CCI+ PHASE 2
PERMAFROST

CCN4
MOUNTAIN PERMAFROST: ROCK GLACIER INVENTORIES (ROGI) AND ROCK GLACIER VELOCITY (RGV) PRODUCTS

D3.2 Climate Research Data Package (CRDP)

VERSION 2.0

15 MAY 2025

PREPARED BY

b·geos
GAMMA REMOTE SENSING
UNIVERSITÉ DE FRIBOURG
UNIVERSITÄT FREIBURG
ALMA MATER STUDIORUM
UNIVERSITÀ DI BOLOGNA
West University of Timisoara
TERRASIGNA
NORCE
UiO : University of Oslo

Document status sheet

Issue	Date	Details	Authors
1.0	15.11.2023	First version CCN4 D3.2	L. Rouyet, T. Echelard, L. Schmid, C. Pellet, R. Delaloye, F. Sirbu, A. Onaca, V. Poncos, F. Brardinoni, A. Kääb, T. Strozzi, N. Jones, A. Bartsch
2.0	15.05.2025	Second version CCN4 D3.2 iteration 2: RoGI in new regions, InSAR-RGV in Switzerland and Italy, and status of the optical-radar RGV work in Norway.	L. Rouyet, C. Pellet, T. Echelard, L. Schmid, R. Delaloye, F. Brardinoni, F. Sirbu, A. Onaca, V. Poncos, T.R. Lauknes, L. Wendt, A. Kääb, T. Strozzi, P. Bernhard, A. Bartsch

Author team

Line Rouyet, Cécile Pellet, Thomas Echelard, Lea Schmid and Reynald Delaloye, UNIFR

Francesco Brardinoni and Thomas Echelard, UniBo

Flavius Sirbu and Alexandru Onaca, WUT

Valentin Poncos, Terrasigna

Line Rouyet, Tom Rune Lauknes and Lotte Wendt, NORCE

Andreas M. Kääb, UiO

Tazio Strozzi and Philipp Bernhard, GAMMA

Annett Bartsch, BGEOS

ESA Technical Officer

Frank Martin Seifert

EUROPEAN SPACE AGENCY CONTRACT REPORT
The work described in this report was done under ESA contract. Responsibility for the contents resides in the authors or organizations that prepared it.

TABLE OF CONTENTS

Executive summary

The European Space Agency (ESA) Climate Change Initiative (CCI) is a global monitoring program, which aims to provide long-term satellite-based products to serve the climate modelling and climate user community. The objective of the ESA CCI Permafrost project (Permafrost_cci) is to develop and deliver the required Global Climate Observation System (GCOS) Essential Climate Variables (ECV) products, using primarily satellite imagery. The two main products associated to the ECV Permafrost, Ground Temperature (GT) and Active Layer Thickness (ALT), were the primary documented variables during Permafrost_cci Phase 1 (2018–2021). Following the ESA Statement of Work for Permafrost_cci Phase 2 (2022–2025) [AD-1], GT and ALT are complemented by a new ECV Permafrost product: Rock Glacier Velocity (RGV). This document focuses on the mountain permafrost component of the Permafrost_cci project and the dedicated rock glacier products.

In periglacial mountain environments, permafrost occurrence is patchy, and the preservation of permafrost is controlled by site-specific conditions, which require the development of dedicated products as a complement to GT and ALT measurements and permafrost models. Rock glaciers are the best visual expression of the creep of mountain permafrost and constitute an essential geomorphological heritage of the mountain periglacial landscape. Their dynamics are largely influenced by climatic factors. There is increasing evidence that the interannual variations of the rock glacier creep rates are influenced by changing permafrost temperature, making RGV a key parameter of cryosphere monitoring in mountain regions.

Two product types are therefore proposed by Permafrost_cci Phase 2: Rock Glacier Inventory (RoGI) and Rock Glacier Velocity (RGV). This agrees with the objectives of the International Permafrost Association (IPA) Standing Committee on Rock Glacier Inventories and Kinematics (RGIK) [RD-4] and concurs with the recent GCOS and GTN-P decisions to add RGV time series as a new product of the ECV Permafrost to monitor changing mountain permafrost conditions [AD-2 to AD-4]. RoGI is an equally valuable product to document past and present permafrost extent. It is a recommended first step to comprehensively characterise and select the landforms that can be used for RGV monitoring. RoGI and RGV products also form a unique validation dataset for climate models in mountain regions, where direct permafrost measurements are very scarce or lacking. Using satellite remote sensing, generating systemic RoGI at the regional scale and documenting RGV interannual changes over many landforms become feasible. Within Permafrost_cci, we mostly use Synthetic Aperture Radar Interferometry (InSAR) technology based on Sentinel-1 images that provide a global coverage, a large range of detection capability (mm–cm/yr to m/yr) and fine spatio-temporal resolutions (tens of m pixel size and 6–12 days of repeat-pass). InSAR is complemented at some locations by SAR offset tracking techniques and spaceborne/airborne optical photogrammetry.

This Climate Research Data Package (CRDP) describes the status of the RoGI and RGV generation for Permafrost_cci Phase 2 and the plan for future work. Both products follow the plan defined in the PSD [RD-2] and will be further described and discussed in the updated PUG and PVIR (Deliverable D4.1 and D4.2 in August 2025). We present the results of the RoGI generation in the new regions selected for the second iteration within Permafrost_cci Phase 2 [RD-2]. We show the results of the RGV production in the Alps as part of the Baseline project (Switzerland) and Option 9 (Italy). We describe the status of the work on RGV using radar and optical remote sensing in Northern Norway (Option 8). This version of the CDRP is still under revision. It will be published open-access when completed.

1 Introduction

1.1 Purpose of the document

The mountain permafrost component of Permafrost_cci Phase 2 focuses on the generation of two products: Rock Glacier Inventory (RoGI) and Rock Glacier Velocity (RGV). The Climate Research Data Package (CRDP) describes the status of the RoGI and RGV generation for Permafrost_cci Phase 2 iteration 2 and the plan for future work.

1.2 Structure of the document

Section 1 provides information about the purpose and background of this document. Section 2 described the RoGI and RGV products generated during Permafrost_cci Phase 2 iteration 2. Section 3 explains the work that is foreseen in the future. A bibliography complementing the applicable and reference documents (Sections 1.3 and 1.4) is provided in Section 4.1. A list of acronyms is provided in Section 4.2. A glossary of the commonly accepted permafrost terminology can be found in [RD-19].

1.3 Applicable documents

[AD-1] ESA. 2022. Climate Change Initiative Extension (CCI+) Phase 2 – New Essential Climate Variables – Statement of Work. ESA-EOP-SC-AMT-2021-27.

[AD-2] GCOS. 2022. The 2022 GCOS Implementation Plan. GCOS – 244 / GOOS – 272. Global Observing Climate System (GCOS). World Meteorological Organization (WMO).

[AD-3] GCOS. 2022. The 2022 GCOS ECVs Requirements. GCOS – 245. Global Climate Observing System (GCOS). World Meteorological Organization (WMO).

[AD-4] GTN-P. 2021. Strategy and Implementation Plan 2021–2024 for the Global Terrestrial Network for Permafrost (GTN-P). Authors: Streletskiy, D., Noetzli, J., Smith, S.L., Vieira, G., Schoeneich, P., Hrbacek, F., Irrgang, A.M.

1.4 Reference Documents

[**RD-1**] Rouyet, L., Pellet, C., Schmid, L., Echelard, T., Delaloye, R., Brardinoni, F., Sirbu, F., Onaca, A., Poncos, V., Kääb, A, Strozzi, T., Bartsch, A. 2024. ESA CCI+ Permafrost Phase 2 – CCN4 Mountain Permafrost: Rock Glacier inventories (RoGI) and Rock glacier Velocity (RGV) Products. D1.1 User Requirement Document (URD), v2.0. European Space Agency.

[RD-2] Rouyet, L., Schmid, L., Pellet, C., Echelard, T., Delaloye, R., Brardinoni, F., Sirbu, F., Onaca, A., Poncos, V., Kääb, A, Strozzi, T., Bernhard, P., Bartsch, A. 2024. ESA CCI+ Permafrost Phase 2 – CCN4 Mountain Permafrost: Rock Glacier inventories (RoGI) and Rock glacier Velocity (RGV) Products. D1.2 Product Specification Document (PSD), v2.0. European Space Agency.

[RD-3] Rouyet, L., Pellet, C., Schmid, L., Echelard, T., Barboux, C., Delaloye, R., Brardinoni, F., Sirbu, F., Onaca, A., Poncos, V., Wendt, L., Lauknes, T. R., Kääb, A, Strozzi, T., Bernhard, P., Bartsch, A. 2024. ESA CCI+ Permafrost Phase 2 – CCN4 Mountain Permafrost: Rock Glacier inventories (RoGI) and Rock glacier Velocity (RGV) Products. D2.2 Algorithm Theoretical Basis Document (ATBD), v2.0. European Space Agency.

[RD-4] Delaloye, R., Barboux, C., Bodin, X., Brenning, A., Hartl, L., Hu, Y., Ikeda, A., Kaufmann, V., Kellerer-Pirklbauer, A., Lambiel, C., Liu, L., Marcer, M., Rick, B., Scotti, R., Takadema, H., Trombotto

Liaudat, D., Vivero, S., Winterberger, M. 2018. Rock glacier inventories and kinematics: a new IPA Action Group. Proceedings of the 5th European Conference on Permafrost (EUCOP), Chamonix, 23 June – 1st July 2018.

[RD-5] RGIK. 2022. Towards standard guidelines for inventorying rock glaciers: baseline concepts (version 4.2.2). IPA Action Group Rock glacier inventories and kinematics, 13 pp.

[RD-6] RGIK. 2022. Towards standard guidelines for inventorying rock glaciers: practical concepts (version 2.0). IPA Action Group Rock glacier inventories and kinematics, 10 pp.

[RD-7] RGIK. 2022. Optional kinematic attribute in standardized rock glacier inventories (version 3.0.1). IPA Action Group Rock glacier inventories and kinematics, 8 pp.

[RD-8] RGIK. 2023. Guidelines for inventorying rock glaciers: baseline and practical concepts (version 1.0). IPA Action Group Rock Glacier Inventories and Kinematics, 25 pp. https://doi.org/10.51363/unifr.srr.2023.002.

[RD-9] RGIK. 2023. InSAR-based kinematic attribute in rock glacier inventories. Practical InSAR guidelines (version 4.0). IPA Action Group Rock glacier inventories and kinematics, 33 pp.

[RD-10] RGIK 2023. Rock Glacier Velocity as an associated parameter of ECV Permafrost: baseline concepts (version 3.2). IPA Action Group Rock glacier inventories and kinematics, 12 pp.

[RD-11] RGIK. 2023. Rock Glacier Velocity as an associated parameter of ECV Permafrost: practical concepts (version 1.2). IPA Action Group Rock glacier inventories and kinematics, 17 pp.

[RD-12] RGIK. 2023. Instructions of the RoGI exercises in the Goms and the Matter Valley (Switzerland). IPA Action Group Rock glacier inventories and kinematics, 10 pp.

[RD-13] Bertone, A., Barboux, C., Delaloye, R., Rouyet, L., Lauknes, T. R., Kääb, A., Christiansen, H. H., Onaca, A., Sirbu, F., Poncos, V., Strozzi, T., Caduff, R., Bartsch, A. 2020. ESA CCI+ Permafrost Phase 1 – CCN1 & CCN2 Rock Glacier Kinematics as New Associated Parameter of ECV Permafrost. D4.2 Climate Research Data Package Product Specification Document (CRDP), v1.0. European Space Agency.

[RD-14] Sirbu, F., Onaca, A., Poncos, V., Strozzi, T., Bartsch, A. 2022. ESA CCI+ Permafrost Phase 1 – CCN1 & CCN2. Rock Glacier Kinematics in the Carpathians (CCN1 Budget Extension). Climate Research Data Package Product Specification Document (CRDP), v1.0. European Space Agency.

[RD-15] Bertone, A., Barboux, C., Bodin, X., Bolch, T., Brardinoni, F., Caduff, R., Christiansen, H. H., Darrow, M. M., Delaloye, R., Etzelmüller, B., Humlum, O, Lambiel, C., Lilleøren, K. S., Mair, V., Pellegrinon, G., Rouyet, L., Ruiz, L., Strozzi, T. 2022. Incorporating InSAR kinematics into rock glacier inventories: insights from 11 regions worldwide. The Cryosphere. 16, 2769–2792. https://doi.org/10.5194/tc-16-2769-2022.

[RD-16] Rouyet, L., Echelard, T., Schmid, L., Pellet, C., Delaloye, R., Onaca, A., Sirbu, F., Poncos, V., Brardinoni, F., Kääb, A, Strozzi, T., Jones, N., Bartsch, A. 2023. ESA CCI+ Permafrost Phase 2 – CCN4 Mountain Permafrost: Rock Glacier inventories (RoGI) and Rock glacier Velocity (RGV) Products. D3.2 Climate Research Data Package (CRDP), v1.0. European Space Agency.

[RD-17] Pellet, C., Bodin, X., Cusicanqui, D., Delaloye, R., Kaufmann, V., Noetzli, J., Thibert, E., Vivero, S., & Kellerer-Pirklbauer, A. (2024). Rock glacier velocity. In Bull. Amer. Soc. Vol. 105(8), State of the Climate in 2023, pp. 44–45. https://doi.org/10.1175/2024BAMSStateoftheClimate.1.

[RD-18] Adler, C., Wester, P., Bhatt, I., Huggel, C., Insarov, G. E., Morecroft, M. D., Muccione, V. and Prakash, A. 2022. Cross-Chapter Paper 5: Mountains. In: Climate Change 2022: Impacts, Adaptation and Vulnerability. Contribution of Working Group II to the Sixth Assessment Report of the

Intergovernmental Panel on Climate Change. Cambridge University Press, Cambridge, UK and New York, NY, USA, pp. 2273–2318. https://doi.org/10.1017/9781009325844.022.

[RD-19] van Everdingen, R. Ed. 1998, revised in May 2005. Multi-language glossary of permafrost and related ground-ice terms. Boulder, CO: National Snow and Ice Data Center/World Data Center for Glaciology. http://nsidc.org/fgdc/glossary.

2 Overview of the mountain permafrost data package

2.1 Rock glacier inventory (RoGI)

In iteration 1, we generated and disseminated RoGI products in 12 areas worldwide (Rouyet et al., 2024; Rouyet et al., 2025, in review; UNIFR, 2025). In iteration 2, we extended the set of RoGI products to **six new regions** [RD-2]. Three RoGI regions are in Europe (Switzerland, Italy and Bulgaria), as part of the Baseline project and the Option 9 (UNIFR, UniBo, WUT). Three others RoGI regions are in South America and Asia (Bolivia–Chile, Nepal, Mongolia), in collaboration with external partners (Université Grenoble Alpes, Chinese University of Hong Kong and Mongolian Academy of Science). **Two additional RoGI** are being developed as part of side-projects in India and Bhutan, not initially promised as Permafrost_cci deliverables, but in synergy with research projects at two partner institutions (UniBo and UNIFR). **Figure 1** shows the locations of the 12 initial inventories (red squares), together with the new regions (blue circles: the six Permafrost_cci regions; orange circles: regions from the two side-projects).

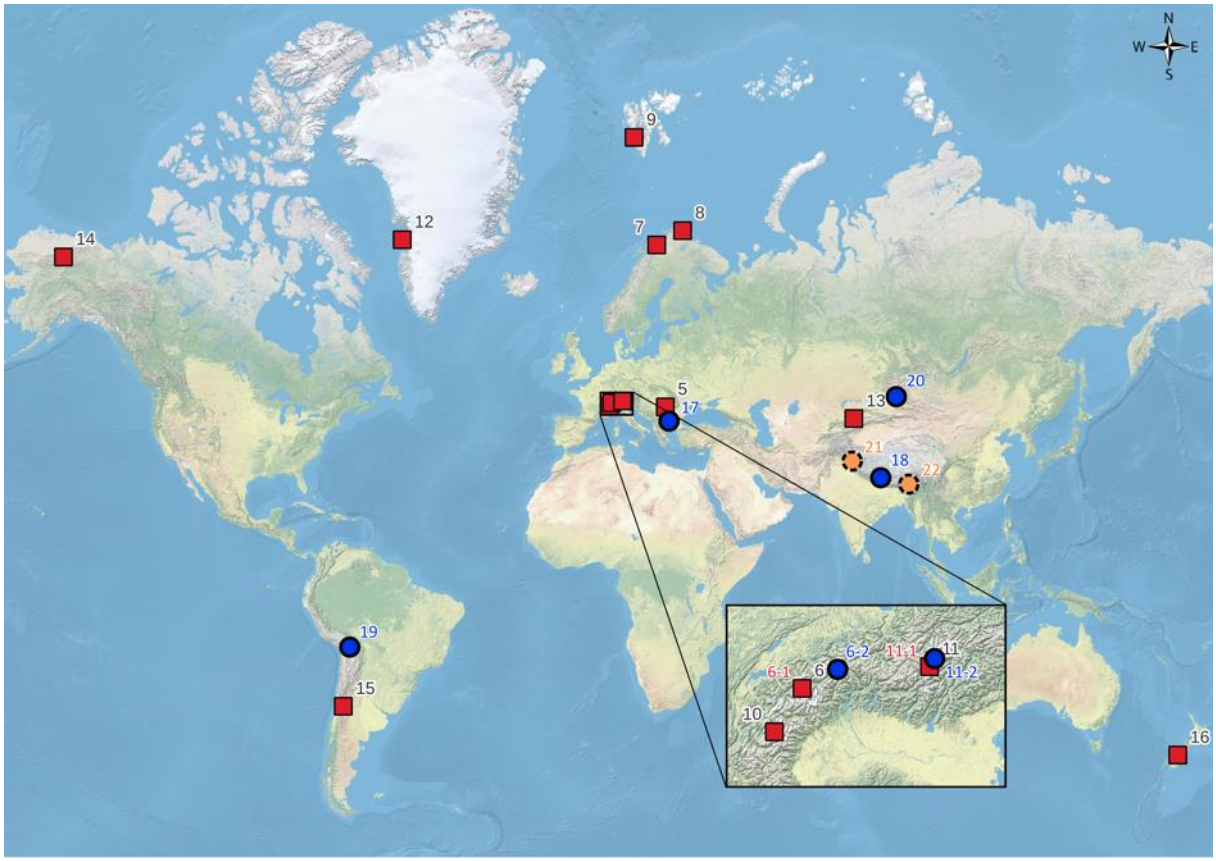

Figure 1. *Location map of areas selected for the RoGI from Permafrost_cci Phase 2 iteration 1 (red squares), new regions from iteration 2 (blue circles) and regions from side-projects (orange circles). The area numbering corresponds to the format defined in the PSD [RD-2].*

All RoGI teams have received QGIS projects, with common file structure, background data and dialog boxes for semi-automatic attribute filling. The InSAR data (single interferograms and stacking) have been provided by GAMMA, except for the RoGI 18 (Manaslu, Nepal) where InSAR data has been processed by an external partner (Chinese University of Hong Kong). The data folder and QGIS

structure have been provided by UNIFR. The inventorying teams have followed the RoGI guidelines developed by the RGIK community. The work has been performed by several teams, building on the tools and recommendations from the multi-operator exercise from the first iteration. The procedure is further explained in the ATBD [RD-3] and follows the inventorying rules defined by RGIK reference documents [RD-5, RD-6, RD-7, RD-8, RD-9]. The number of RoGI operators and the way the tasks has been shared within the team varies from a team to another and is described in **Annex 1**.

For each region, the RoGI data consists of set of three geopackage files: 1) the Primary Markers (PM), a point vector file showing the locations of the rock glaciers, and including several standard morpho-kinematic attributes; 2) the Moving Areas (MA), a polygon vector file showing the extent and velocity of the detected surface movement based on spaceborne InSAR; 3) the Geomorphological Outlines (GO), a polygon vector file showing the restricted and/or the extended boundaries of the mapped landforms.

The status of the work varies from a region to another: from partially compiled to completely finished. Here is the summary of the status in each region:

- **RoGI area 6-2 in Goms–Binntal, Switzerland:** The inventory is completed. Minor adjustments might still occur during the final review of the product.
- **RoGI area 11-2 in Northern Venosta, Italy:** The RoGI process is finished. The inventory is completed. Last technical adjustments (field labelling) are ongoing.
- **RoGI area 17-1 in Pirin and Rila Mountains, Bulgaria:** The RoGI process is finished in the Pirin area. Similar work is ongoing in the Rila area.
- **RoGI area 18-1 in Manaslu, Nepal:** PM identification is completed. MA step is ongoing. Past version of the GO will be updated based on the finalised PM/MA.
- **RoGI area 19-1 in Sajama, Bolivia–Chile:** PM identification is completed in Bolivia. MA and GO are ongoing (70–90% completed).
- **RoGI area 20-1 in Tsengel Khairkhan, Mongolia:** All RoGI steps are finished. The inventory is completed. Further analysis and plan for publication is ongoing.
- **RoGI area 21-1 in Himachal Pradesh, India:** A preliminary version of all RoGI files has been compiled. Quality-check and adjustments are ongoing.
- **RoGI area 22-1 in Thana, Bhutan:** Data compilation and sharing with operators is completed. The RoGI process is about to start.

In **Annex 1**, the regional specificities, work status and main findings of each RoGI team/region is summarised in a common template. Examples of PM, MA and GO results are selected in small subareas of the inventoried regions for visualisation purposes. The current data in each region is included in the **attached data package**. The datasets are **under embargo**, due to upcoming adjustments, further developments and/or specific plans for scientific publications in all regions. See **Section 3** for information about the future workplan.

2.2 Rock glacier velocity (RGV)

In the Alps, Sentinel-1 InSAR has been processed by GAMMA over **21 rock glaciers in the Alps**: five sites in Switzerland (Baseline project) and 15 sites in Italy (Option 9), and one additional landform in France (see PSD [RD-2]). The results include the complete velocity and coherence time series for each generated InSAR pair, as well as the final averaged RGV product. The velocity time series are extracted at selected locations (manual selection) and/or spatially averaged for several pixels after filtering (see ATBD [RD-3]), depending on the results quality and the identified challenged at each site. The high-coherent June–September interferograms are averaged for each summer season, to provide an annualized surface velocity time series, following the RGV requirements [AD-3, AD-4] [RD-10, RD-11]. The InSAR results based on 12 days temporal baseline (2015–2024) are compared with 6 days temporal baseline (2016–2021) to verify if the trends are similar or affected by significant bias from phase aliasing and unwrapping errors. The resulting InSAR-RGV document interannual trends of velocity changes assumed to be representative of the rock glacier units. The method remains semi-automatic due to site-specific challenges leading the spatial and temporal heterogeneous quality of the InSAR signal, both temporally and spatially. These challenges will be discussed in the PVIR and PUG.

Examples of results are shown in **Figures 2 and 3** (Switzerland) and **Figure 4** (Italy). Detailed presentation of all InSAR-RGV results is provided in **Annex 2**. The data for all sites are included in the **attached data package.** This dataset is **under embargo**, due to upcoming adjustments and expected extensions to new sites. The future workplan is described in **Section 3**.

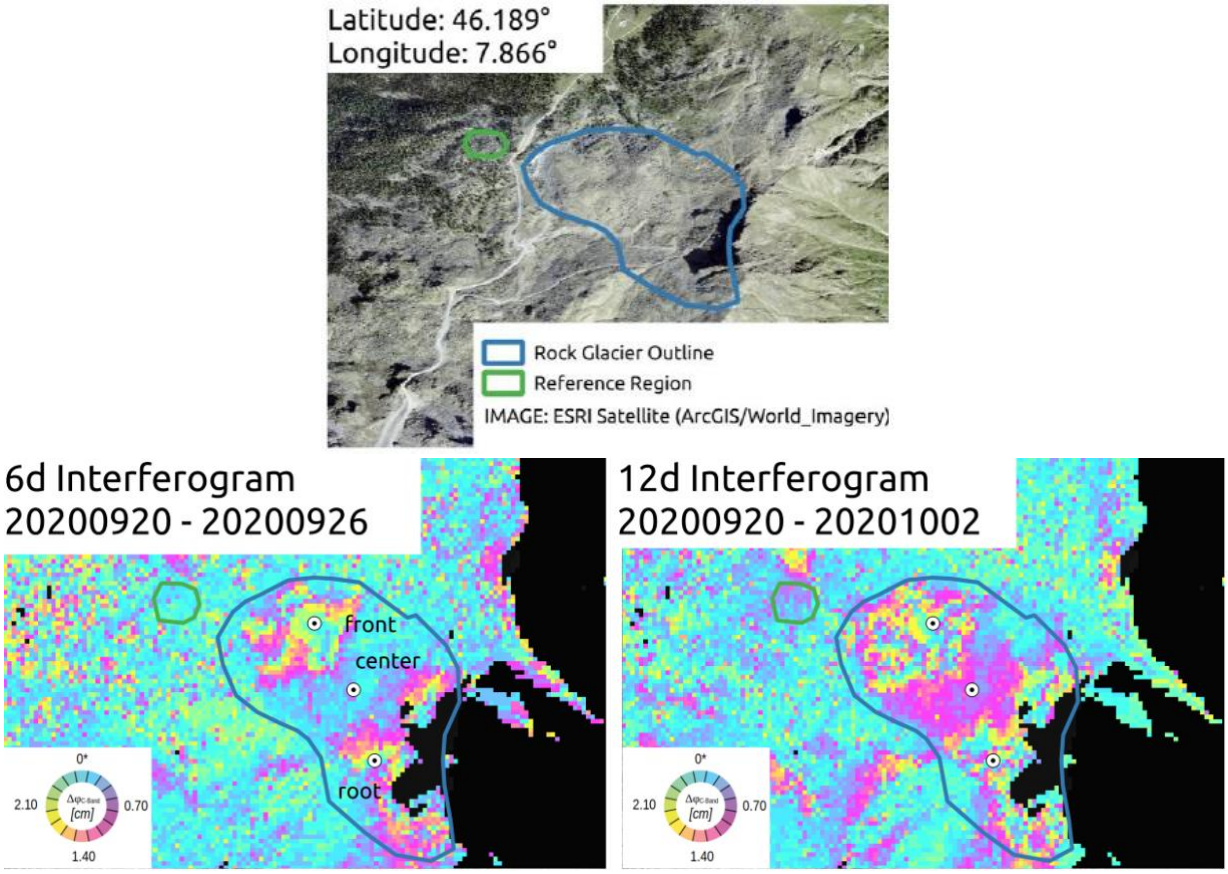

Figure 2. *Example of location map (upper) and Sentinel-1 interferograms and selected points (lower) on Diestelhorn rock glacier, Switzerland.*

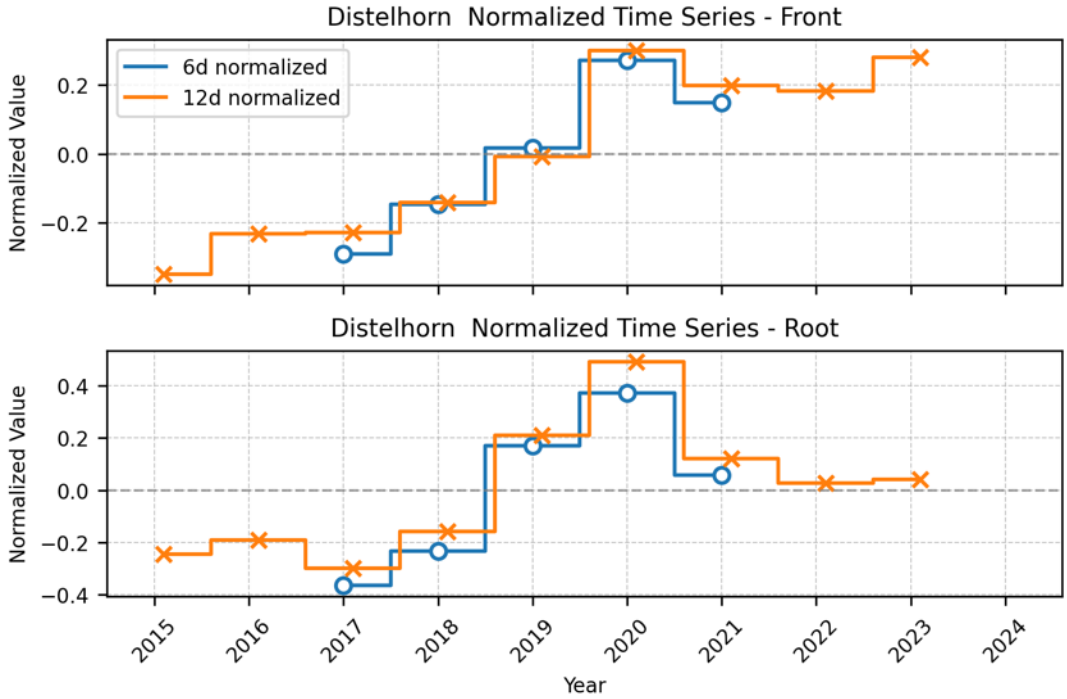

Figure 3. *InSAR-RGV on Diestelhorn rock glacier. Front and root locations are shown in Figure 2.*

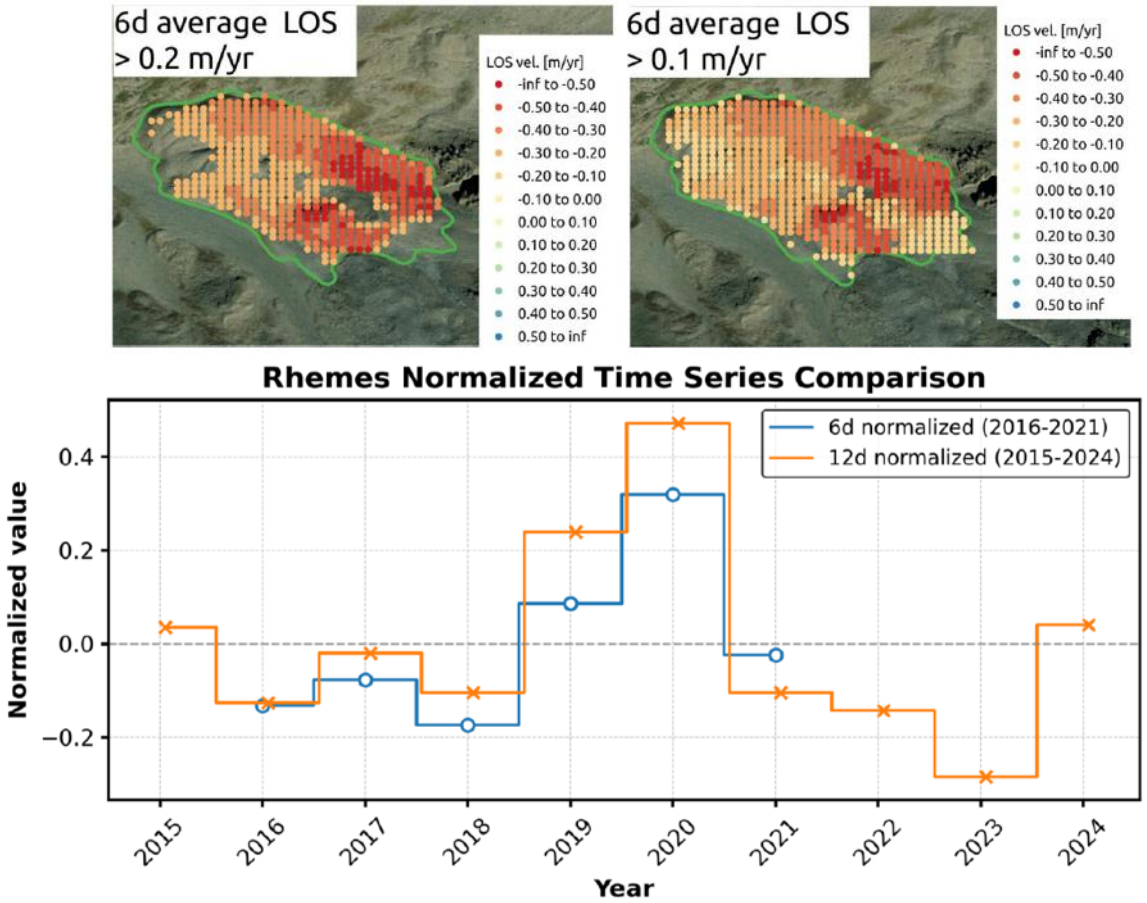

Figure 4. *InSAR-RGV on Rhemes rock glacier, Italy. Example of Sentinel-1 interferograms and pixels selected for aggregated (upper maps) and resulting RGV product (lower graphs).*

In Norway, the objective of the Option 8 'PermaSeries' is to compare and possibly integrate rock glacier velocity time series processed with a set of complementary data (airphotos, spaceborne SAR and ground-based radar) and techniques (optical feature tracking, SAR offset tracking and InSAR). One challenge was to find locations with good data availability/quality and a variety of rock glaciers with variable sizes and velocity ranges to be documented by the various techniques. The Ádjet mountain ridge (Troms, Northern Norway) was selected for this purpose (see PSD [RD-2]).

Examples of preliminary results using optical photogrammetry, InSAR and SAR offset tracking are shown in **Figure 5** and **Figure 6**. Until now, the work has been performed separately for the optical and radar components. We will then compare the results and integrate the findings with previously published data at the same location (Eriksen et al., 2018). Detailed presentation of the current results is provided in **Annex 2**. The future workplan is described in **Section 3**.

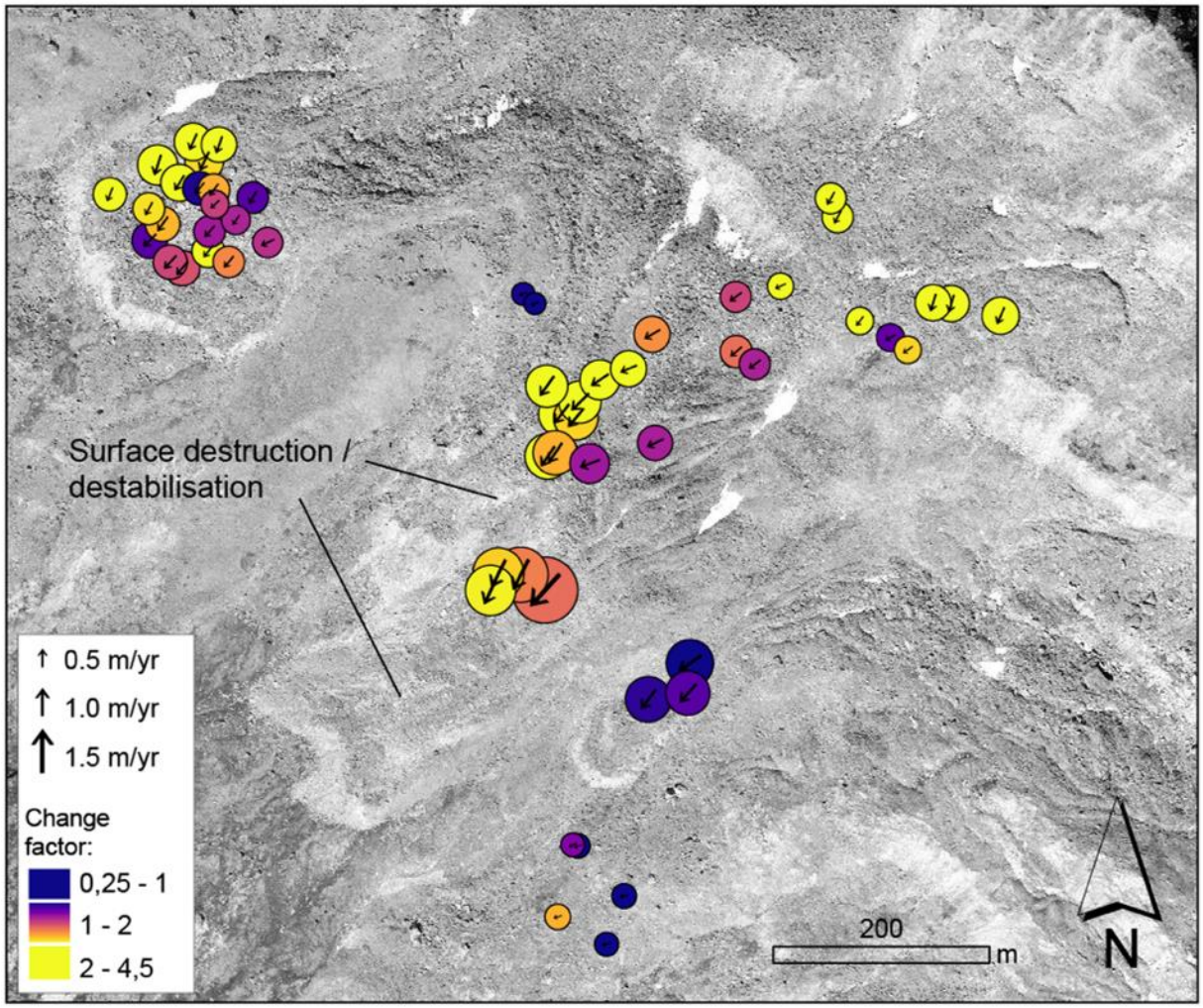

Figure 5. *Changes in speed between 1977–2006 and 2006–2016 for the rock glaciers in the eastern part of the Ádjet mountain slope. The factor "fact" is 2nd velocity/1st velocity, i.e. 1 means no change, >1 means acceleration over time.*

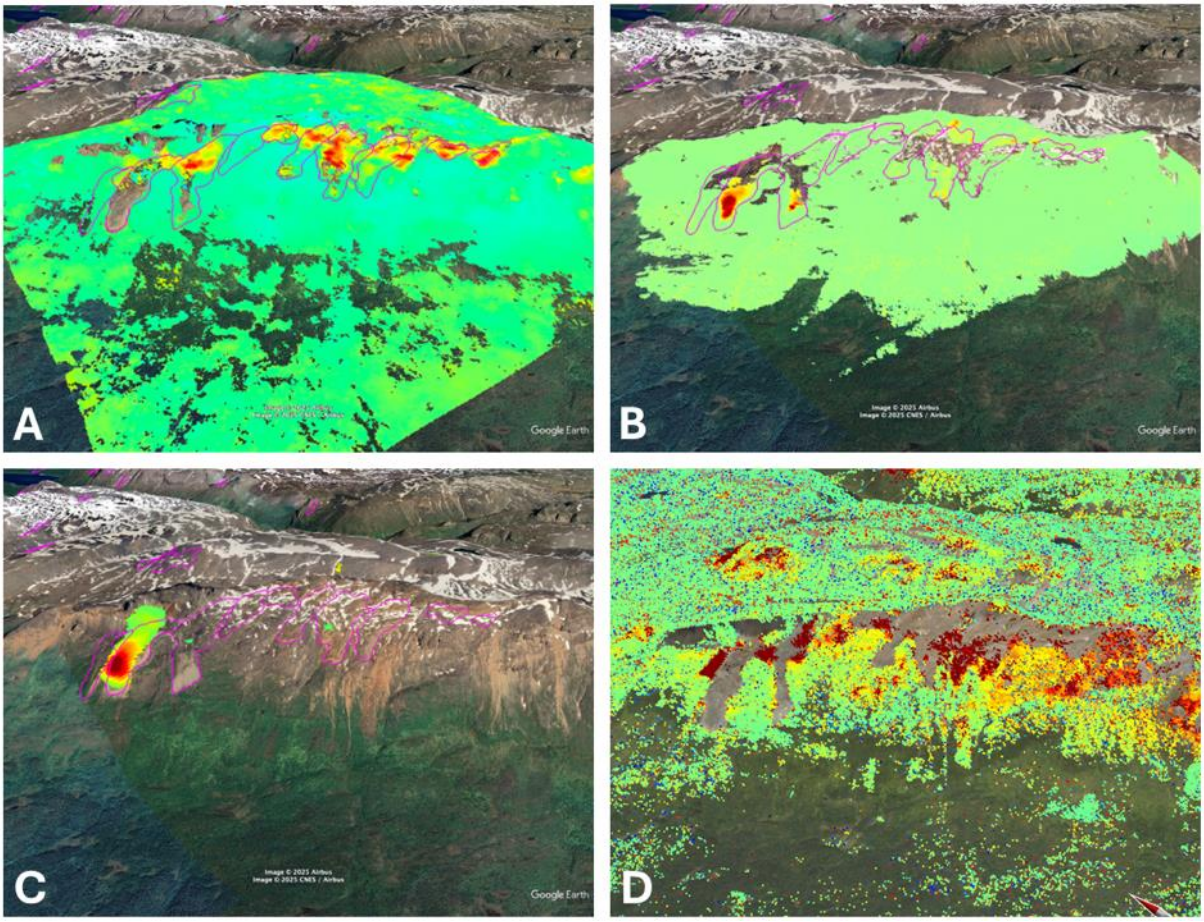

Figure 6. *Overview of complementary datasets used in the radar analysis.* ***A.*** *COSMO-SkyMed interferogram stacking from 2023–2024. Scale ±50 cm/year.* ***B.*** *GPRI ground-based radar from 2014.* ***C.*** *COSMO-SkyMed offset tracking from 2023–2024.* ***D.*** *Sentinel-1 PSI 2020–2024 from InSAR Norway. Note that colour scales differ across panels, and each sensor has distinct line-of-sight sensitivity. Despite these differences, spatial patterns are consistent. The different sensors and methods are highly complementary, offering a robust picture of the rock glacier dynamics. Magenta outline shows mapped rock glacier extent from Rouyet et al. (2021). COSMO-SkyMed Product/COSMO Second Generation Product © ASI: 2023–2024 processed under license from ASI - Agenzia Spaziale taliana. All rights reserved. Distributed by e-GEOS.*

In 2024, we kicked off a **RGV working group** and designed an intercomparison exercise over common landforms. The first objectives of the group were to simultaneously generate RGV on three landforms (see PSD [RD-2]), to intercompare the results using various data sources (GNSS, airphotos, Sentinel-1 SAR images), and to identify concrete issues occurring during the production. Three alpine rock glaciers were selected to perform an intercomparison exercise based on variable data sources (GNSS, airphotos, Sentinel-1 SAR images) (see PSD [RD-2] and ATBD [RD-3]). The selected rock glaciers (Gran Sometta, Grosses Gufer and Laurichard) are included in the InSAR-RGV products delivered by GAMMA (**Annex 2**). The results of the intercomparison between different techniques will be discussed in the PVIR. The future workplan of this initiative is described in **Section 3**.

3 Summary and prospects

3.1 Rock glacier inventory (RoGI)

The results from multi-operator exercise in 12 areas from iteration 1 is now published in the Zenodo repository (Rouyet et al., 2024). The data can also be viewed in an online WebGIS (UNIFR, 2025). The methodology and data properties are described in an ESSD paper (Rouyet et al., 2025, in review). A peer-reviewed paper summarising the common inventorying guidelines is being finalized and will be submitted before summer 2025 (Vivero et al., in prep.). The work to develop alternative training tools to further explain and promote the guidelines (video tutorial, online exercise) is ongoing as part of the RGIK initiative. RoGI Permafrost_cci products are key examples for this purpose.

The inventorying progress in the new regions of Permafrost_cci Phase 2 iteration 2 is variable due the different AOI sizes, the various numbers of involved internal and external partners, and the different timelines of connected projects. In some regions, the RoGI is fully completed but must still be comprehensively summarised and analysed for future scientific publications. In other regions, the results are partial: either some parts of the AOI have not been fully covered, or some steps of the RoGI procedures have not been finalized yet (e.g., MA, GO, attribute characterisation or full quality-check and consensus-based final decision based on individual operator results).

Here is the summary of the future workplan in each region:

- **RoGI area 6-2 in Goms–Binntal, Switzerland):** The work is in synergy with the RoDynAlpS project (SNSF) that is currently finishing the RoGI production for the whole Switzerland. A publication is under development, as part a related PhD project.
- **RoGI area 11-2 in Northern Venosta, Italy:** Final adjustments will be made before summer. Further analysis towards a publication is likely. The timeline will depend on the workplan foreseen by the CCI project extension in 2025–2026.
- **RoGI area 17-1 in Pirin and Rila Mountains, Bulgaria:** The Pirin RoGI is completed. The results will be analysed against other available data in the area and integrated in a multi-method paper. The Rila RoGI is expected to be completed by late summer.
- **RoGI area 18-1 in Manaslu, Nepal:** The ongoing RoGI steps (MA/GO) are expected to be completed in June–July 2025. Further work on analysis and publication will start this summer.
- **RoGI area 19-1 in Sajama, Bolivia–Chile:** The Bolivian RoGI will be completed by end of spring. Similar work will then start in the Chilean AOI. A joint publication is planned in 2026.
- **RoGI area 20-1 in Tsengel Khairkhan, Mongolia:** Work on the results analysis will start this summer. A conference contribution is planned for the next RCOP in Mongolia (June 2026), likely in relation with an article submission.
- **RoGI area 21-1 in Himachal Pradesh, India:** The final version is expected in June 2025. The analysis and dissemination will be performed in summer–fall, in relation with a PhD project.
- **RoGI area 22-1 in Thana, Bhutan:** The RoGI process is linked to the SNSF-funded Cryo-SPIRIT project. The work is starting in June 2025. The results are expected to be used in synergy with the permafrost map being developed by a PhD candidate in Bhutan.

We expect all inventories to be completed before the end of the CCI programme and related scientific publications are planned in most regions. The release of an open RoGI database to store and share is planned for 2026 and the Permafrost_cci RoGI will be the first products to be integrated, as showcasing examples.

The results are planned to be used as training data for RoGI using machine learning. A collaboration with third parties is ongoing (University of Bergen, Norway; University of Canterbury, New Zealand), in synergy with an upcoming RGIK working group on the same topic.

3.2 Rock glacier velocity (RGV)

During iteration 1, the RGV component remained at a pilot stage, with a focus on consolidating the baseline principles to monitor rock glaciers. As the decision of including RGV as ECV product is recent [AD-3], the requirements and guidelines for generating such products were still at an embryonic stage at the beginning of CCI Permafrost Phase 2. Since then, a first version of the practical guidelines for RGV generation has been released [RD-10] and integrated in the WMO Guide for Measurement of Cryospheric Variables (WMO, 2025). A review paper on RGV has been published (Hu et al., 2025). Several recently published publications documenting RGV at the regional scale involve Permafrost_cci partners (Kääb & Røste, 2024; Kellerer-Priklbauer et al., 2024; Pellet et al., 2024).

In iteration 2, several questions remain to design an easily transferable method to automate the production of RGV using InSAR and provide consistent results, comparable with other data sources and techniques (in-situ, optical photogrammetry, SAR offset tracking). It is the reason we created a RGV working dedicated to such questions. In November 2024, we organised a first RGV workshop in Fribourg (Switzerland) co-funded by Permafrost_cci (ESA, 2024). The conclusions of the intercomparison will be presented in several scientific conferences in 2025 (EGU, ESA LPS, IAG), and will be summarised in the next PVIR.

In 2025, the work of the RGV working group continues. We aim to summarise our recommendations in Best Practice documents that will help the community members to produce and disseminate comparable RGV in the future. The RGV Best Practices are meant to be technical reference documents, complementary to the current RGIK baseline [RD-10, RD-11]. To wrap up this phase, a second 2-days workshop is planned in Switzerland, between the end of 2025 and early 2026. The comparison and potential integration of time series from different methods is also in synergy with the objectives of the Option 8.

In the Alps, Permafrost_cci partners (GAMMA, UNIFR, UniBo) have implemented a semi-automated processing chain for intensifying the production of InSAR-RGV products. Currently, 21 rock glaciers are being documented with RGV, mostly in the Swiss and Italian Alps. Gradually more landforms are included, which is a promising development for the future use of such products as regional climate change indicators. In the next PVIR, we aim to combine the individual RGV products to describe the regional trends, and compare them to similar analysis based on in-situ velocity time series (Kellerer-Pirklbauer, 2024; PERMOS, 2024).

In Norway, Permafrost_cci partners (NORCE, UiO) have started the Option 8 a year later than the Baseline, so that a similar processing chain is not implemented yet. The focus is placed on the area covered by RoGI 7-1 (Troms, Norway), where velocity time series from various data and techniques (optical photogrammetry, InSAR and SAR offset tracking) are being processed and compared. This intercomparison objective is in synergy with the goals of the RGV working group. Until now, the work has been performed independently for the optical and radar components. The next step is to compare the results and integrate the findings with previously published data (Eriksen et al., 2018). The work is continuing until Spring 2026, according to the shifted Option 8 timeline.

RGV processing in the other Permafrost_cci areas covered by RoGI products is not foreseen before the end of the iteration 2 but is foreseen in the extension phase.

4 References

4.1 Bibliography

Eriksen, H. Ø., Rouyet, L., Lauknes, T. R., Berthling, I., Isaksen, K., Hindberg, H., Larsen, Y. and Corner, G. D. (2018). Recent acceleration of a rock glacier complex, Ádjet, Norway, documented by 62 years of remote sensing observations. *Geophysical Research Letters*, *45*(16), 8314–8323. https://doi.org/10.1029/2018GL077605.

ESA (2024). New Rock Glacier Velocity (RGV) Working Group kicks off! Climate Change Initiative (CCI) News. European Space Agency (ESA) Climate Office. https://climate.esa.int/en/projects/permafrost/news-and-events/news/Rock-Glacier-Velocity-Working-Group-kicks-off/.

Kääb, A. and Røste, J. (2024). Rock glaciers across the United States predominantly accelerate coincident with rise in air temperatures. *Nature Communications*, *15*(1), 7581. https://doi.org/10.1038/s41467-024-52093-z.

Kellerer-Pirklbauer, A., Bodin, X., Delaloye, R., Lambiel, C., Gärtner-Roer, I., Bonnefoy-Demongeot, M., Carturan, L., Damm, B., Eulenstein, J., Fischer, A., Hartl, L., Ikeda, A., Kaufmann, V., Krainer, K., Matsuoka, N., Morra Di Cella, U., Noetzli, J., Seppi, R., Scapozza, C., Schoeneich, P., Stocker-Waldhuber, M., Thibert, E. and Zumiani, M. (2024). Acceleration and interannual variability of creep rates in mountain permafrost landforms (rock glacier velocities) in the European Alps in 1995–2022. *Environmental Research Letters*, *19*(3), 034022. https://doi.org/10.1088/1748-9326/ad25a4.

Hu, Y., Arenson, L., Barboux, C., Bodin, X., Cicoira, A., Delaloye, R., Gärtner-Roer, I., Kääb, A., Kellerer-Pirklbauer, A., Lambiel, C., Liu, L., Pellet, C., Rouyet, L., Schoeneich, P., Seier, G. and Strozzi, T. (2025). Rock Glacier Velocity: An Essential Climate Variable Quantity for Permafrost, *Reviews of Geophysics*, *63*(1), e2024RG000847. https://doi.org/10.1029/2024RG000847.

Pellet, C., Bodin, X., Cusicanqui, D., Delaloye, R., Kaufmann, V., Noetzli, J., Thibert, E., Vivero, S. and Kellerer-Pirklbauer, A. (2024). Rock glacier velocity. In *Bull. Amer. Soc. Vol. 105(8), State of the Climate in 2023*, pp. 44–45. https://doi.org/10.1175/2024BAMSStateoftheClimate.1.

PERMOS 2024. Swiss Permafrost Bulletin 2023. Noetzli, J. and Pellet, C. (eds.) 25 pp, https://doi.org/10.13093/permos-bull-2024.

Rouyet, L., Bolch, T., Brardinoni, F., Caduff, R., Cusicanqui, D., Darrow, M., Delaloye, R., Echelard, T., Lambiel, C., Ruiz, L., Schmid, L., Sirbu, F. and Strozzi, T. (2024). Rock Glacier Inventories (RoGI) in 12 areas worldwide using a multi-operator consensus-based procedure [Data set]. *Zenodo*. https://doi.org/10.5281/zenodo.14501399.

Rouyet, L., Bolch, T., Brardinoni, F., Caduff, R., Cusicanqui, D., Darrow, M., Delaloye, R., Echelard, T., Lambiel, C., Ruiz, L., Schmid, L., Sirbu, F. and Strozzi, T. (2025, in review). Rock Glacier Inventories (RoGI) in 12 areas worldwide using a multi-operator consensus-based procedure. *Earth System Science Data Discussion* [preprint]. https://doi.org/10.5194/essd-2024-598.

Rouyet, L., Lilleøren, K. S., Böhme, M., Vick, L. M., Delaloye, R., Etzelmüller, B., Lauknes, T. R., Larsen, Y. and Blikra, L. H. (2021). Regional morpho-kinematic inventory of slope movements

in northern Norway. *Frontiers in Earth Science*, *9*, 681088. https://doi.org/10.3389/feart.2021.681088.

UNIFR (2025). RoGI WebGIS: ESA CCI+ Permafrost project – Rock glacier inventories. https://bigweb.unifr.ch/Science/Geosciences/Geomorphology/Pub/Website/CCI/CCI_qgis2web_2025_04/#2/28.5/0.0. University of Fribourg, Switzerland.

Vivero, S., Barboux, C., Bodin, X., Cicoira, A., Delaloye, R., Echelard, T., Hu, Y., Jones, N., Lambiel, C., MacDonnell, S., Pellet, C., Rouyet L., Ruiz, L., Schaffer, N., Wehbe, M. and Brardinoni, F. (in prep.). RGIK guidelines for compiling consistent rock glacier inventories.

WMO (2025). Guide to Instruments and Methods of Observation. Volume II – Measurement of Cryospheric Variables. WMO-No.8. 2024 Edition. Chapter 4. Measurement of Permafrost. Section 4.4. Measurements of Rock Glacier Velocity. https://doi.org/10.59327/WMO/CIMO/2.

4.2 Acronyms

AD	Applicable Document
AI	Artificial Intelligence
ALT	Active Layer Thickness
ADP	Algorithm Development Plan
ATBD	Algorithm Theoretical Basis Document
BR	Breakthrough Requirement
CAR	Climate Assessment Report
CCI	Climate Change Initiative
CCN	Contract Change Notice
CRDP	Climate Research Data Package
DEM	Digital Elevation Model
E3UB	End-to-End ECV Uncertainty Budget
ECV	Essential Climate Variable
EO	Earth Observation
ESA	European Space Agency
GAMMA	Gamma Remote Sensing AG
GCOS	Global Climate Observing System
GNSS	Global Navigation Satellite System
GR	Goal Requirement
GT	Ground Temperature
GTN-P	Global Climate Observing System
GTOS	Global Terrestrial Observing System
InSAR	Interferometric Synthetic Aperture Radar
IPA	International Permafrost Association
KA	Kinematic Attribute
LOS	Line-of-sight
MA	Moving Area
MAGT	Mean Annual Ground Temperature
MAGT	Mean Annual Ground Surface Temperature
NORCE	Norwegian Research Centre AS
OT	Offset Tracking

PERMOS	Swiss Permafrost Monitoring Network
PI	Principal Investigator
PM	Primary Marker
PSD	Product Specification Document
PUG	Product User Guide
PVASR	Product Validation and Algorithm Selection Report
PVIR	Product Validation and Intercomparison Report
PVP	Product Validation Plan
RD	Reference Document
RG	Rock Glacier
RGIK	Rock Glacier Inventories and Kinematics
RGU	Rock Glacier Unit
RGV	Rock Glacier Velocity
RoGI	Rock Glacier Inventory
RMSE	Root Mean Square Error
SAR	Synthetic Aperture Radar
SfM	Surface from Motion
TR	Threshold Requirement
UAV	Unmanned Aerial Vehicle
UiO	University of Oslo
UniBo	University of Bologna
UNIFR	University of Fribourg
URD	User Requirement Document
URq	User Requirement
UTM	Universal Transverse Mercator
WUT	West University of Timisoara
WMO	World Meteorological Organization

Annex 1: Permafrost_cci RoGI products

RoGI reports for each region of the second iteration of Permafrost_cci Phase 2 are listed in the next pages, in the following order:

- RoGI area 6-2 in Goms–Binntal, Switzerland
- RoGI area 11-2 in Northern Venosta, Italy
- RoGI area 17-1 in Pirin and Rila Mountains, Bulgaria
- RoGI area 18-1 in Manaslu, Nepal
- RoGI area 19-1 in Sajama, Bolivia–Chile
- RoGI area 20-1 in Tsengel Khairkhan, Mongolia
- RoGI area 21-1 in Himachal Pradesh, India
- RoGI area 22-1 in Thana, Bhutan

Status of RoGI area 6-2 in Goms–Binntal, Switzerland

RoGI PI: Reynald Delaloye, University of Fribourg, Switzerland

Contributors: Thibaut Duvanel, University of Lausanne; Christophe Lambiel, University of Lausanne; Marc O'Callaghan, University of Lausanne; Paula Johns, University of Fribourg; Matthias Lichtenegger, WSL SLF Davos; Cécile Pellet, University of Fribourg (all Switzerland).

Introduction

The Goms-Binntal study area is located in easternmost part of the Valais Alps in Switzerland and also comprises a part of the southeasternmost Bernese Alps. The area covers about 400 km^2 with elevation ranging from 1300 to more than 3500 m a.s.l. for the highest peaks.

The RoGI process started in February 2024 and involved 7 operators. A previous multi-operator inventory was conducted by people from the University of Fribourg in two sub-sections of the Goms-Binntal area in 2022 and serves as training tool within the framework of RGIK.

The present extended Goms-Binntal RoGI has been established by applying the procedure operated within the RoDynAlpS project (Rock glacier Dynamics in the Swiss Alps) for conducting the whole inventory of rock glacier in Switzerland. The procedure has followed the recommendations of the RGIK guidelines. A first screening of the whole area has been performed by various operators (in different sub-areas) in order to identify rock glacier units (RGUs) but also landforms, which could be considered as potential rock glaciers, but whose attribution is uncertain without further in-depth investigation. The primary RGUs marking has been checked, confirmed or altered, by a single expertized operator. In parallel, MAs mapping and characterization has mostly been performed based on a set of Sentinel-1 data dating from 2020 to 2022. This information, as well as a 0.5 m Lidar DEM recently produced by Swisstopo and interpretation of orthoimages from different times (made available every 3 years by Swisstopo for the recent period) have formed the basis for both outlining the confirmed RGUs and characterizing them. These last steps have also been checked by a further expertized operator.

Current work status

The inventory is completed. Some minor adjustments might still occur during final review of the product.

Key findings

In total 178 certain rock glacier units have been identified, while 54 landforms have been set as uncertain. Based on InSAR, 140 moving areas have been outlined and categorized with velocity classes ranging from 1–3 cm/a to > 100 cm/a. Most RGUs are talus-connected, whereas some are connected to glacier forefields.

Identified challenges

Many RGUs are small and difficult to either be identified or considered as a rock glacier. Some landforms are also difficult to distinguish from morainic bastions, namely the terminal morainic construction of small glaciers which developed during the cold phases of the Holocene and recently during the Little Ice Age, and have nowadays retreated, when not fully disappeared. The same challenge occurs for relict rock glaciers connected to Late glacial glacier forefields. Relict landforms are also often difficult to identify without the use of the high-resolution Lidar DEM.

Next steps

Publication is planned as part of the RoDynAlpS project. The final version will be made available for CCI Permafrost within the next months after last check.

Example of results

A bit less than half of the 178 inventoried RGUs in the Goms-Binntal area are active or active uncertain, a quarter are transitional, and a last third are relict or relict uncertain (**Figure 1A**). It has been possible to characterize 98 among the transitional to active landforms with a kinematic attribute. A large majority of them are moving slowly (dm/a) to very slowly (cm/a). 20 are moving several dm/a, whereas only 3 RGUs are moving in the order of the m/a or faster (**Figure 1B**).

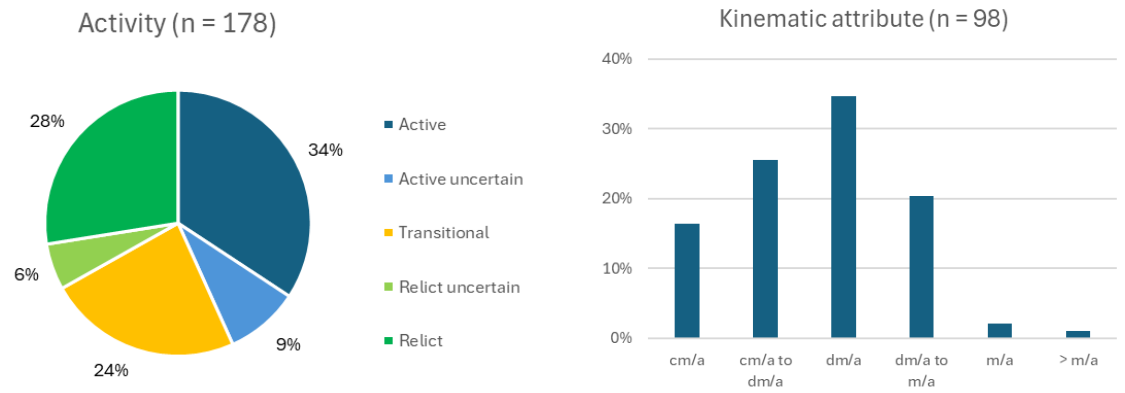

Figure 1. *A (left) – Relative frequency distribution of rock glaciers units according to their activity state. B (right) – Relative distribution of rock glaciers with kinematic attribute.*

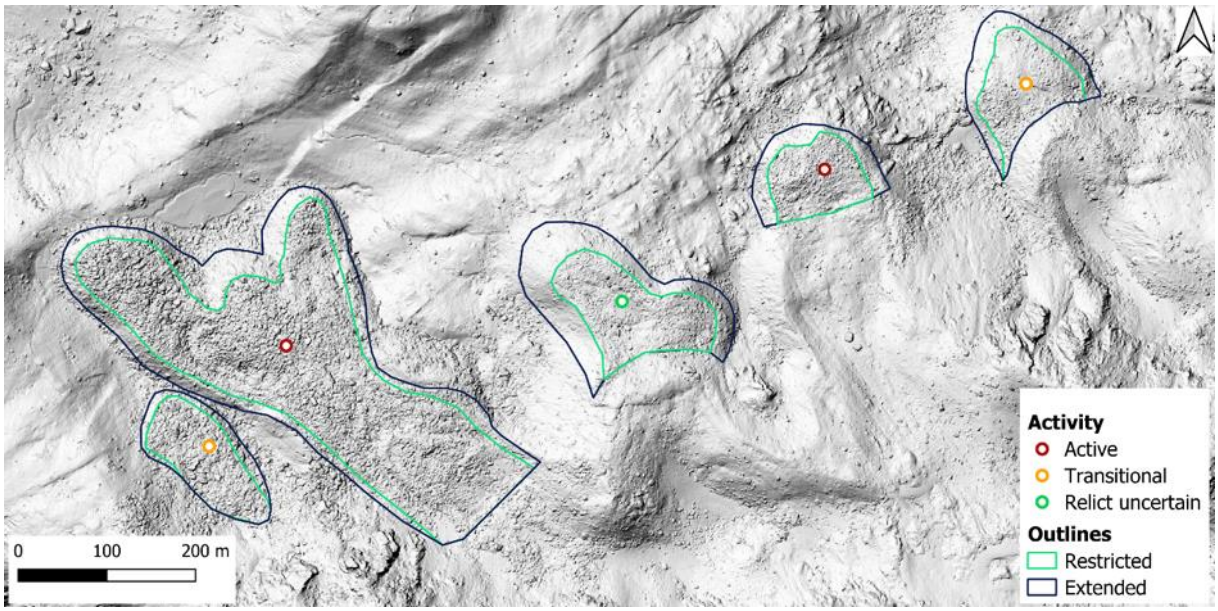

Figure 2. *Examples of Primary Markers (PM), with coloured Activity, and Geomorphological Outlines (GO). Except the westernmost unit, which is talus-connected, all RGUs are glacier forefield-connected. They expose various activity states. Both active RGUs develop in the continuation of areas glacierized during the Little Ice Age (LIA). Their uppermost boundary has been drawn in accordance with the uppermost signs of ground motion. The two other RGUs were partly overridden by the LIA glacier advance. Background: 0.5 m Lidar DEM by Swisstopo.*

Status of RoGI area 11-2 in Northern Venosta, Italy

RoGI PI: Brardinoni, Francesco, UniBo (University of Bologna)

Contributors: Brardinoni, Francesco, UniBo; Bertone, Aldo, UniBo; Echelard, Thomas, UniBo.

Introduction

The Northern Venosta study area is located in western South Tyrol, Italy. The area covers 770 km^2 with elevation ranging from 620 (Parcines/Partschins) to 3738 m a.s.l (Palla Bianca/Weisskugel). Lithology is metamorphic, dominated by paragneiss, micaschist and lesser orthogneiss.

The inventory relies on a regional geomorphological inventory completed in 2019 across South Tyrol (Scotti et al., 2024). In this inventory, each RGU polygon encloses the extended footprint; it contains a number of morphological attributes but RGUs are not grouped into RGS, the upslope connection is not characterized and "uncertain rock glaciers" are not envisaged. To fit the RGIK basic format, a PM layer was created on purpose. The kinematic characterization started in 01/2022 and consisted of two phases. In the first phase, the central portion of the study area (green polygon, **Figure 1**) was covered by two operators (one expert and a less experienced one), who cross-checked their respective products. Subsequently, a third (expert) operator worked independently on the remaining portions (blue polygons, **Figure 1**). The delineation and kinematic characterization of MAs have been conducted on S1 interferograms (2017–2020) and subsequently replicated on CSK interferograms (2016–2020). Thus, each RGU has two distinct kinematic attributes, one associated with S1, and one associated with CSK.

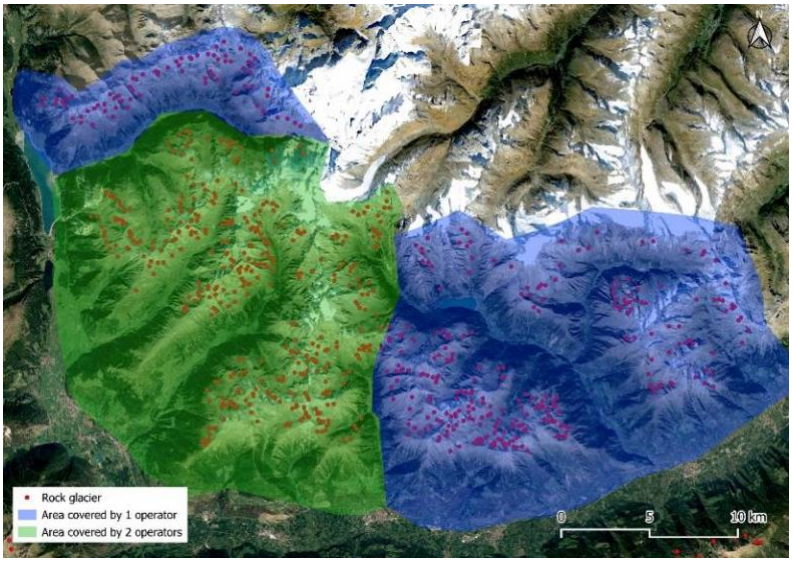

Figure 1. *Map showing the portions of Northern Venosta in which the InSAR-based kinematic characterization was conducted respectively by two operators (green polygon) and by one operator (blue polygons). Primary markers associated with single RGUs are represented by red dots.*

Current work status

The morphological inventory is regarded as completed and the implementation of additional attributes is not envisaged. At the beginning of Phase 2, the PI and Dr. Strozzi agreed that the focus for Northern Venosta area was to conduct RGU kinematic characterization using S1 and CSK acquisitions independently. The relevant PM and MA geopackages have been completed. While the respective MA attribute tables are in order, the PM counterparts are not entirely consistent with each other and some homogenization in terms of field labelling is still needed for S1.

The geopackages enclosed to this document are: (1) [ma_north_venosta_csk.gpkg]: moving areas based on CSK interferograms from 2016 to 2020; (2) [ma_north_venosta_S1.gpkg]: moving areas based on S1 interferograms from 2017 to 2020; (3) [pm_north_venosta_csk.gpkg]: primary markers of rock

glaciers including kinematic attributes and activity class based on CSK moving areas; (4) [pm_north_venosta_S1.gpkg]: primary markers of rock glaciers including kinematic attributes and activity class based on S1 moving areas; and (5) [outline_north_venosta.gpkg]: Outline of each PM.

Key findings

In total, 708 rock glacier units have been characterized kinematically. Based on InSAR, 2911 moving areas have been outlined and categorised with velocity classes ranging from <1 cm/y to >100 cm/yr. Among these, 1942 and 696 were delineated on CSK and S1 interferograms respectively. Although, the relevant CSK and S1 frequency distributions may look similar (**Figure 2**), a systematic analysis for evaluating the (possible) advantages of integrating the two constellations is missing.

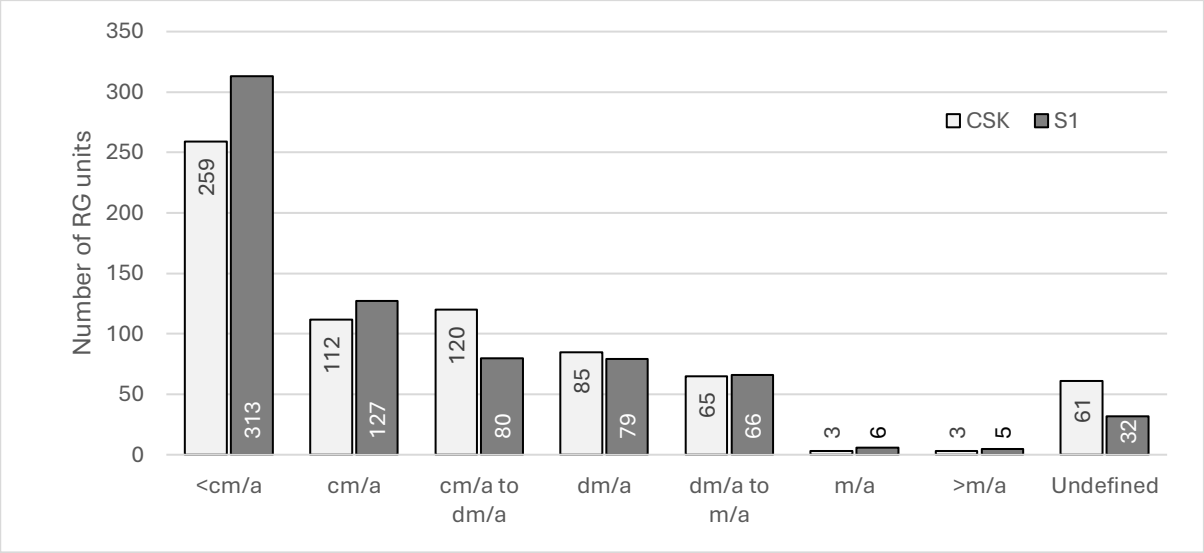

Figure 2. *Rock glacier count across kinematic classes: CSK vs S1.*

Identified challenges

No specific challenges, besides the well-known issue with north and south facing units. Mapping and interpretation of MAs conducted on CSK interferograms proved being much more time consuming than in S1. However, this extra time is rewarded with MAs delineated at much higher resolution.

Next steps

The geopackages will be finalized by 19.05.2025. Subsequently, we expect to be able to finalize a systematic analysis on the differences (and redundancies) that characterize S1 and CSK kinematic classification (e.g., confusion matrix across kinematic classes) by the end of July. This analysis will form the basis for pursuing a publication, the timeline of which, however, will depend on the work plan foreseen by the CCI project extension in 2025–2026.

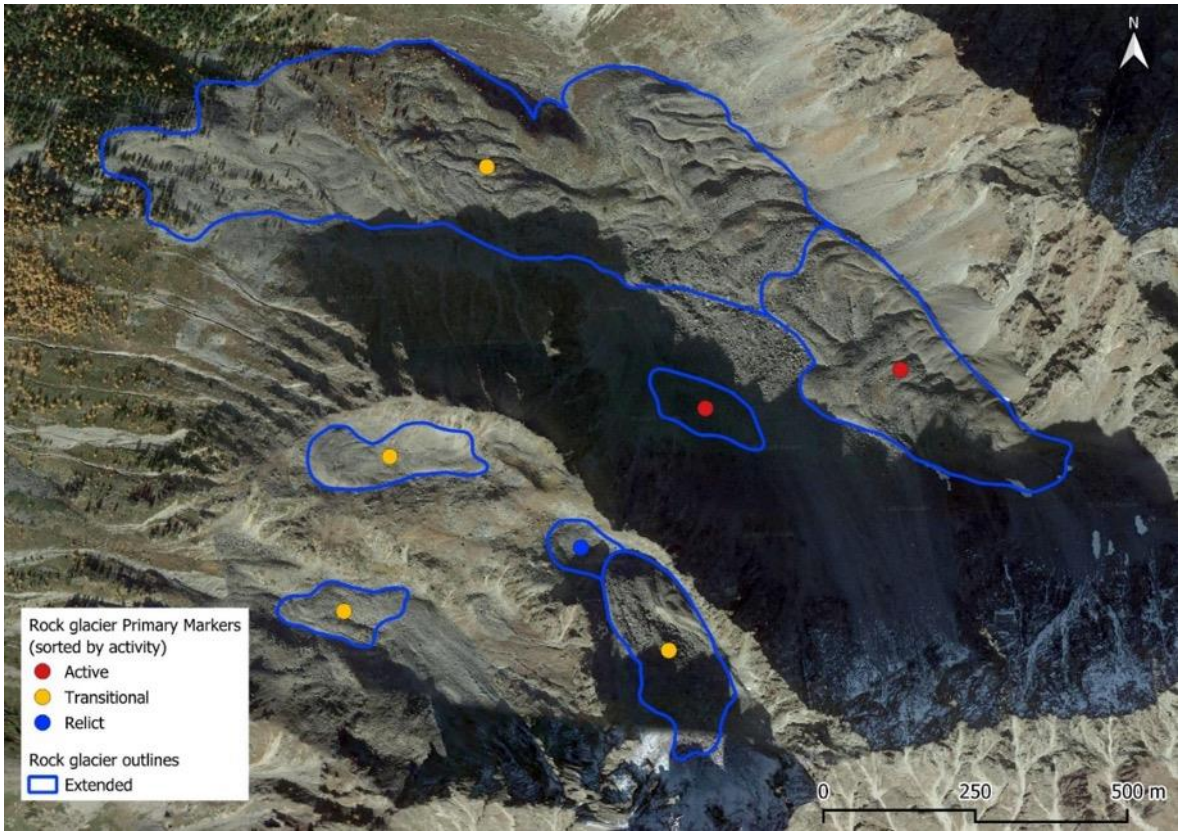

Figure 3: *Northern Vensota, Italy. Examples of Primary Markers (PM) and Geomorphological Outlines (GO).*

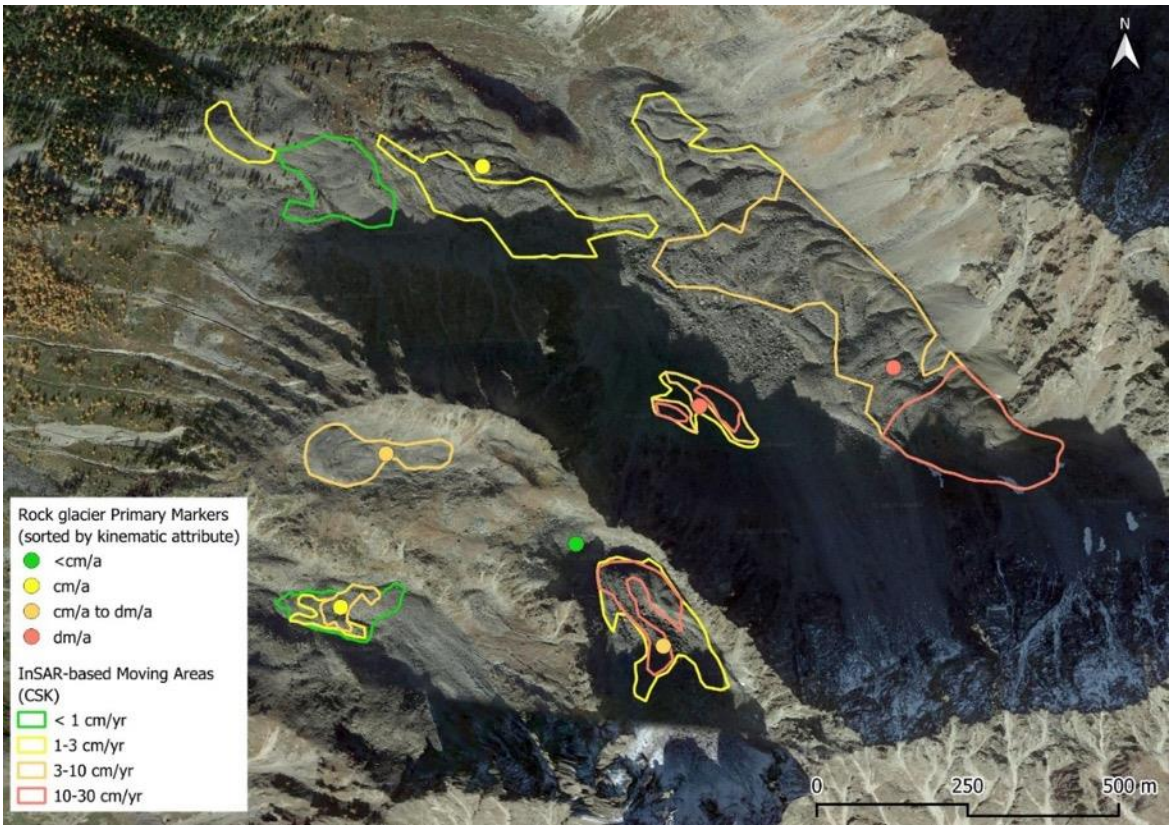

Figure 4: *Northern Vensota, Italy. Examples of Kinematic Attributes (KA) and Moving Areas (MA).*

Status of RoGI area 17-1 in Pirin and Rila Mountains, Bulgaria

RoGI PI: Flavius Sirbu, West University of Timișoara

Contributors: Alexandru Onaca, West University of Timișoara; Adrian Ardelean, National Museum of Bana, Petru Urdea, West University of Timișoara, Emil Gachev Bulgarian Academy of Science, Mirela Vasile, University of Bucharest

Introduction

The Pirin Mountains study area is located in Rhodope Massif in south-western Bulgaria. The area covers 700 km^2 with elevation ranging from 1100 and 2914 m a.s.l.

The RoGI process started in April 2024 and involved 6 operators. A multi-operator procedure is applied, following RGIK recommendations.

The work on RoGI production in Bulgaria is related to the ChronoCaRP (chronocarp.unibuc.ro) project. ChronoCaRP aims to date various glacial and periglacial features, including rock glaciers, for a "better understanding of past response of geological and environmental systems to climate oscillations in SE Europe, with main emphasis on global warming after the Last Glacial Maximum (LGM) in high mountain environment". Having a reliable RoGI is important in selecting sampling sites and in data interpretation.

Current work status

The work on RoGI in Pirin Mountains is finished. Similar RoGI process in Rila in still ongoing. We finished the first step (primary markers). The plan is to complete the inventory by the end of the summer 2025.

Key findings

For Pirin, 73 certain rock glacier units have been identified, while 5 landforms have set as uncertain. Based on InSAR, 62 moving areas have been outlined and categorised with velocity classes ranging from <1 cm yr^{-1} to 3-10 cm yr^{-1}. Both extended and restricted outlines have been drawn for the certain rock glaciers. One key finding could be the use of PSI mean velocity maps instead of single interferograms for mapping MAs.

For Rila, 38 certain rock glacier units have been identified, while 9 landforms have set as uncertain.

Identified challenges

The biggest challenge is to identify, map and classify moving area. This is mostly to the small velocity and steep terrain. Using PSI, instead of InSAR, helps in identifying slow moving areas (< 1 cm/year) but also makes it harder to map the boundaries of the MA.

Another challenge is to map old relict rock glaciers that are completely covered by vegetation. A high-resolution LiDAR-derived DEM would help in this regard.

Next steps

For Pirin, we intend to publish a multi-method paper focusing on rock glaciers that will combine thermal and kinematic data with the aim of better understanding rock glacier evolution and various periglacial processes (i.e. permafrost, rock glacier creep).

For Rila, we intend to continue the in-depth study of two rock glaciers, in the upper part of Bistrita valley (north of Musala peak). This will focus on continues thermal monitoring, differential GNSS

monitoring and periodical geophysical surveys. We have no immediate plans for any research paper, but some data might be use in support of other studies (e.g. in the whole region, on SE European permafrost in general).

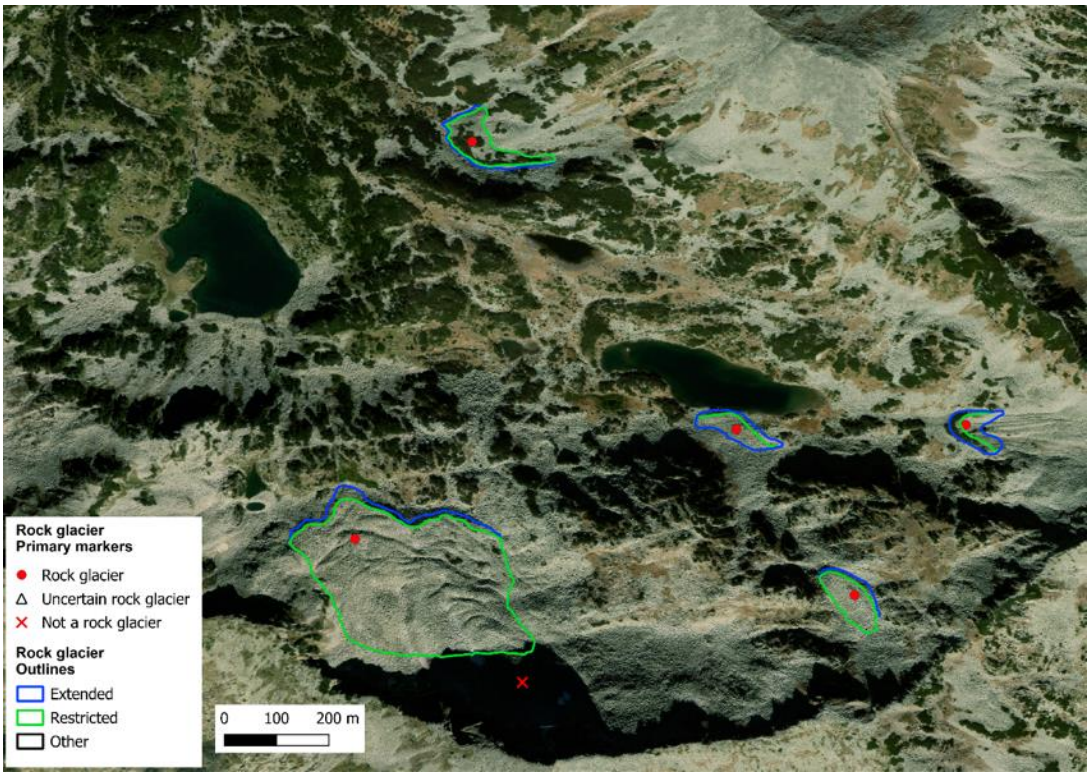

Figure 1: *Pirin, Bulgaria. Examples of Primary Markers (PM) and Geomorphological Outlines (GO).*

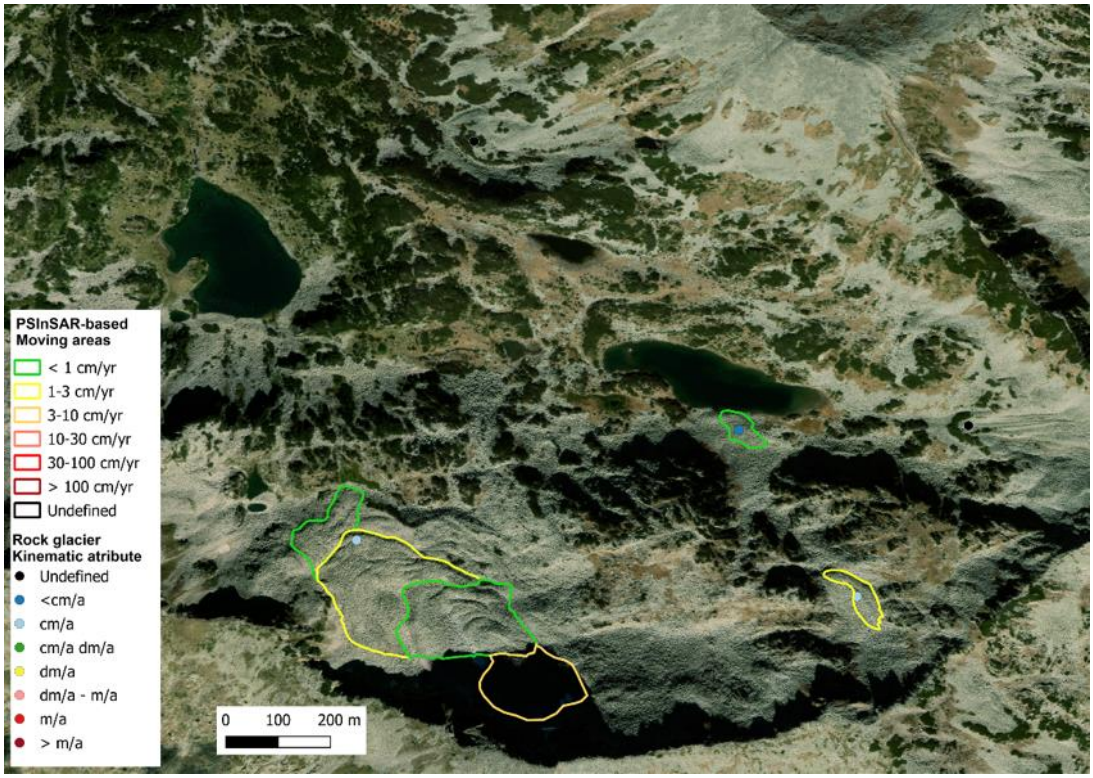

Figure 2: *Pirin, Bulgaria. Examples of Kinematic Attributes (KA) and Moving Areas (MA).*

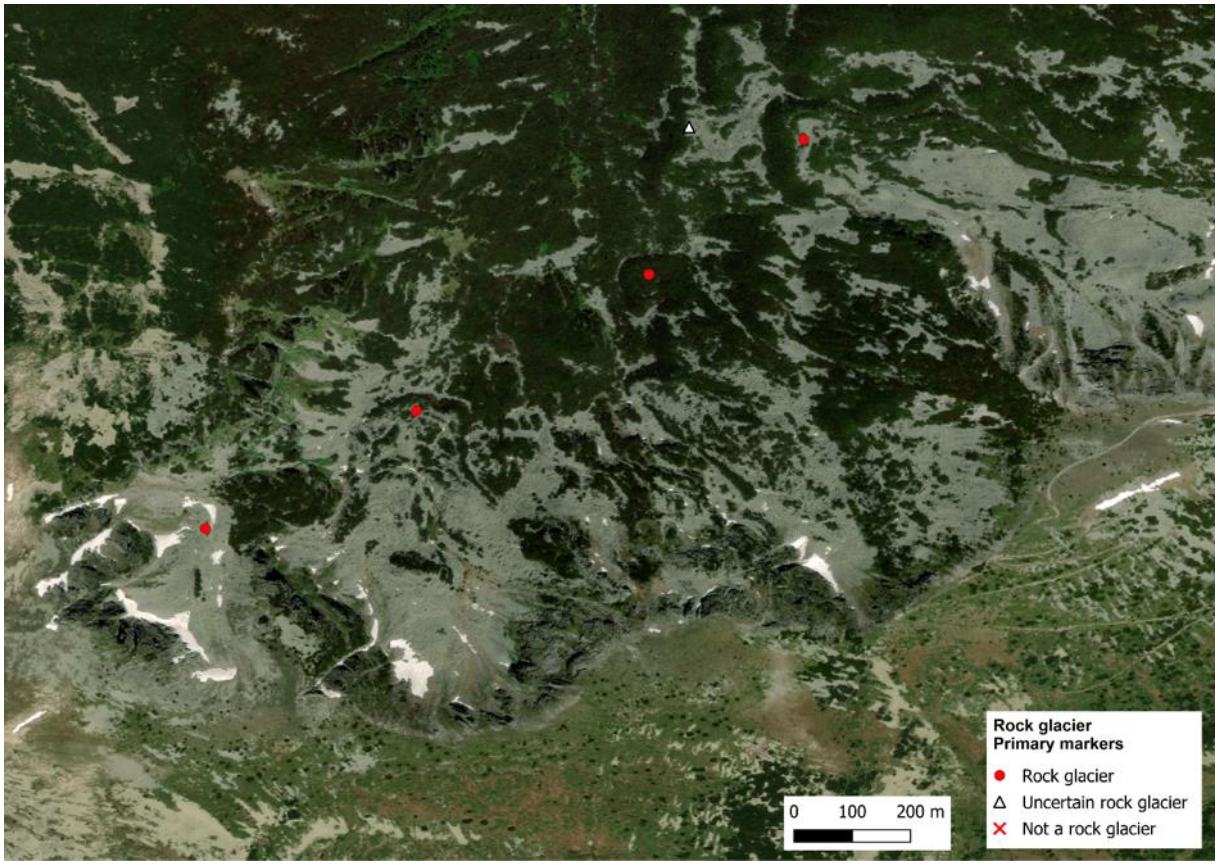

Figure 3: *Rila, Bulgaria. Examples of Primary Markers (PM) and Geomorphological Outlines (GO).*

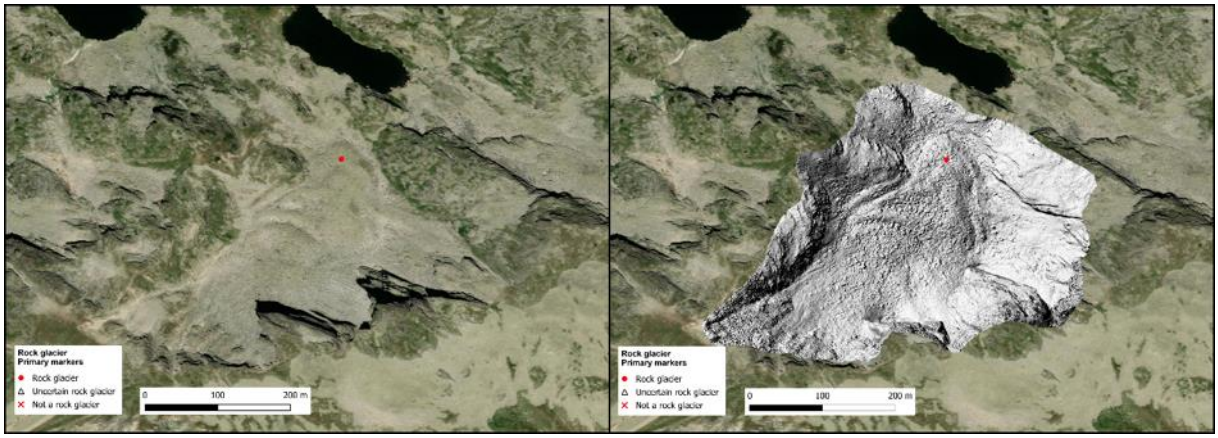

Figure 4: *Rila, Bulgaria. Detailed view of an identified rock glacier.*

Status of RoGI area 18-1 in Manaslu, Nepal

RoGI PI: Adina Racoviteanu, Univ. Grenoble Alpes / IGE, France; Lin Liu, Chinese University of Hong Kong

Contributors: Mengze Li, Zhangyu Sun – Chinese University of Hong Kong; Darren Jones (previously Exeter University, UK) – for use of his dataset

Introduction

The Manaslu study area is located in the central Himalaya range in Nepal (**Figure 1**). The initial region covered ~1970 km^2 with elevation ranging from ~858 m to 8054 m a.s.l. Given the large size of the domain, we chose a subset of the AOI, with an area of 188,5 km^2 (**Figure 1**, inset) which contained a high density of rock glaciers based on previous estimates (Harrison et al., 2024). For this smaller area, elevations range from 3710 to 6462 m a.s.l. This area contains a multitude of complex landforms (debris-covered glaciers-ice debris landforms).

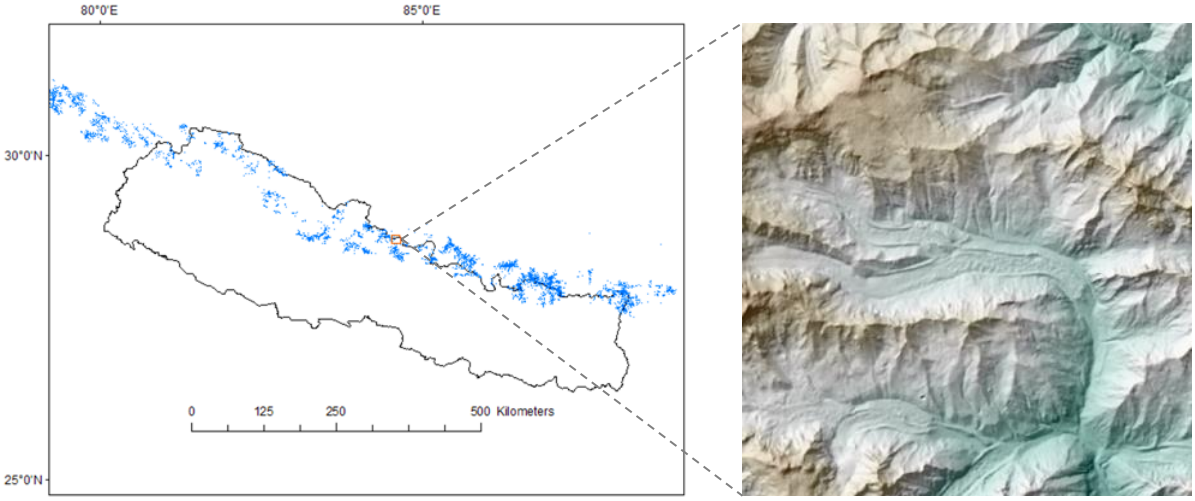

Figure 1. *Location of the study area and shaded relief map*

The RoGI processes started with defining the study area in September 2024 and the analysis started in January 2025, and involved a total of 5 operators, of which one is virtual as we just used previously published data (point locations of rock glaciers), available here: https://zenodo.org/records/11237094.

We applied a multi-operator procedure: 2 operators from CUHK; each pinned the RG individually; and the dataset from Darren Jones was used as a surrogate operator, providing a third dataset. Also, we split the PI tasks as follows: A Racoviteanu supervised the RG primary markers and Lin Liu supervised the moving areas delineation. In January 2025, we had a cross-check among operators in Hong Kong to discuss uncertain cases. Based on this, all 3 operators were taken into account by PI A.R. who produced a first consensus; this was once again reviewed by second PI L.L. to achieve a final consensus.

Primary markers were slightly adjusted based on all operators and PI expertise. When uncertain RGs were marked as such, these were discussed among the two PI before finalizing.

The work was conducted in line with the PROCORE France-Hong Kong project, which funded A.R.'s visit to Hong Kong in Jan 2025.

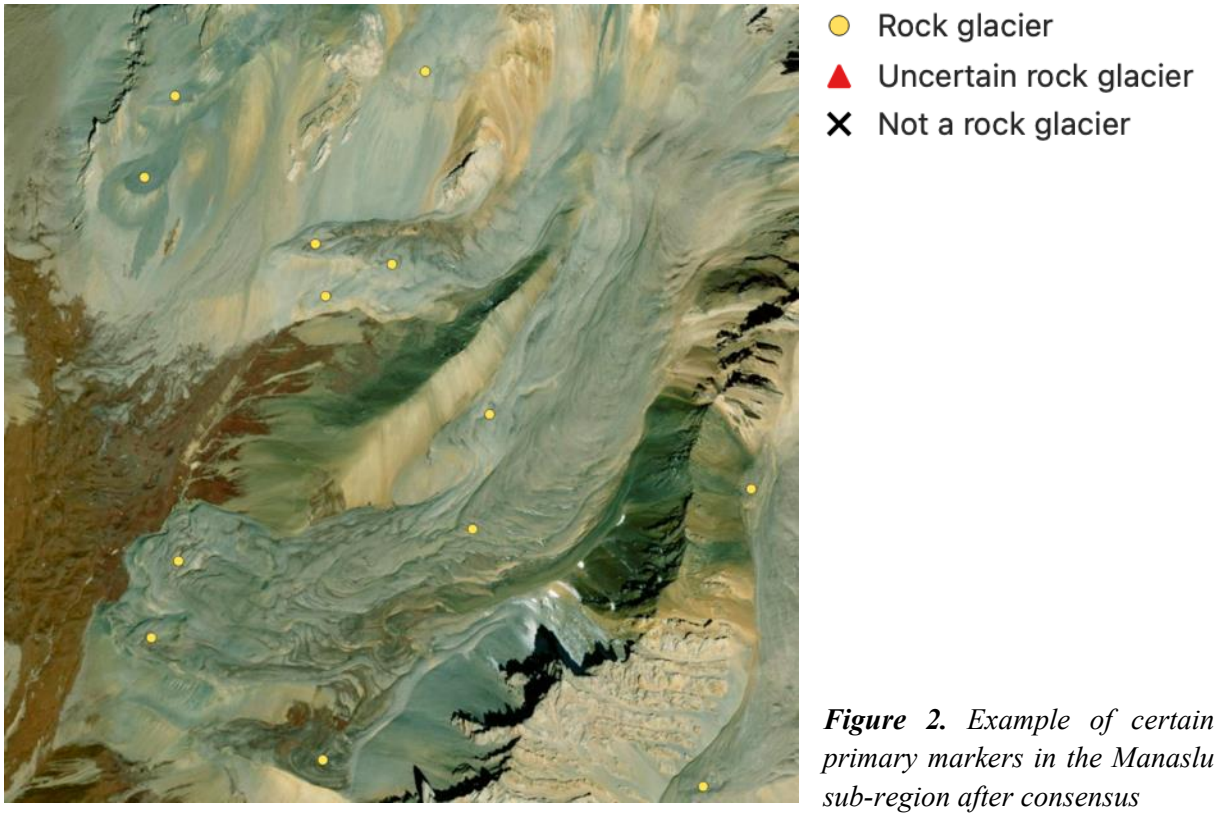

Figure 2. *Example of certain primary markers in the Manaslu sub-region after consensus*

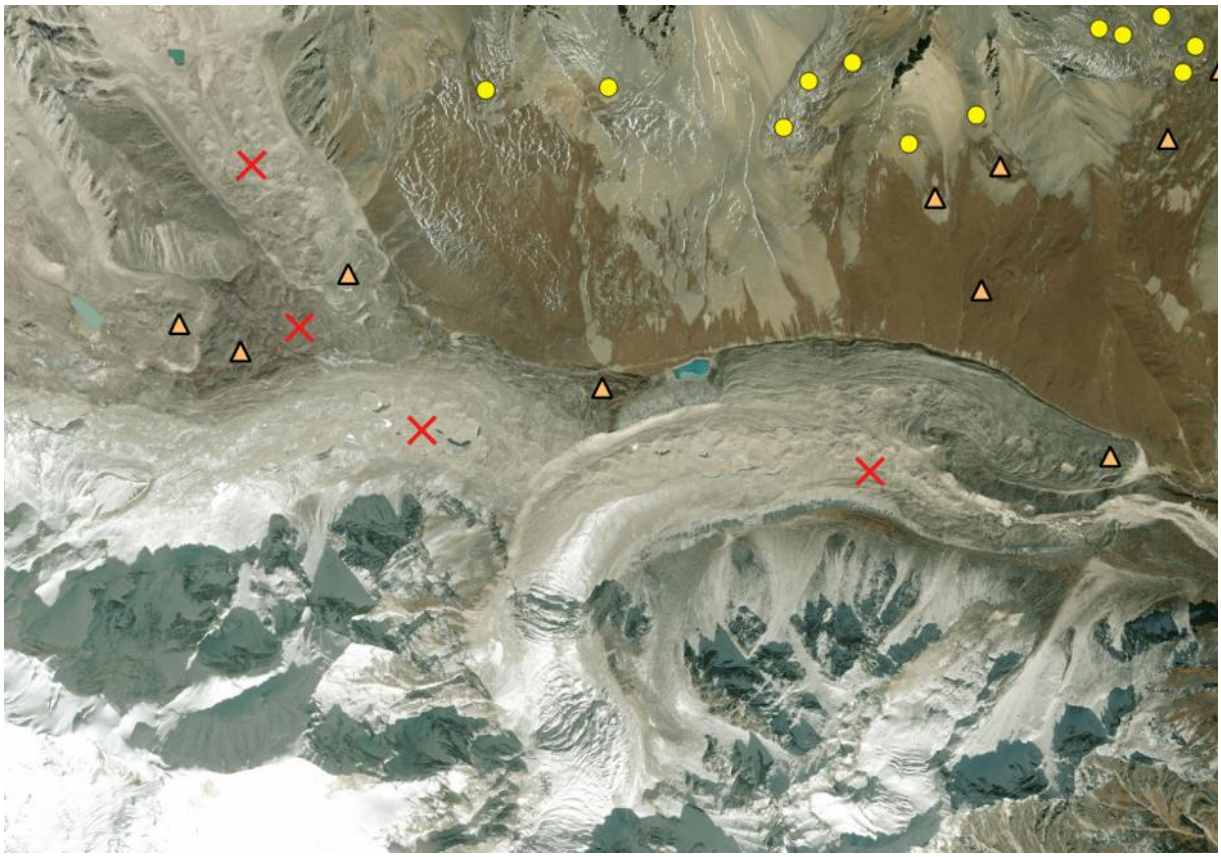

Figure 3. *Example of complex landforms with uncertain RG and non-RG (debris-covered glaciers).*

Current work status

As of May 2025, we have completed the first step, Primary Markers. Step two (Moving Areas) is in progress and partly finished (1 analyst). We have gathered the InSAR data needed for the delineation, including interferograms with temporal baselines of 12, 24, 36, 48, 60 days and 1 year in both ascending and descending orbits generated based on Sentinel-1 data using ASF HyP3 service.

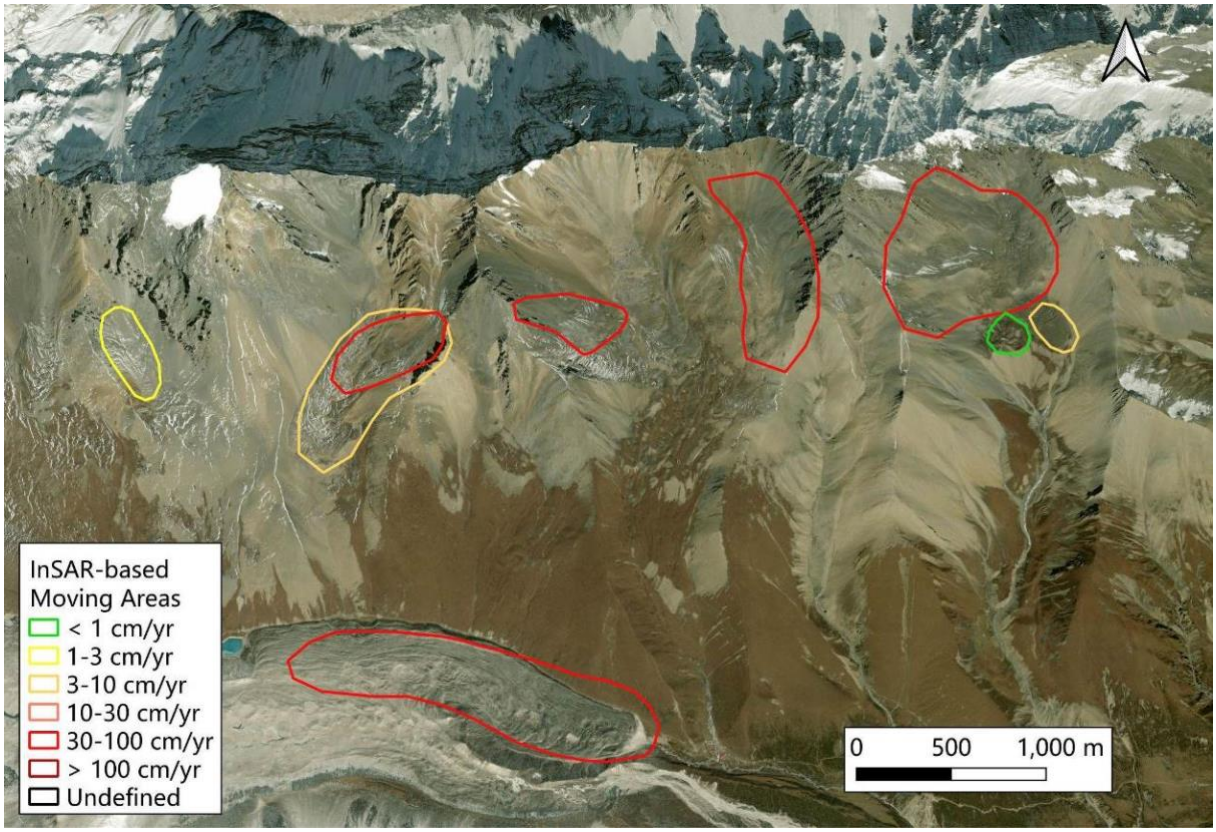

Figure 4. *Example of Moving Areas in the Manaslu area, Nepal.*

Key findings

In total, 111 certain rock glacier units have been identified, while 19 landforms have been set as uncertain. A total of 7 landforms were marked as "not a rock glacier" (red cross symbol) because they are complex landforms, with debris-covered glaciers with a rock glacier-like terminus, or glacier moraine forefield (see **Figure 3**). Based on InSAR, 36 moving areas have been outlined and categorised with velocity classes ranging from < 1 cm/yr to > 100 cm/yr (see **Figure 4**).

Identified challenges

No significant issues applying the guideline; one challenge posed by the ice-debris terminus of some debris-covered glaciers (not a fully developed rock glacier), making it tricky to label.

Next steps

We aim to finalise the moving areas (2 analysts minimum) in order to add the kinematics. Timeline envisioned: June–July 2025 to finish the datasets (during Lin Liu's visit in Grenoble). We then plan to work on a paper this summer.

Status of RoGI area 19-1 in Sajama, Bolivia–Chile

RoGI PI: Diego CUSICANQUI, Institut des Sciences de la Terre (ISTerre), Univ. Grenoble Alpes, Grenoble, France.

Contributors: Alvaro SORUCO, Instituto de Geologia y Medio Ambiente (IGEMA), Univ. Mayor San Andres, Bolivia; Marco CONDORI, Instituto de Geologia y Medio Ambiente (IGEMA), Univ. Mayor San Andres, Bolivia.

Introduction

The Sajama volcano study area is located in occidental Cordillera in Bolivia. The area covers 383 km^2 with elevation ranging from 4200 and 6542 m a.s.l.

This stratovolcano is part of the Andean volcanic belt, situated in the Western Cordillera of the Andes. Its geological origin is linked to the subduction of the Nazca Plate beneath the South American Plate, which has caused significant volcanic activity in the region over time (de Silva & Francis, 1991).

Sajama is an inactive volcano, with eruptive activity dated to the Pleistocene. Its morphology is composed of dacitic and andesitic lava flows, indicating an explosive eruptive behaviour in the past. The surrounding region features geothermal manifestations, such as hot springs and geysers, suggesting the presence of a still-hot magmatic system at depth. Its elevation places it among the snow-covered Andean peaks, with the summit permanently covered in ice and snow.

The RoGI processes started in January 2025 and involved 3 operators. We applied a multi-operator procedure. The cross-check operators were made through several videoconferences between the PI and the operators. An existing inventory exists in the region (Rangercroft et al., 2015). However, we do not take into account the existing inventory.

The results are part of a bachelor thesis (M. Condori) at Univ. San Andres, Bolivia.

Current work status

The inventory is not yet complete. However, it is well advanced. A brief explanation follows:

- Primary marker identification is complete.
- The outlining of moving areas is 70% complete. Verification by operators is still pending.
- The outlining of rock glacier outlines is 90% complete. Some complex areas are still lacking.

The attached files contain the first consensus among all operators regarding the primary markers, outlines and moving areas.

Key findings

A total of 93 rock glacier units have been identified, while 43 landforms have been classified as uncertain. Based on a geomorphological inspection, several of these landforms appear to be solifluction lobes. This should be confirmed.

Based on InSAR analysis, 63 moving areas have been outlined and categorised into velocity classes ranging from 1–3 cm/yr to >100 cm/yr. Extended and restricted outlines have been drawn for the certain rock glaciers. Some complex landforms still require full interpretation.

Overall, the Sajama volcano area is 80% complete. However, the outlining of moving areas and rock glacier units is 70% and 90% complete, respectively.

From our current results, talus-connected rock glaciers predominate in the region. As it is a volcanic region, the current dataset is well distributed among all orientations. However, a slight preference for the south-west, south and south-east orientations can be seen.

Identified challenges

From a geomorphological point of view, this region is complicated. First, the context of an extinct volcano means that several lava flows can be confused with rock glaciers. Geomorphological aspects also present challenges, with at least three study sites being very complex to interpret due to the presence of poly-connected rock glaciers and debris-covered glaciers. The high erosion rate in the region, together with the geology, makes interpretation more difficult. In both cases, InSAR enables the rock glacier section to be distinguished more clearly.

From a kinematic point of view, some small landforms lack kinematic interpretation due to the resolution of the interferograms.

No issues with the RGIK guidelines or the provided templates were identified.

Next steps

Complete the Sajama Volcano region by the end of spring. The second stage is to extend the work to cover the entire S1 InSAR area, across the Chilean border, in collaboration with Chilean colleagues. A joint publication is planned for mid-2026.

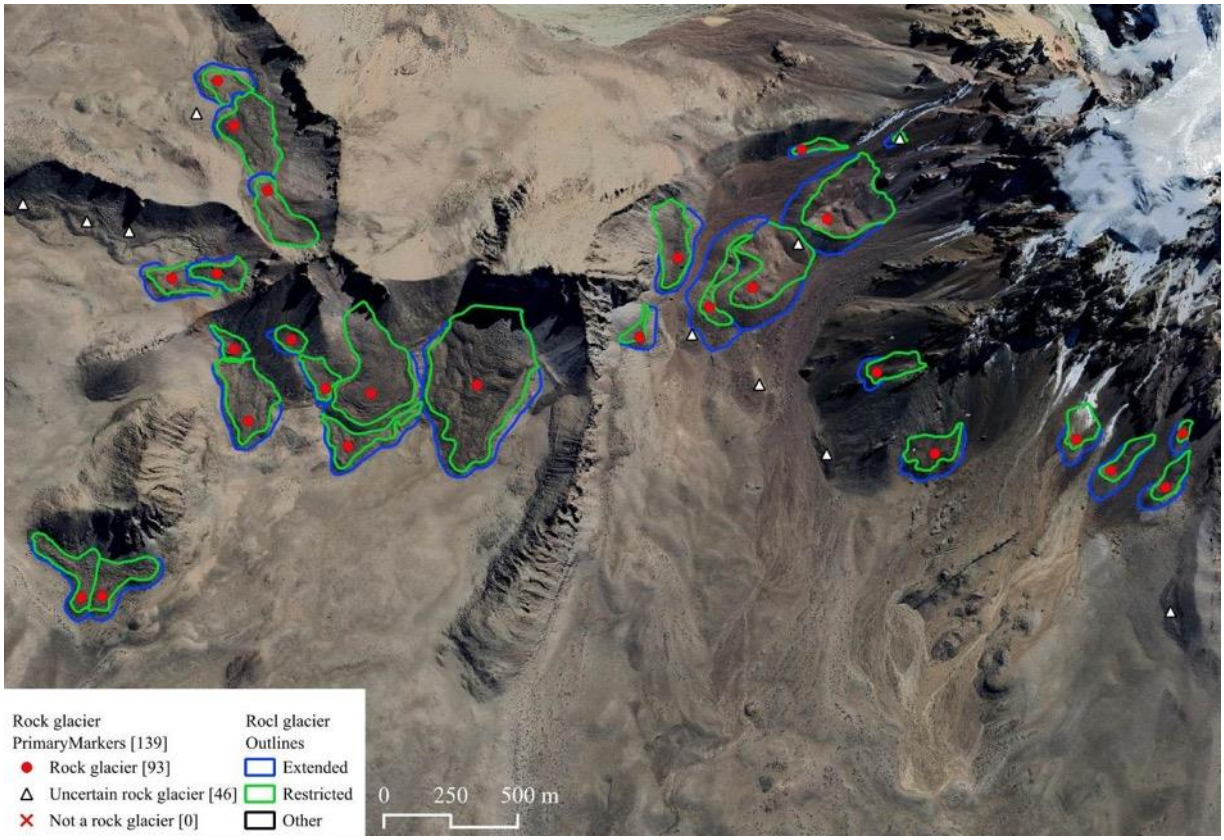

Figure 1. *Sajama, Bolivia. Example of Primary Markers (PM) and Geomorphological Outlines (GO).*

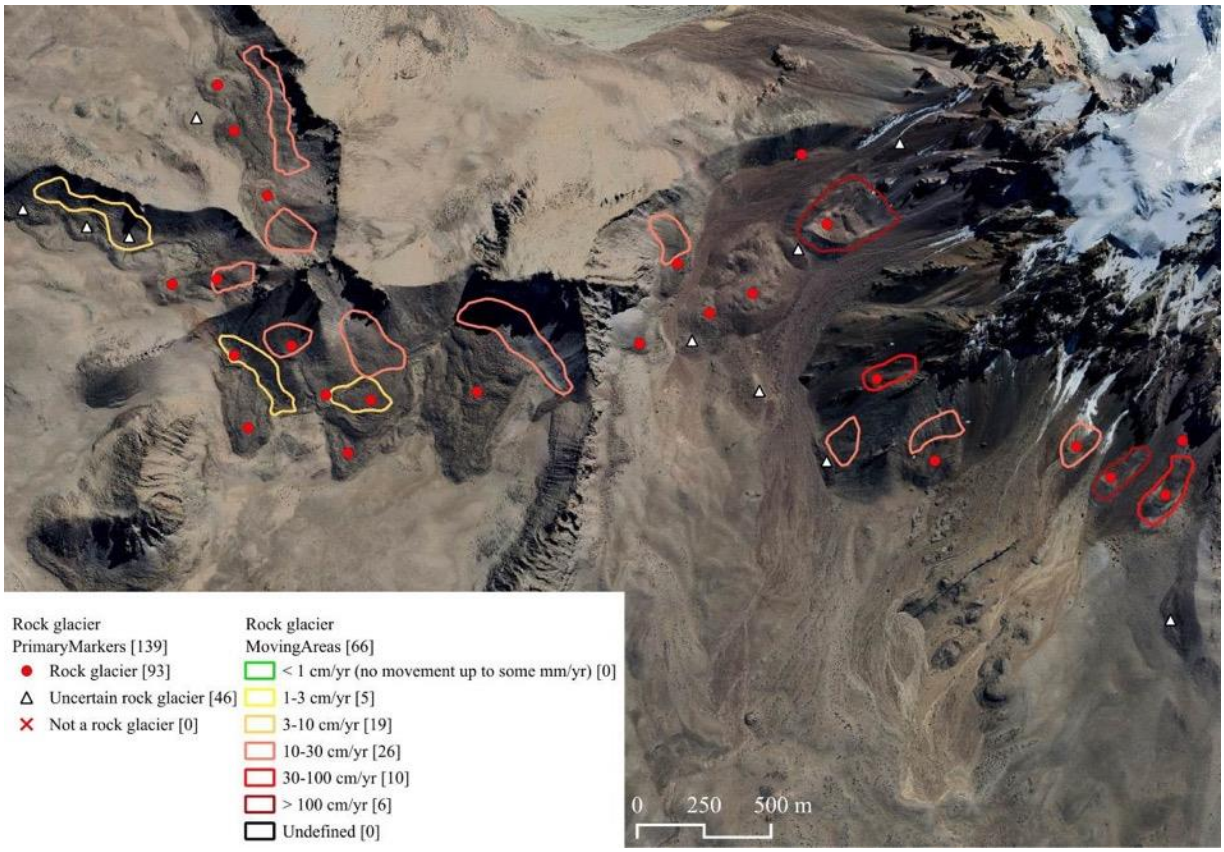

Figure 2. *Sajama, Bolivia. Example of Kinematic Attributes (KA) and Moving Areas (MA).*

Status of RoGI area 20-1 in Tsengel Khairkhan, Mongolia

RoGI PI: Avirmed Dashtseren, Institute of Geography and Geoecology, Mongolian Academy of Sciences

Contributors: Tsogoo Bilguun**,** Institute of Geography and Geoecology of Mongolian Academy of Sciences; Line Rouyet, University of Fribourg; Reynald Delaloye, University of Fribourg; Alina Milceva, University of Fribourg; Sebastian Westermann, University of Oslo, Norway, Thomas Echelard, University of Fribourg, Tazio Strozzi, GAMMA Remote Sensing AG.

Introduction

The Tsengel Khairkhan study area is located in the Altai range, in western Mongolia. The area covers approximately 208 km^2, with elevations ranging from approximately 2,610 and 3,943 m a.s.l. The Tsengel Khairkhan mountain is covered by a small ice cap ("flat top glacier") in the north and valley glaciers in the eastern and southern parts (total area: 8.2 km^2). This inventory contributes to the broader effort of documenting periglacial landforms in the Mongolian Altai and supports a better understanding of mountain permafrost dynamics in the region. This project is the first study mapping rock glaciers in Mongolia.

The first meeting between Mongolian, Swiss and Norwegian partners was in August 2024. The RoGI process started in the Fall 2024 and involved one operator from Mongolia (A. Dashtseren) and three operators from UNIFR (L. Rouyet, R. Delaloye and A. Milceva). We followed a standardized multi-operation RoGI procedure in line with the RGIK guidelines. Based on optical images and InSAR data, all operators generated their PM/MA/GO results, and the team had several meetings on discuss and adjust the results for the final version. Team meetings involved the four operators, as well as the other contributors listed above for discussions on the data package, the workplan and the interpretation.

Current work status

The work in the study area is now completed. All four operators finalized their tasks, and the individual outputs were reviewed, discussed and consolidated through joint sessions to reach a common interpretation and consensus-based decisions.

The final dataset has been compiled according to the standard GeoPackage format. It includes Primary Markers (PM), which locate and characterize the identified Rock Glacier Units (RGU); Moving Areas (MA), which delineate zones of surface displacement associated with rock glacier creep based on spaceborne Interferometric Synthetic Aperture Radar (InSAR); and Geomorphological Outlines (GO), which show both restricted and extended RGU boundaries.

Key findings

In total, 63 certain rock glacier units have been identified, while 111 landforms have been set as uncertain. Based on InSAR, 91 moving areas have been outlined and categorised with velocity classes ranging from 0.01 to 0.3 m/yr. Extended and restricted outlines have been drawn for the certain rock glaciers.

The activity classification for certain rock glaciers was assigned based on InSAR kinematics and geomorphological indicators. In total, 55 RGU were classified as transitional. One unit was categorized as relict uncertain. Four faster-moving RGU (dm/yr and over) were classified as active. Three RGU were classified as active uncertain. In term of upslope connection, most rock glaciers (57 RGU) were categorized as talus-connected. Two RGU were identified as debris-mantled slope-connected, two are

glacier forefield-connected, and two remained unknown. The landforms are evenly divided between mono-unit and multi-unit systems, with simple morphologies (40 RGU) being more frequent than complex ones (23 RGU). The majority of rock glaciers are N-facing, while S-facing landforms are less common. No destabilized rock glacier was observed in the study area.

Identified challenges

Many (possible) rock glaciers were identified during the first phase, which made the work more extensive than initially expected. For pragmatic reasons, we decided to keep several landforms as uncertain. Several landforms in this category are likely rock glaciers but assessed to be too complex to be fully mapped and characterized at this stage.

The variable quality of online imagery sources is another challenge. The basemaps (Bing Maps, Google, ESRI Satellite) were updated during the analysis period to imagery with substantial snow cover, which complicated the delineation of rock glacier boundaries in the second stage.

Next steps

The team plans to further analysis the results and work on a common publication. The results are also expected to be presented at the next ACOP in Mongolia (June 2026).

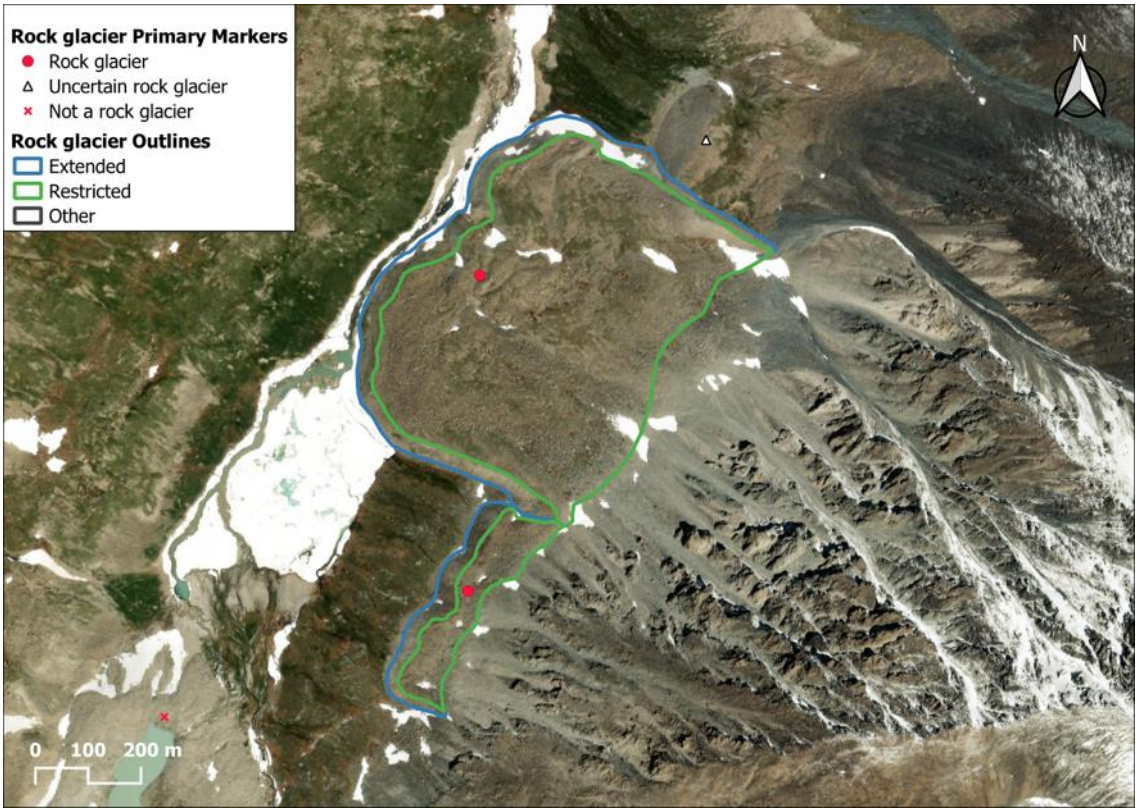

Figure 1. *Tsengel Khairkhan, Mongolia. First example of Primary Markers (PM) and Geomorphological Outlines (GO).*

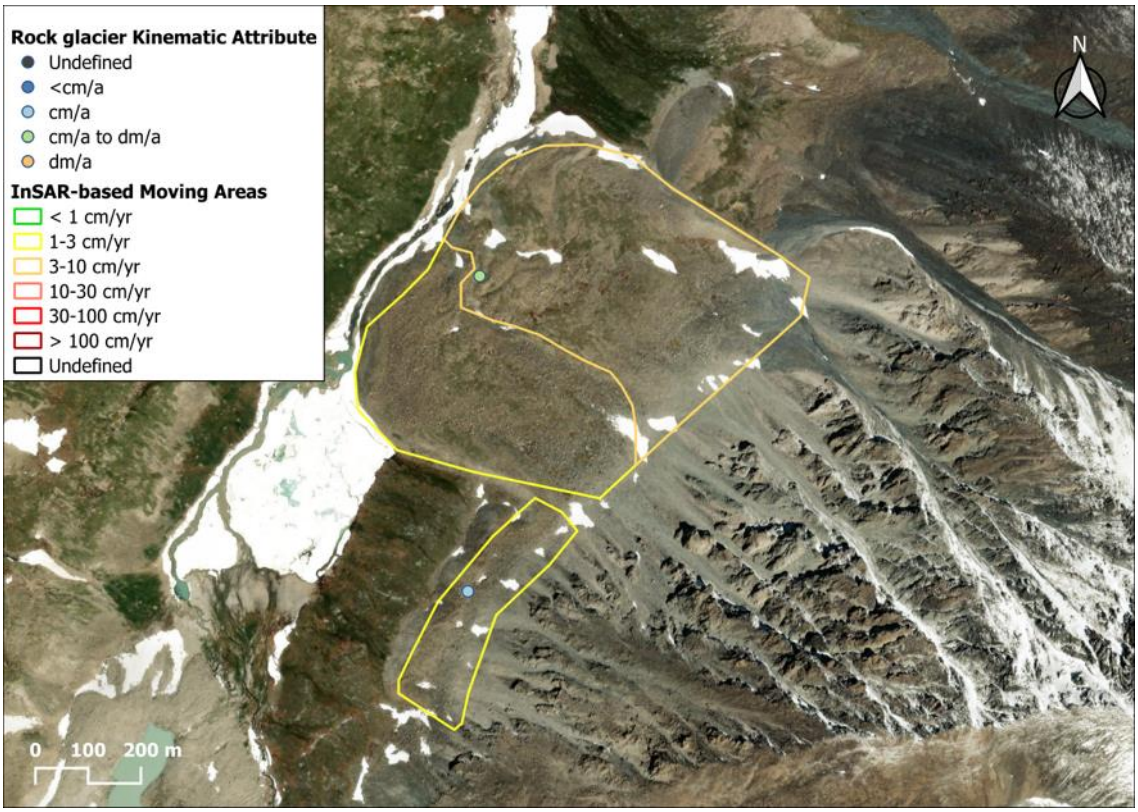

Figure 2. *Tsengel Khairkhan, Mongolia. First example of Kinematic Attributes (KA) and Moving Areas (MA).*

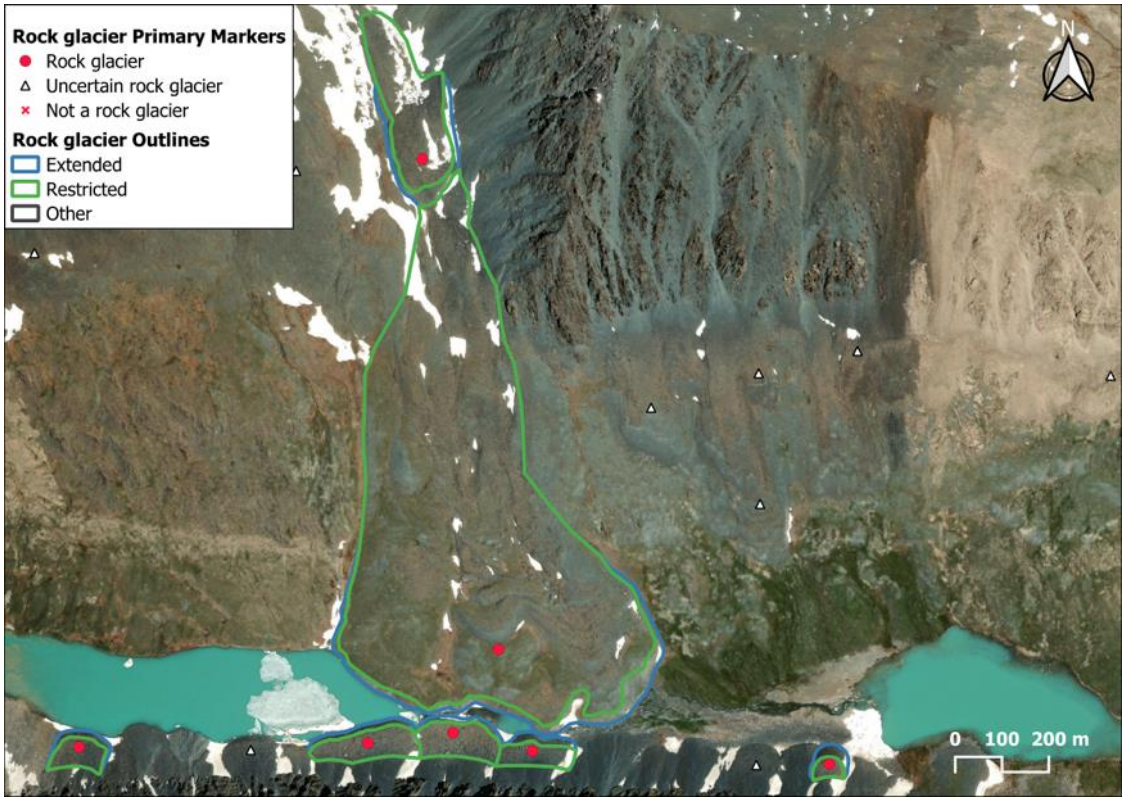

Figure 3. *Tsengel Khairkhan, Mongolia. First example of Primary Markers (PM) and Geomorphological Outlines (GO).*

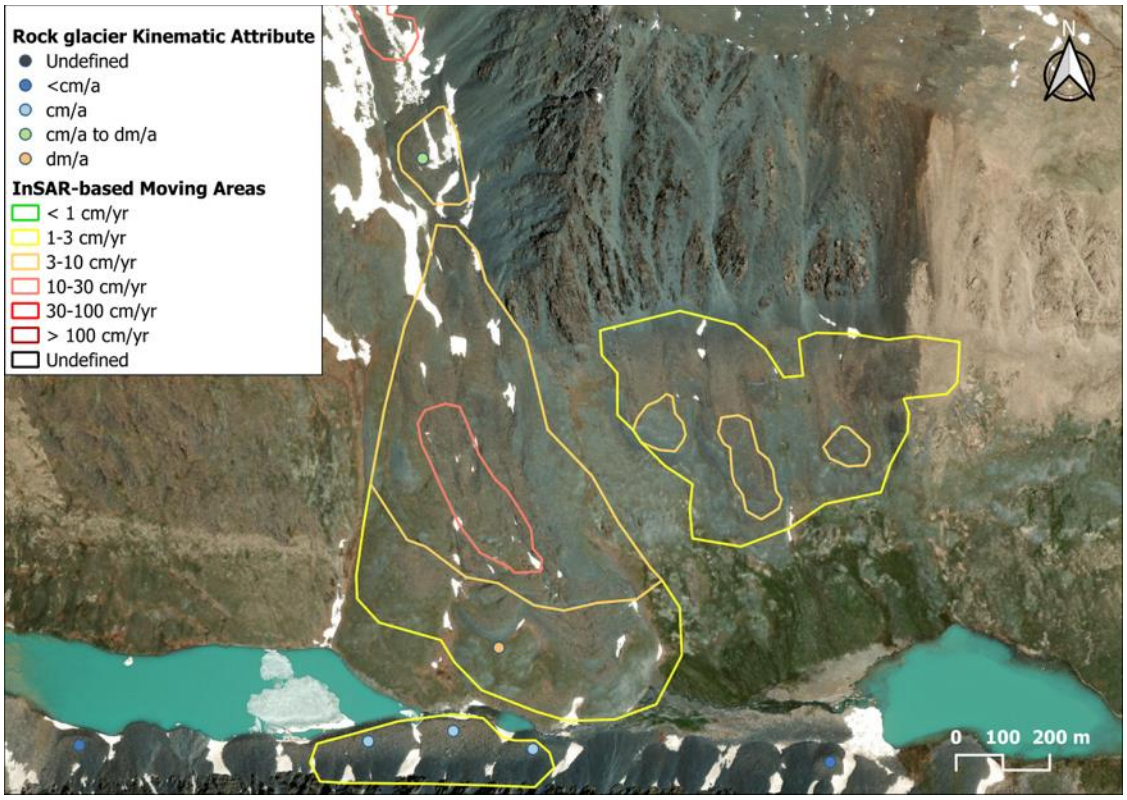

Figure 4. *Tsengel Khairkhan, Mongolia. Second example of Kinematic Attributes (KA) and Moving Areas (MA).*

Status of RoGI area 21-1 in Baralacha La, India

RoGI PI: Francesco Brardinoni, UniBo

Contributors: Tara T. Mantha, UniBo; Thomas Echelard, UniBo; Pratima Pandey, IIRS; Sheikh N. Ali, BISP

Introduction

The Baralacha La study area is located in Western Himalaya, India, along the border between Himachal-Pradesh and Ladakh states. The area covers about 530 km^2 with elevation ranging from 3752 m a.s.l. (Bhaga River floodplain) to 6111 m a.s.l. (Mount Yunam). Glaciers occupy about 20% of the terrain. The area is strategic, as it hosts key transportation corridors linking the regional centers of Leh and Zanskar with Manali and includes the proposed Leh-Manali Railway line.

The RoGI compilation started in July 2024 and involved 5 operators. The dataset adopts the RGIK specifics. It forms a prominent part of Tara T. Mantha's PhD project at UniBo. The morphological approach was implemented starting from version1 compiled by the PhD student, which subsequently underwent four sets of revisions supervised by the other operators. The kinematic approach, implemented on S1 interferograms (2020–2024), differs from the morphological one in that version1 undertaken by the PhD student is being revised by one expert operator only. Two weeks of confirmatory fieldwork were conducted in September 2024.

Current work status

The morphological approach has been completed both in terms of primary markers and polygon outlines (i.e., version 5). All attributes have been considered. The InSAR-based kinematic approach has been completed (i.e., version 1). A thorough revision of the kinematic version 1 has been conducted on a subset of rock glaciers (24 out of 82). Based on this revision, and the set of recommendations that stemmed from it, the PhD student is now revising the moving areas on the remaining 58 rock glaciers. We expect that this iteration will induce significant changes to morphological version 5 too.

We are attaching the PMs, MAs, and GOs files in their present state. In the PM attribute table, RGUs that underwent kinematic and morphological revisions are marked by TE in the "Revised" field. In the RGU_outlines attribute tables, additional fields (currently not labelled appropriately) indicate the median elevation, min elevation, max elevation, dominant aspect, and area of the extended footprint.

Key findings

In total, 82 certain rock glacier units have been identified, while 46 landforms have been classified as uncertain. Based on InSAR (2020–2024), 166 moving areas have been outlined and categorised with velocity classes ranging from 3–10 cm/yr to > 100 m/yr. Extended outlines have been drawn for the certain rock glaciers.

Within the landscape, most of the rock glaciers display upslope connection modulated by talus slopes (66.7%), followed by poly connections (18.1 %) – mostly jointly fed by talus slopes and glacier forefields –, glacier forefields (8.3 %), debris-mantled slopes (5.5%), and lastly glaciers (1.4 %).

Identified challenges

Geomorphological interpretation is made challenging by the physical setting that hosts a number of complex glacial and periglacial landforms. Visual interpretation can rely on GE imagery only, whose resolution is coarser than what typically available across the European Alps.

Next steps

A finalized version of the RoGI – including PMs, MAs and GOs – is expected by 30.06.2025. The relevant statistical analysis is expected by the 31.08.2025, since the PhD student must complete her thesis by the 30.09.2025. An abstract was submitted to IAG 2025 Regional Conference on Geomorphology in Timisoara.

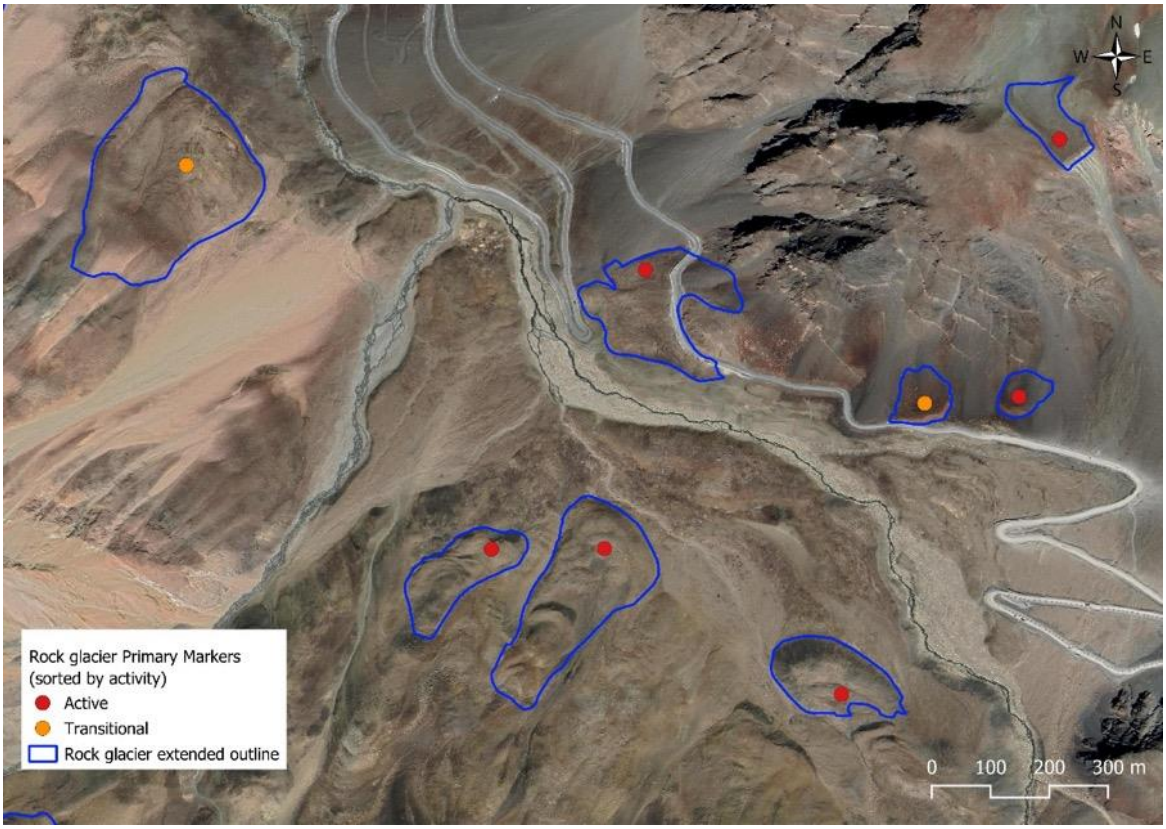

Figure 1. *The Baralacha, India. First example of Primary Markers (PM) and Geomorphological Outlines (GO).*

Figure 2. *The Baralacha, India. Example of Kinematic Attributes (KA) and Moving Areas (MA).*

Status of RoGI area 22-1 in Thana, Bhutan

RoGI PI: Pellet Cécile, University of Fribourg, Switzerland

Contributors: Eden Pema, College of Natural Resources, Royal university of Bhutan; Alina Milceva, University of Fribourg, Switzerland; Mishelle Wehbe, University of Ottawa

Introduction

The Thana study area is located in the Himalayas in Bhutan. The area covers ~775 km^2 with elevation ranging from around 3000 to 7500 m a.s.l (**Figure 1**). The study area is in the headwater of the Chamkar Chhu river.

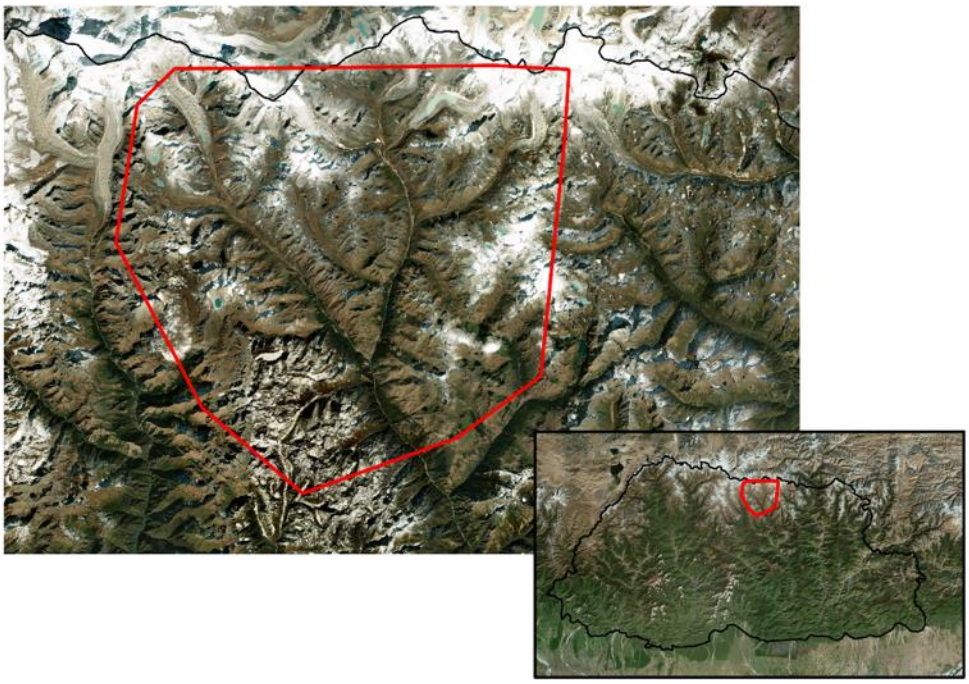

Figure 1. *Location map of the Thana RoGI area in Bhutan.*

The RoGI process is linked to the SNSF-funded Cryo-SPIRIT project (2024–2027), which aims at improving our understanding of rapidly changing high-mountain cryosphere and its impacts in Bhutan focusing on permafrost and snow. Within the Cryo-SPIRIT project, the RoGI in the Thana area will be used as validation for a new potential permafrost map of Bhutan and to assess potential risks related to permafrost in Bhutan.

Current work status

The preparation of the RoGI project has started this Spring (AOI definition, InSAR data processing and sharing, and QGIS folder structure).

Next steps

The RoGI process will start in June 2025 and involve 4 operators. A multi-operator procedure is foreseen as well as a two-step inventorying process (first: primary marker and moving areas identification; second: characterisation and outlining). The inventory and review process will take place in June and July 2025.

Annex 2: Permafrost_cci RGV products

In the following, the status of the Option 8 work in Norway is described. All RGV results in the Alps (Baseline project) are provided at the end, in a similar factsheet format.

Status of the optical analysis in Ádjet, Troms, Norway (UiO)

Author: Andreas Kääb (UiO)

The Ádjet rock glacier in Northern Norway (most western rock glacier in **Figure 1**) is the fastest rock glacier known today in Norway. It shows exceptionally high speeds that could be described as persistent destabilization. Here, we extend the time series of rock glacier velocities until 2014 from repeat airphotos by Eriksen et al. (2018) and also investigate the dynamics of other rock glaciers along the same mountain ridge. We follow the Permafrost_cci methodology developed by Kääb and Røste (2024). For the purpose of the current study, we have to rely on readily orthorectified sporadic airphotos provided by the Norwegian mapping authority through their "Norge i bilder" service (Norway in images). We find that these orthoimages have in parts considerable distortions to each other, which creates an artificial offset field that combines with offsets from real terrain movement. Both components cannot be separated from each other, cause hidden errors in the terrain displacements retrieved, and render in particular slow surface velocities very uncertain. In addition, some orthoimages show extensive snow remains (**Figure 1**), excluding large areas from measurements. In the following we summarise highlights from our measurements.

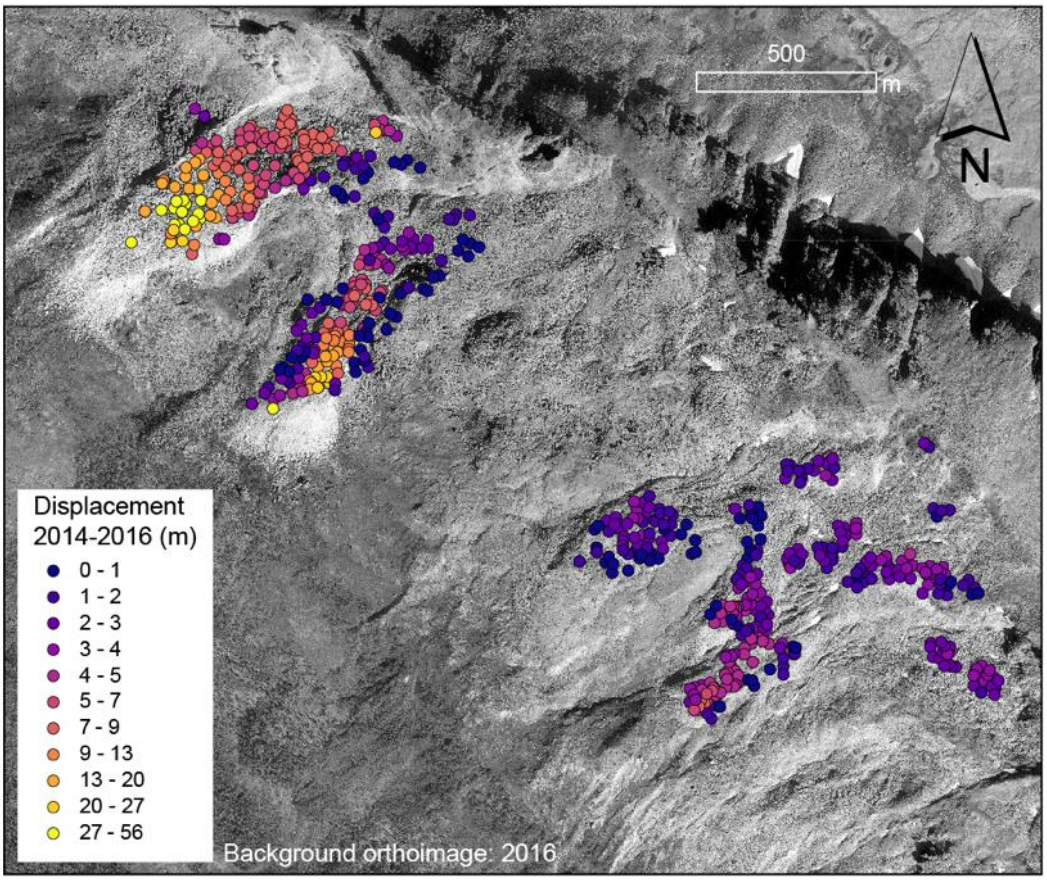

Figure 1. Colour-coded displacement magnitudes between airphotos of 2014 and 2016.

Between 2014 and 2016, we find maximum displacements of 56 m, i.e. 26.4 m/yr (**Figure 1** and **Figure 2**). For rock glaciers, this is an extremely high velocity, perhaps unprecedented. These high speeds are found for the Ádjet rock glacier, but the other investigated rock glaciers also show very high speeds, at the upper end of worldwide known rock glacier speeds.

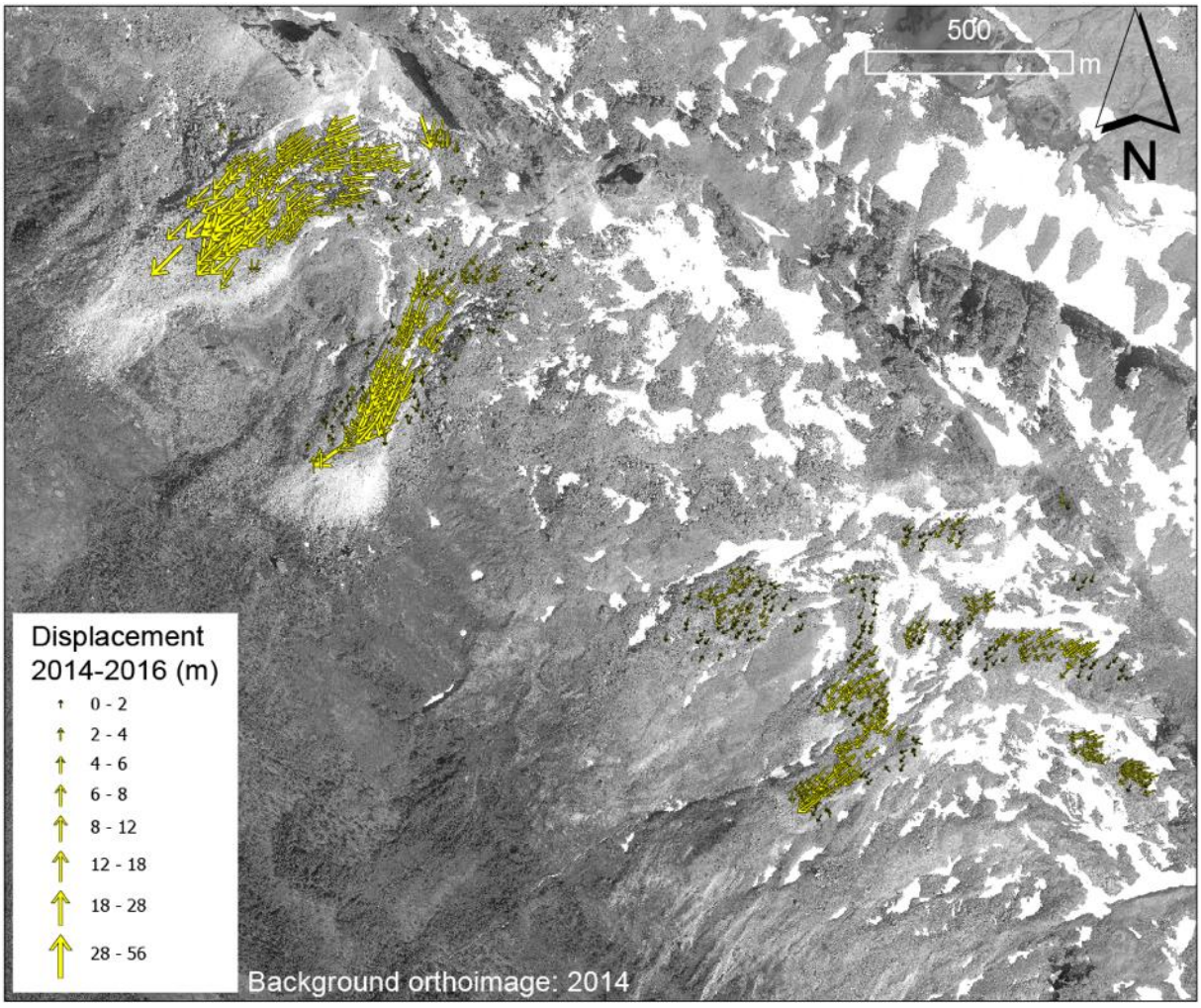

Figure 2. Displacement vectors between airphotos of 2014 and 2016. Same data as in Figure 1 but displayed as vectors.

For the westernmost rock glaciers, we investigate changes in speed between 1977, 2006 and 2016 (**Figure 3**) by comparing offsets between these three years at close-by measuring points. As these measuring points have to be identifiable in the airphotos of all three years, their number is limited, and smaller than the number of measuring points, for instance, between 2014 and 2016. **Figure 3** shows speed changes for the "slower" rock glaciers in the eastern part of the mountain slope. Most points show acceleration over time. Speed changes over two rock glaciers in the western part of the mountain slope have been previously investigated by Eriksen et al. (2018).

We also extended the photogrammetric measurements by Eriksen et al. (2018) after 2014. **Figure 4** shows rock glacier displacements on the westernmost rock glaciers for 2016–2023. Maximum displacements are nearly 230 m, i.e. around 32 m/yr. We also measure displacements of selected points over 2023–2024, revealing also speeds of up to 32 m/yr. This means the Ádjet rock glacier maintains its extremely high velocities over the last 8 years. Such behaviour is to our best knowledge undocumented

so far for rock glaciers and rises pressing questions about the mechanism behind these dynamics, and about the associated mass transfer within the rock glacier, and mass supply into it. Or in simple words, where and how does the extreme shearing within the rock glacier work, and how is the rock glacier able to maintain its exceptional speeds, seemingly without exceptional mass supply?

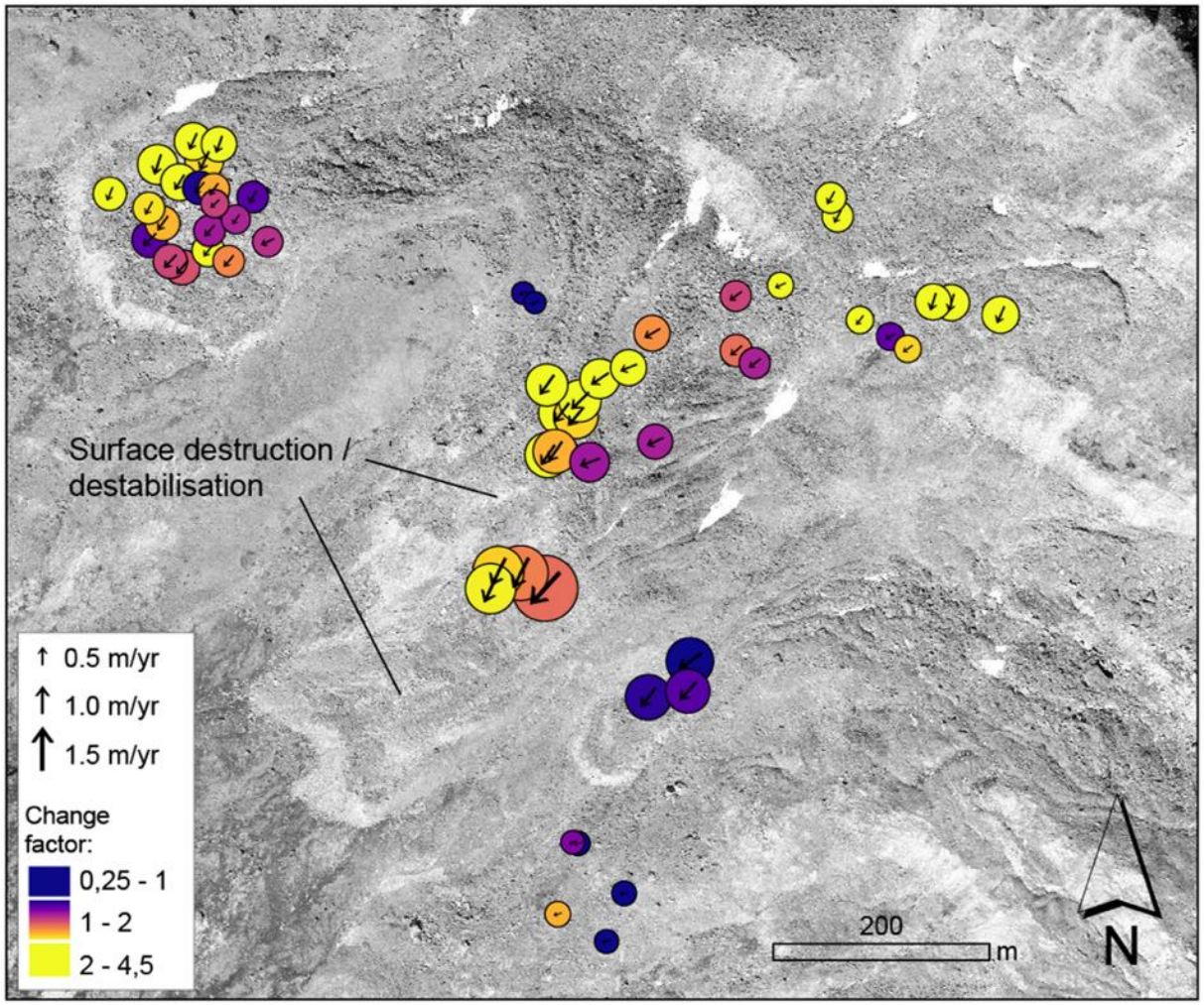

Figure 3. Changes in speed between 1977–2006 and 2006–2016 for the rock glaciers in the part eastern part of the Ádjet mountain slope. The factor "fact" is 2nd velocity/1st velocity, i.e. 1 means no change, >1 means acceleration over time.

We also extended the photogrammetric measurements by Eriksen et al. (2018) after 2014. **Figure 4** shows rock glacier displacements on the two western rock glaciers for 2016–2023. Maximum displacements are nearly 230 m, i.e. around 32 m/yr. We also measure displacements of selected points over 2023-2024, revealing also speeds of up to 32 m/yr. This means that the Ádjet rock glacier maintains its extremely high velocities over the last 8 years. Such behaviour is to our best knowledge undocumented so far for rock glaciers and rises pressing questions about the mechanism behind these dynamics, and about the associated mass transfer within the rock glacier, and mass supply into it. Or in simple words, where and how does the extreme shearing within the rock glacier work, and how is the rock glacier able to maintain its exceptional speeds, seemingly without exceptional mass supply?

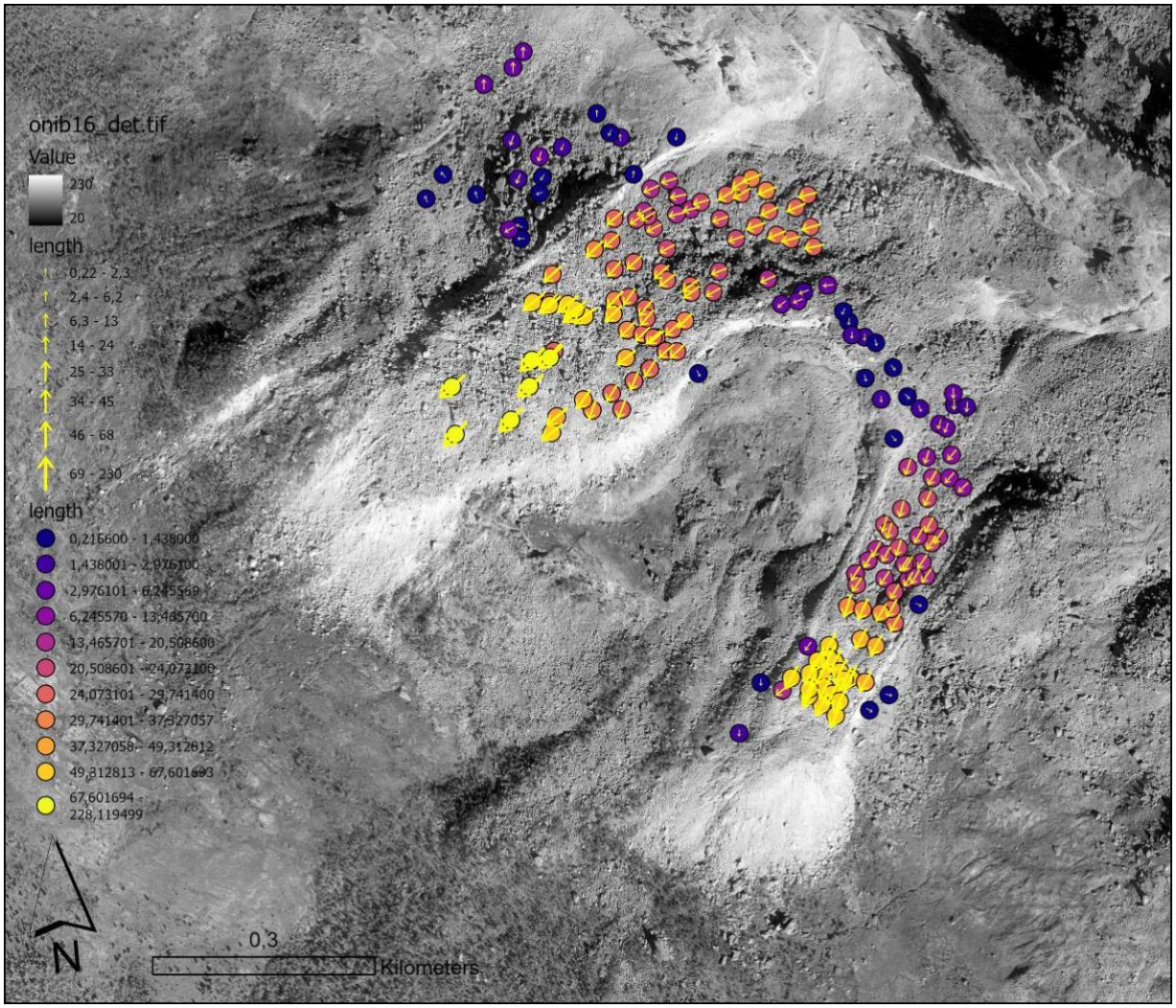

Figure 4. Displacement vectors and colour-coded displacement magnitudes over 2016–2023 over the westernmost rock glaciers. The Ádjet rock glacier is the biggest and fastest unit in the upper-left.

Status of the radar analysis in Ádjet, Troms, Norway (NORCE)

Author: Tom Rune Lauknes (NORCE). Contributors: John Dehls (NGU), Line Rouyet (NORCE).

The analysis integrates both ground-based real aperture radar and satellite-based synthetic aperture radar (SAR) observations to characterize surface displacement of the Adjet rock glacier.

Ground-based measurements from the Gamma Portal Radar Interferometer (GPRI), presented in Eriksen et al. (2018), provide high-resolution observations from 2014–2015 and serve as a valuable reference dataset. The study also included TerraSAR-X offset-tracking results from 2009–2014.

Satellite observations from COSMO-SkyMed were processed using both interferometric SAR (InSAR) stacking and amplitude-based offset-tracking. Interferogram stacking with short temporal baselines improves coherence and enhances the signal-to-noise ratio for detecting moderate displacement rates, while offset-tracking of image pairs separated by 16 days enables detection of faster surface motion that often exceeds InSAR's decorrelation limits. All COSMO-SkyMed data used are in descending geometry.

Figure 1 presents an overview of the different SAR products used in this study. While the colour scales differ across the panels, and each sensor has a distinct line-of-sight (LOS) sensitivity based on its acquisition geometry and wavelength, the spatial patterns of movement are consistent and provide crucial insight into the kinematics of the rock glacier. The combination of ground-based radar, high-resolution SAR (e.g., TerraSAR-X and COSMO-SkyMed), and long-term monitoring from Sentinel-1 PSI highlights how different sensors and processing methods are highly complementary—each contributing with unique strengths in terms of spatial resolution, temporal coverage, and sensitivity to deformation direction. The magenta outlines shown in **Figure 1** correspond to mapped rock glacier boundaries from Rouyet et al. (2021).

Figure 2 presents preliminary time-series results for a point located in the fastest-moving area of the Adjet rock glacier. The data are based on offset tracking of COSMO-SkyMed StripMap imagery from 2023–2024, using image pairs with a 16-day temporal baseline. The figure shows displacements estimated in the satellite line-of-sight (range) direction only. Although the results are preliminary, they suggest a potential velocity decrease in 2025. The method also appears capable of capturing relatively consistent intra-seasonal velocity variations. These findings require further verification through additional analysis and comparison with other datasets. If confirmed, the trend may indicate that the rock glacier has recently reached its peak activity, following several years of exceptionally high velocities (see optical analysis by Andreas Kääb).

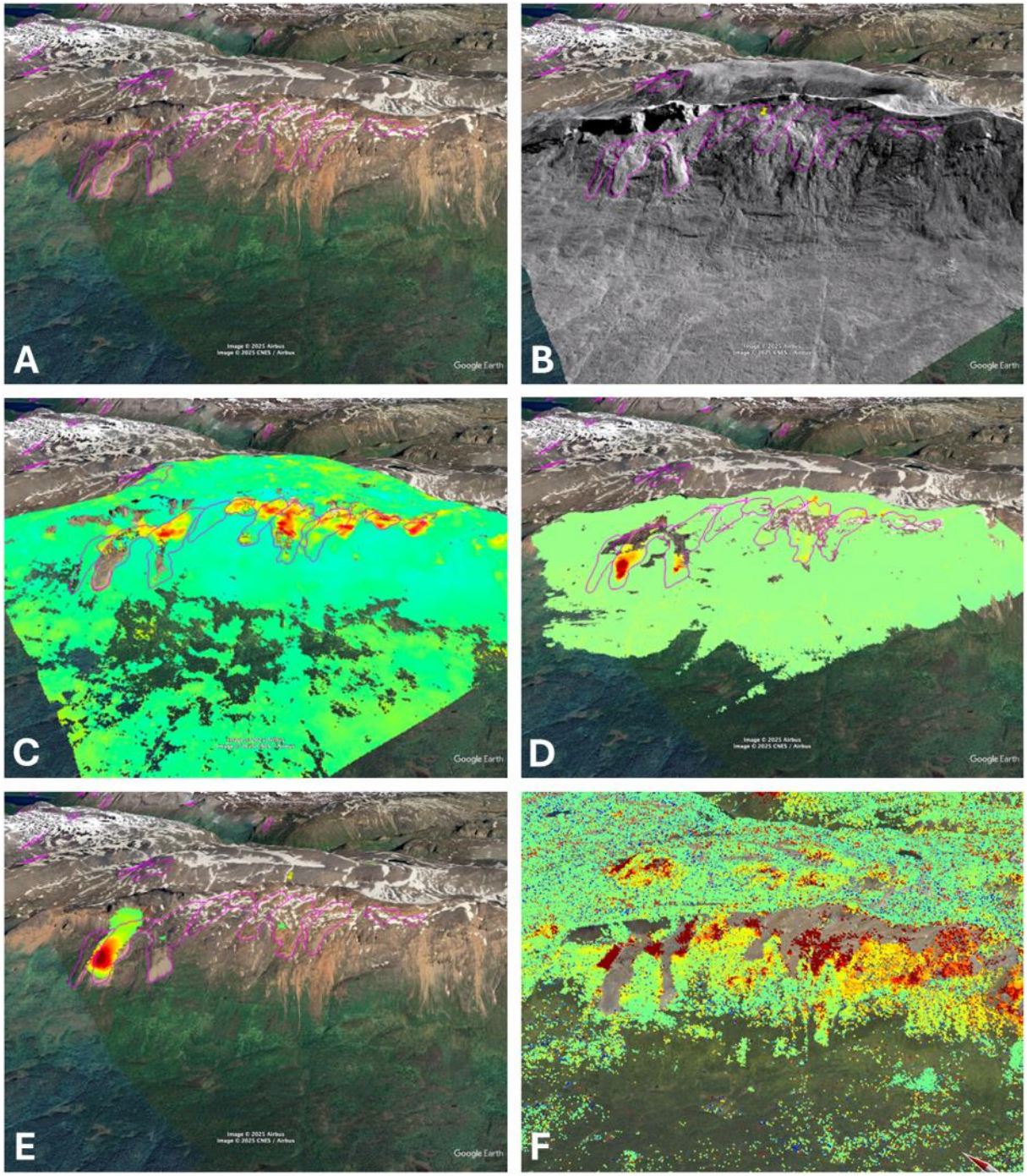

Figure 1: ***A.*** *Adjet rock glacier complex;* ***B.*** *COSMO-SkyMed SAR backscatter;* ***C.*** *COSMO-SkyMed interferogram stacking from 2023–2024. Scale ±50 cm/year.* ***D.*** *GPRI ground-based radar from 2014.* ***E.*** *COSMO-SkyMed offset tracking from 2023–2024.* ***F.*** *Sentinel-1 PSI 2020–2024 from InSAR Norway. Note that colour scales differ across panels, and each sensor has distinct line-of-sight sensitivity. Despite these differences, spatial patterns are consistent. The different sensors and methods are highly complementary, offering a robust picture of the rock glacier dynamics. Magenta outline shows mapped rock glacier extent from Rouyet et al. (2021). COSMO-SkyMed Product/COSMO Second Generation Product © ASI: 2023–2024 processed under license from ASI - Agenzia Spaziale taliana. All rights reserved. Distributed by e-GEOS.*

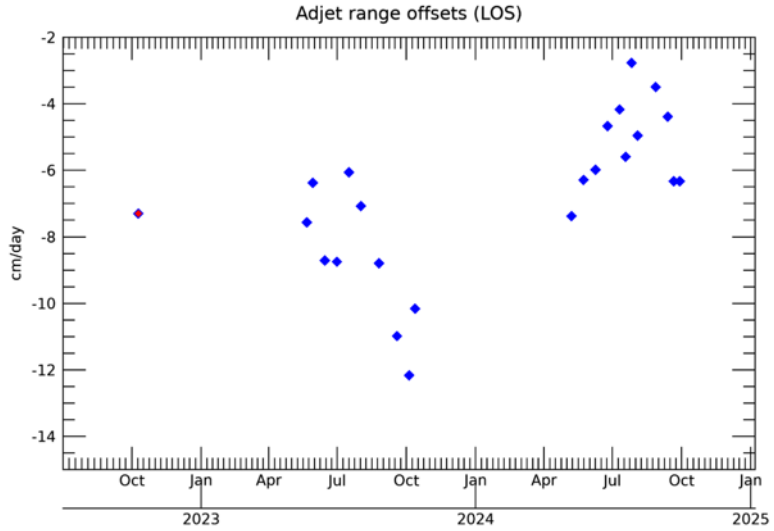

Figure 2: *Preliminary velocity time series for a point located in the fastest-moving area of the Adjet rock glacier, derived from offset tracking of COSMO-SkyMed StripMap data (2023–2024) using 16-day temporal baselines. Only range-direction displacements are shown. The results suggest a potential decrease in velocity into 2025, along with indications of intra-seasonal variability. Further validation is required to confirm these trends. COSMO-SkyMed Product/COSMO Second Generation Product © ASI: 2023–2024 processed under license from ASI - Agenzia Spaziale taliana. All rights reserved. Distributed by e-GEOS.*

Future Work

Future work will focus on the interannual analysis of surface velocities from various sensors:

- Upcoming 2025 COSMO-SkyMed snow-free images will be processed, and preliminary results showed in **Figure 2** extended and quality-checked.
- Offset-tracking results from Eriksen et al. (2018) using TerraSAR-X data from 2009–2014 will be compared to COSMO-SkyMed offset-tracking data from 2023–2025.
- As part of the EPOS-NG Infrastructure project (RCN-funded and kicked-off in 2025), a new ground-based radar campaign is planned in summer 2025. The resulting dataset will be valuable to compare with COSMO-SkyMed offset-tracking the same year.
- The integration of InSAR and offset-tracking is essential for capturing the full range of displacements, especially in fast-moving sectors where InSAR coherence is lost.
- Differences in LOS geometry between sensors will be addressed by extracting and comparing displacement profiles across the rock glacier, using an approach similar to Eriksen et al. (2018).
- Further analysis will include Sentinel-1 data (short-baseline interferograms and PSI time series) with a focus on identifying temporal variability in velocity patterns and the onsets of acceleration or deceleration phases.
- By integrating all radar observations with the optical observations described in the previous chapters, we will test the feasibility of providing RGV products for the various rock glaciers along this mountain ridge.

This multi-sensor approach will improve our understanding of the Ádjet rock glacier's dynamic behaviour and demonstrate the value of integrating complementary SAR datasets for operational monitoring in periglacial environments.

Status of RGV production in the Alps (GAMMA)

GAMMA factsheets for each selected rock glaciers in the Swiss, Italian and French Alps are listed in the next pages, in the following order:

- Swiss Alps
  - Bru Latitude: 46.122º Longitude: 7.828º
  - Diestelhorn Latitude: 46.189º Longitude: 7.866º
  - Grosses Gufer Latitude: 46.425º Longitude: 8.082º
  - Réchy Latitude: 46.173º Longitude: 7.512º
  - Steintälli Latitude: 46.129º Longitude: 7.831º
- Italian Alps – Aosta
  - Gran Sometta Latitude: 45.921º Longitude: 7.669º
  - La Thuile Latitude: 45.700º Longitude: 7.000º
  - Luseney Latitude: 45.863º Longitude: 7.501º
  - Moline Latitude: 45.886º Longitude: 7.221º
  - Monte Emilius Range 1 Latitude: 45.635º Longitude: 7.459º
  - Monte Emilius Range 2 Latitude: 45.661º Longitude: 7.367º
  - North Arpignan Latitude: 45.651º Longitude: 7.367º
  - Rhemes Latitude: 45.562º Longitude: 7.159º
  - Val Grisenche 2 Latitude: 45.629º Longitude: 7.101º
  - Val Grisenche 3 Latitude: 45.525º Longitude: 7.064º
  - Valnontey Latitude: 45.568º Longitude: 7.362º
  - Valsavarenche 1 Latitude: 45.566º Longitude: 7.177º
  - Valsavarenche 3 Latitude: 45.511º Longitude: 7.234º
- Italian Alps – Venosta
  - Lazaun Latitude: 46.742º Longitude: 10.755º
  - Similaun Latitude: 46.756º Longitude: 10.862º
- French Alps
  - Laurichard Latitude: 45.017º Longitude: 6.399º

At this stage, the RGV product names do not follow the convention defined in the PSD. The recent developments show the need to adjust the formatting.

Bru RGV Analysis

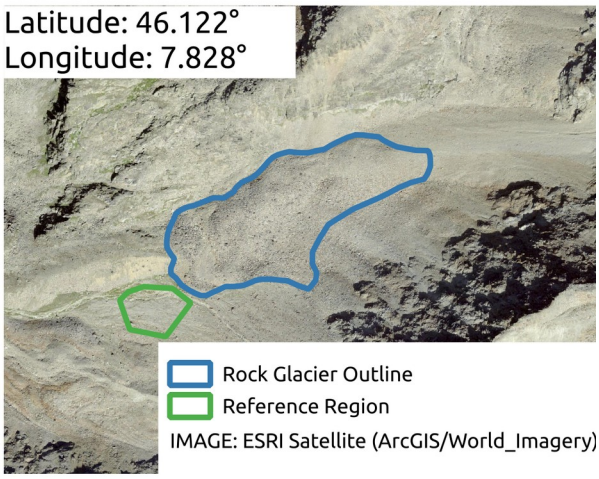

T088A

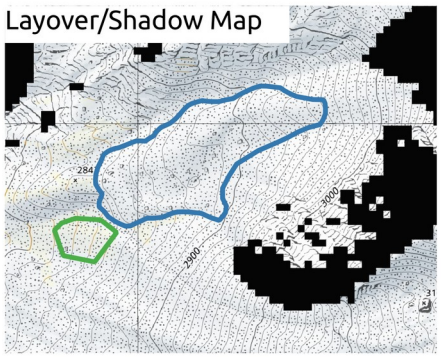

T066D

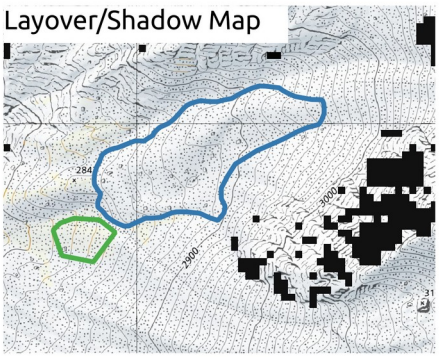

Layover/Shadow
Sentinel-1 data are acquired from two orbits (T088A and T066D). In both orbits the rock glacier region is not affected by layover or shadow effects.

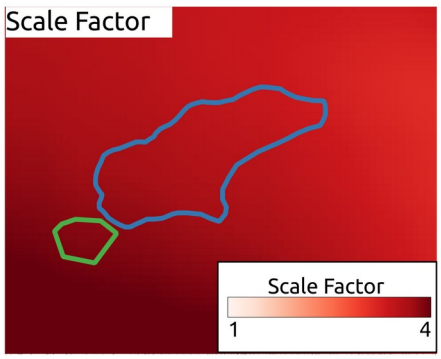

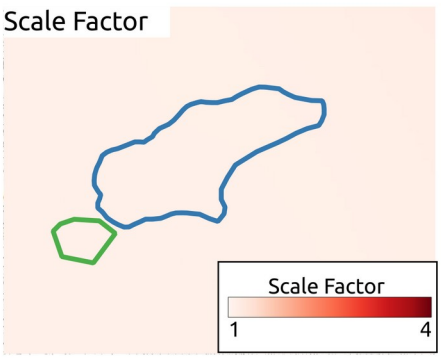

Scale Factor
T088A exhibits an unfavorable viewing geometry with a Scale Factor abroaching 4. The Line-of-Sight for orbit T066D aligns better with the flow direction of the RG. Scale Factors for orbit T066D are in the range of 1.1 to 1.3 over the RG.

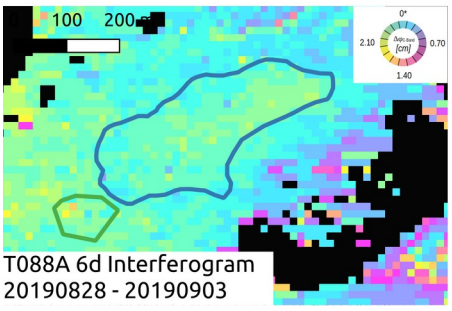

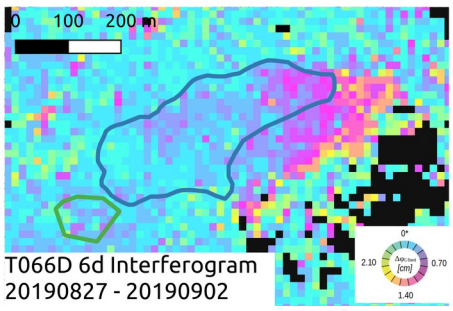

Initial assessment
The T139D interferogram shows movement of up to 1 cm/6d (0.6m/yr) at the root of the RG. Outside the RG boundaries some regions move faster. Phase unwrapping should proceed without complications.

Line-of-Sight

For the RGV Analysis we use orbit T139D descending data.

Bru RGV Analysis – Descending orbit T066D

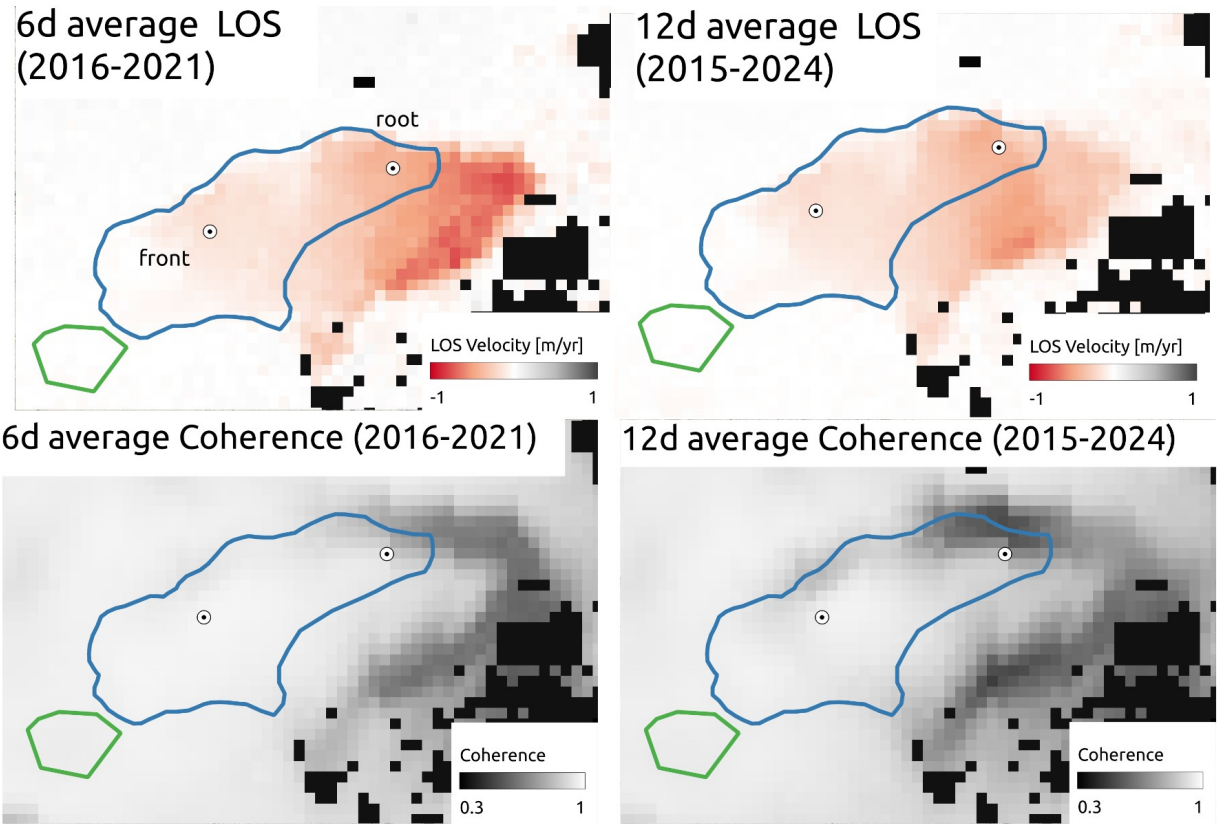

Overview

The figures above show averaged Line-of-Sight (LOS) velocities over all available summer seasons (July to October) (top) as well as the average coherence over the same period (bottom). 6-day interferograms are available from October 2016 to December 2021, 12-day interferograms are available from October 2015 to the start of 2025. Negative LOS values indicate a displacement away from the sensor. A selection of coherent interferograms was made manually for the further analysis. We selected three points (front, root1 and root2) to extract LOS velocities time series. On the bottom we show additionally two example interferograms from summer 2020 for the 6d and 12d period as well as the associated coherence.

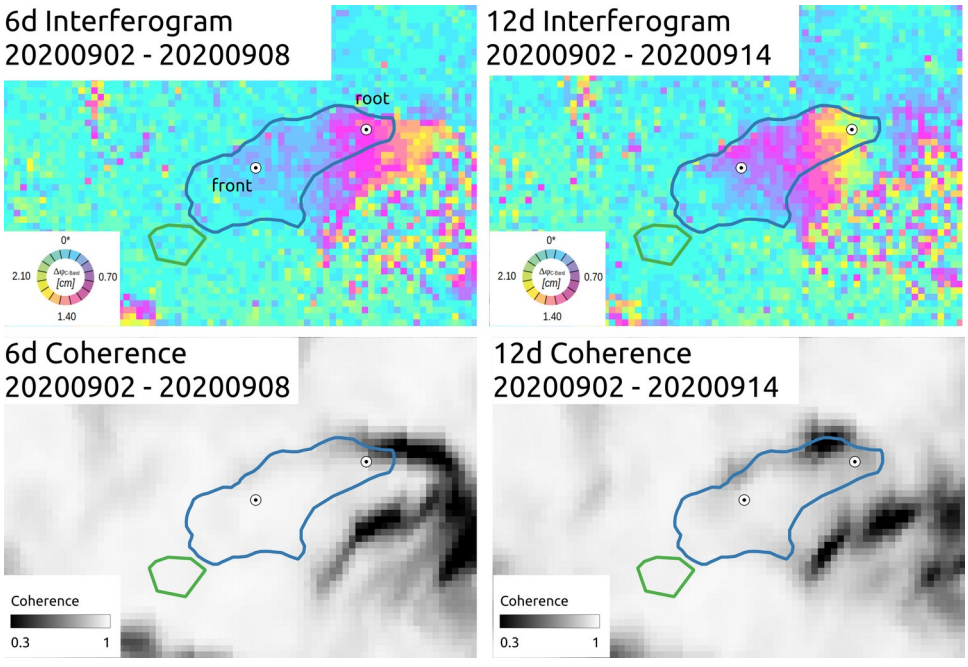

Bru RGV Analysis – Descending orbit T066D

Point Time Series

For two monitoring points (front [46.1223, 7.8276] and root [46.1230, 7.8307] highlighted in the plots from the previous page, we extracted LOS velocity time series, carefully checking and correcting any unwrapping issues. Each figure showing the time series on the next page displays the LOS displacement rates in m/yr in the top panel and the coherence in the bottom panel. For the LOS displacement, only the coherent measurements are shown. For the coherence time series, all available pairs are shown. The coherence was obtained at the point location in the individual interferograms. Blue circles represent 6-day interferometric measurements, while orange crosses show 12-day measurements, with summer months (June-September) highlighted by gray vertical bands.

For the selected interferograms the coherence values are generally high (>0.7) and are obtained mainly in the summer season. In general, the 12-day interferogram coherence values are lower than the 6-day. Higher velocities as well as unfavorable conditions such as snow cover can decrease the coherence.

The highest velocities are measured at the root location (~0.5-0.6 m/yr ~> 0.55-0.65 m/yr when assuming slope-parallel movement) with acceleration and deceleration during the summer of about 0.2-0.3 m/yr. At the front, the velocities are overall lower with velocities up to 0.4m/yr and similar fluctuations within the summer of up to0.3 m/yr. Scale Factors at the two points are 1.10 for front and 1.11 for root.

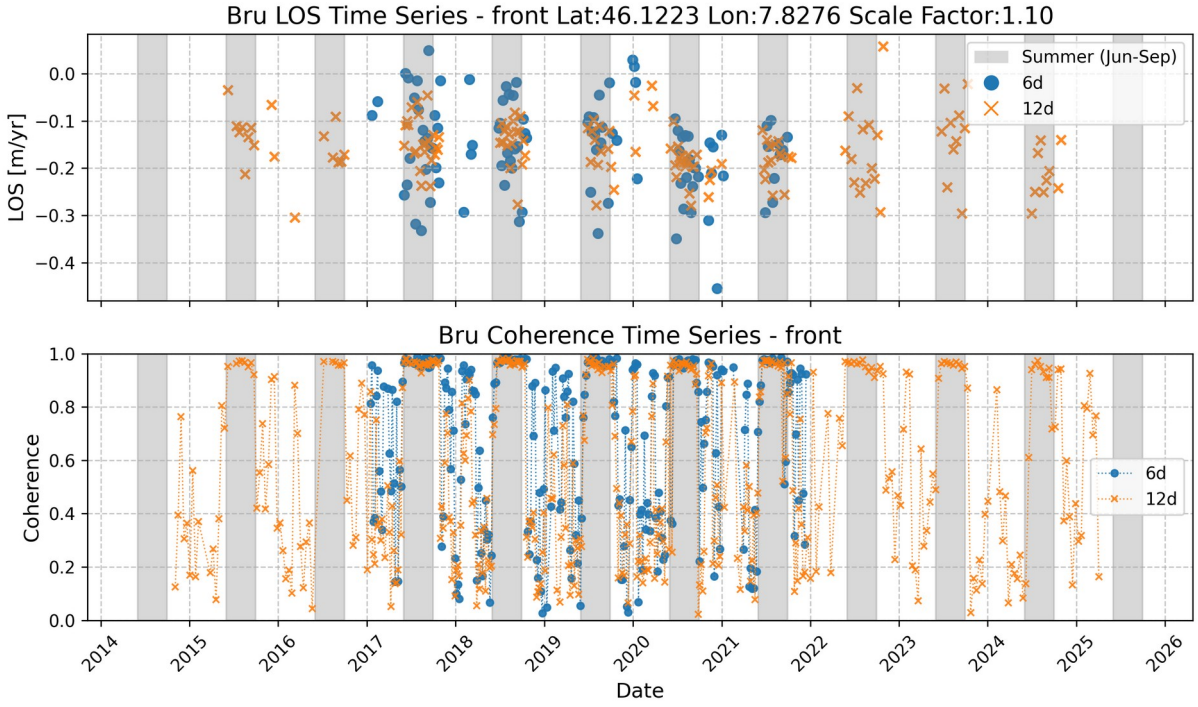

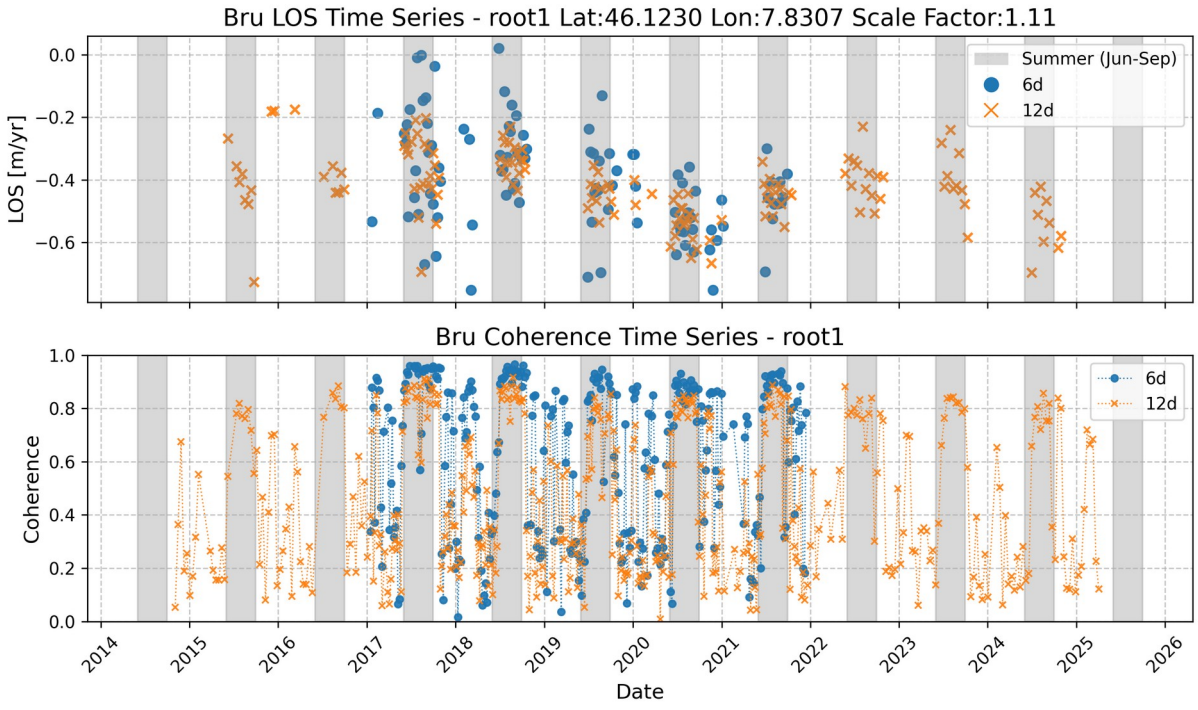

Bru RGV Analysis – Descending orbit T066D

Velocity variation over the years: We averaged the obtained LOS velocity rates from all three monitoring points to generate yearly velocity estimates. In the top three figures, the averaged LOS velocities per summer are shown. The error bars represent the standard deviation per year. The three bottom figures show the normalized values ((Avg_year/mean_overall)-1) to highlight relative changes independent of the absolute velocities. Note that higher variations are expected as the measured velocities approach the sensitivity/noise level.

Both locations exhibit fluctuations and seasonal variations, showing a relatively consistent temporal pattern: stable displacement in 2015 to 2018, followed by a strong acceleration in 2019 and 2020 and a subsequent deceleration until 2023, with a renewed acceleration in 2024. Nevertheless, for the front location the error bars are larger and closer to the sensitivity limit and thus also the normalized time-series shows a less clear pattern. The good agreement between 6-day (blue circles, 2016-2021) and 12-day (orange crosses, 2015-2024) interferometric measurements for the Root location indicates reliability in the observations.

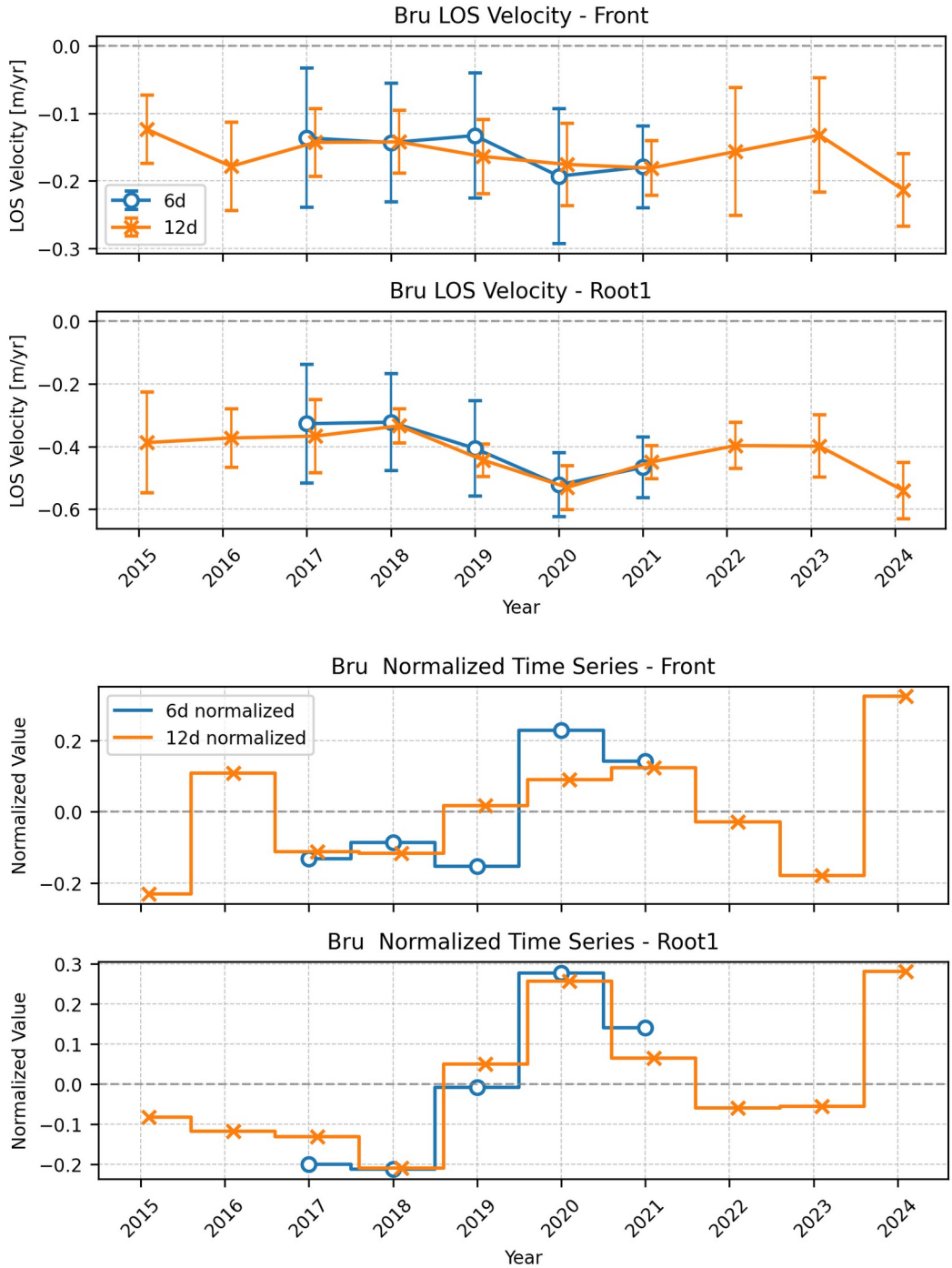

Bru RGV Analysis – Descending orbit T066D

The number of unwrapping errors over the whole RG was small which allowed the spatial aggregation of LOS velocities for all points on the RG. We kept points with average LOS displacement rates above the approximate sensitivity (0.2m/yr for 6d and 0.1m/yr for the 12d). The points above the sensitivity limit can be seen in the bottom figures and the relative changes averaged over all points in the bottom plot. The behavior is consistent with the individual points.

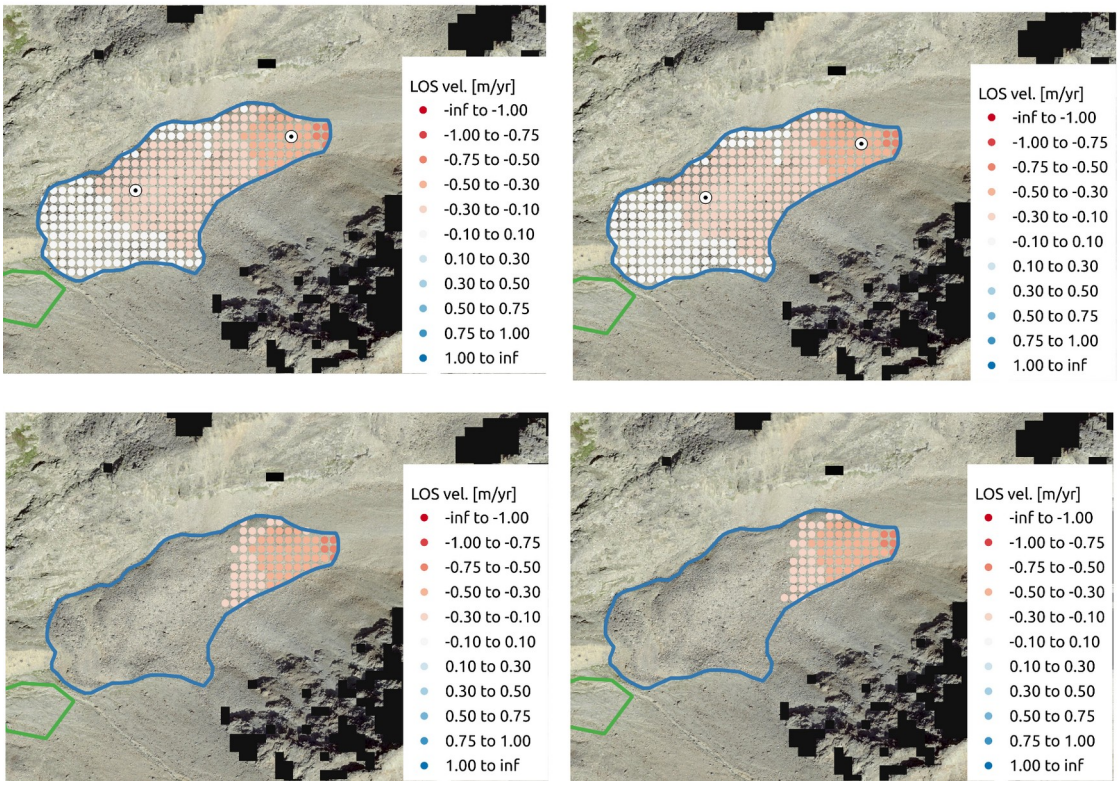

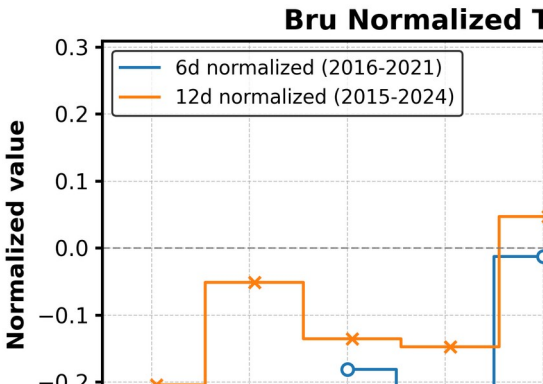

Distelhorn RGV Analysis

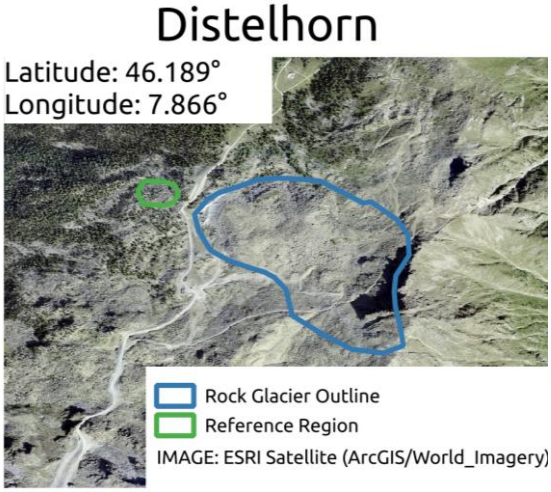

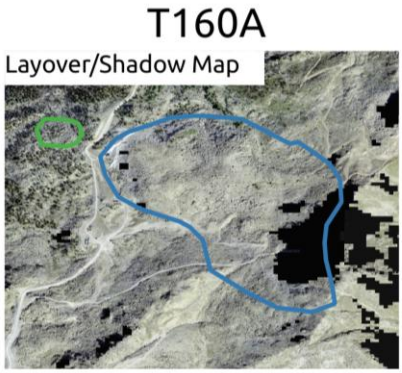

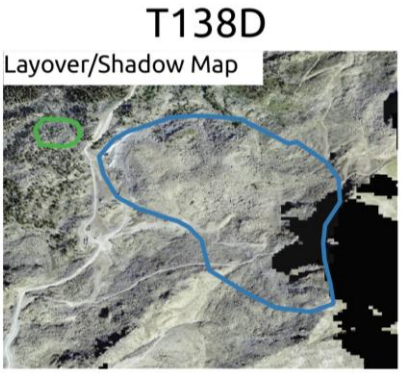

Layover/Shadow
Sentinel-1 data are acquired from two orbits (T160A and T138D). In both orbits the rock glacier region is mostly not affected by layover or shadow effects except for a small steep part at the root of the RG.

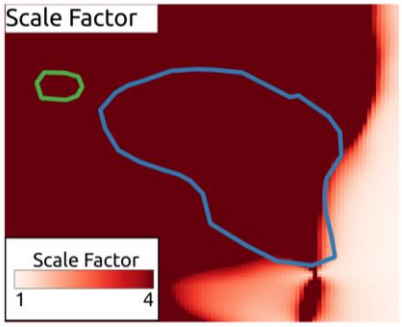

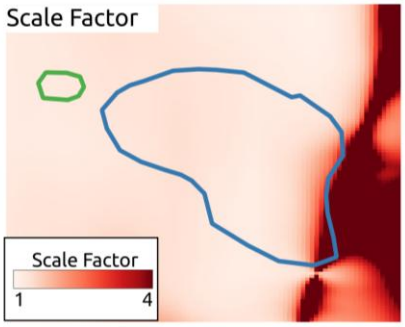

Scale Factor
T160A exhibits a more unfavorable viewing geometry with a Scale Factor mostly above 4.
The Line-of-Sight for orbit T138D aligns well with the flow direction of the RG.
Scale Factors for orbit T138D are in the range 1.1 to 1.4 over the RG.

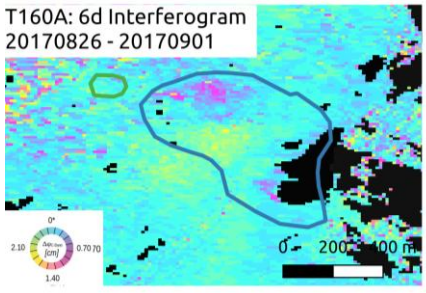

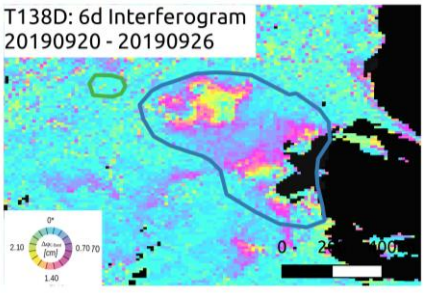

Initial assessment
The T138D interferogram shows significant movement across the RG, with deformation rates ranging from 2.1-2.4cm/6d (approximately 1.3-1.5m/yr).
The displacement pattern exhibits notable spatial variation, with higher velocities concentrated in the front and root of the RG. These variations create steep velocity gradients that likely require attention and corrections during phase unwrapping.

Line-of-Sight

For the RGV Analysis we use descending orbit 138.

Distelhorn RGV Analysis – Descending orbit 138

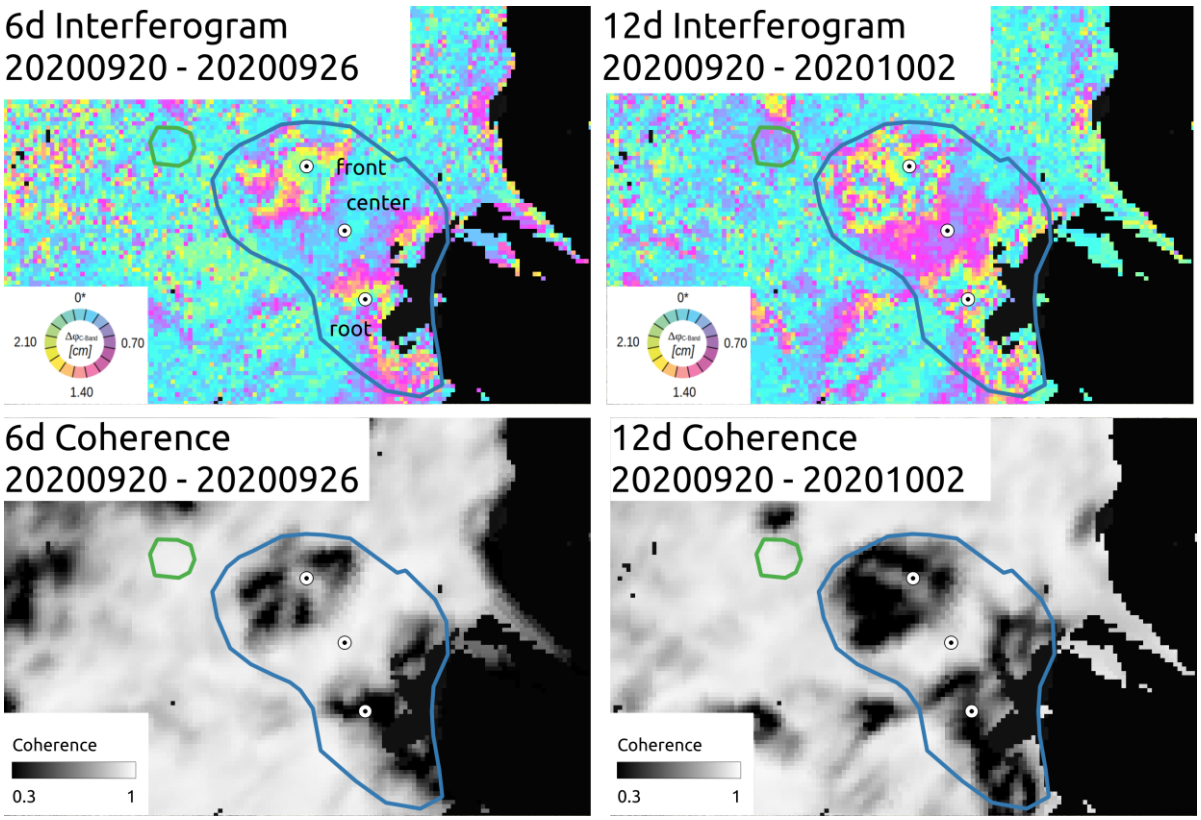

Overview

The figure above shows a 6d and 12d interferogram as well as the associated coherence from end of summer 2019. A selection of coherent interferograms was made manually for the further analysis. Many unwrapping issues are present due to high LOS velocities (> 1.5 m/yr) as well as abrupt changes. We selected three points (front, center, root) across the RG to extract LOS velocities time series.

Point Time Series

For the three monitoring points (front [46.1908, 7.8628], center [46.1895, 7.8664], and root [46.1875, 7.8672]) highlighted in the upper figures, we extracted LOS velocity time series, carefully checking and correcting any unwrapping issues. Each figure showing the time series on the next page displays the LOS displacement rates in m/yr in the top panel and the coherence in the bottom panel. For the LOS displacements, the coherent values are shown. For the coherence time series, all available 6-day pairs are shown. The coherence was obtained at the point location in the individual interferograms. Blue circles represent 6-day interferometric measurements, while orange crosses show 12-day measurements, with summer months (June-September) highlighted by gray vertical bands. 12-day measurements were excluded due to poor unwrapping results. For all three locations the coherence values in the summer season are generally high (>0.6) except for the root location for two years in 2019 and 2020 where very high velocities lead to coherences of 0.4-0.6. Higher velocities as well as unfavorable conditions such as snow cover can decrease the coherence.

The highest velocities are measured at the front and root locations (~1.0-1.5 m/yr ~> 1.5-2.0 m/yr when assuming slope-parallel movement). The fluctuations during the individual summer months was relatively small. LOS velocities at the center are were slow and just above the sensitivity threshold of 0.1-0.2 m/yr. Scale Factors for the three points are 1.33 for front, 1.25 for center and 1.18 for root.

Distelhorn RGV Analysis – Descending orbit 138

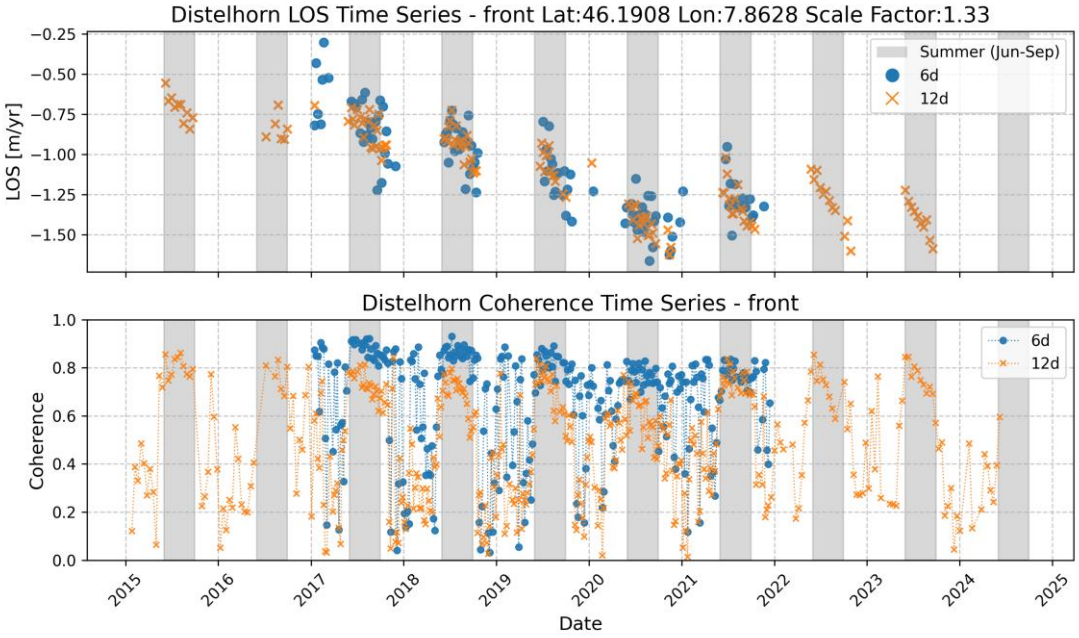

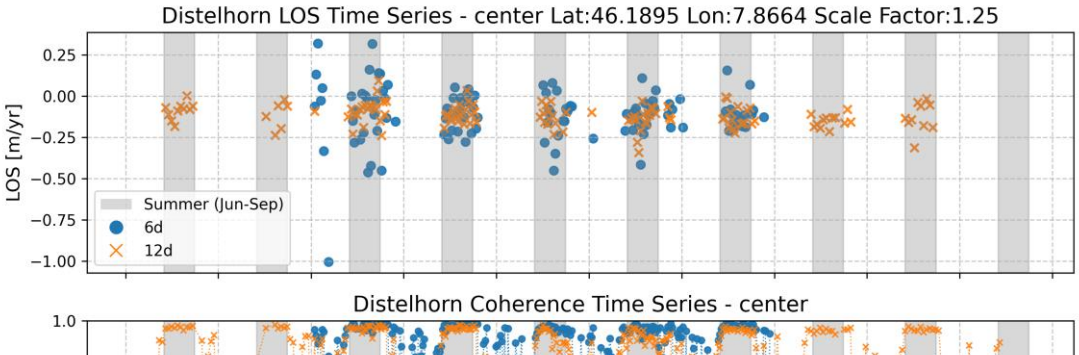

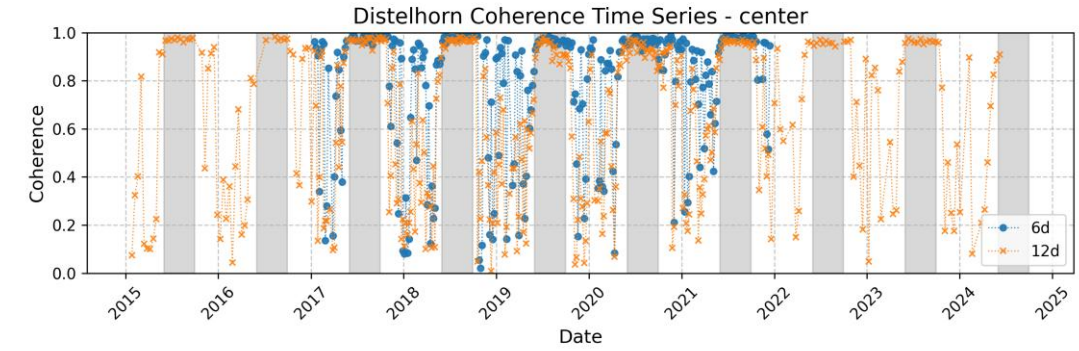

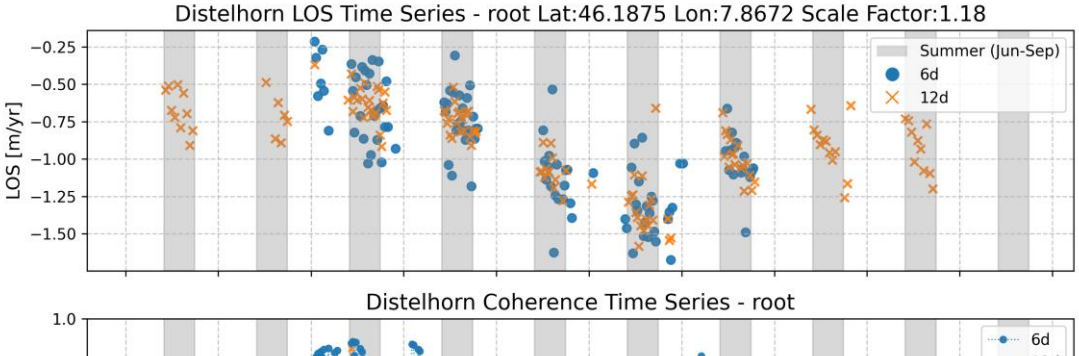

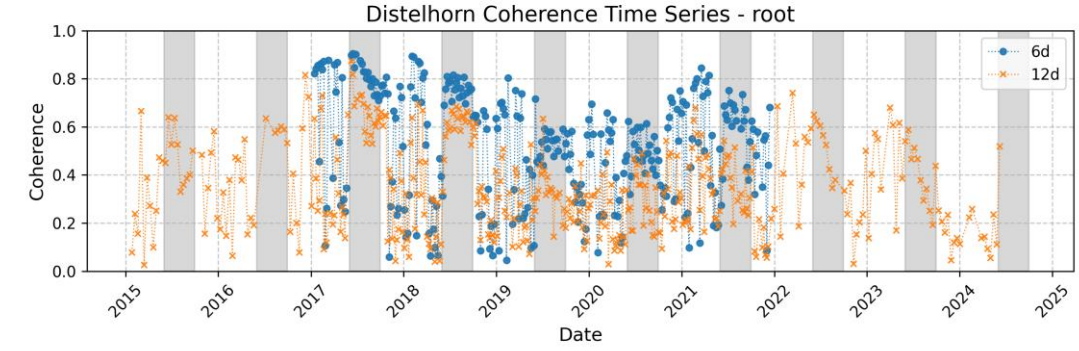

Distelhorn RGV Analysis – Descending orbit 138

Velocity variation over the years: We averaged the obtained LOS velocity rates from all three monitoring points to generate yearly velocity estimates. In the top three figures, the averaged LOS velocities per summer are shown. The error bars represent the standard deviation per year. The three bottom figures show the normalized values ((Avg_year/mean_overall)-1) to highlight relative changes independent of the absolute velocities. Note that higher variations are expected as the measured velocities approach the sensitivity/noise level.

Since the center location is close to the sensitivity limit we don't show the averaged yearly changes. The two locations front and root show a very similar temporal pattern, with slightly higher error bars at the root location compared to the front. The LOS displacement shows an overall acceleration from 2016 to 2020, followed by a subsequent deceleratio. The 6 day and 12 day data as well as the two points show very good agreement indicating a high reliability of the data.

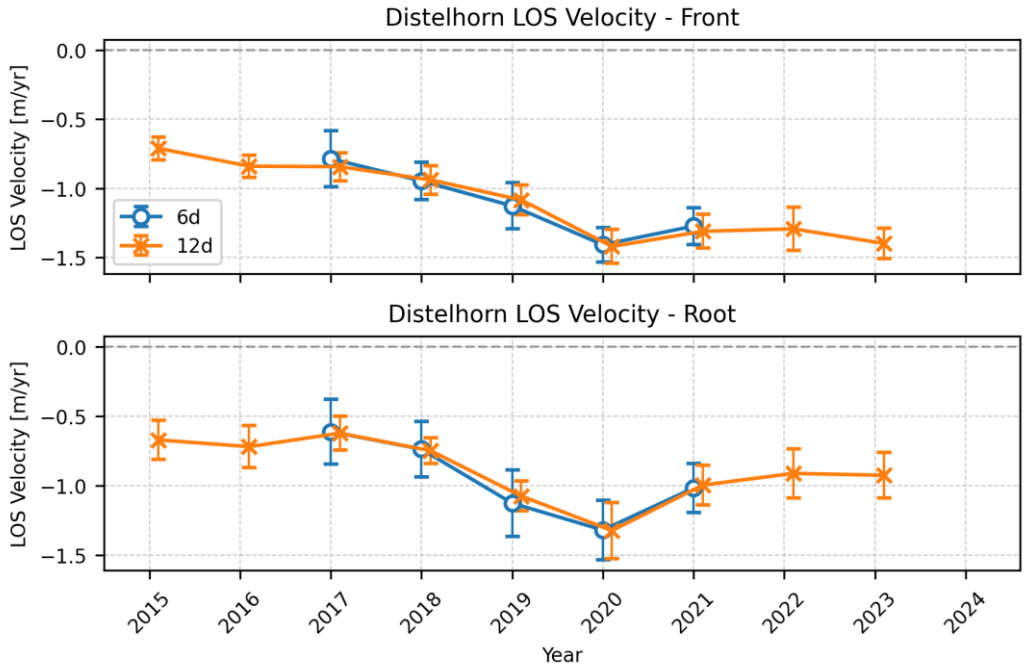

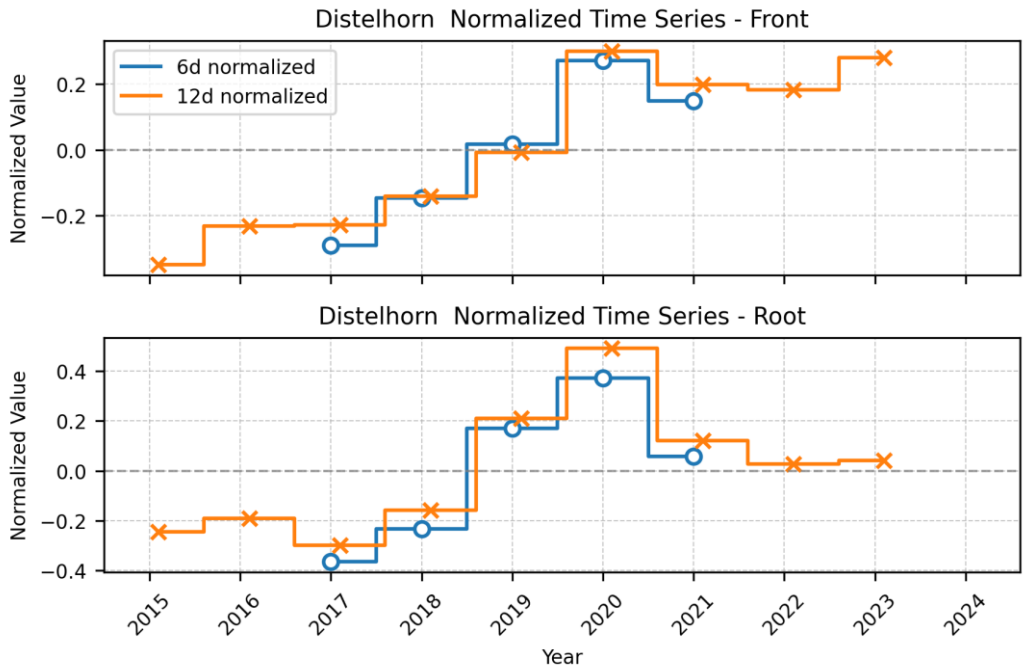

Grosses Gufer RGV Analysis

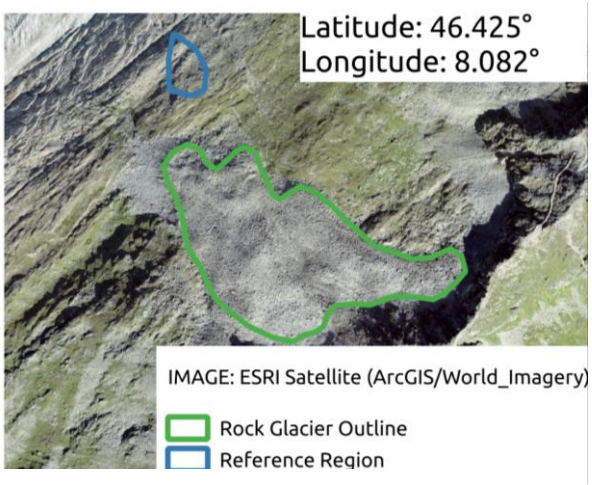

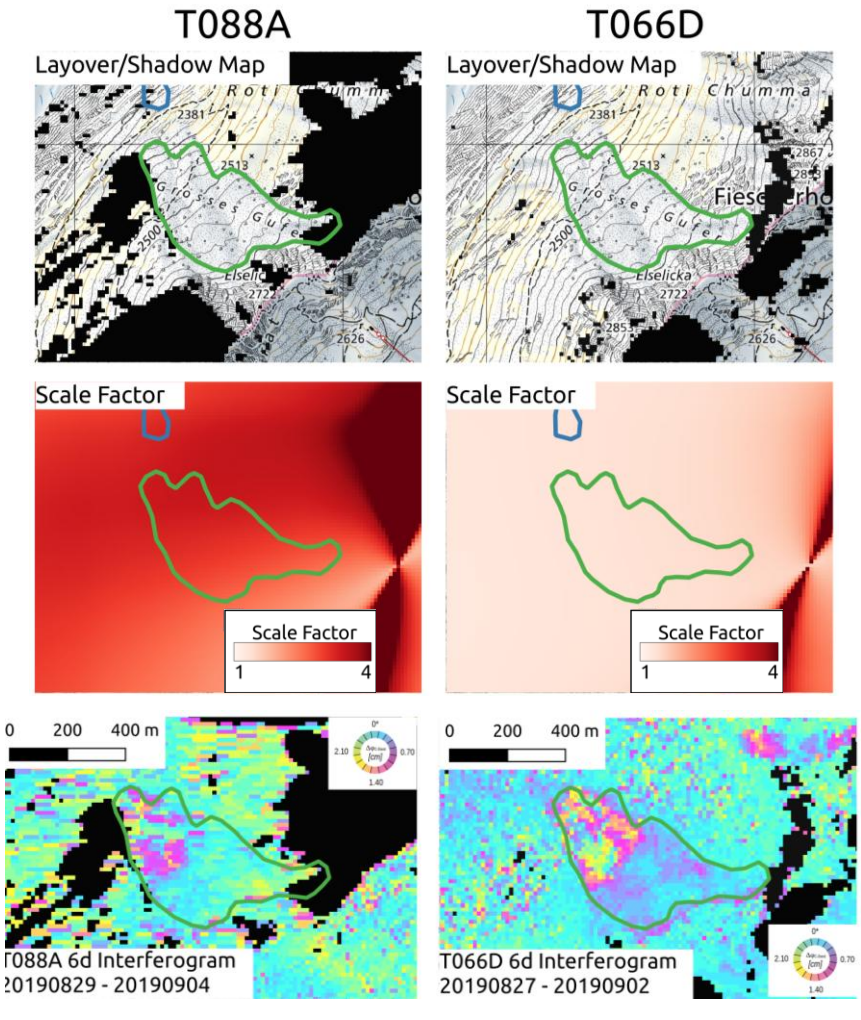

Layover/Shadow
Sentinel-1 data are acquired from two orbits (T088A and T066D). In both orbits the rock glacier region is mostly not affected by layover or shadow effects except for a small steep part at the root of the RG.

Scale Factor
T088A exhibits a more unfavorable viewing geometry with a Scale Factor approaching 4.
The Line-of-Sight for orbit T066D aligns well with the flow direction of the RG. Scale Factors for orbit T066D are in the range 1.3 to 1.4 over the RG.

Initial assessment
The T066D interferogram shows significant movement mainly at the front of the RG. Here with deformation rates are above 2.4cm/6d (approximately1.5 m/yr). The displacement pattern exhibits notable spatial variation. These variations create steep velocity gradients that likely require attention and corrections during phase unwrapping.

Line-of-Sight

For the RGV Analysis we use descending orbit 66.

Grosses Gufer RGV Analysis – Descending orbit 66

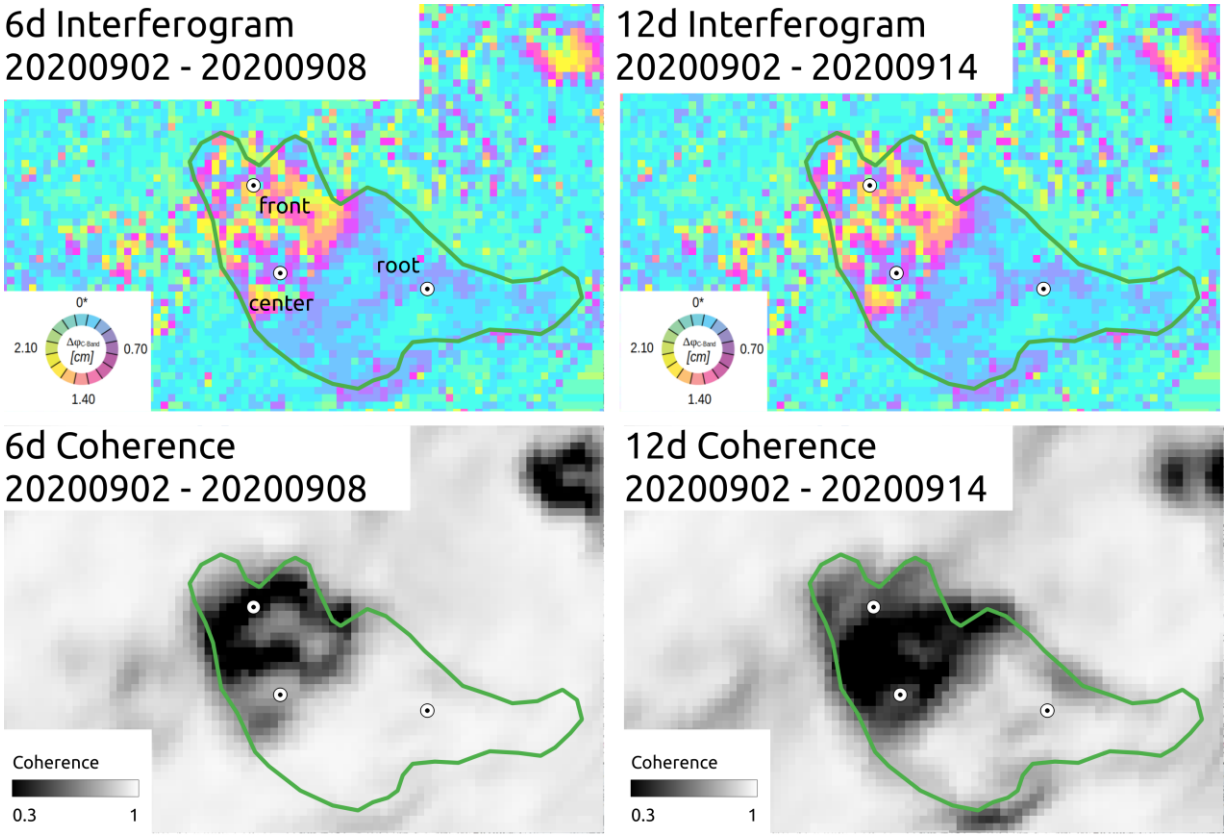

Overview

The figure above shows a 6d and 12d interferogram as well as the associated coherence from end of summer 2019. A selection of coherent interferograms was made manually for the further analysis. Many unwrapping issues are present due to high LOS velocities (> 1.5 m/yr) as well as abrupt changes. We selected three points (front, center, root) across the RG to extract LOS velocities time series.

Point Time Series

For the three monitoring points (front [46.4268, 8.0808], center [46.4253, 8.0814], and root [46.4250, 8.0851]) highlighted in the upper figures, we extracted LOS velocity time series, carefully checking and correcting any unwrapping issues. Each figure showing the time series on the next page displays the LOS displacement rates in m/yr in the top panel and the coherence in the bottom panel. For the LOS displacements, the coherent values are shown. For the coherence time series, all available 6-day pairs are shown. The coherence was obtained at the point location in the individual interferograms. Blue circles represent 6-day interferometric measurements, while orange crosses show 12-day measurements, with summer months (June-September) highlighted by gray vertical bands. 12-day measurements were excluded due to poor unwrapping results. For all root locations the coherence values in the summer season are generally high (>0.8). Both other points show significant lower coherence values going down to 0.3, likely due to the high displacement rates. Higher velocities as well as unfavorable conditions such as snow cover can decrease the coherence.

The highest velocities are measured at the front and center locations (~2.0-2.5 m/yr ~> 2.5-3.5 m/yr when assuming slope-parallel movement). The fluctuations during the individual summer months was high with rates of up to 1m/yr. LOS velocities at the root are were slow and below the sensitivity threshold of 0.1-0.2 m/yr. Scale Factors for the three points are 1.33 for front, 1.33 for center and 1.39 for root.

Grosses Gufer RGV Analysis – Descending orbit 66

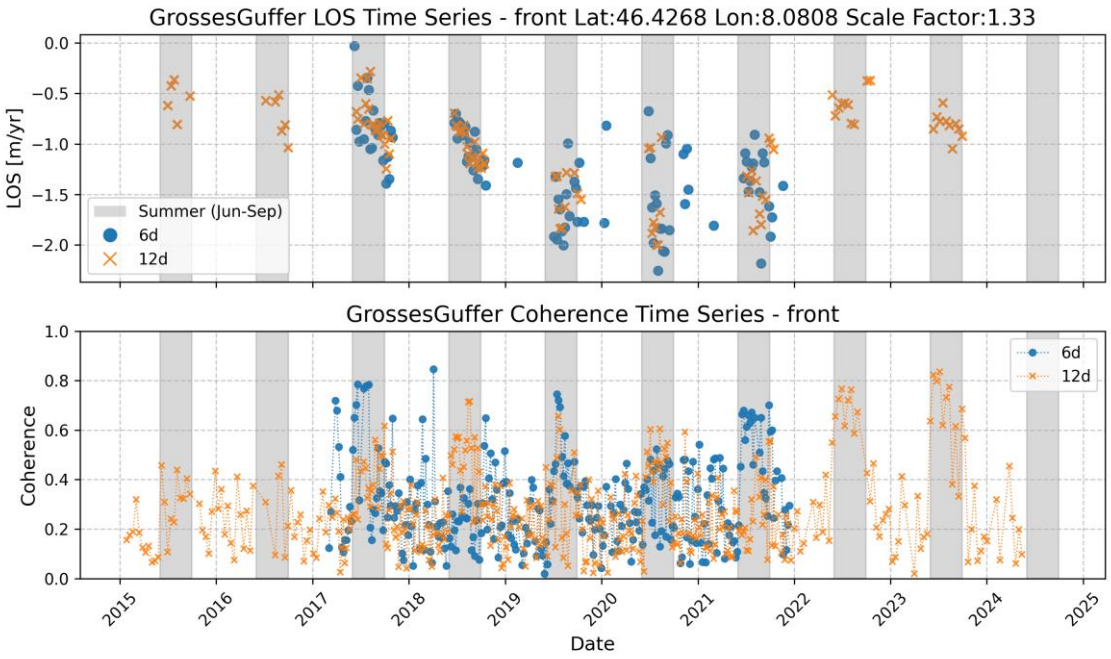

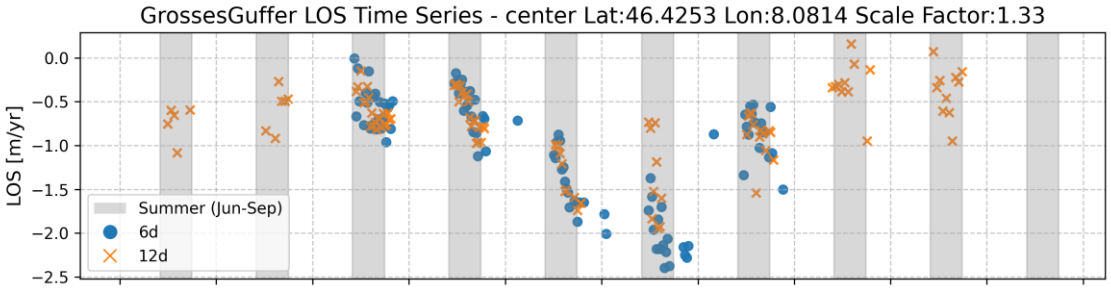

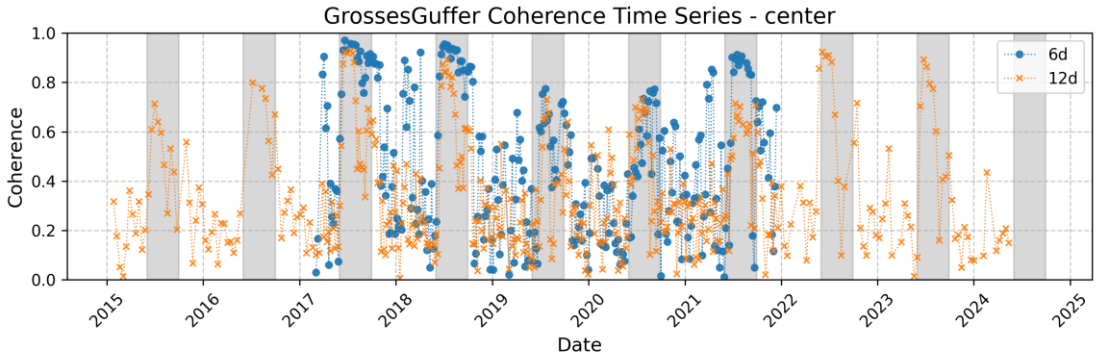

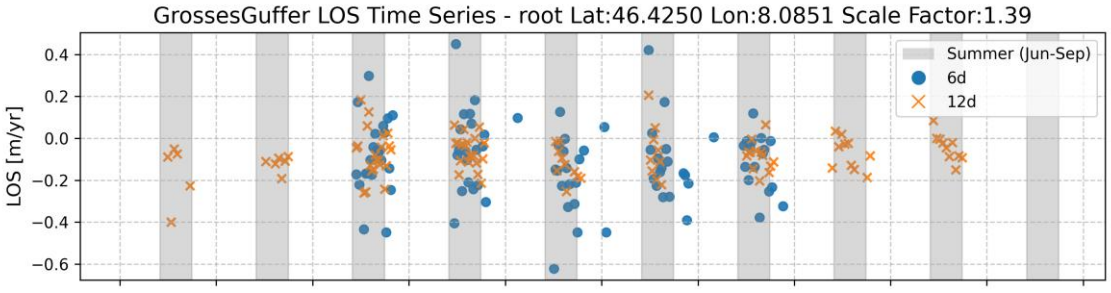

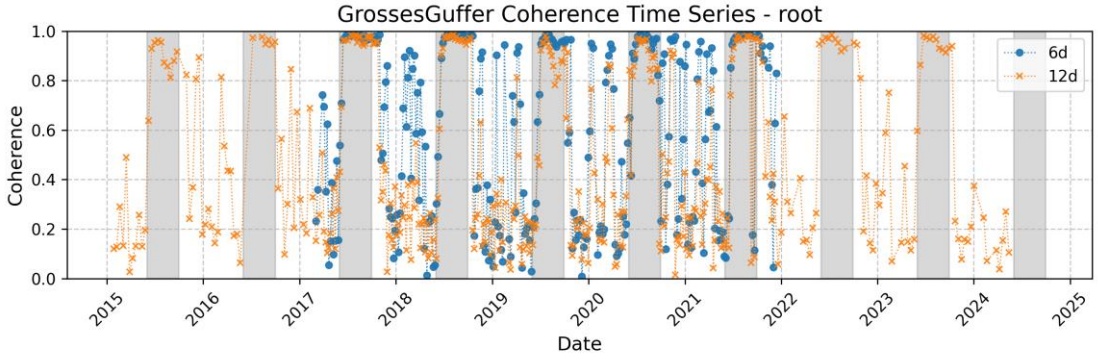

Grosses Gufer RGV Analysis – Descending orbit 66

Velocity variation over the years: We averaged the obtained LOS velocity rates from all three monitoring points to generate yearly velocity estimates. In the top three figures, the averaged LOS velocities per summer are shown. The error bars represent the standard deviation per year. The three bottom figures show the normalized values ((Avg_year/mean_overall)-1) to highlight relative changes independent of the absolute velocities. Note that higher variations are expected as the measured velocities approach the sensitivity/noise level.

Since the root location is bewlow the sensitivity limit we don't show the averaged yearly changes. The two locations front and center show a very similar temporal pattern, except for a discrepance between the 6-day and 12-day measurements for the center location in 2020. Due to the high velocities it is likely that the 12-day interferograms underestimate the displacement rates. The LOS displacement shows an overall acceleration from 2015 to 2020, followed by a subsequent deceleration.

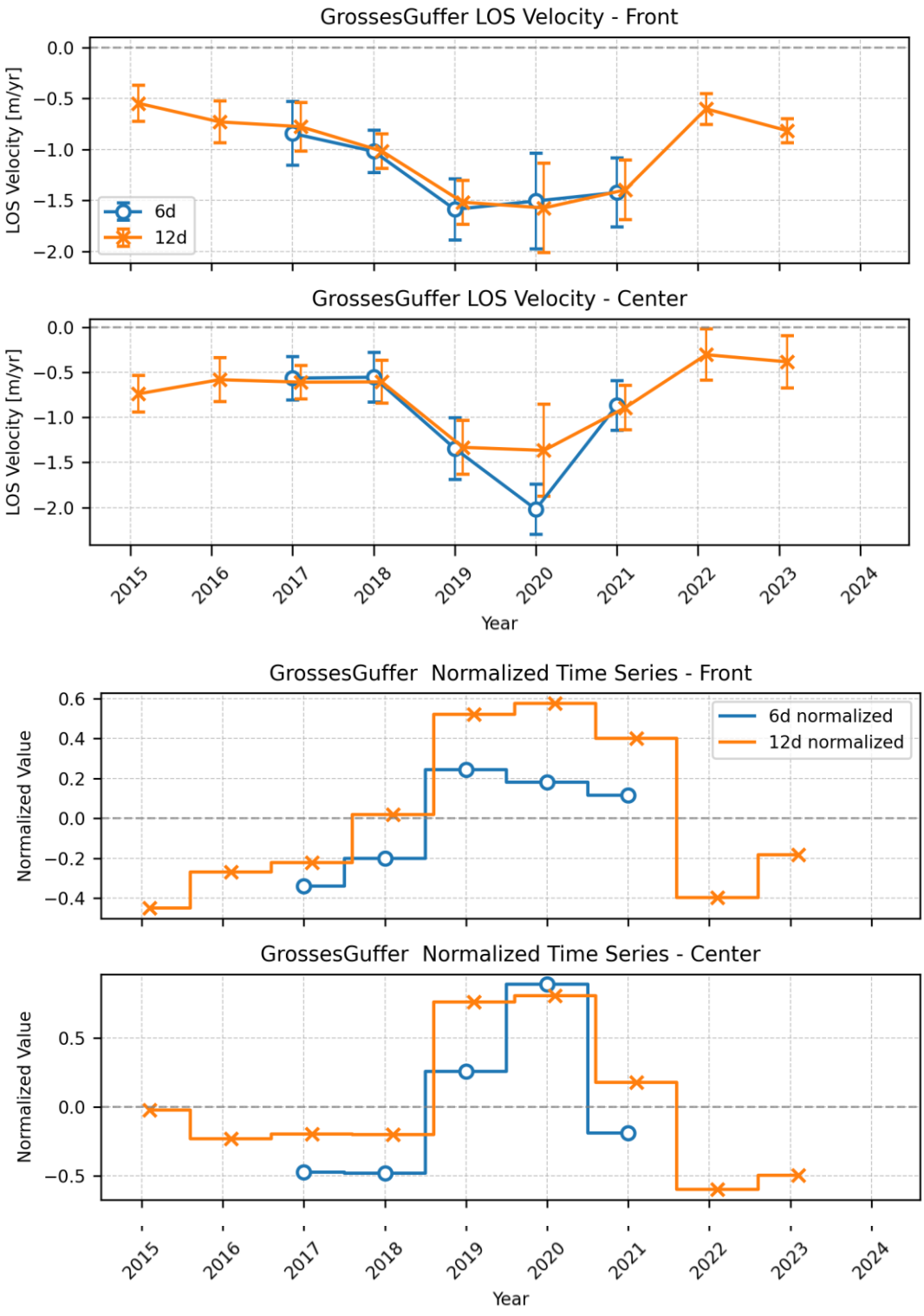

Rechy RGV Analysis

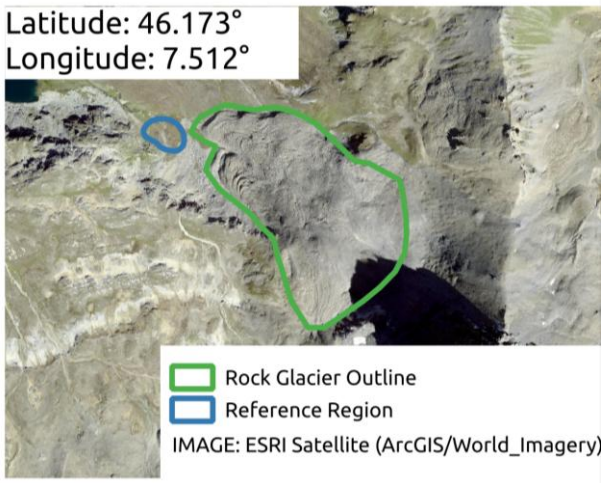

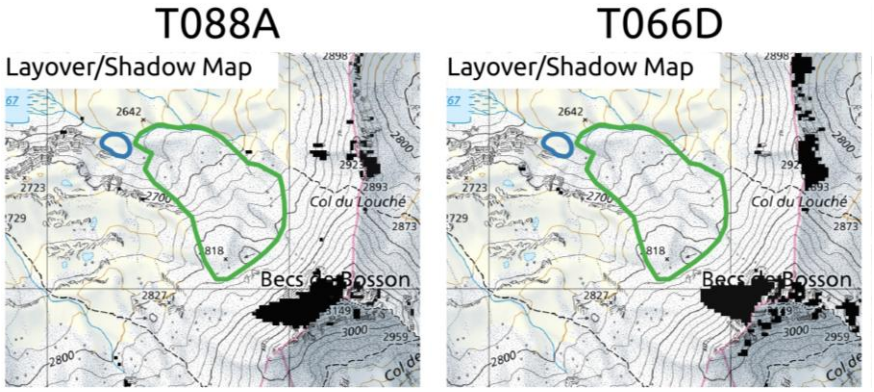

Layover/Shadow
Sentinel-1 data are acquired from two orbits (T088A and T066D). In both orbits the rock glacier region is mostly not affected by layover or shadow effects.

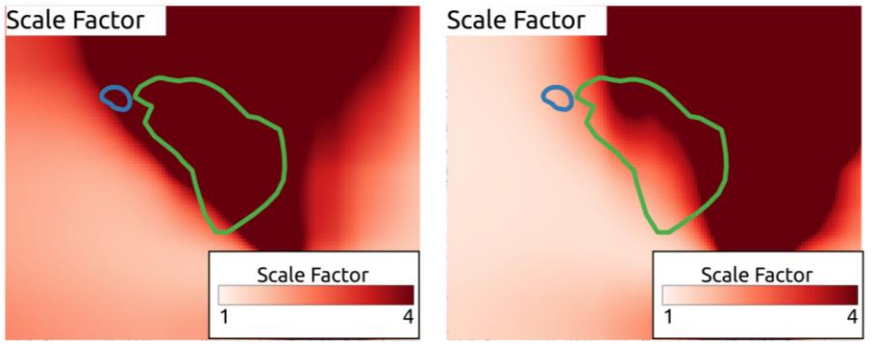

Scale Factor
T088A exhibits a more unfavorable viewing geometry with a Scale Factor mostly above 4.
The Line-of-Sight for orbit T066D aligns better with the flow direction of the RG. Scale Factors for orbit T066D are in the range 2 to 4.5 over the RG. The north-eastern part of the RG is not well aligned with either Line-of-Sight direction.

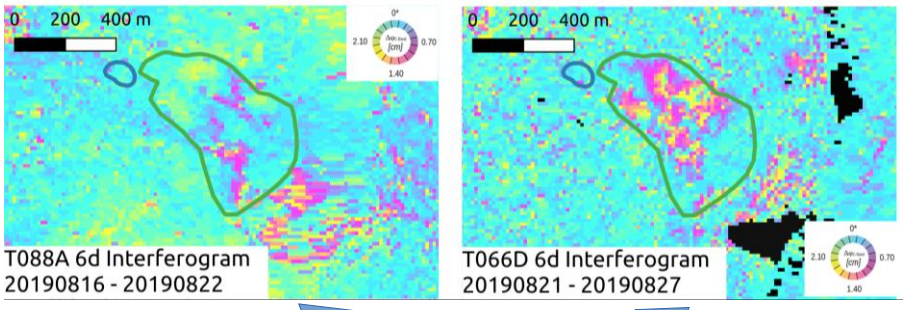

Line-of-Sight

Initial assessment
The T066D interferogram shows significant movement across the RG, with deformation rates ranging up to 2.4cm/6d (approximately 1.5m/yr). The displacement pattern exhibits notable spatial variation, with higher velocities concentrated in the front and center of the RG. These variations create steep velocity gradients that likely require attention and corrections during phase unwrapping.

For the RGV Analysis we use descending orbit 138.

Rechy RGV Analysis – Descending orbit 66

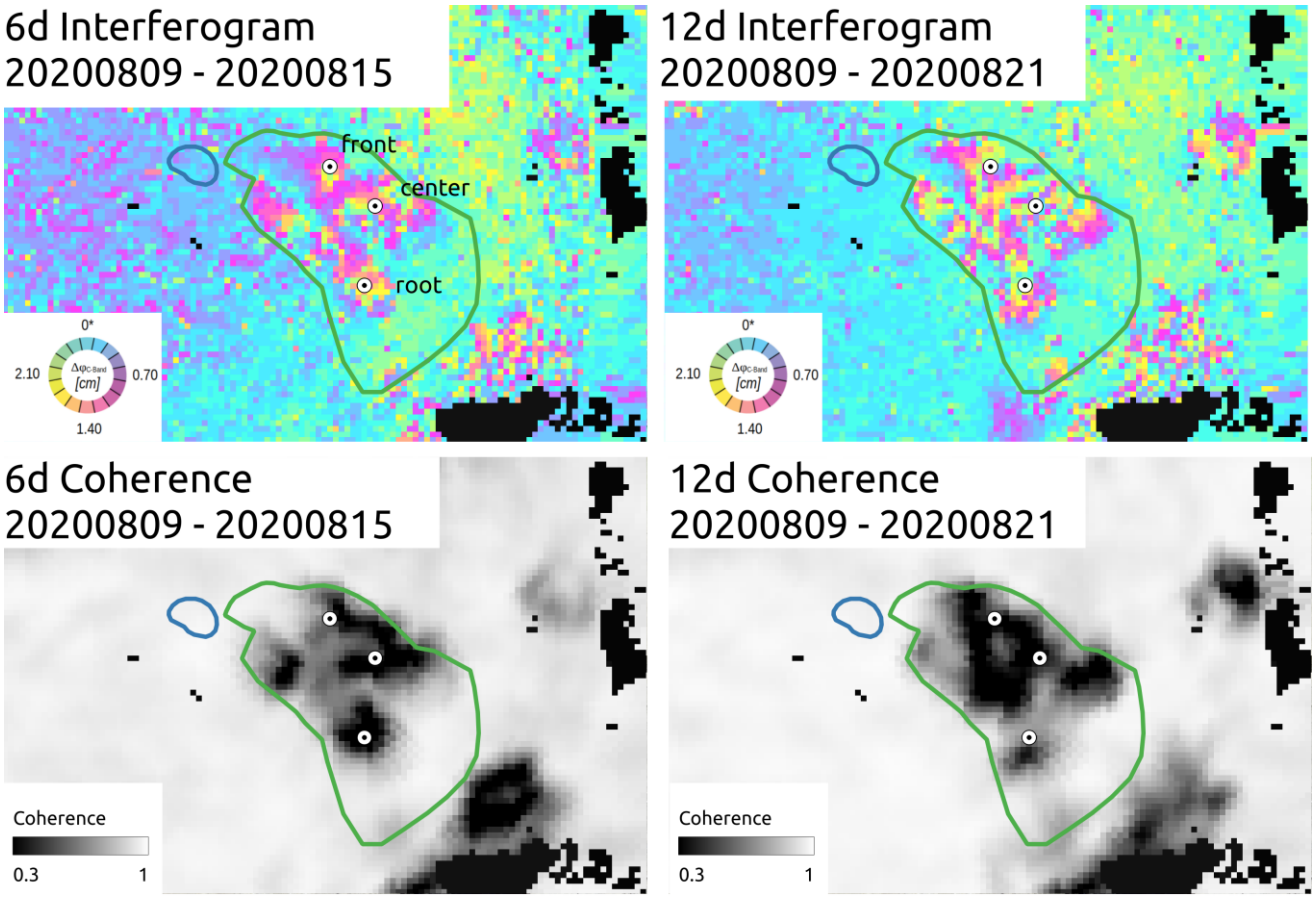

Overview

The figure above shows a 6d and 12d interferogram as well as the associated coherence from end of summer 2019. A selection of coherent interferograms was made manually for the further analysis. Many unwrapping issues are present due to high LOS velocities up to 1.5 m/yr as well as abrupt changes. We selected three points (front, center, root) across the RG to extract LOS velocities time series.

Point Time Series

For the three monitoring points (front [46.1738, 7.5114], center [46.1729, 7.5128], and root [46.1712, 7.5125]) highlighted in the upper figures, we extracted LOS velocity time series, carefully checking and correcting any unwrapping issues. Each figure showing the time series on the next page displays the LOS displacement rates in m/yr in the top panel and the coherence in the bottom panel. For the LOS displacements, the coherent values are shown. For the coherence time series, all available 6-day pairs are shown. The coherence was obtained at the point location in the individual interferograms. Blue circles represent 6-day interferometric measurements, while orange crosses show 12-day measurements, with summer months (June-September) highlighted by gray vertical bands. 12-day measurements were excluded due to poor unwrapping results. For all three locations the coherence values in the summer season are in mid range from 0.3 to 0.7, indicating high velocities. Higher velocities as well as unfavorable conditions such as snow cover can decrease the coherence.

All three locations show high LOS velocities of about 1.0 to 1.5 m/yr (up 3 to 5 m/yr when assuming slope-parallel movement). The fluctuations during the individual summer months is high with up to 1 m/yr. Scale Factors for the three points are 4.45 for front, 3.95 for center and 2.61 for root.

Rechy RGV Analysis – Descending orbit 66

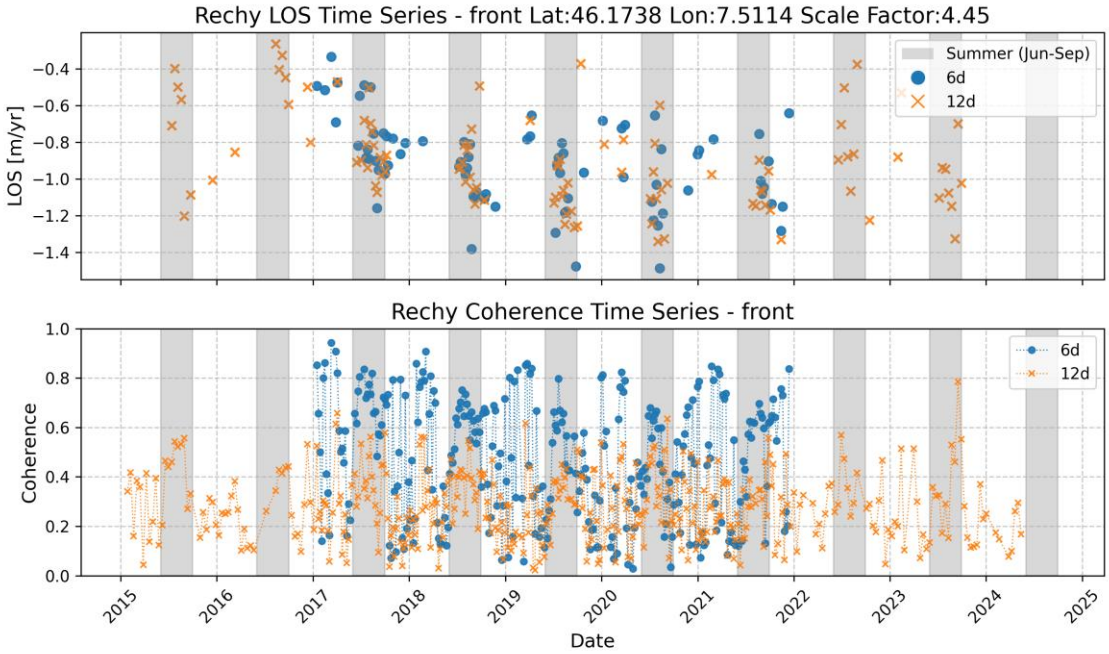

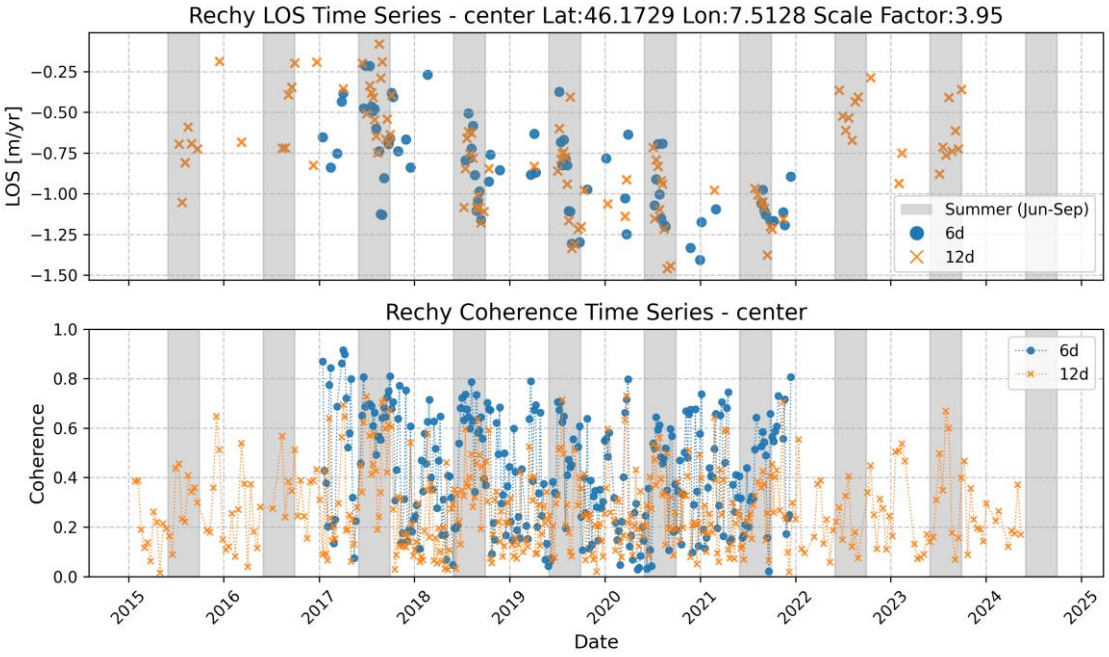

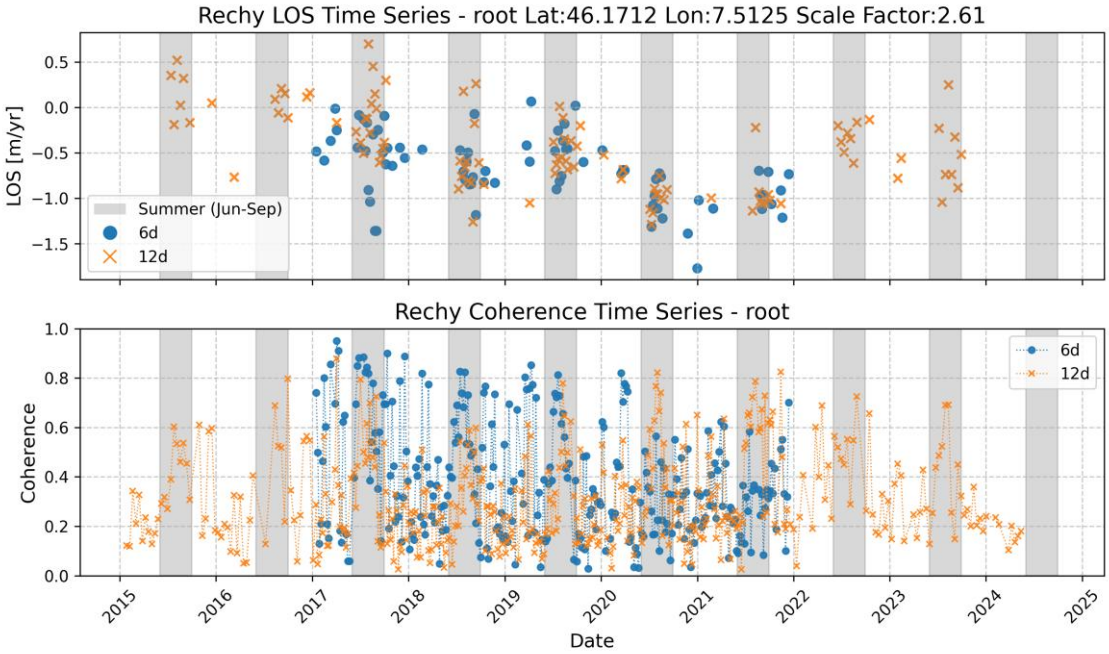

Rechy RGV Analysis – Descending orbit 66

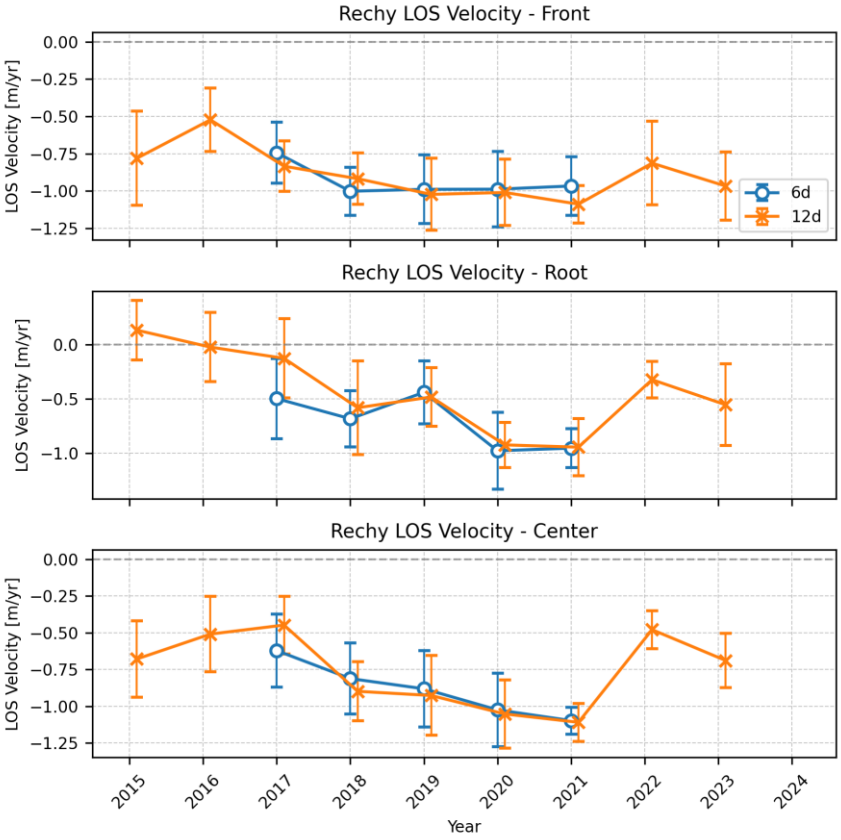

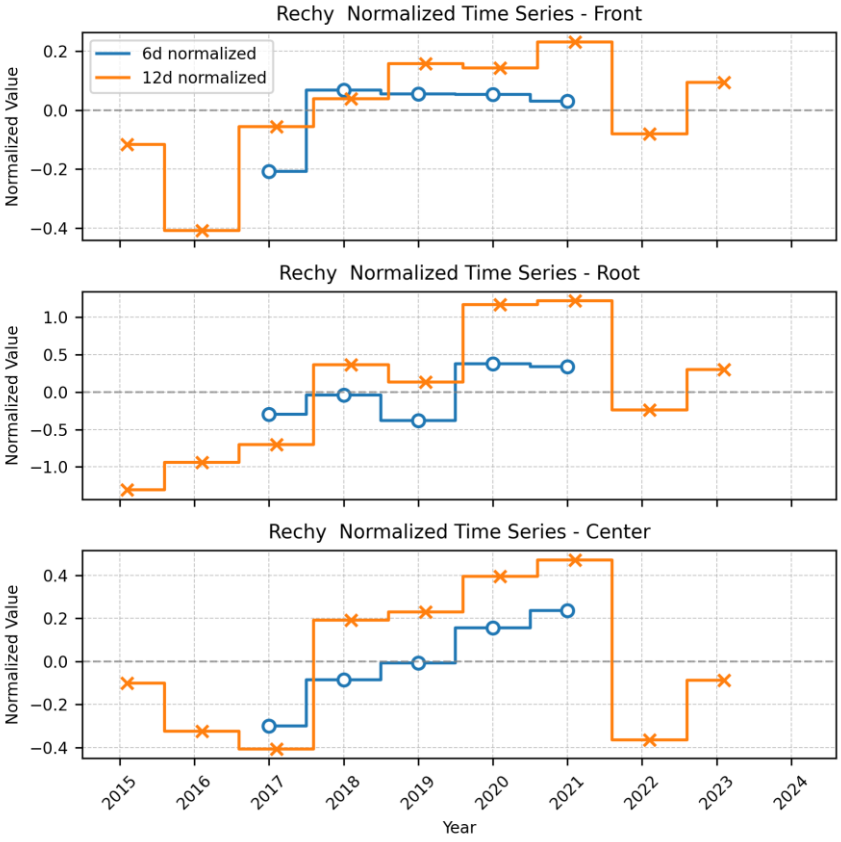

Velocity variation over the years: We averaged the obtained LOS velocity rates from all three monitoring points to generate yearly velocity estimates. In the top three figures, the averaged LOS velocities per summer are shown. The error bars represent the standard deviation per year. The three bottom figures show the normalized values ((Avg_year/mean_overall)-1) to highlight relative changes independent of the absolute velocities. Note that higher variations are expected as the measured velocities approach the sensitivity/noise level.

All three locations show a very similar temporal pattern, with an overall acceleration from 2015/16 to 2021, followed by a subsequent deceleration in 2022/23. The 6-day and 12-day data sjpw a realative good agreement but the errorbar and thus the variation during the years are large. The relative changes show thus some variation and need to interpreted with caution.

Steintälli RGV Analysis

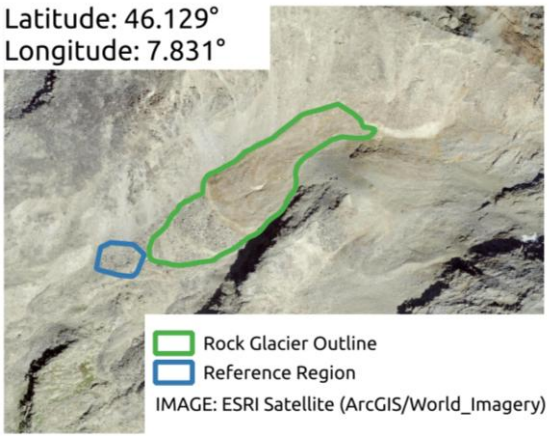

T088A

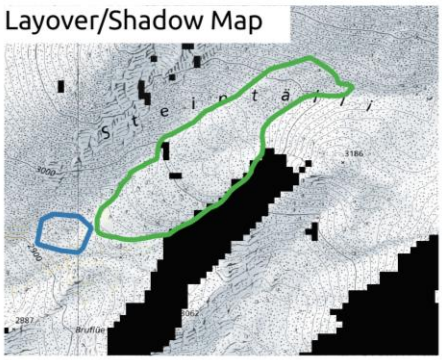

T066D

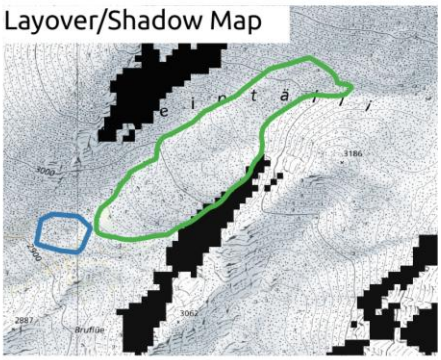

Layover/Shadow
Sentinel-1 data are acquired from two orbits (T088A and T066D). In both orbits the rock glacier region is not affected by layover or shadow effects.

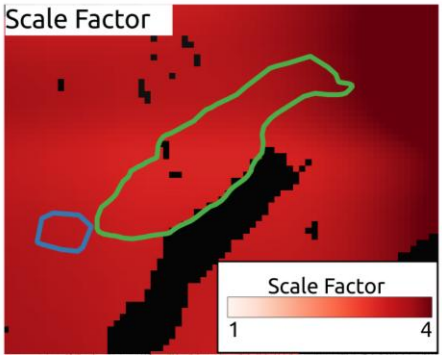

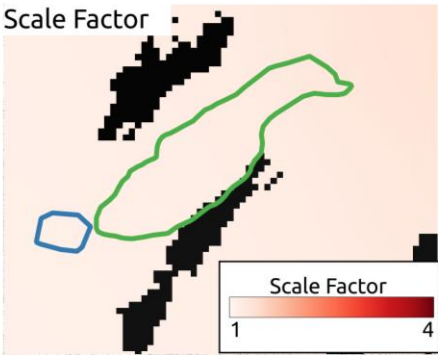

Scale Factor
T088A exhibits a more unfavorable viewing geometry with a Scale Factor abroaching 4.
The Line-of-Sight for orbit T066D aligns well with the flow direction of the RG.
Scale Factors for orbit T066D are in the range 1.1 to 1.4 over the RG.

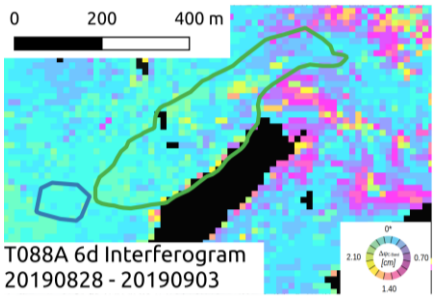

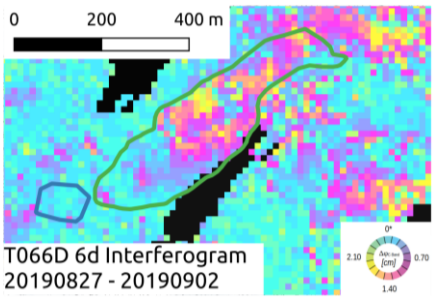

Initial assessment
The T066D interferogram shows significant movement across the RG, with deformation rates up to 2cm/6d (approximately 1.2 m/yr). The displacement pattern exhibits notable spatial variation, with higher velocities concentrated in center of the RG. These variations create steep velocity gradients that likely require attention and corrections during phase unwrapping.

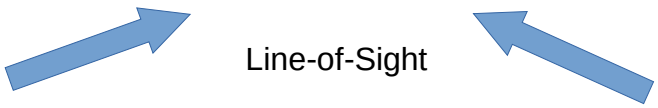

For the RGV Analysis we use descending orbit 66.

Steintälli RGV Analysis
Descending orbit 66

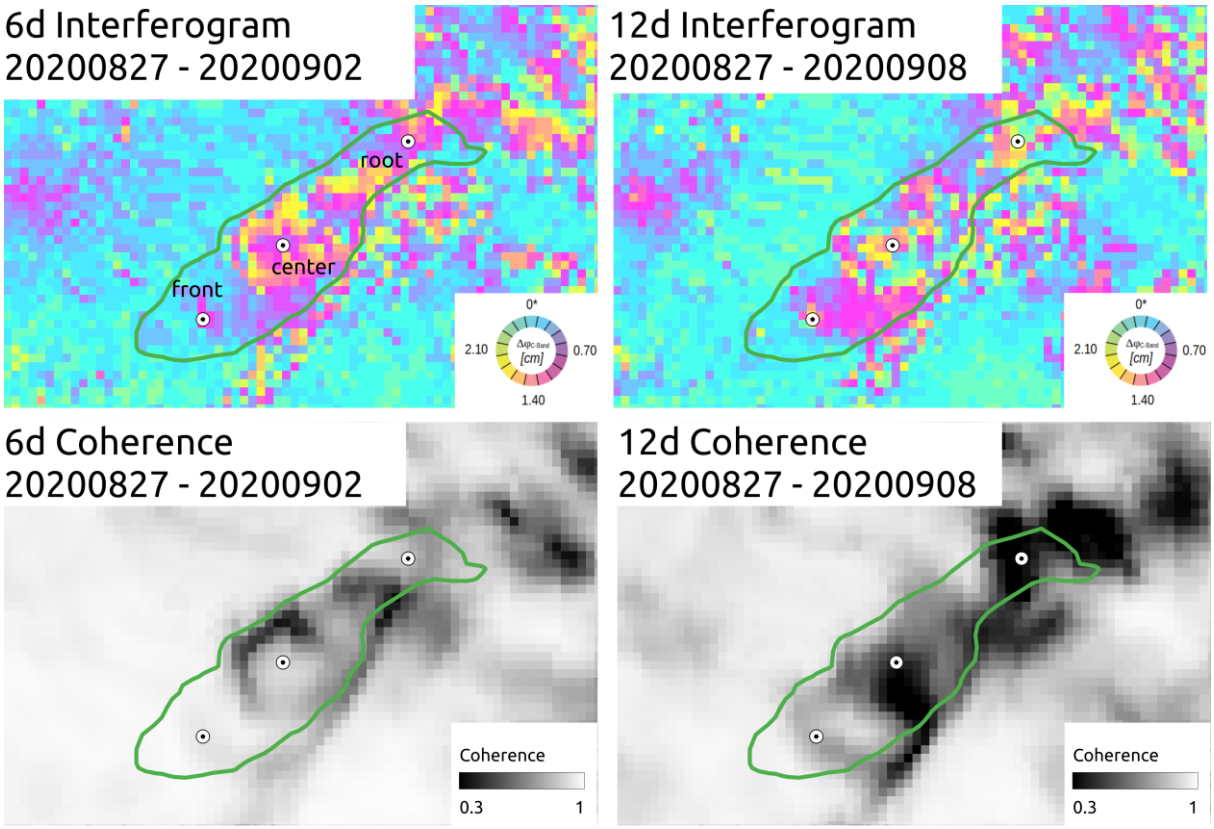

Overview

The figure above shows a 6d and 12d interferogram as well as the associated coherence from end of summer 2019. A selection of coherent interferograms was made manually for the further analysis. Many unwrapping issues are present due high phase noise. We selected three points (front, center, root) across the RG to extract LOS velocities time series.

Point Time Series

For the three monitoring points (front [46.1276, 7.8287], center [46.1302, 7.8331], and root [46.1302, 7.8331]) highlighted in the upper figures, we extracted LOS velocity time series, carefully checking and correcting any unwrapping issues. Each figure showing the time series on the next page displays the LOS displacement rates in m/yr in the top panel and the coherence in the bottom panel. For the LOS displacements, the coherent values are shown. For the coherence time series, all available 6-day pairs are shown. The coherence was obtained at the point location in the individual interferograms. Blue circles represent 6-day interferometric measurements, while orange crosses show 12-day measurements, with summer months (June-September) highlighted by gray vertical bands. 12-day measurements were excluded due to poor unwrapping results. For all three locations the coherence values in the summer season are generally high (>0.6). Higher velocities as well as unfavorable conditions such as snow cover can decrease the coherence.

The velocities at the three locations are relatively similar (~0.5-0.8 m/yr ~> 0.6-1.0 m/yr when assuming slope-parallel movement). The fluctuations during the individual summer months was big and vary up to 0.6 m/yr. Scale Factors for the three points are 1.12 for front, 1.14 for center and 1.22 for root.

Steintälli RGV Analysis
Descending orbit 66

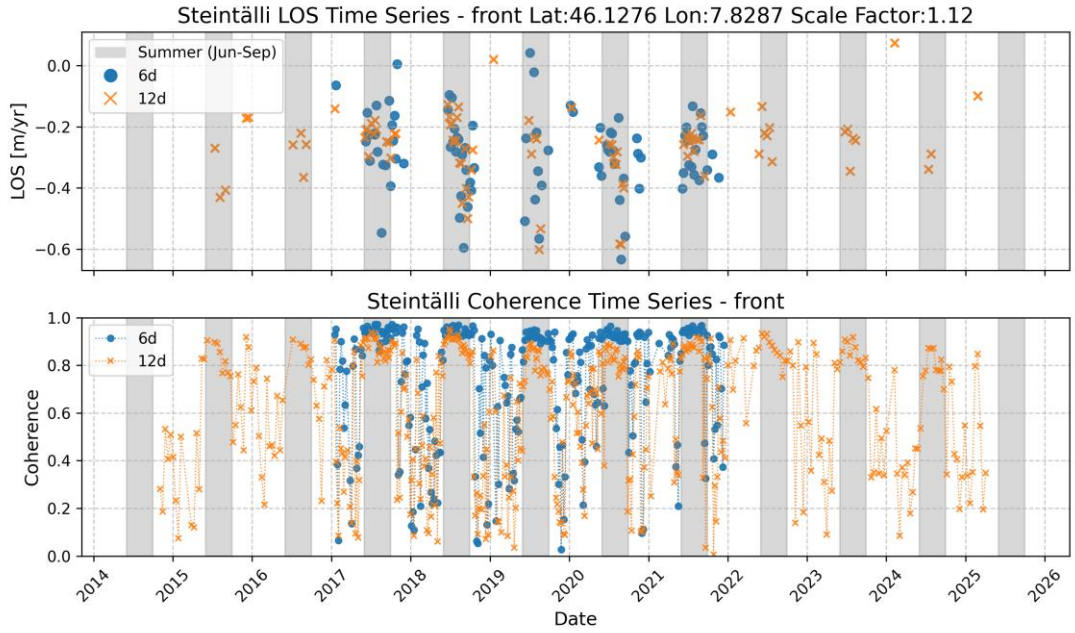

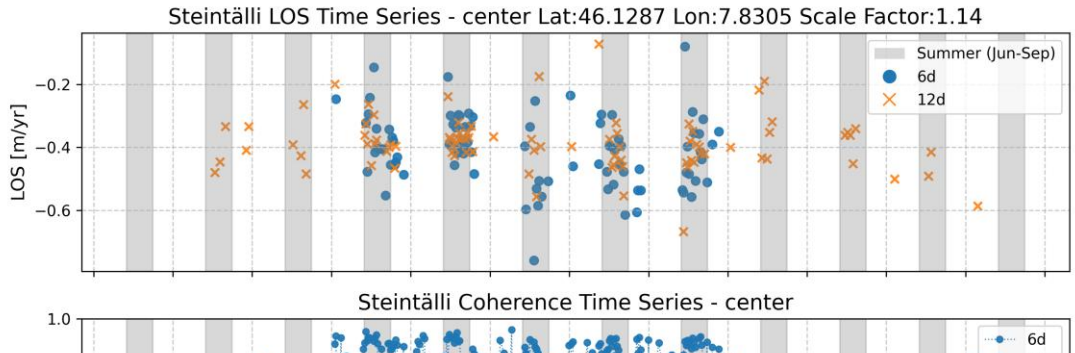

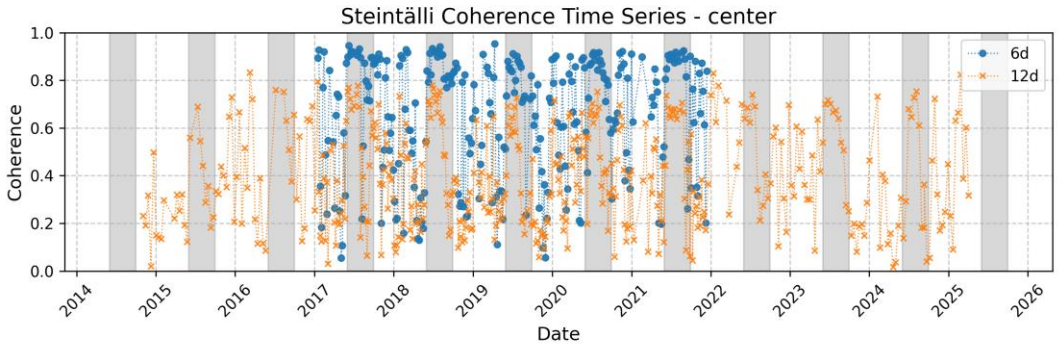

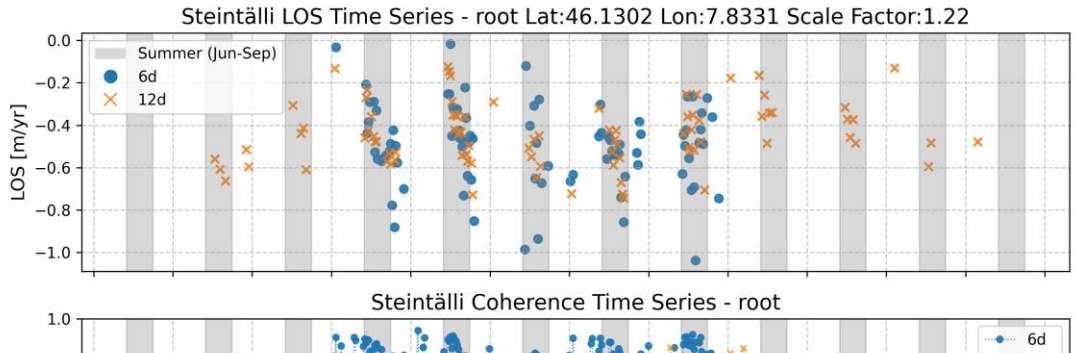

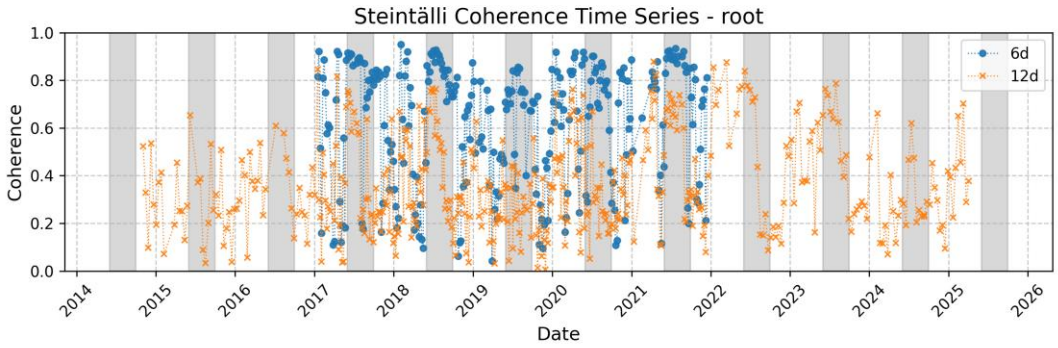

Steintälli RGV Analysis
Descending orbit 66

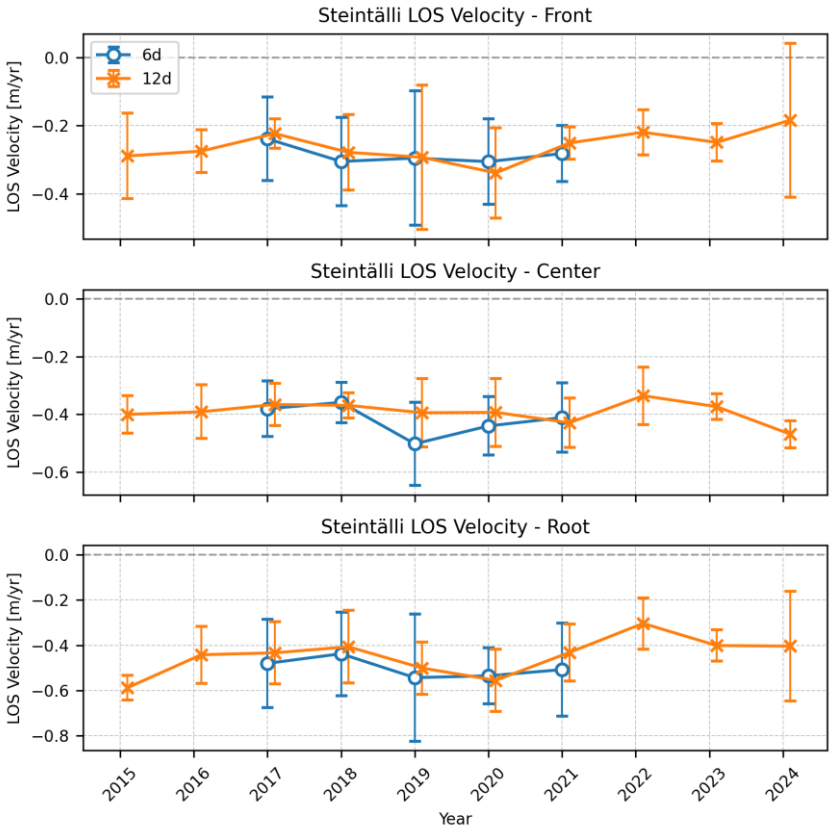

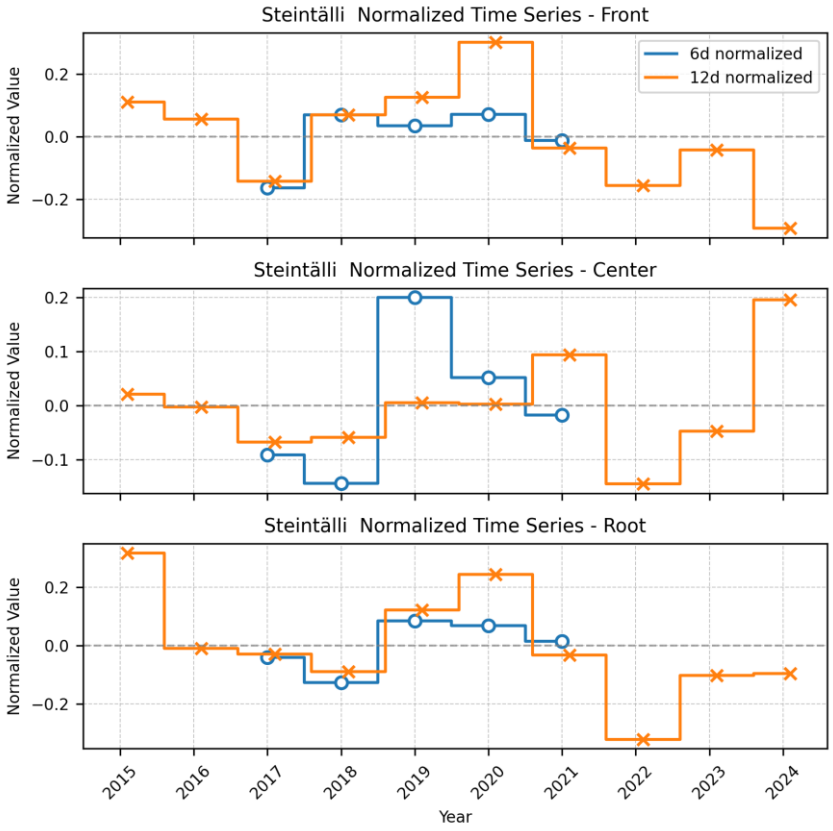

Velocity variation over the years: We averaged the obtained LOS velocity rates from all three monitoring points to generate yearly velocity estimates. In the top three figures, the averaged LOS velocities per summer are shown. The error bars represent the standard deviation per year. The three bottom figures show the normalized values ((Avg_year/mean_overall)-1) to highlight relative changes independent of the absolute velocities. Note that higher variations are expected as the measured velocities approach the sensitivity/noise level.

For all three measurement location the error bars are big due to the large fluctuation during the summer months. The LOS displacement rates vary only slightly but are generally highest in 2019/ 2020.

Gran Sometta RGV Analysis

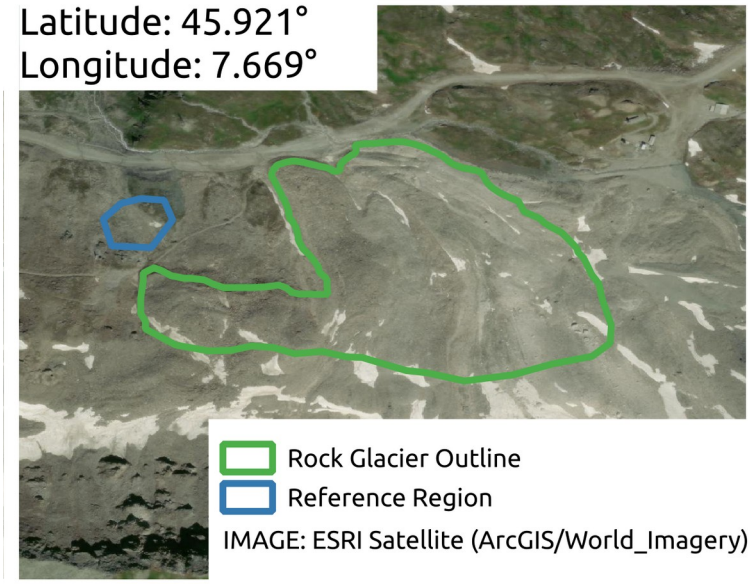

T088A

T139D

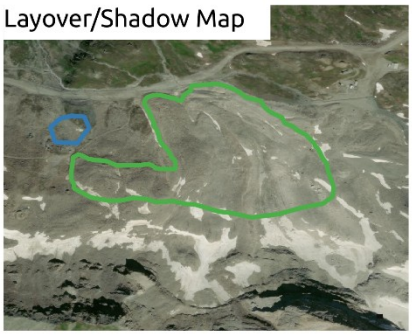

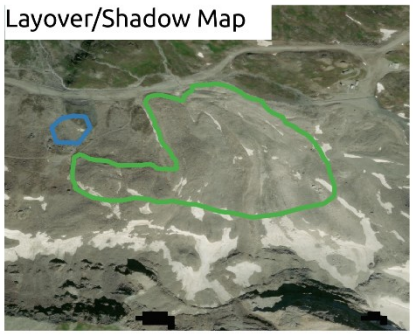

Layover/Shadow
Sentinel-1 data are acquired from two orbits (T088A and T139D). In orbit T139D the rock glacier is strongly affected by layover/shadow. In orbit T088A the rock glacier region is not affected by layover or shadowing effects.

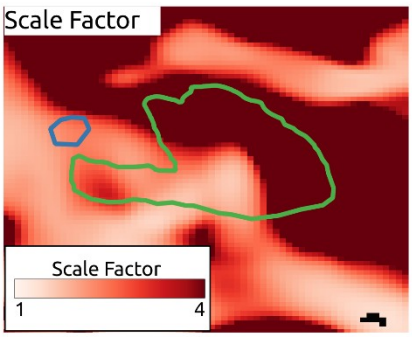

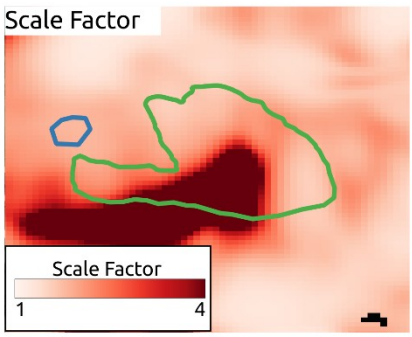

Scale Factor:
The Line-of-Sight for both orbits align only for part of the RG. For orbit T088A the western part of the RG is covered with scale factors in the range 1.1 to 2.5.
For orbit T139D the eastern part of the RG is covered with similar scale factors in the range 1.5 to 2.2.

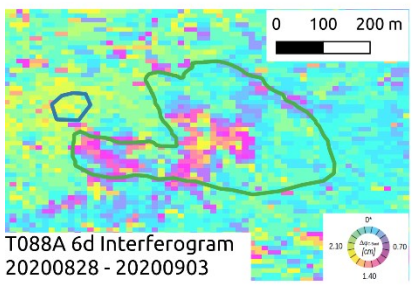

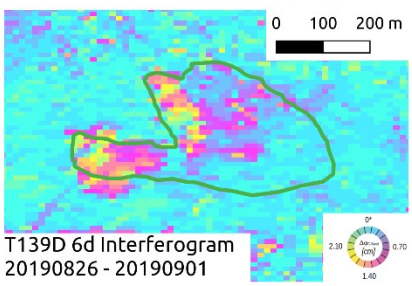

Initial assessment
Both interferograms show significant movement of up to 2 to 3cm over the 6-day period (equivalent to approximately 1.2-1.8m/year). These localized high-velocity zones likely present challenges for phase unwrapping procedures in subsequent processing stages.

Line-of-Sight

For the RGV Analysis we use both orbits.

Gran Sometta RGV Analysis – Ascending orbit 88

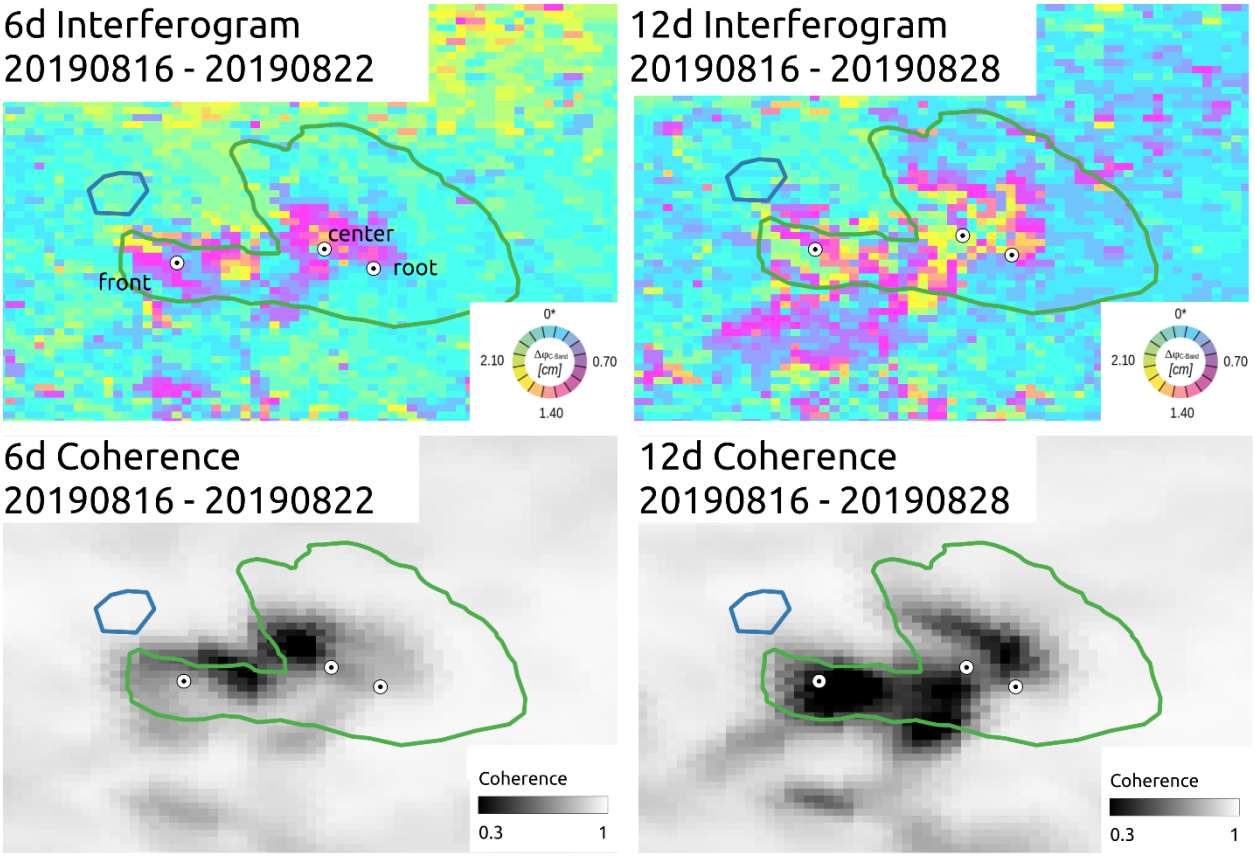

Overview

The figure above shows a 6d and 12d interferogram as well as the associated coherence from end of summer 2019. A selection of coherent interferograms was made manually for the further analysis. Many unwrapping issues are present due to high LOS velocities (up to 2 m/yr) as well as abrupt changes. We selected three points (front, center, root) across the RG to extract LOS velocities time series.

Point Time Series

For the three monitoring points (front [45.9203, 7.6663], center [45.9206, 7.6690], and root [45.9203 7.6699]) highlighted in the upper figures, we extracted LOS velocity time series, carefully checking and correcting any unwrapping issues. Each figure showing the time series on the next page displays the LOS displacement rates in m/yr in the top panel and the coherence in the bottom panel. For the LOS displacements, the coherent values are shown. For the coherence time series, all available pairs are shown. The coherence was obtained at the point location in the individual interferograms. Blue circles represent 6-day interferometric measurements, while orange crosses show 12-day measurements, with summer months (June-September) highlighted by gray vertical bands. In general, the 12-day interferogram coherence values are lower than the 6-day. For the locations center and root the coherence values in the summer season are generally high (>0.6). Higher velocities as well as unfavorable conditions such as snow cover decrease the coherence.

The highest velocities are measured at the center location (~1-1.2 m/yr ~> 2.3-3 m/yr when assuming slope-parallel movement). The variability during the summer months is high with large increases/decrease of up to 0.8 m/yr (see figure on next page). The LOS velocity at the front is up to 0.7 m/yr with also large seasonal fluctuations. At the root, the velocities are relatively stable around 0.2 m/yr and thus just the sensitivity limits. Scale Factors for the three points are 2.77 for front, 2.28 for center and 1.17 for root.

Gran Sometta RGV Analysis – Ascending orbit 88

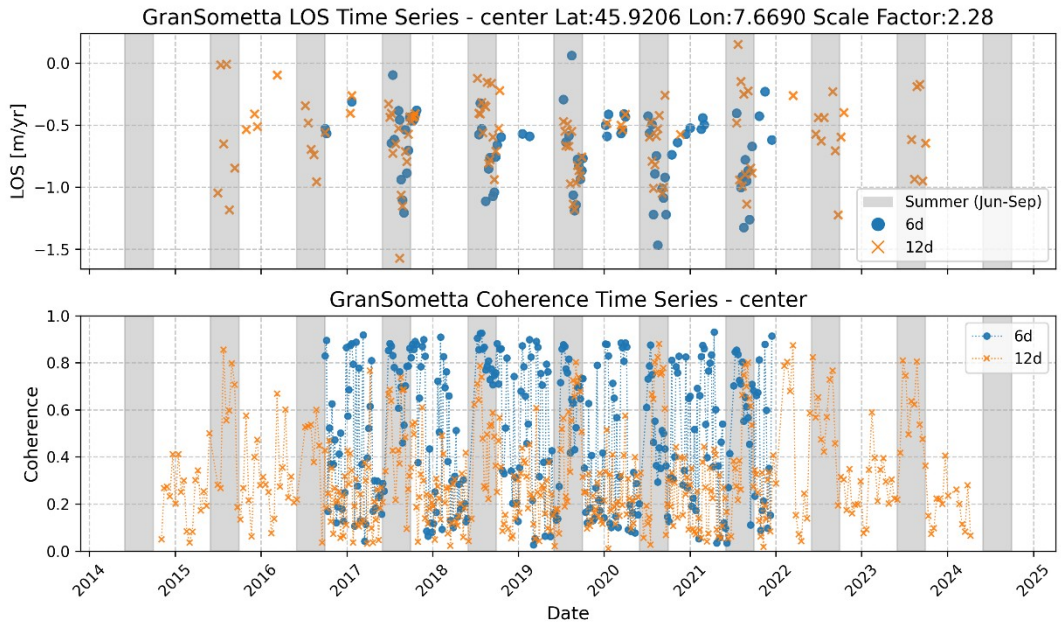

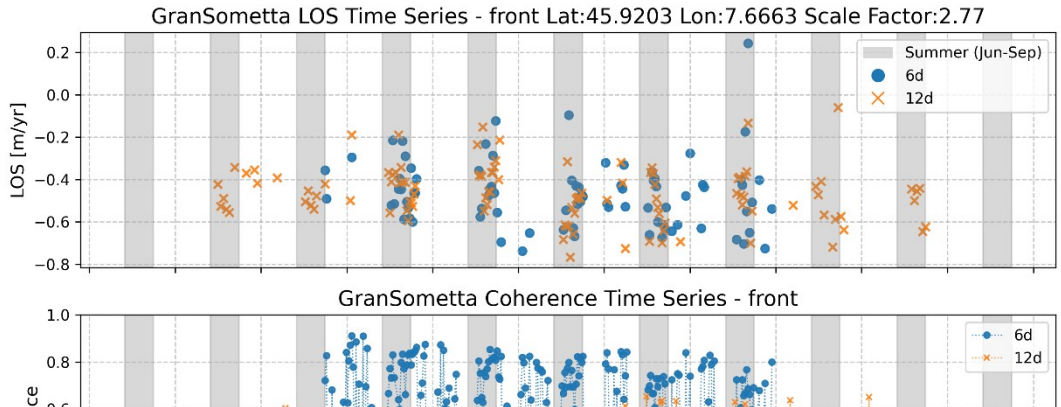

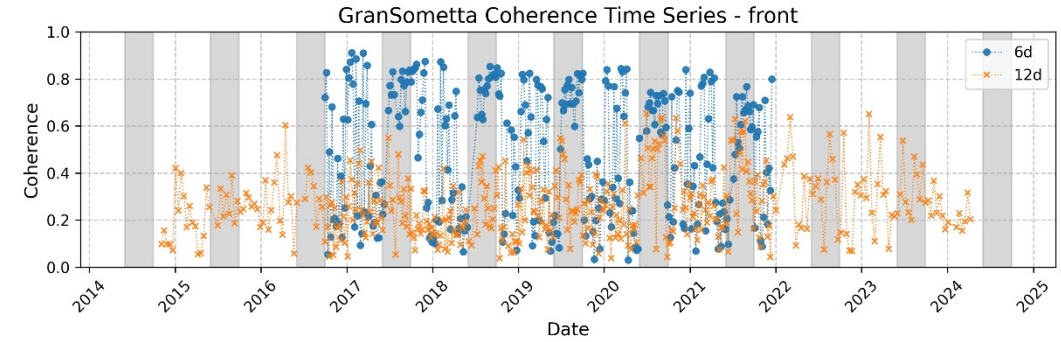

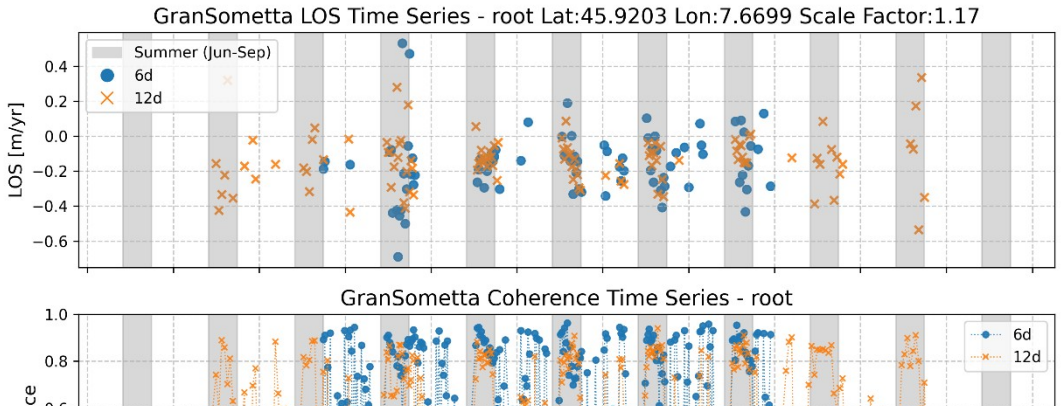

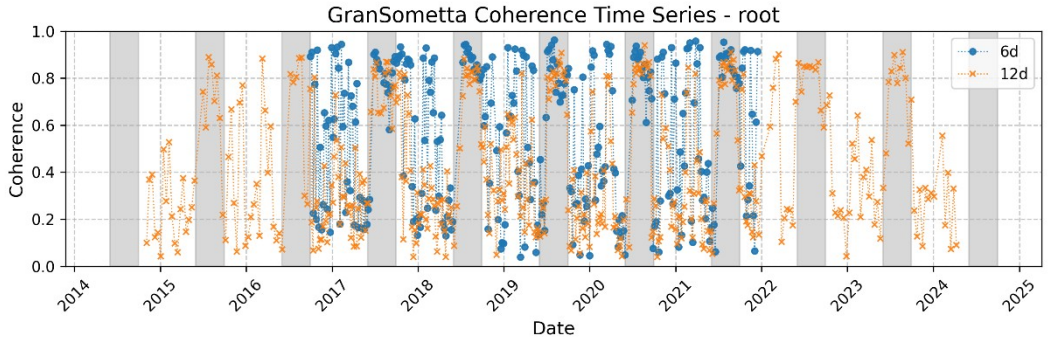

Gran Sometta RGV Analysis – Ascending orbit 88

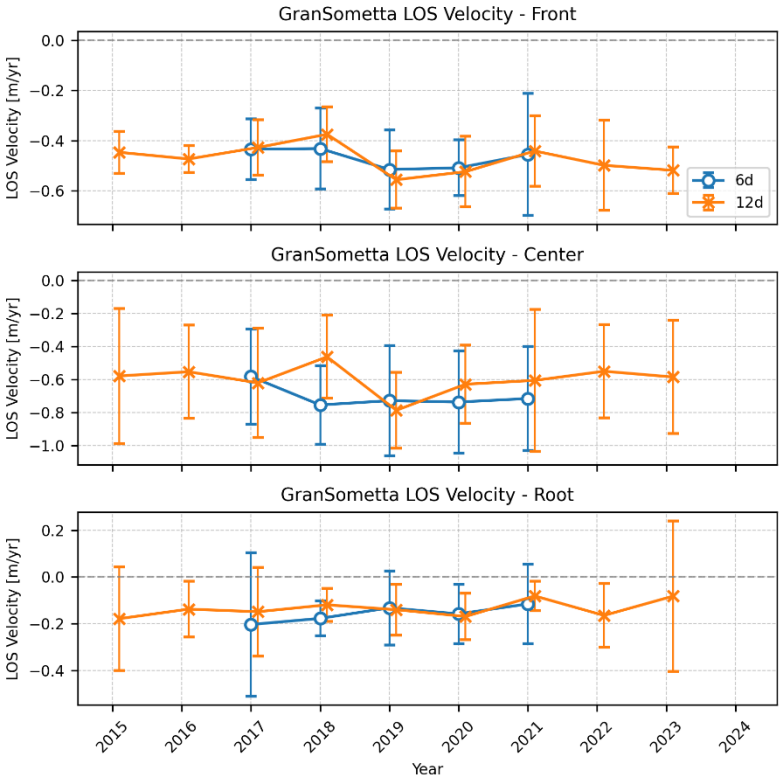

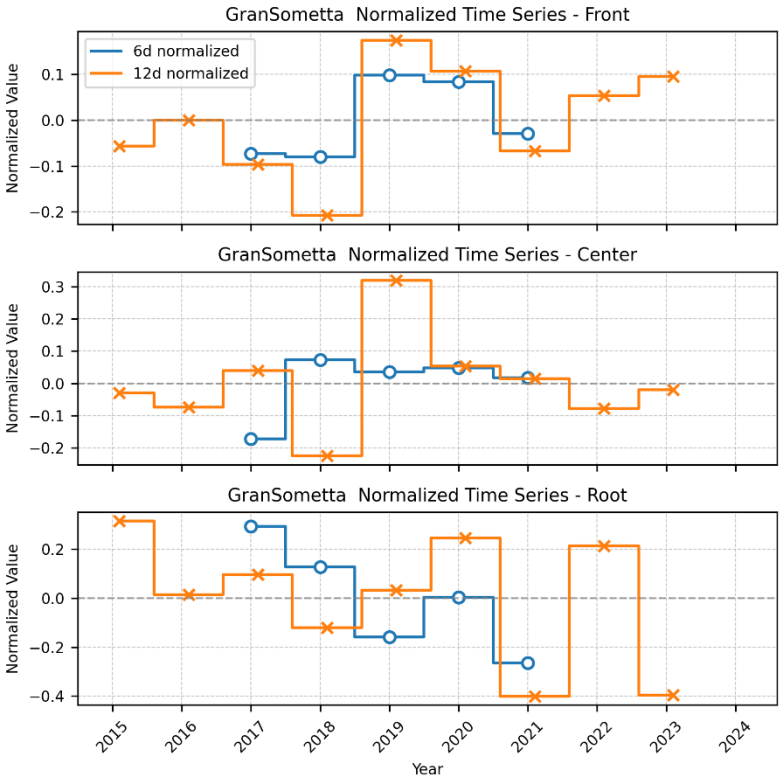

Velocity variation over the years: We averaged the obtained LOS velocity rates from all three points to generate yearly velocity estimates. In the top figures, the averaged LOS velocities per summer are shown. The error bars represent the standard deviation per year. The two bottom figures show the normalized values ((Avg_year/mean_overall)-1) to highlight relative changes independent of the absolute velocities. Note that higher variations are expected as the measured velocities approach the sensitivity/noise level.

All points show large error bars. This is due to strong seasonal variations with large increases starting at nearly no movement during winter and reaching up to 1 m/yr for the center location. The selection of which points to use in the analysis thus plays a significant role. For example, in 2018 the 12d LOS velocity appears significantly lower than the 6d LOS velocity for the center location, because fast-moving points were excluded from the analysis due to decorrelation. For the root location the velocities are close to the sensitivity limit and thus, small seasonal variations can not be measured accurately. The time series displayed should thus be interpreted with caution.

Gran Sometta RGV Analysis – Descending orbit 139

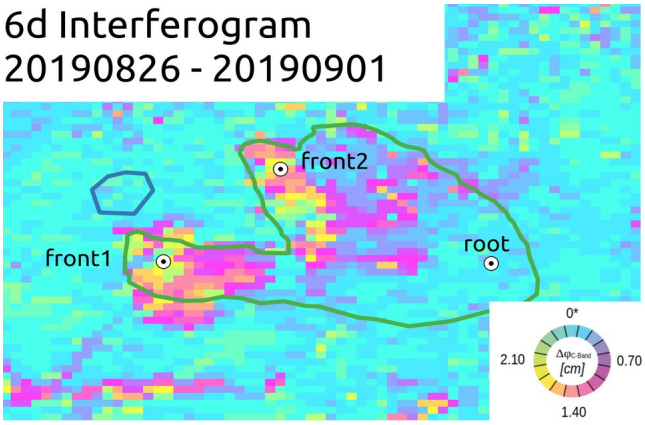

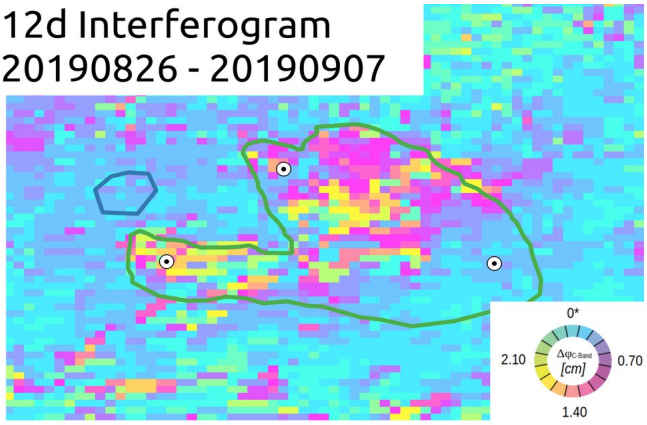

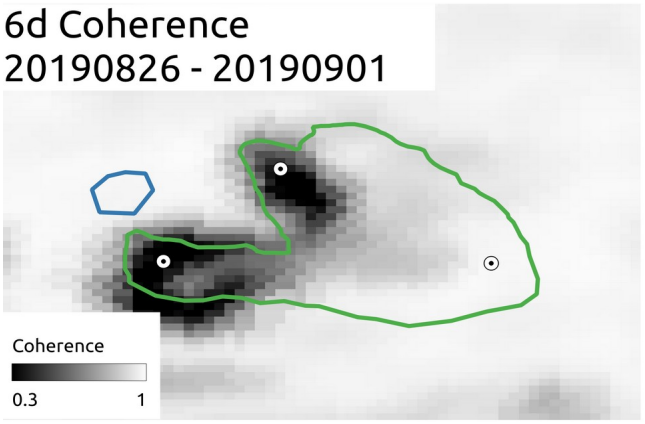

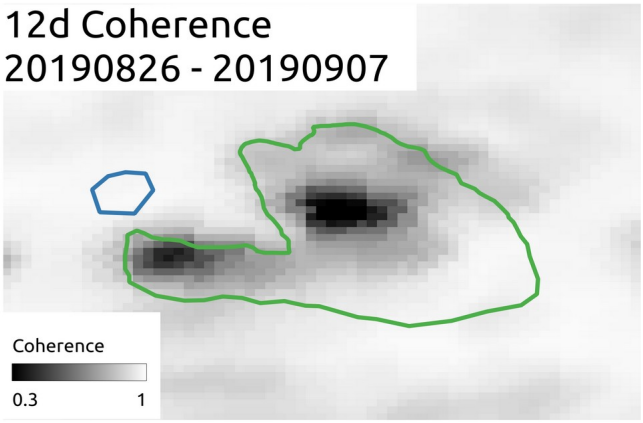

Overview

The figure above shows a 6d and 12d interferogram as well as the associated coherence from end of summer 2019. A selection of coherent interferograms was made manually for the further analysis. Many unwrapping issues are present due to high LOS velocities (up to 2 m/yr) as well as abrupt changes. We selected three points (front, center, root) across the RG to extract LOS velocities time series.

Point Time Series

For the three monitoring points (front1 [45.9204, 7.6660], front2 [45.9221, 7.6680], and root [45.9203 7.6717]) highlighted in the upper figures, we extracted LOS velocity time series, carefully checking and correcting any unwrapping issues. Each figure showing the time series on the next page displays the LOS displacement rates in m/yr in the top panel and the coherence in the bottom panel. For the LOS displacements, the coherent values are shown. For the coherence time series, all available pairs are shown. The coherence was obtained at the point location in the individual interferograms. Blue circles represent 6-day interferometric measurements, while orange crosses show 12-day measurements, with summer months (June-September) highlighted by gray vertical bands. In general, the 12-day interferogram coherence values are lower than the 6-day. For the root locations the coherence values in the summer season are generally high (>0.8). For the two front locations the coherence was significantly lower (0.3-0.5). Due to the high velocities for front 1 only a processing of the 6d-interferograms was possible. Higher velocities as well as unfavorable conditions such as snow cover decrease the coherence.

The highest velocities are measured at the front1 location (~1.5-2.0 m/yr ~> 3-4 m/yr when assuming slope-parallel movement) with large fluctuations due to the low data quality (see figures on next page). . The LOS velocity at the front2 location was also high with LOS velocities up to 1.5 m/yr. Here a large seasonal variation is visible. At root, the velocities are relatively stable around 0 m/yr and thus inside the sensitivity limits. Scale Factors for the three points are 2.01 for front, 1.59 for center and 1.57 for root.

Gran Sometta RGV Analysis – Descending orbit 139

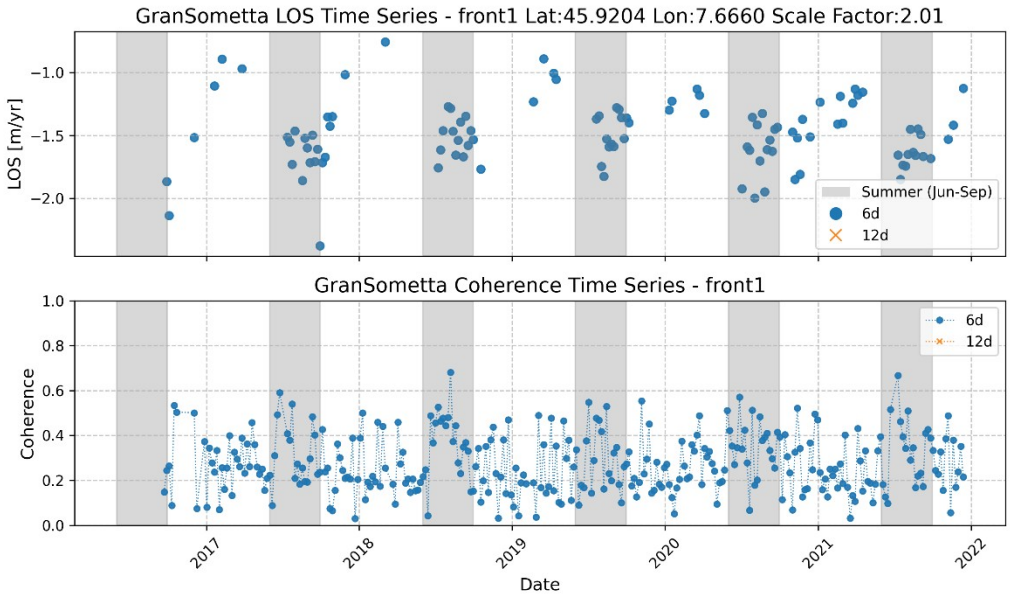

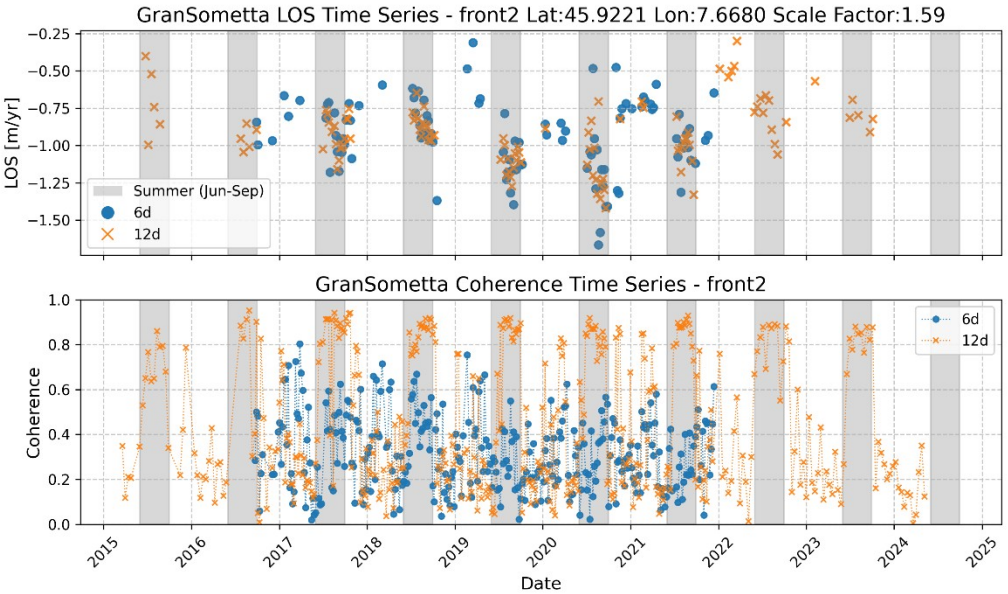

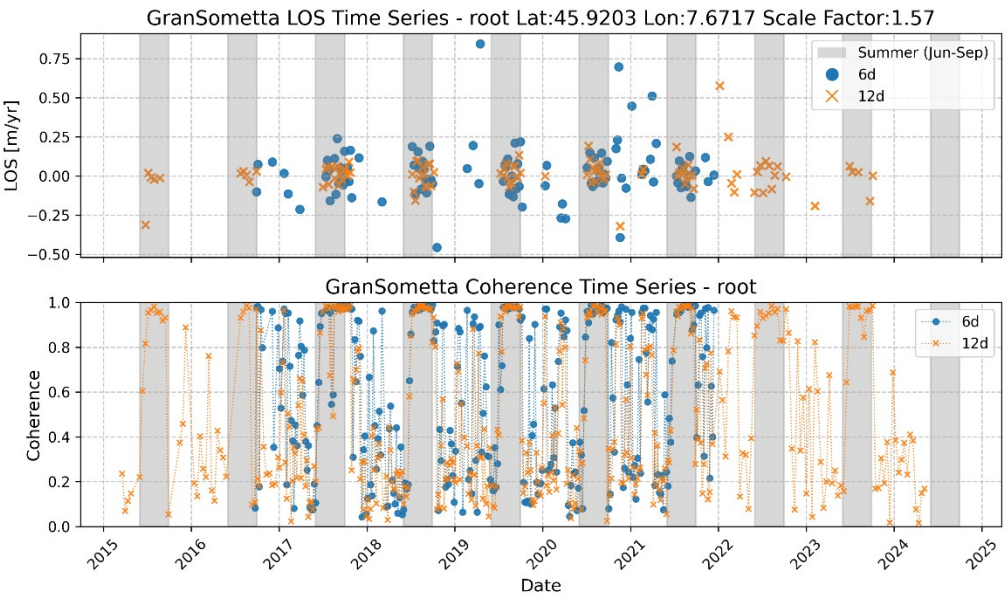

Gran Sometta RGV Analysis – Descending orbit 139

Velocity variation over the years: We averaged the obtained LOS velocity rates from the front1 and front2 monitoring points to generate yearly velocity estimates. In the top two figures, the averaged LOS velocities per summer are shown. The error bars represent the standard deviation per year. The two bottom figures show the normalized values ((Avg_year/mean_overall)-1) to highlight relative changes independent of the absolute velocities. Note that higher variations are expected as the measured velocities approach the sensitivity/noise level.

For location front 1 the variations over the year are small and at the size of the error bars. The relative changes should thus be interpreted with caution. For front2 the variation are slightly larger, especially considering the longer period of the 12d interferogram data. The highest velocities are measured in 2019 and 2020.

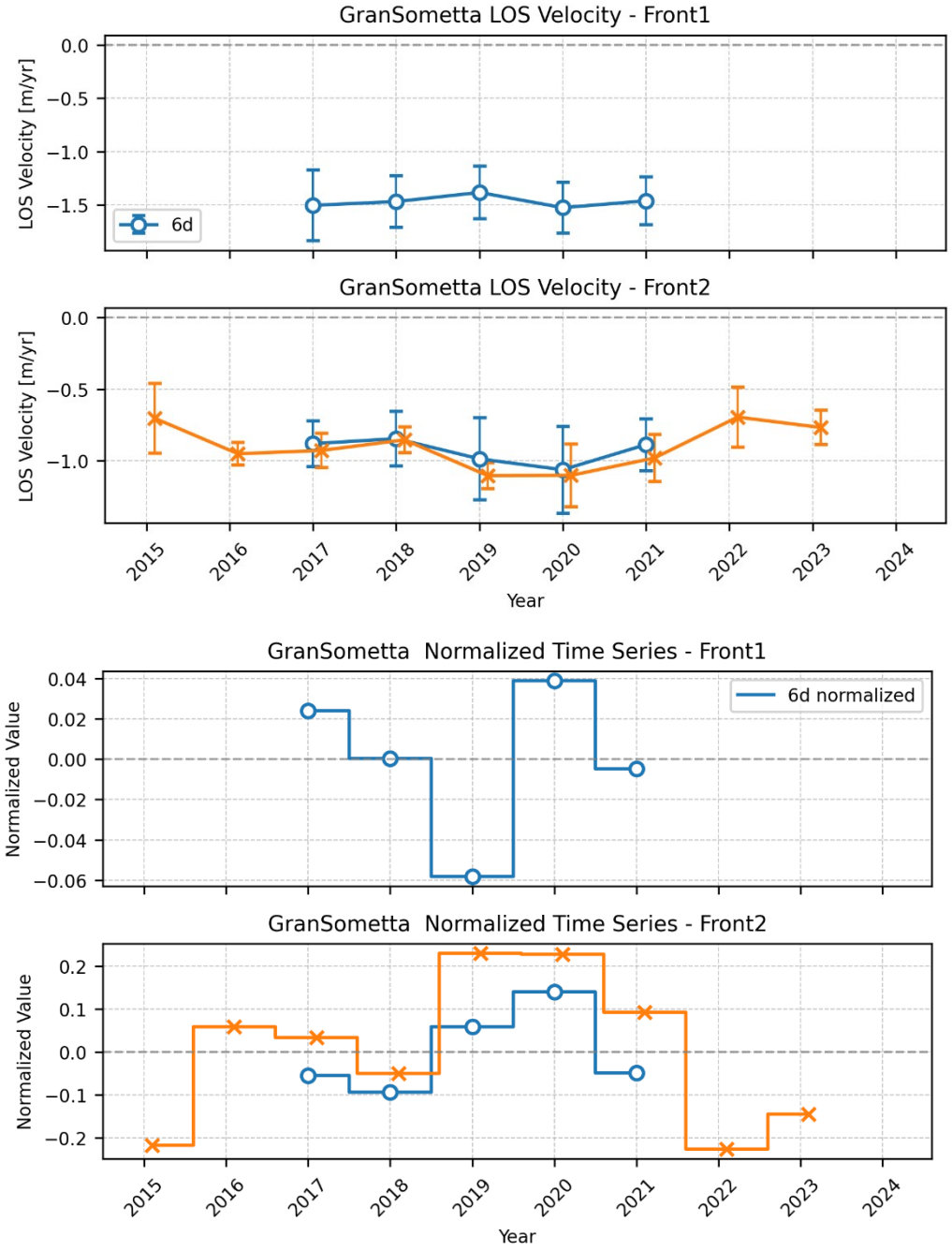

La Thuile RGV Analysis

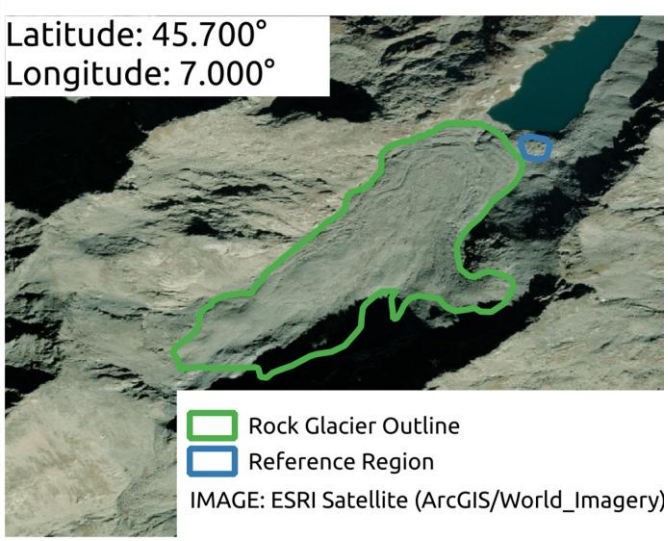

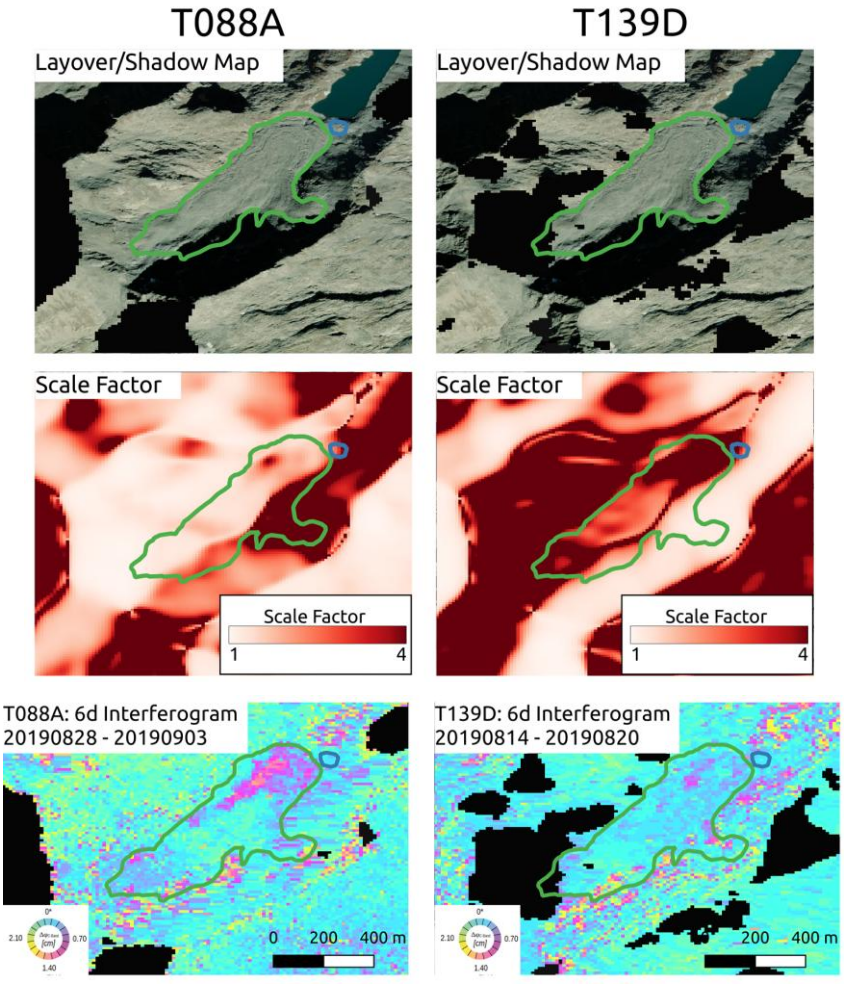

For the RGV Analysis we use mostly orbit T088A ascending data except for the most eastern part were orbit T139D descending data is more suitable.

Layover/Shadow
Sentinel-1 data are acquired from two orbits (T088A and T139D). In both orbits the rock glacier region is not affected by layover or shadow effects.

Scale Factor
The Line-of-Sight (LOS) direction for orbit T088A aligns well with the flow direction of most of the RG with Scale Factors in the range 1.1 to 1.8, except the eastern part with unsuitable conditions and Scale Factors above 4.
T139D exhibits an unfavorable viewing geometry over most of RG with a Scale Factor above 4. Here the most eastern part of the RG aligns well with scale factors of 1.1 to 1.4.

Initial assessment
The front western region covered by T088A shows movement approaching 1cm/6d in LOS, most other areas are at or below the detection limit (6d sensitivity ~0.2m/yr). For most of the 6d interferograms phase unwrapping should proceed without complications.
The eastern region, monitored using T139D, reveals a smaller zone of accelerated movement ranging from 1 to 2cm/6d (approximately 0.6-1.2m/yr). This localized high-velocity area may present challenges during the unwrapping process.

La Thuile RGV Analysis – Ascending orbit 88

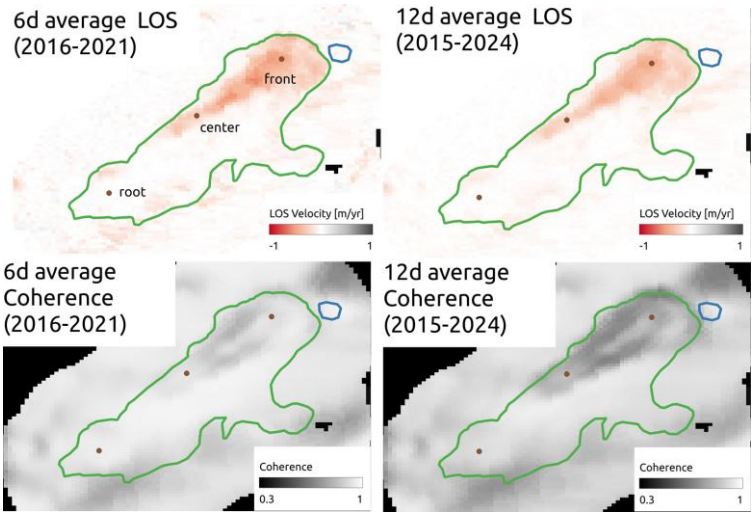

Overview

The figures to the left show averaged Line-of-Sight (LOS) velocities over all available summer seasons (July to October) (top) as well as the average coherence over the same period (bottom). 6-day interferograms are available from October 2016 to December 2021, 12-day interferograms are available from October 2015 to the start of 2025. Negative LOS values indicate a displacement away from the sensor.

A selection of coherent interferograms was made manually for the further analysis. Based on the analysis of the Scale Factor, we focus on the western part of the rock glacier. Here, average velocities of up to 0.5 m/yr are measured.

We selected three points (front, center and root) to extract LOS velocities time series.

Point Time Series

For the three monitoring points (front [45.7056, 7.00116], center [45.7033, 6.9975], and root [45.7017, 7.0011]) highlighted in the upper plots, we extracted LOS velocity time series, carefully checking and correcting any unwrapping issues. Each figure showing the time series displays the LOS displacement rates in m/yr in the top panel and the coherence in the bottom panel. For the LOS displacement, only the coherent measurements are shown. For the coherence time series, all available pairs are shown. The coherence was obtained at the point location in the individual interferograms. Blue circles represent 6-day interferometric measurements, while orange crosses show 12-day measurements, with summer months (June-September) highlighted by gray vertical bands.

For the selected interferograms the coherence values are generally high (>0.6) and are obtained mainly in the summer season. In general, the 12-day interferogram coherence values are lower than the 6-day. Higher velocities as well as unfavorable conditions such as snow cover can decrease the coherence.

The highest velocities are measured at the front (~0.7 m/yr ~> 1.27 m/yr when assuming slope-parallel movement) with acceleration and deceleration during the summer of about 0.5m/yr. At the center (see figure on next page), the velocities are relatively stable around 0.2 m/yr and thus just at the sensitivity limit. The root is stable with variability around 0, indicating no movement above the sensitivity thresholds (6d: ~0.2 m/yr, 12d: ~0.1 m/yr). Scale Factors for the three points are 1.81 for front, 1.35 for center and 1.26 for root.

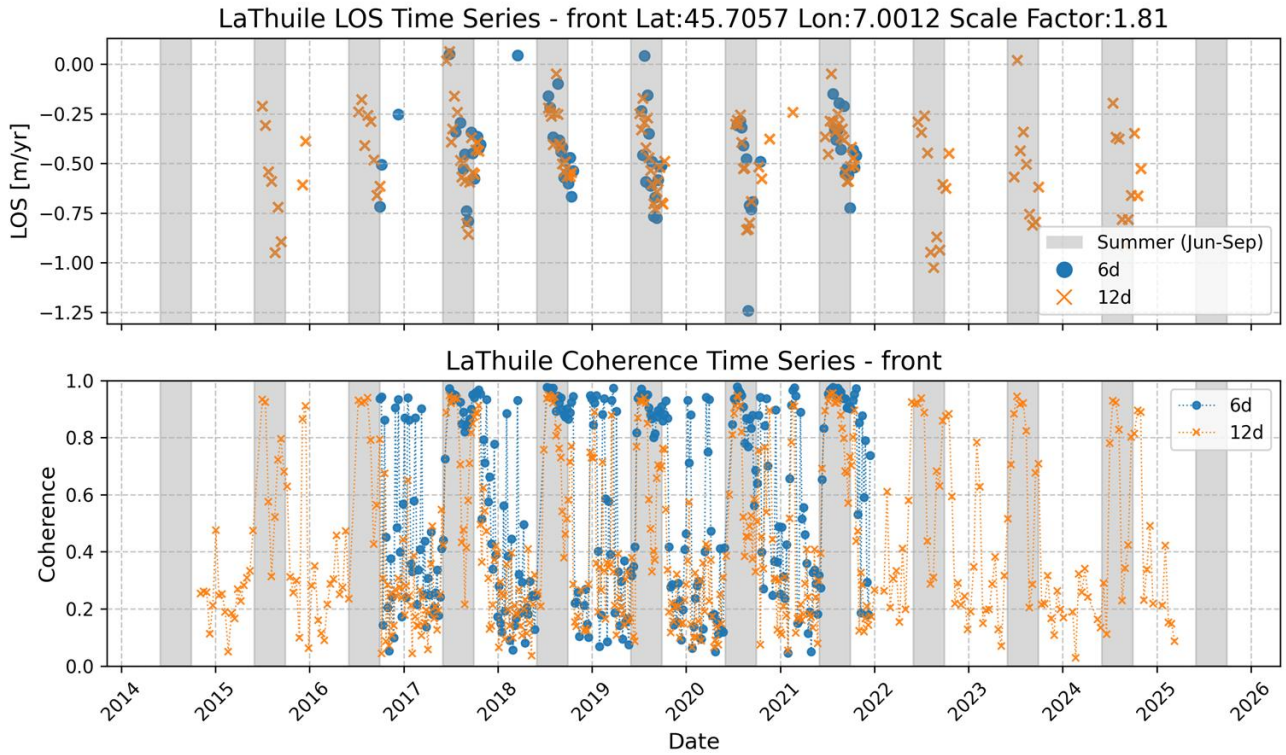

La Thuile RGV Analysis – Ascending orbit 88

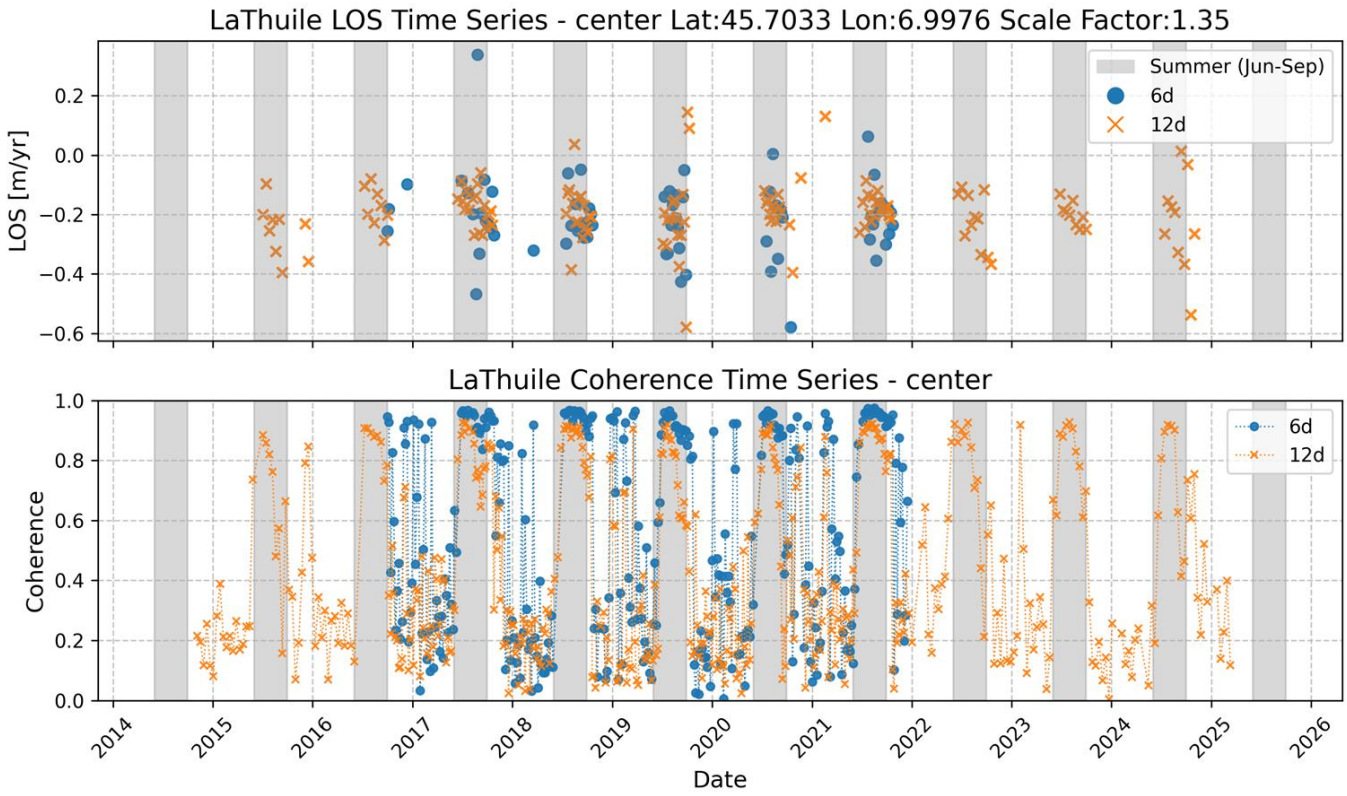

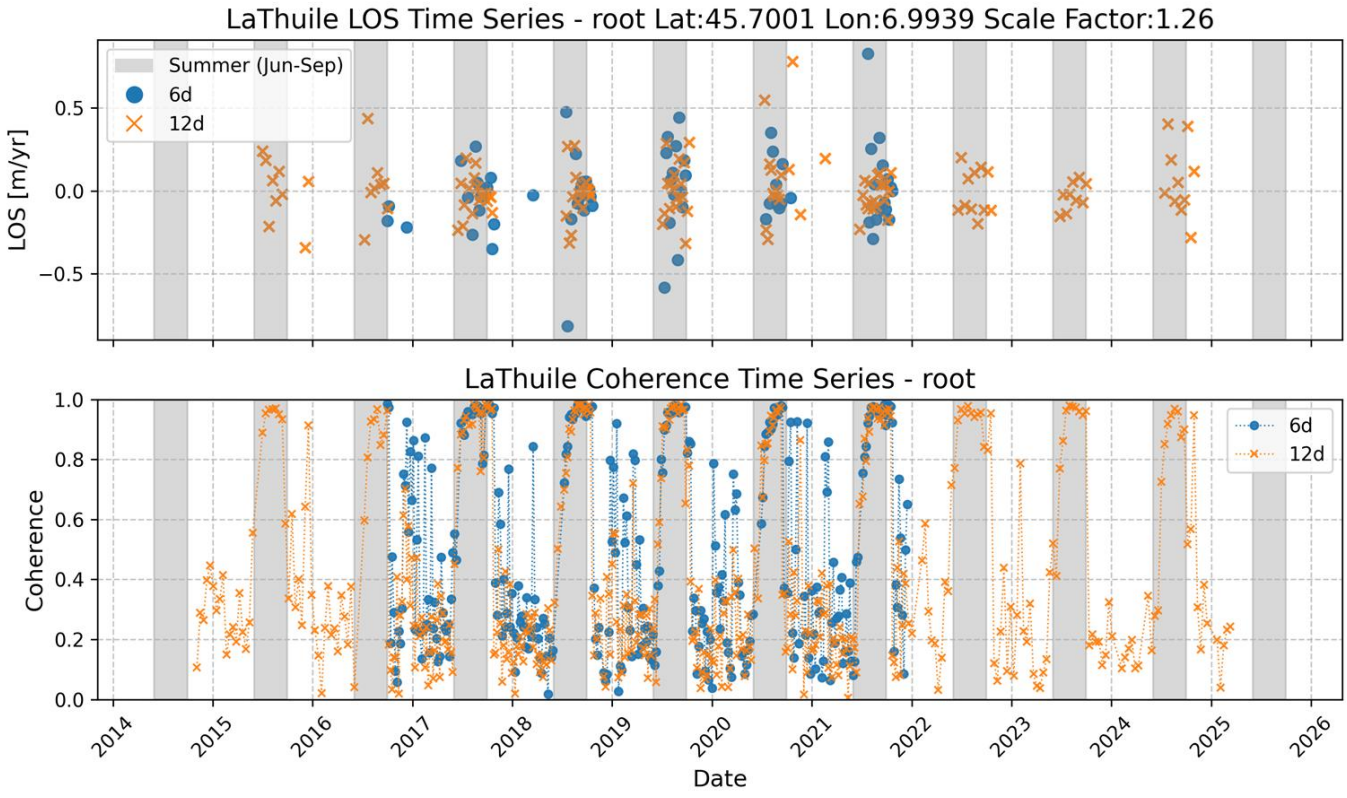

La Thuile RGV Analysis – Ascending orbit 88

Velocity variation over the years: We averaged the obtained LOS velocity rates from the center and front monitoring points to generate yearly velocity estimates. In the top two figures, the averaged LOS velocities per summer are shown. The error bars represent the standard deviation per year. The two bottom figures show the normalized values ((Avg_year/mean_overall)-1) to highlight relative changes independent of the absolute velocities. Note that higher variations are expected as the measured velocities approach the sensitivity/noise level.

The front location exhibits more pronounced variations with stronger negative velocities compared to the center. Both locations show a consistent temporal pattern: initial deceleration from 2015 to 2017, followed by acceleration through 2019/2020, a decrease again in 2021, and another subsequent acceleration. The similar pattern between both points in the normalized plot indicates that while absolute movement intensity differs between locations, the proportional changes over time are consistent. The good agreement between 6-day (blue circles, 2016-2021) and 12-day (orange crosses, 2015-2024) interferometric measurements indicates reliability in the observations.

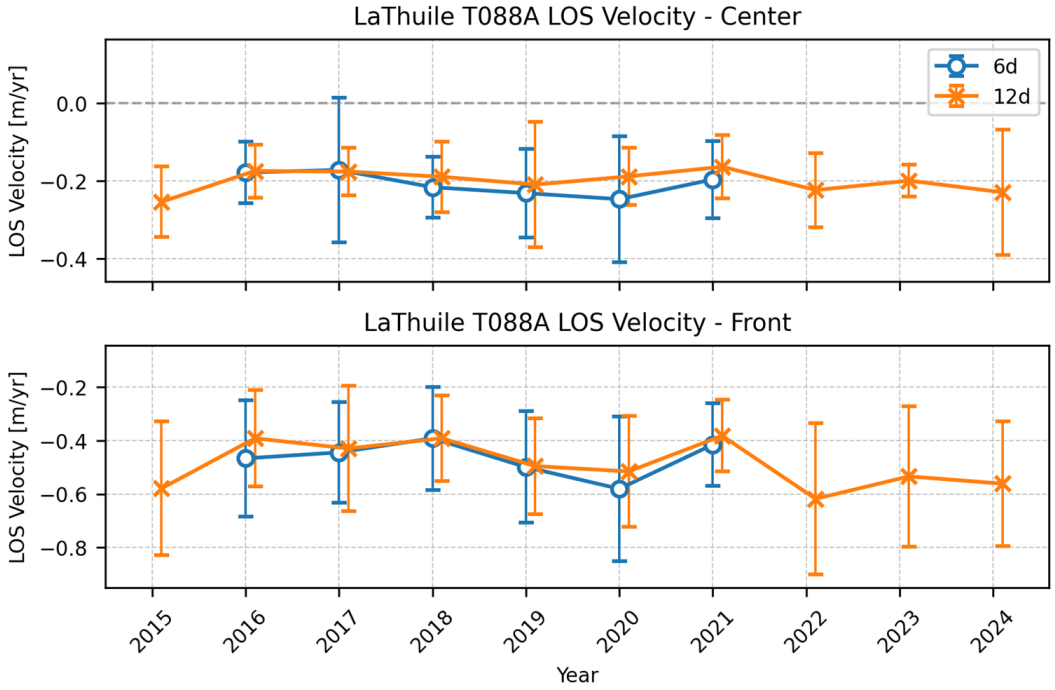

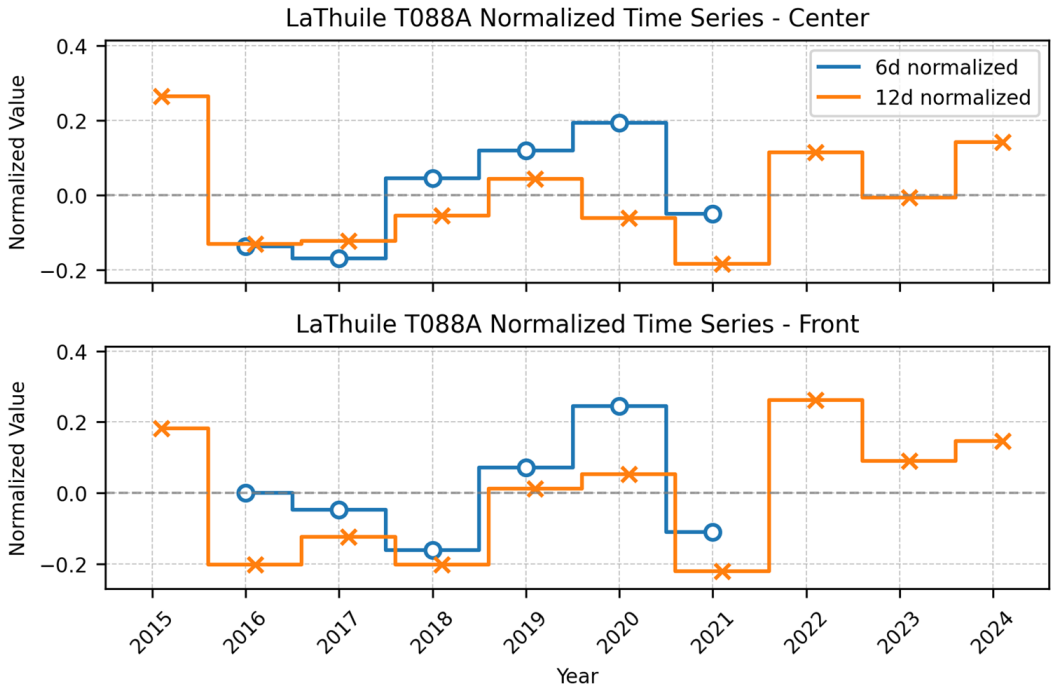

La Thuile RGV Analysis – Ascending orbit 88

The number of unwrapping errors over the whole RG was small which allowed the spatial aggregation of LOS velocities for all points on the RG. We found some small unwrapping issues in the 12d interferograms in the region between center and front which lead to an underestimation in the 12d average LOS displacement rates.
We kept points with average LOS displacement rates above the approximate sensitivity (0.2m/yr for 6d and 0.1m/yr for the 12d). The points above the sensitivity limit can be seen in the top figures and the relative changes averaged over all points in the bottom figure.

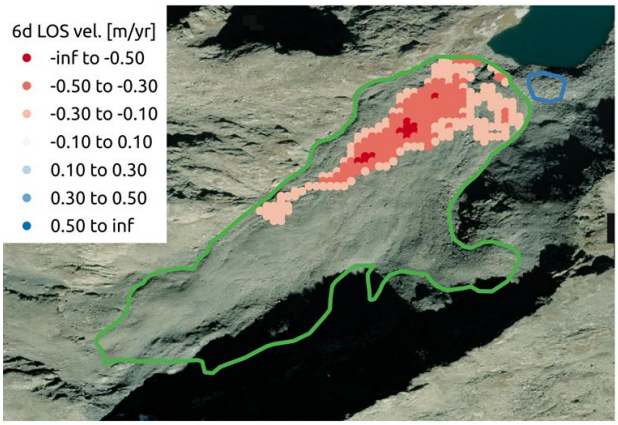

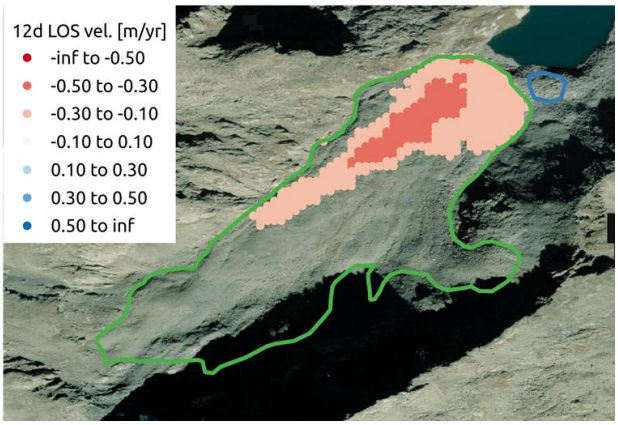

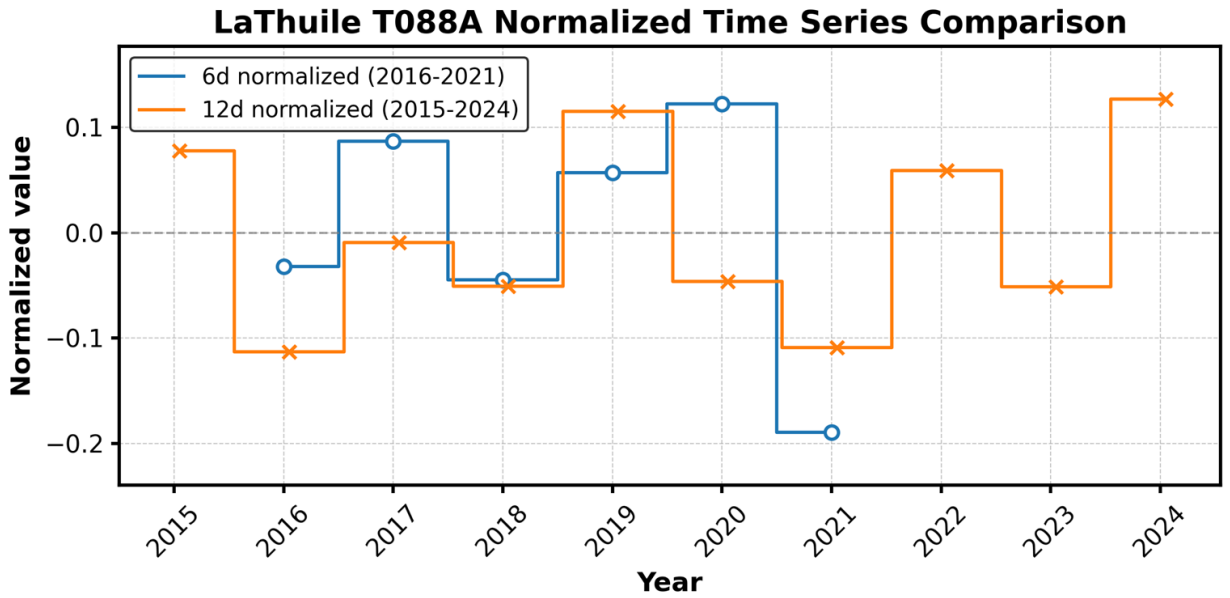

La Thuile RGV Analysis – Descending orbit 139

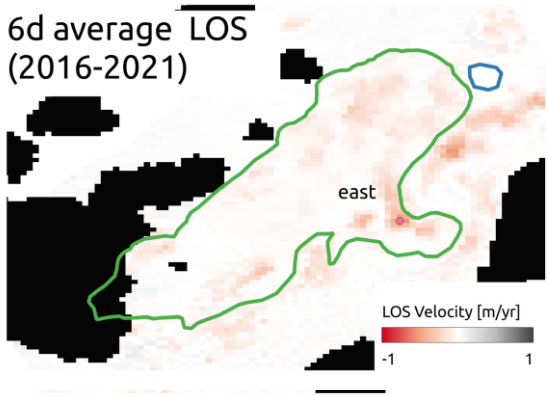

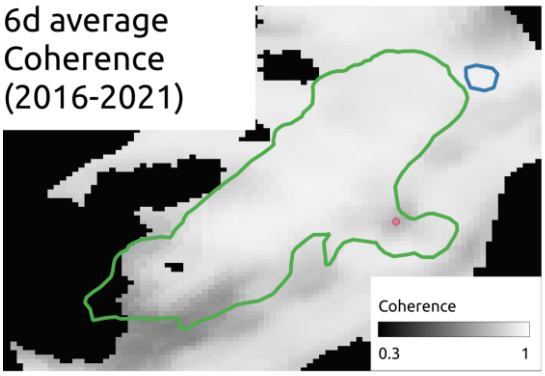

For the analysis of orbit T139D, we are interested in the region on the eastern part of the RG since this part is not well aligned with the ascending LOS. The figures on the left show time series and spatial patterns of surface displacement in LOS as well as the average coherence from 2016 to 2021 (6-day interferograms). We only processed the 6d data since the 12d data had low quality.

As for ascending orbit, a manual selection of coherent interferograms was conducted. Average velocities of up to 1.0-1.4 m/yr (1.2-1.6 m/yr assuming slope-parallel movement) are observed. We found some small unwrapping issues also in the 6d interferograms. These were corrected for the time series plots. Scale Factor for the point location is 1.13.

We can observe a similar behavior as for the ascending case with an increase in velocity towards 2019 and a deceleration afterwards.

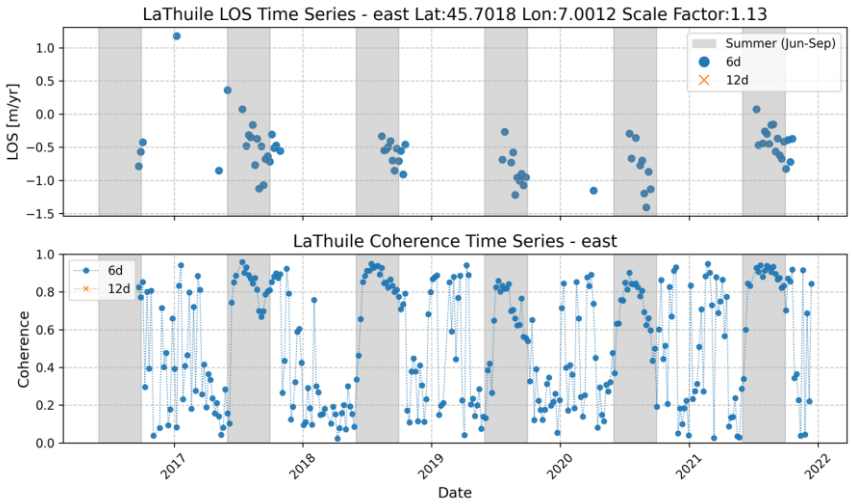

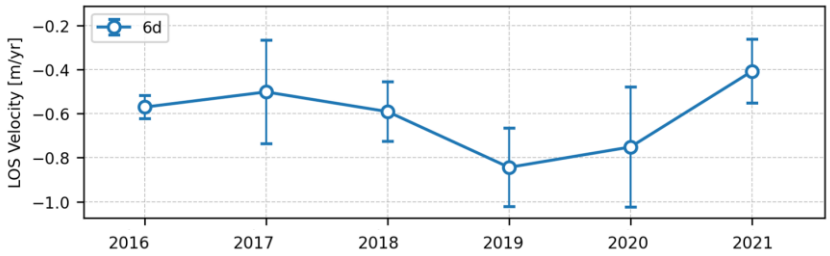

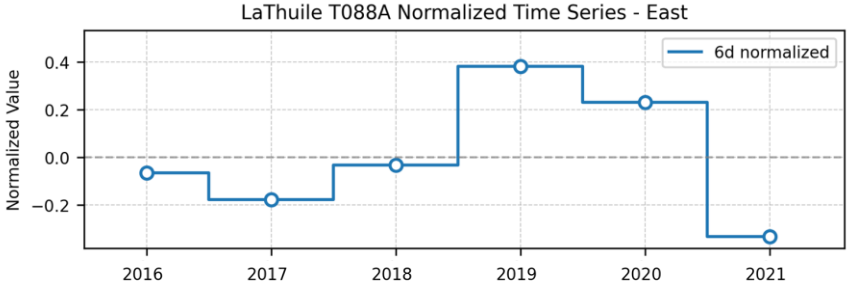

Luseney RGV Analysis

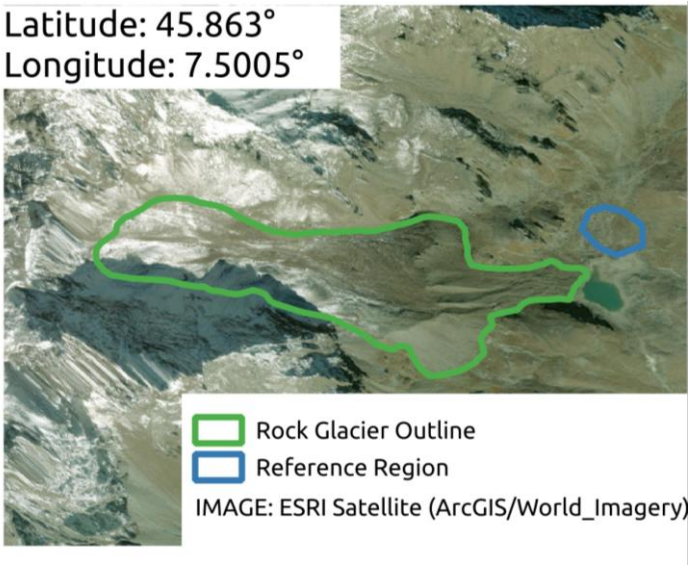

T088A

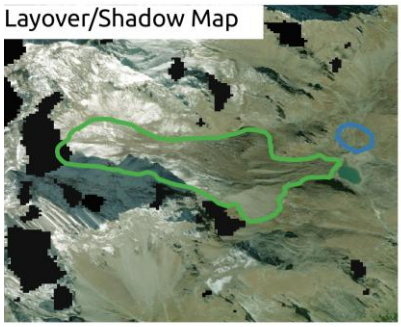

T139D

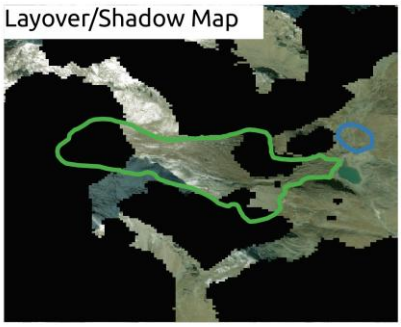

Layover/Shadow
Sentinel-1 data are acquired from two orbits (T088A and T139D). In orbit T139D the rock glacier is strongly affected by layover/shadow. In orbit T088A the rock glacier region is not affected by layover or shadowing effects.

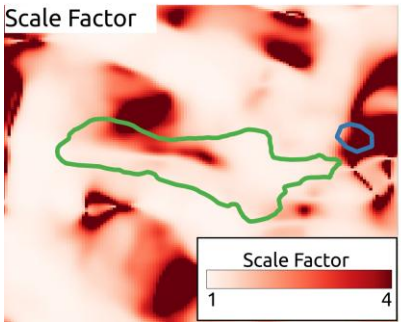

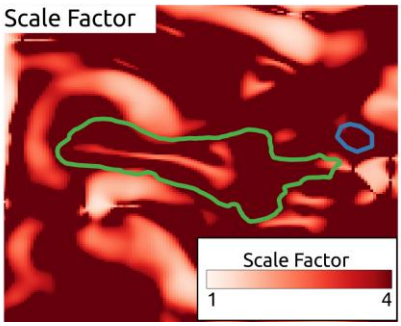

Scale Factor:
The Line-of-Sight for orbit T088A aligns well with the flow direction of the RG. Scale Factors for orbit T088A are in the range 1.1 to 2 over the majority of the RG. In the middle top part of the RG, a region reaches scale factors of up to 4 and is not well covered by the InSAR analysis. T139D exhibits an unfavorable viewing geometry with a Scale Factor above 4.

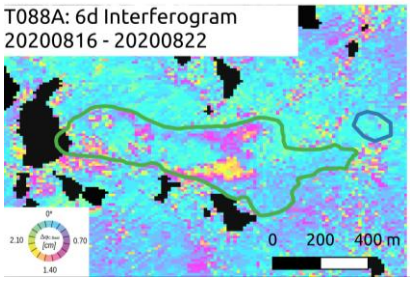

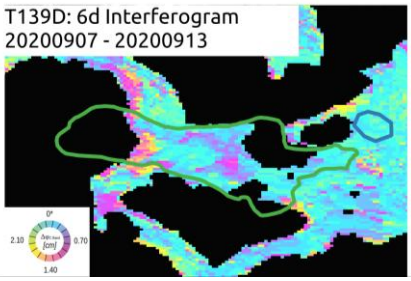

Initial assessment
The T088A interferogram (left) shows minimal surface deformation across most of the RG (sensitivity ~0.2m/yr). However, two notable anomalies appear in the central region, exhibiting movement of up to 2cm over the 6-day period (equivalent to approximately 1.2m/year). These localized high-velocity zones may present challenges for phase unwrapping procedures in subsequent processing stages. Furthermore, at the top of the RG (west), some decorrelated regions are present.
The T139D interferogram is not well suited for an InSAR analysis.

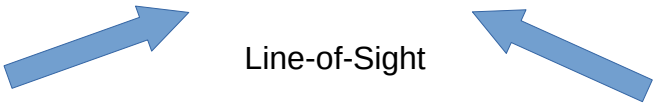

For the RGV Analysis we use orbit T088A ascending data.

RG Luseney RGV Analysis – Ascending orbit 88

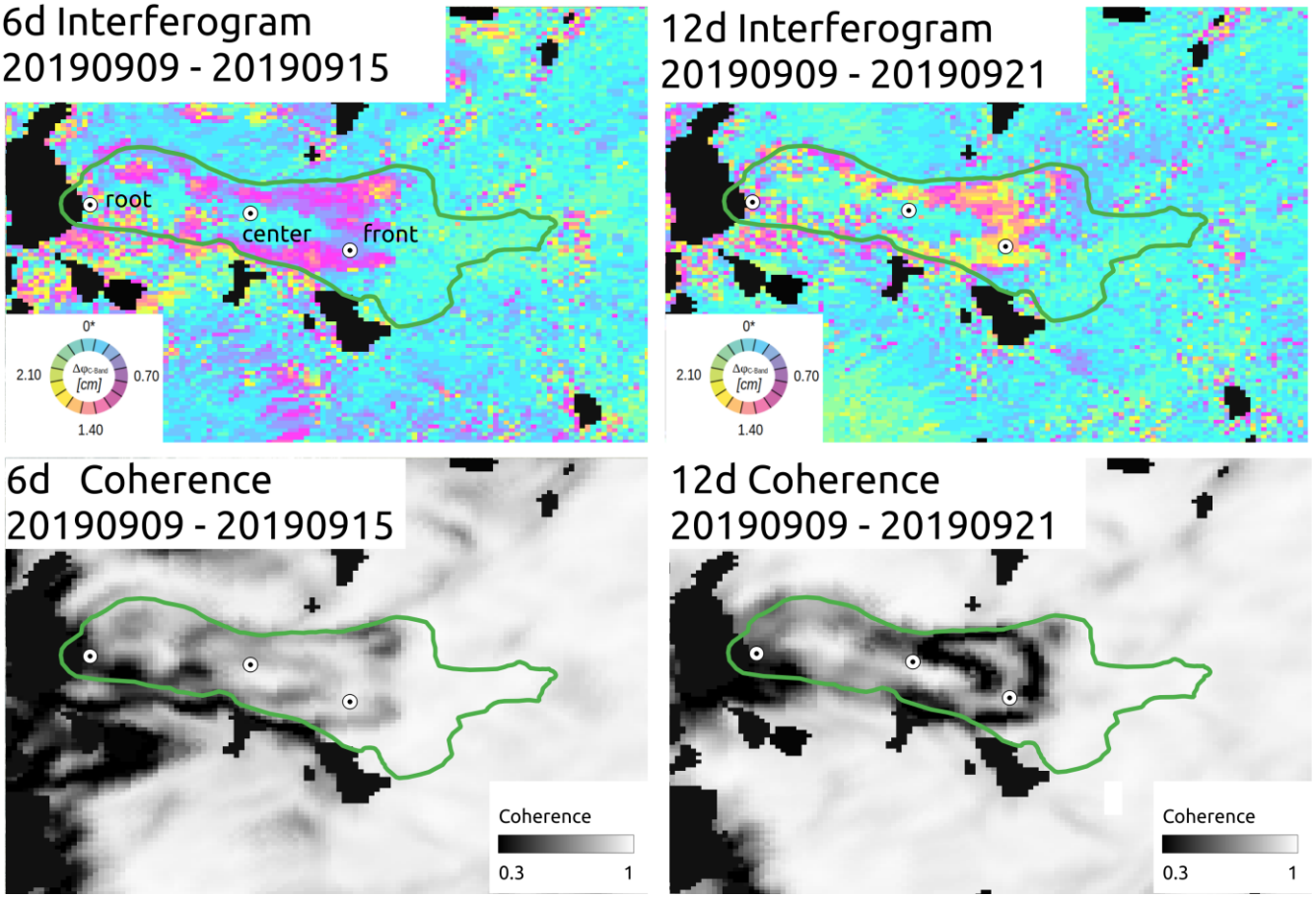

Overview

The figure above shows a 6d and 12d interferogram as well as the associated coherence from end of summer 2019. A selection of coherent interferograms was made manually for the further analysis. Many unwrapping issues are present due to high LOS velocities (up to 2 m/yr) as well as abrupt changes. We selected three points (front, center, root) across the RG to extract LOS velocities time series.

Point Time Series

For the three monitoring points (front [45.8627, 7.5022], center [45.8639, 7.4989], and root [45.8642 7.4937]) highlighted in the upper figures, we extracted LOS velocity time series, carefully checking and correcting any unwrapping issues. Each figure showing the time series on the next page displays the LOS displacement rates in m/yr in the top panel and the coherence in the bottom panel. For the LOS displacements, the coherent values are shown. For the coherence time series, all available pairs are shown. The coherence was obtained at the point location in the individual interferograms. Blue circles represent 6-day interferometric measurements, while orange crosses show 12-day measurements, with summer months (June-September) highlighted by gray vertical bands. In general, the 12-day interferogram coherence values are lower than the 6-day. For the locations center and root the coherence values in the summer season are generally high (>0.6). For the front location the coherence was significantly lower and only a processing of the 6d-interferograms was possible, Higher velocities as well as unfavorable conditions such as snow cover decrease the coherence.

The highest velocities are measured at the root location (~1-1.5 m/yr ~> 1.2-1.8 m/yr when assuming slope-parallel movement) with large fluctuations due to the low data quality (see figure on next page). At the center, the velocities are relatively stable around 0 m/yr and thus inside the sensitivity limits. The LOS velocity at the front is up to 1 m/yr with a large seasonal increase, thus no movement outside the summer period. Scale Factors for the three points are 1.31 for front, 1.65 for center and 1.17 for root.

RG Luseney RGV Analysis – Ascending orbit 88

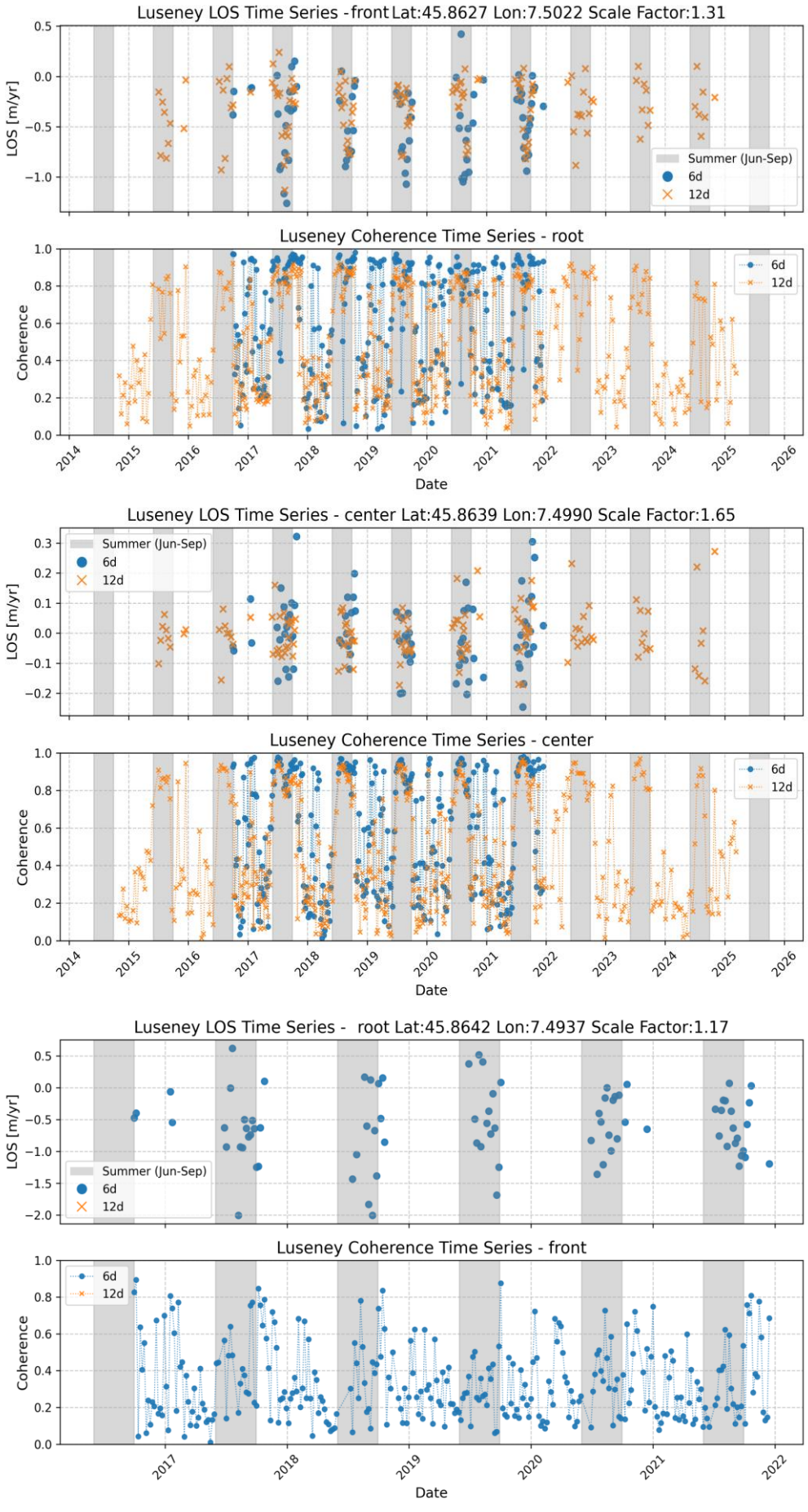

RG Luseney RGV Analysis – Ascending orbit 88

Velocity variation over the years: We averaged the obtained LOS velocity rates from the root and front monitoring points to generate yearly velocity estimates. In the top two figures, the averaged LOS velocities per summer are shown. The error bars represent the standard deviation per year. The two bottom figures show the normalized values ((Avg_year/mean_overall)-1) to highlight relative changes independent of the absolute velocities. Note that higher variations are expected as the measured velocities approach the sensitivity/noise level.

Both points show large error bars. This is due to strong seasonal variations with large increases starting at nearly no movement during winter and reaching up to 1 m/yr for the front location and up to 2 m/yr for the root location. The selection of which points to use in the analysis thus plays a highly significant role. For example, in 2020 the 12d LOS velocity appears significantly lower than the 6d LOS velocity, because fast-moving points were excluded from the analysis due to decorrelation. The time series displayed should thus be interpreted with caution.

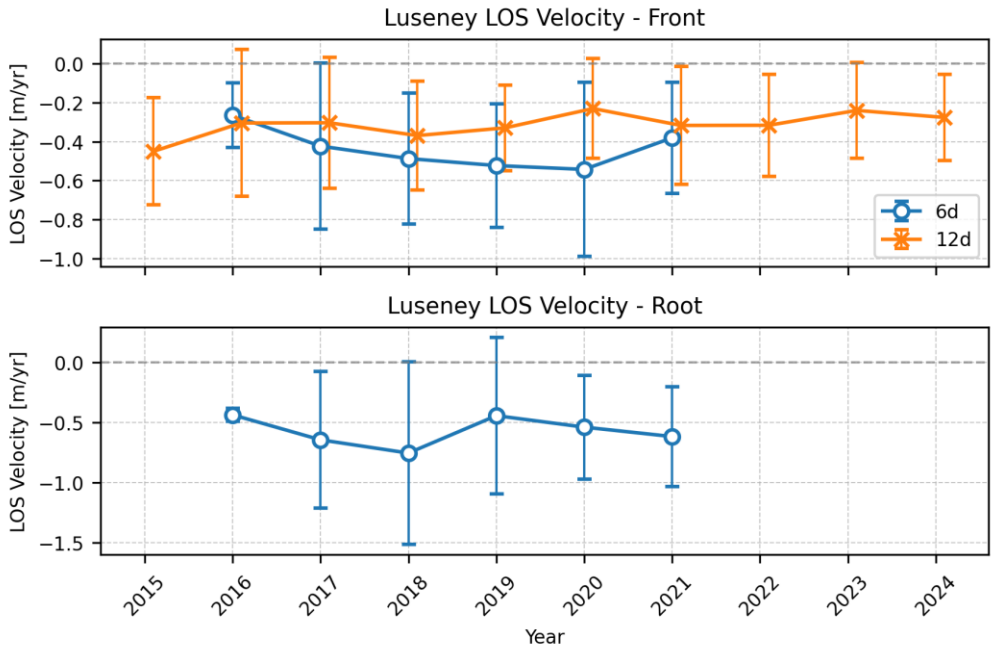

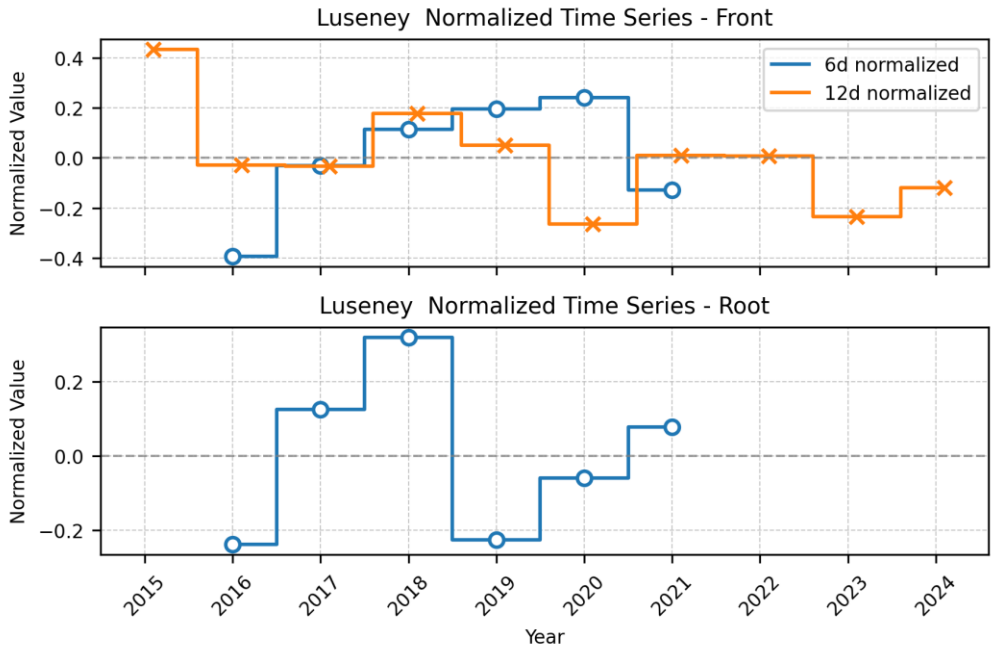

Moline RGV Analysis

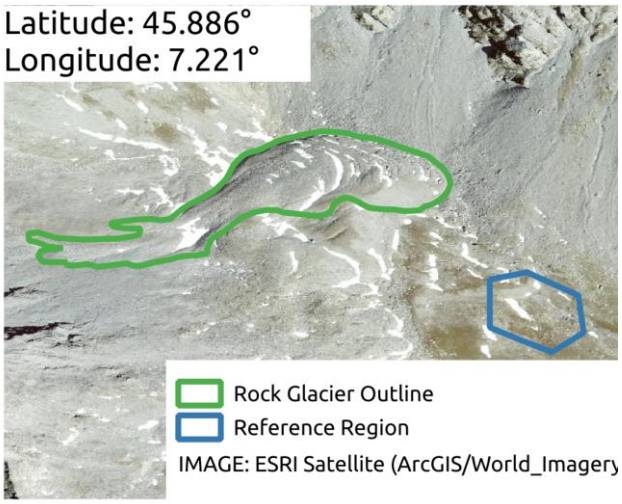

T088A

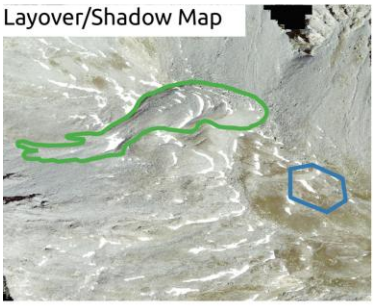

T139D

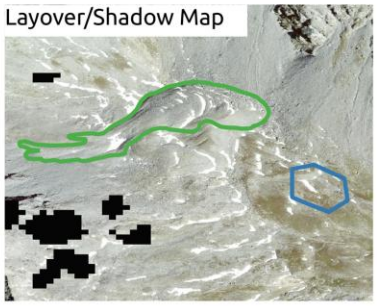

Layover/Shadow
Sentinel-1 data are acquired from two orbits (T088A and T139D). In both orbits the rock glacier region is not affected by layover or shadow effects.

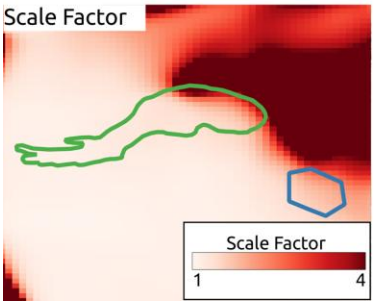

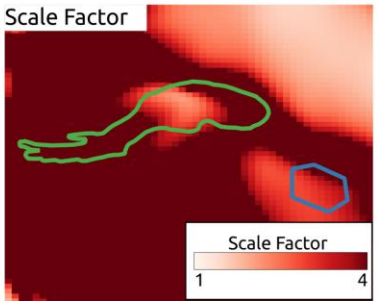

Scale Factor:
T139D exhibits an unfavorable viewing geometry with a Scale Factor above 4. The Line-of-Sight for orbit T088A aligns well with the flow direction of the RG. Scale Factors for orbit T088A are in the range 1.1 to 1.8 over the majority of the RG.

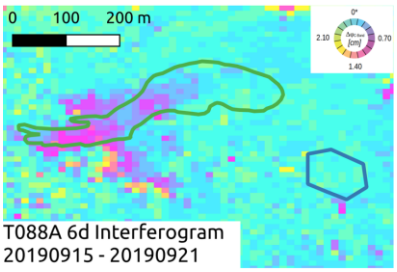

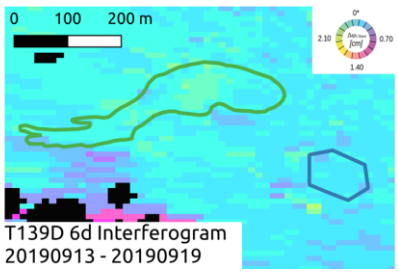

Initial assessment
The T088A interferogram reveals movement in the upper parts of the RG, reaching up to half a phase cycle (1.4cm/6d or approximately 0.6m/yr). In the lower parts no movement is detected (sensitivity ~0.2m/yr). The deformation gradually decreases downhill, with notable movement also detected outside the indicated region towards the south. Given the observed velocity patterns, phase unwrapping challenges should be minimal during processing.
The T139D interferogram shows no movement as expected.

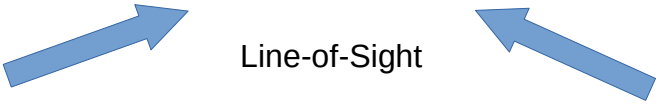

For the RGV Analysis we use orbit T088A ascending data.

Moline RGV Analysis – Ascending orbit 88

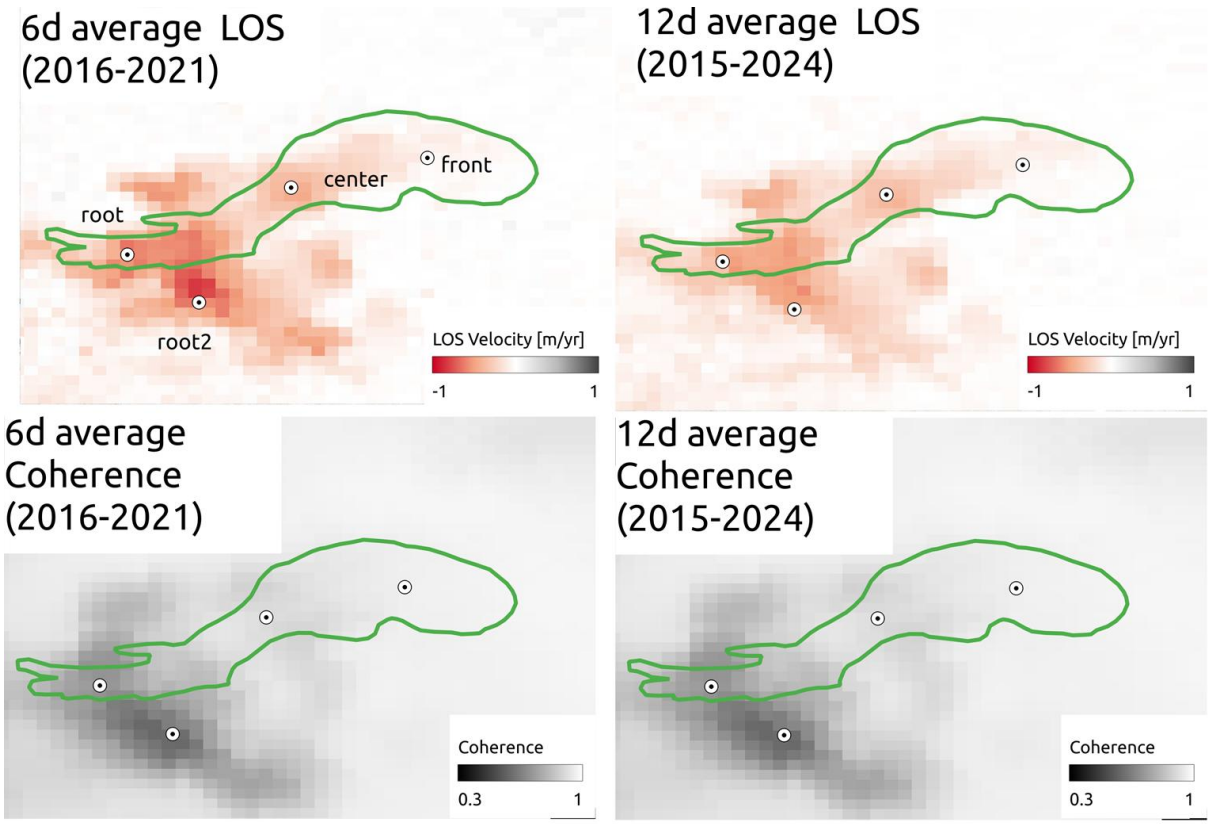

Overview
The figures above show averaged Line-of-Sight (LOS) velocities over all available summer seasons (July to October) (top) as well as the average coherence over the same period (bottom). 6-day interferograms are available from October 2016 to December 2021, 12-day interferograms are available from October 2015 to the start of 2025. Negative LOS values indicate a displacement away from the sensor. A selection of coherent interferograms was made manually for averaging. In the spatial aggregate, we observe LOS velocities above 1 m/yr in the 6-day interferograms, with some of these high velocities occurring outside the RG outline. We found unwrapping issues in the 12-day interferograms that required correction for the time-series plots; consequently, the spatial aggregate for the 12-day interferograms is inaccurate in high velocity regions.

Point Time Series
For the three monitoring points (front [45.88654, 7.22190], center [45.88614, 7.22015], root [45.88527, 7.21801] and root2 [45.88466, 7.21893]) highlighted in the upper plots, we extracted point time series, carefully checking and correcting any unwrapping issues. The respective top panel shows the LOS displacement rates in m/yr, whereas the lower panel shows the coherence. The coherence was obtained at the point location in the individual interferograms. Blue circles represent 6-day interferometric measurements, while orange crosses show 12-day measurements, with summer months (June-September) highlighted by gray vertical bands. The coherence values are generally lower in the upper, faster-moving part of the RG (root). The highest velocities inside the RG outline were measured at the root location, with peak velocities of up to 1 m/yr observed in 2020. Outside the RG at location root2 LOS velocities reached 2m/yr. At the center position, velocities reach up to 0.6 m/yr. The front location shows lower movement rates, below the sensitivity threshold of approximately 0.2 m/yr for 6-day interferograms. Scale Factor values are 1.72 for front, 1.27 for center, 1.11 for root and 1.09 at root2. Smaller scale factors in the root region explain part of the higher LOS velocities.

Moline RGV Analysis – Ascending orbit 88

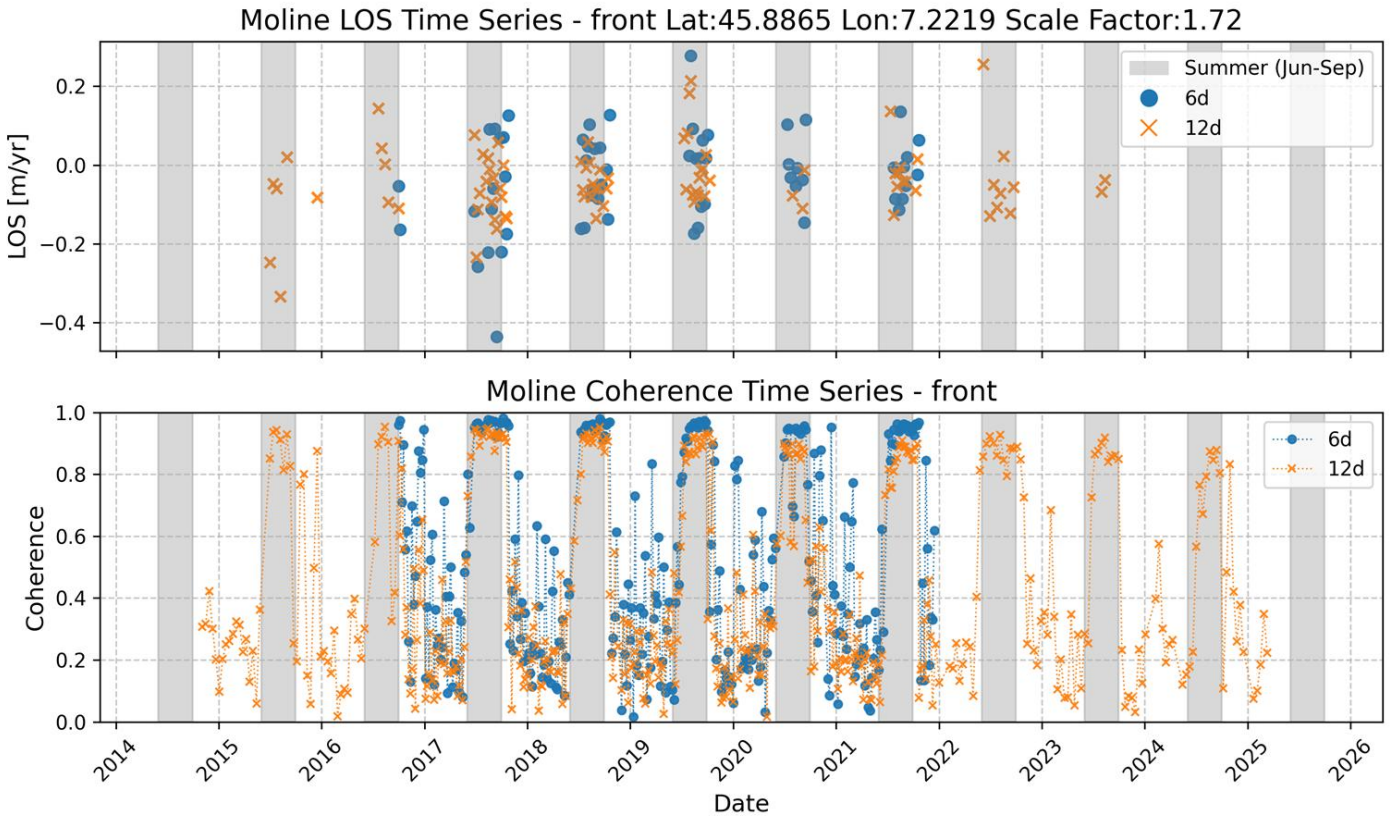

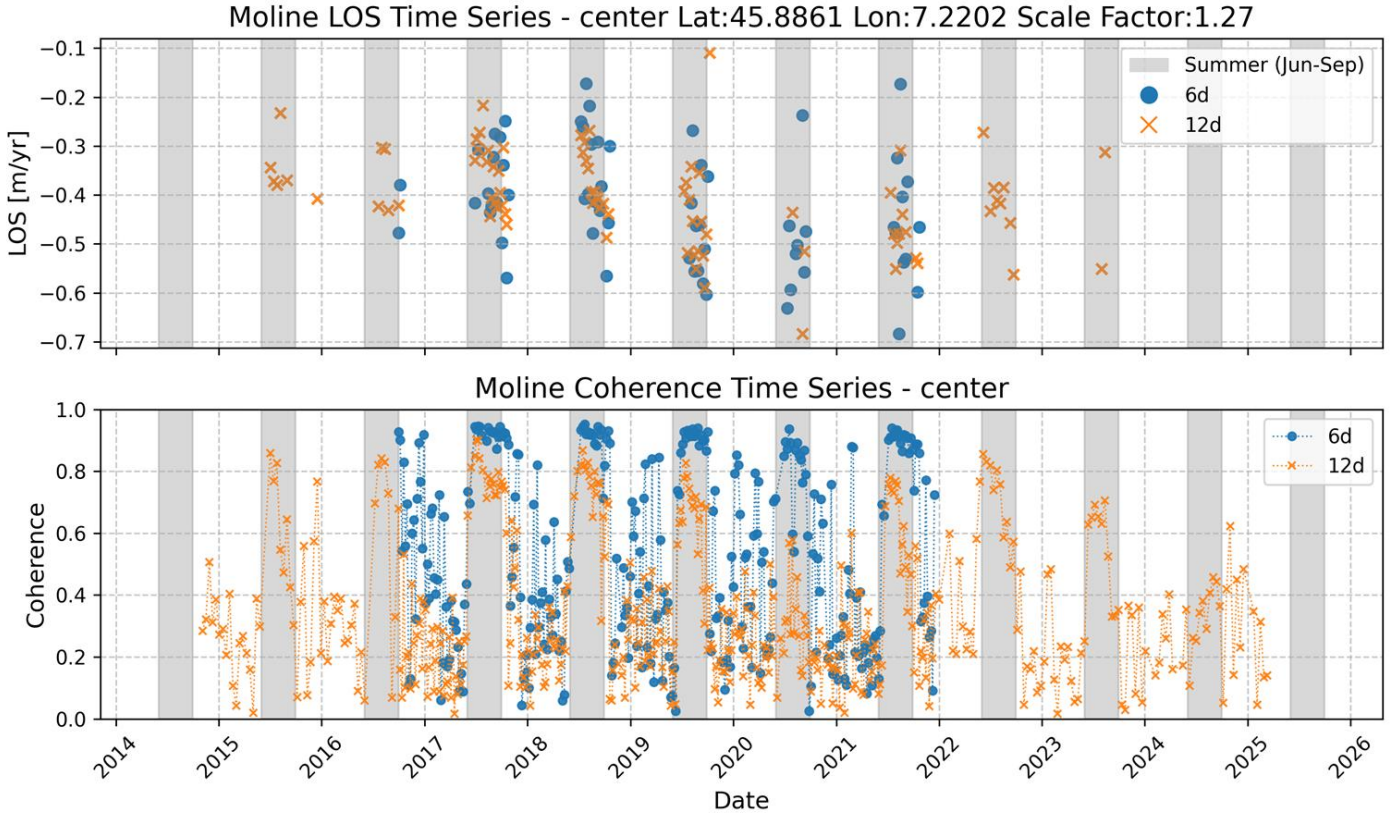

Moline RGV Analysis – Ascending orbit 88

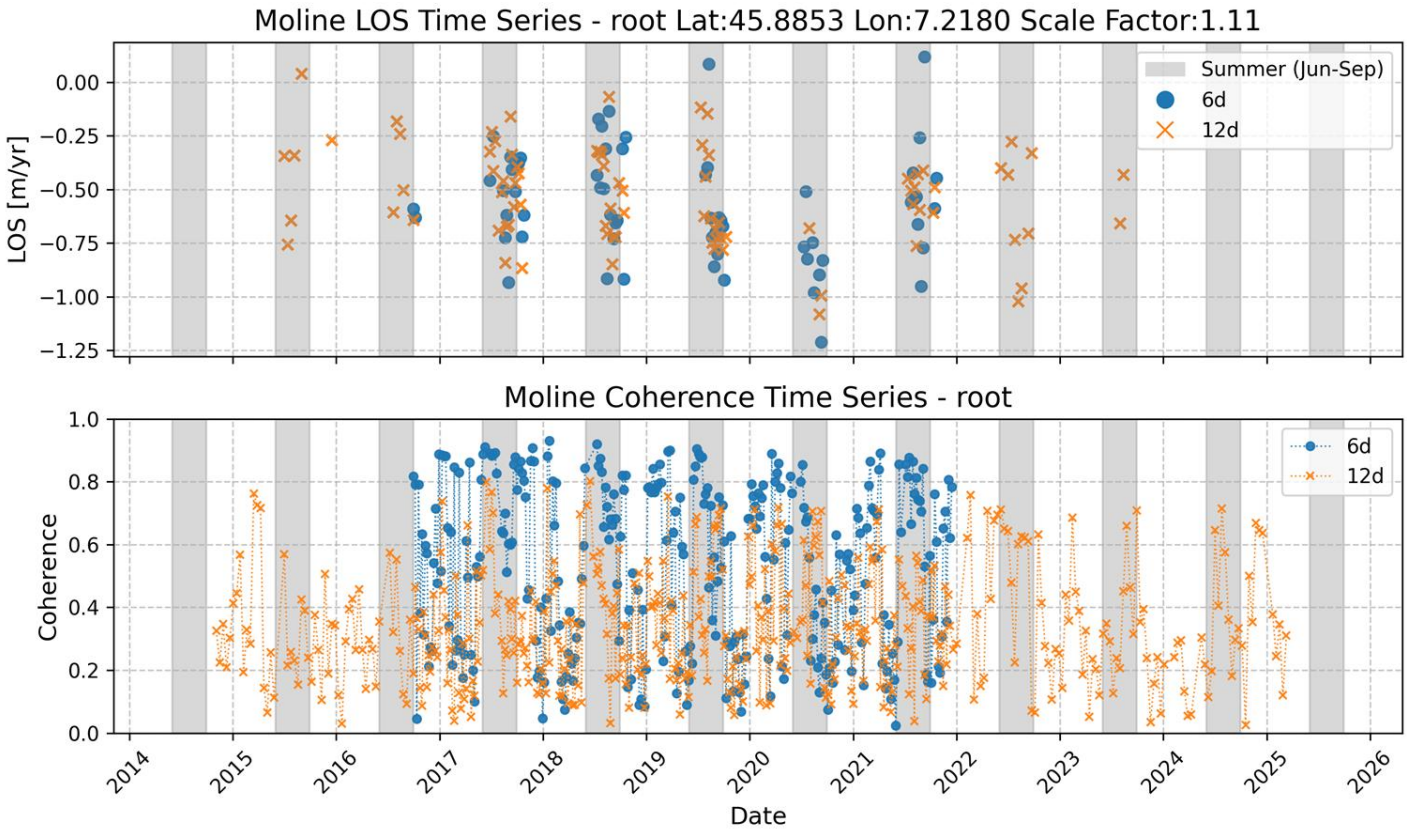

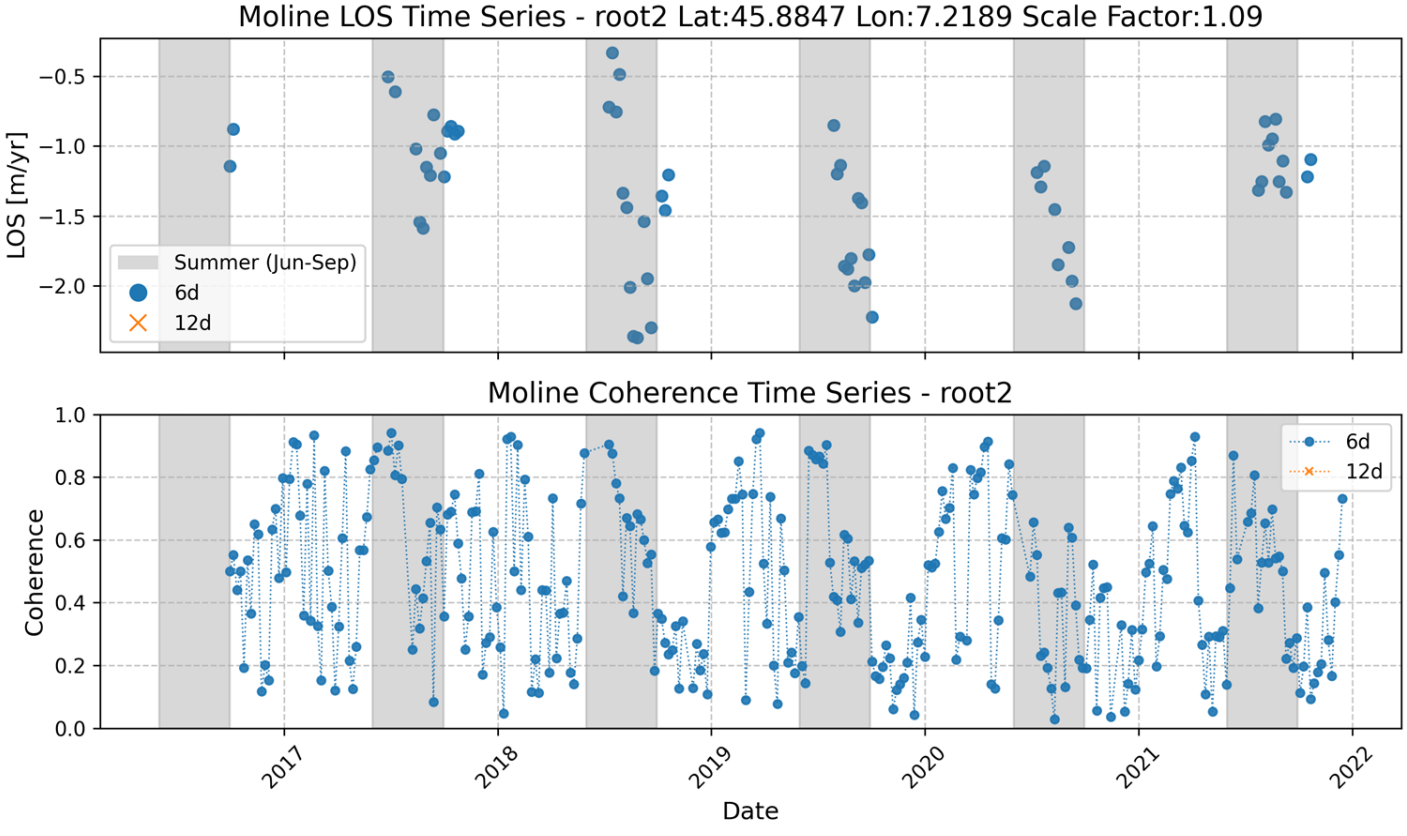

Moline RGV Analysis – Ascending orbit 88

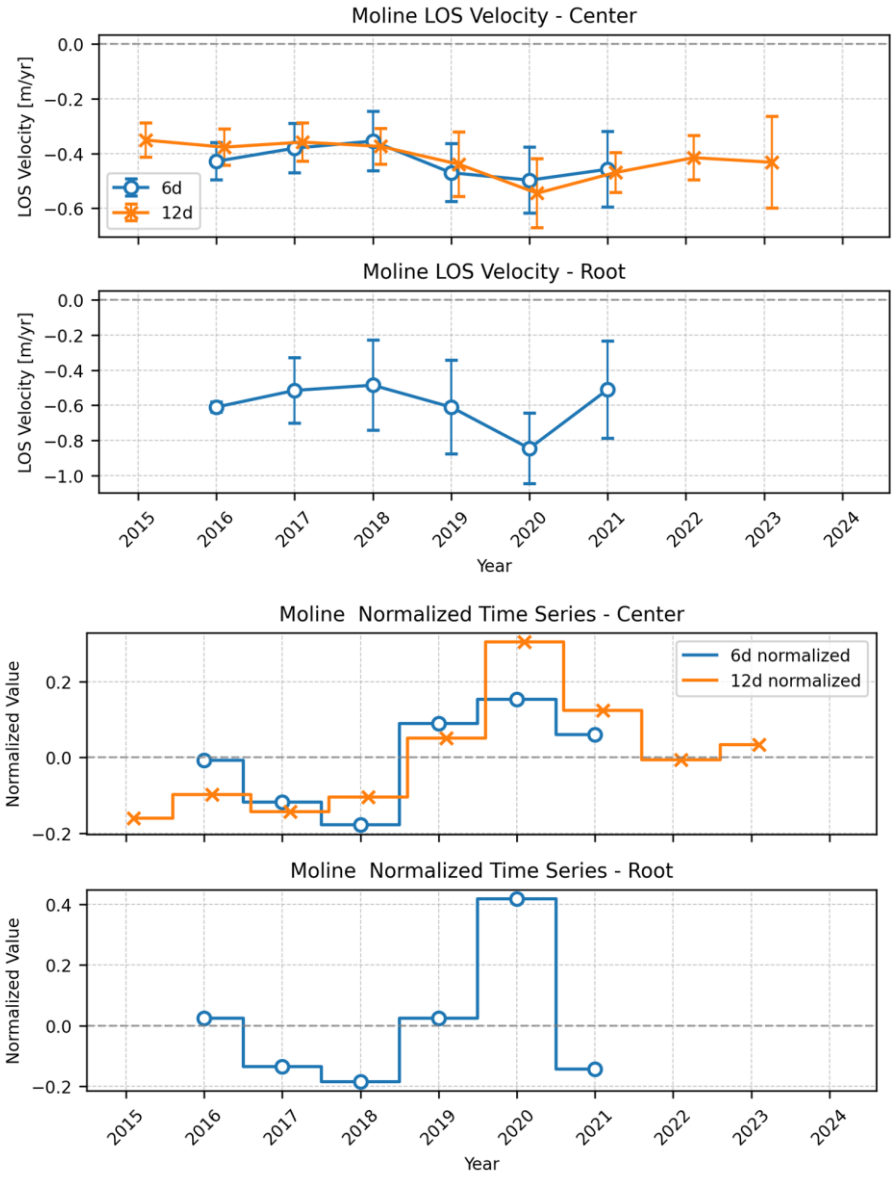

Velocity variation over the years: We averaged the obtained LOS velocity rates from the center and root monitoring points of the Moline RG to generate these comparative time series. The top two figures show absolute velocities with error bars representing yearly averaging uncertainty, while the lower two figures show normalized values ((value/mean_value)-1) to highlight relative changes.

The front location is not shown in this analysis as its movement rates fall below the sensitivity threshold. For the root location, only 6-day interferograms are presented due to the high velocities and limited number of observations, which could otherwise lead to under- or overestimation in the 12-day data.

The root location exhibits more pronounced variations compared to the center. Both locations show peak velocities in 2020, with consistent patterns observed in both 6-day and 12-day measurements. The similar pattern in normalized values indicates that while absolute movement intensity differs between locations, the proportional changes over time are consistent across the RG. This synchronized behavior suggests the RG responds as a coherent unit to external forcing factors.

The good agreement between available measurements reinforces the reliability of these observations. Notably, the spatial average plots (with points used for normalization computation shown in the bottom panel) confirm the previously observed patterns, with a more pronounced increase evident in 2023 for the central point.

Moline RGV Analysis – Ascending orbit 88

The number of unwrapping errors over the whole RG was small which allowed the spatial aggregation of LOS velocities for all points on the RG. We found some small unwrapping issues in the 12d interferograms in the fast-moving region at the root.
We kept points with average LOS displacement rates above the approximate sensitivity (0.2m/yr for 6d and 0.1m/yr for the 12d). The points above the sensitivity limit can be seen in the top four figures. The relative changes averaged over all points for descending orbit T139D are shown in the bottom figure.

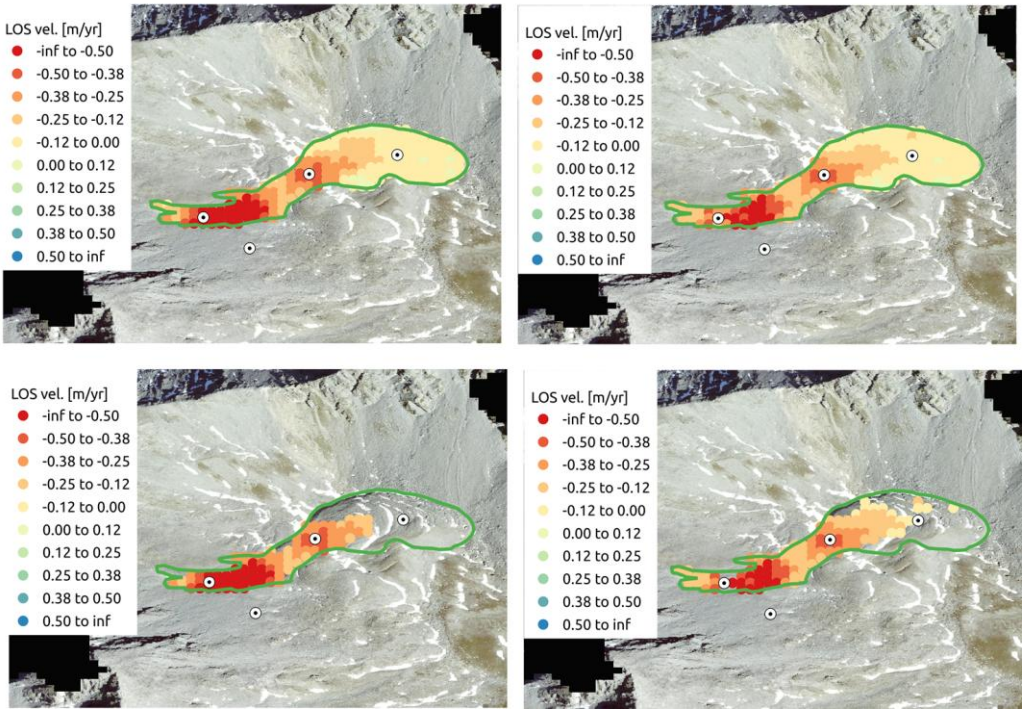

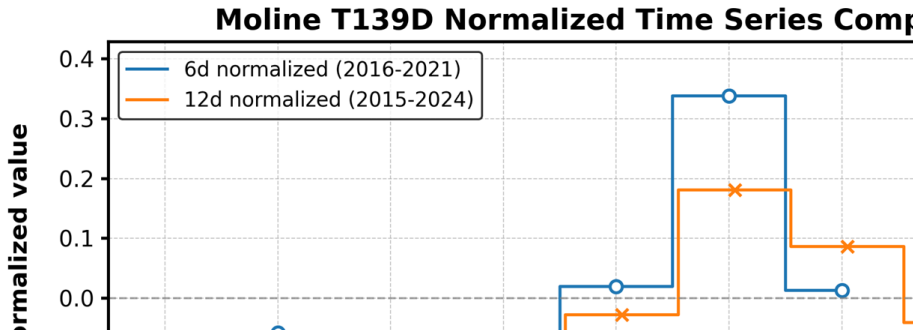

Monte Emilius Range 1 RGV Analysis

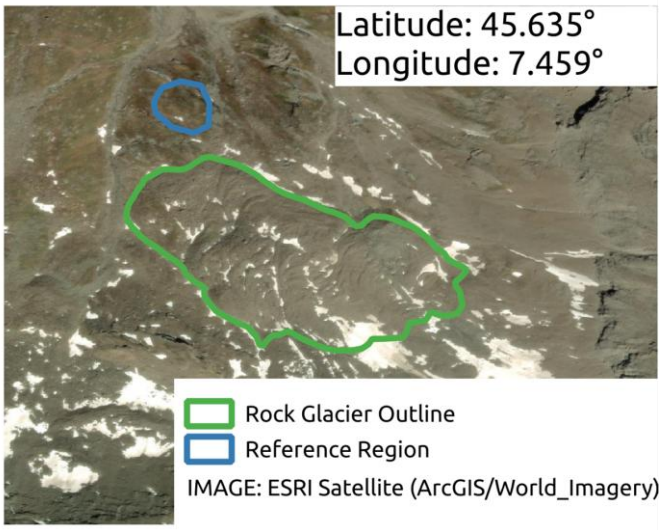

T088A

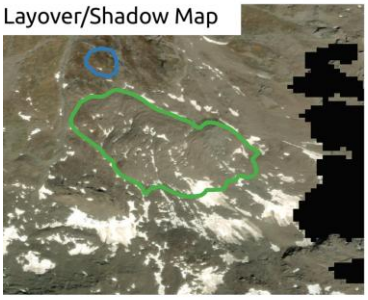

T139D

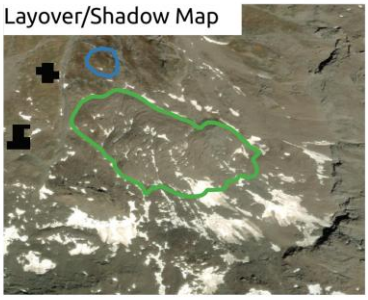

Layover/Shadow
Sentinel-1 data are acquired from two orbits (T088A and T139D). In both orbits the rock glacier region is not affected by layover or shadow effects.

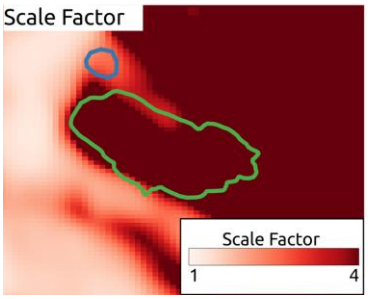

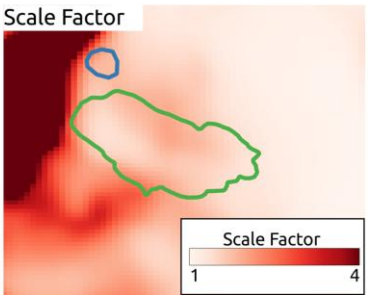

Scale Factor:
T088A exhibits an unfavorable viewing geometry with a Scale Factor above 4. The Line-of-Sight for orbit T139D aligns well with the flow direction of the RG. Scale Factors for orbit T139D are in the range 1.3 to 2.4 over the majority of the RG.

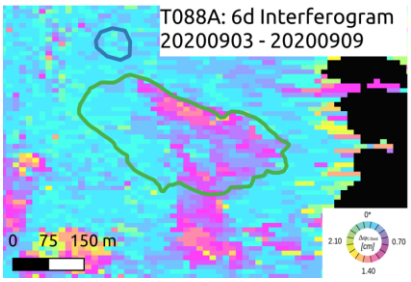

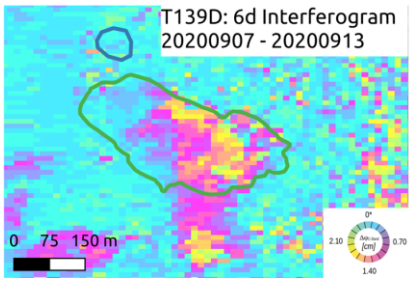

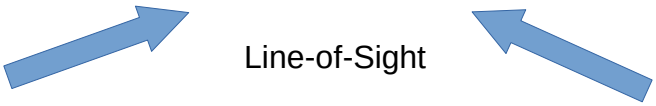

Initial assessment
The T139D interferogram shows contrasting deformation patterns within the RG. The lower part exhibits slow movement at or below the detection limit (sensitivity ~0.2m/yr), while the upper part displays faster movement of up to 2.2cm/6d (equivalent to approximately 1.2m/yr). This sharp velocity transition towards the edge of the RG may introduce phase unwrapping challenges during processing. Significant movement is also detected further upslope, extending beyond the provided RG outline boundaries.

For the RGV Analysis we use orbit T139D descending data.

RG Monte Emilius Range 1
RGV Analysis – Descending orbit 139

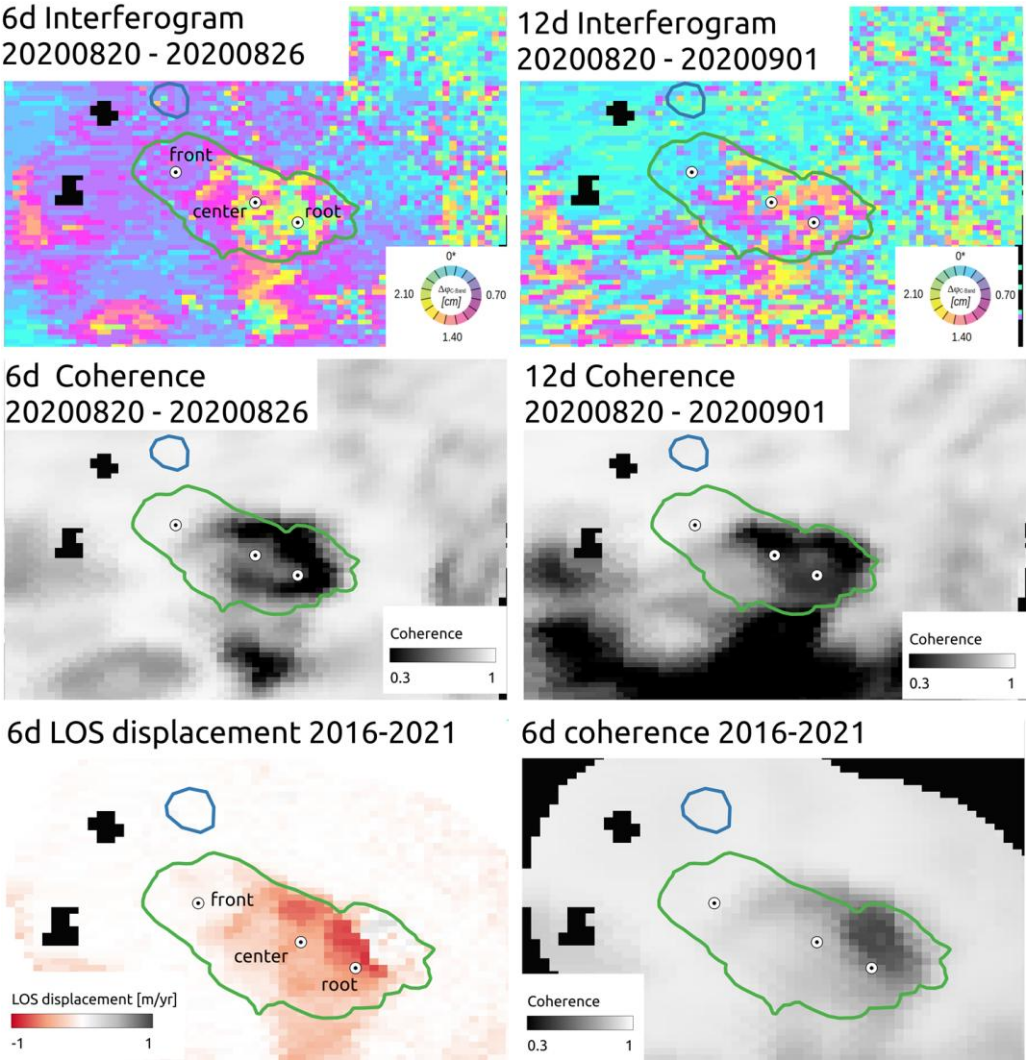

Overview

The figure above shows a 6d and 12d interferogram as well as the associated coherence from mid summer 2020. A selection of coherent interferograms was made manually for the further analysis. Many unwrapping issues are present due to high LOS velocities (> 1.2 m/yr) as well as abrupt changes. We selected three points (front, center, root) across the RG to extract LOS velocities time series. We additionally computed the yearly averages. The averaged values for all years can be seen in the bottom figure (left – LOS displacement, right – coherence). Close to the root location a region showing unwrapping issues is visible, indicated by a sharp transition in displacement rates in a low coherence region. Due to these errors, we focus on the three selected points where we check and correct any unwrapping errors.

Point Time Series

For the three monitoring points (front [45.6396, 7.4551], center [45.6388, 7.4571], and root [45.6383, 7.4582]) highlighted in the upper figures, we extracted LOS velocity time series, carefully checking and correcting any unwrapping issues. Each figure showing the time series on the next page displays the LOS displacement rates in m/yr in the top panel and the coherence in the bottom panel. For the LOS displacements, the coherent values are shown. For the coherence time series, all available pairs are shown. The coherence was obtained at the point location in the individual interferograms. Blue circles represent 6-day interferometric measurements, while orange crosses show 12-day measurements, with summer months (June-September) highlighted by gray vertical bands. In general, the 12-day interferogram coherence values are lower than the 6-day. For the locations center and front the coherence values in the summer season are generally high (>0.6-0.8), while for the root location the coherence values in summer are overall slightly lower. Higher velocities as well as unfavorable conditions such as snow cover can decrease the coherence.

The highest velocities are measured at the root location (~1-1.2 m/yr ~> 1.5-1.8 m/yr when assuming slope-parallel movement) with large fluctuations due to the low data quality (see figure on next page). At the center, the velocities also fluctuate from >0.2 to up to 0.6 m/yr (1.1m/yr slope parallel). The LOS velocity at the front is overall lowest with values generally within the sensitivity threshold of 0.2 m/yr. Scale Factors for the three points are 1.41 for front, 1.85 for center and 1.54 for root.

RG Monte Emilius Range 1
RGV Analysis – Descending orbit 139

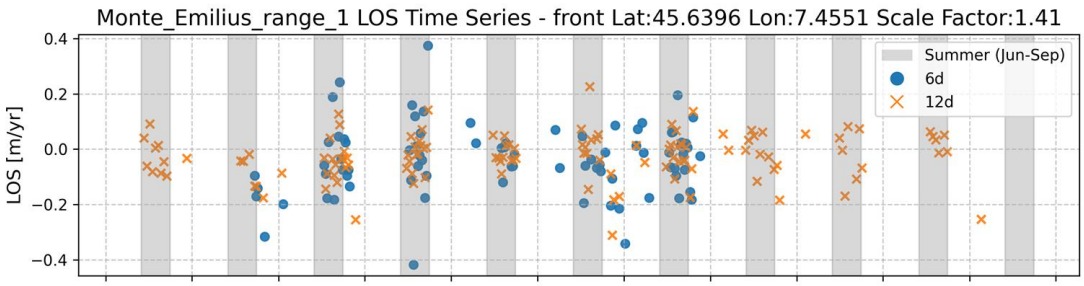

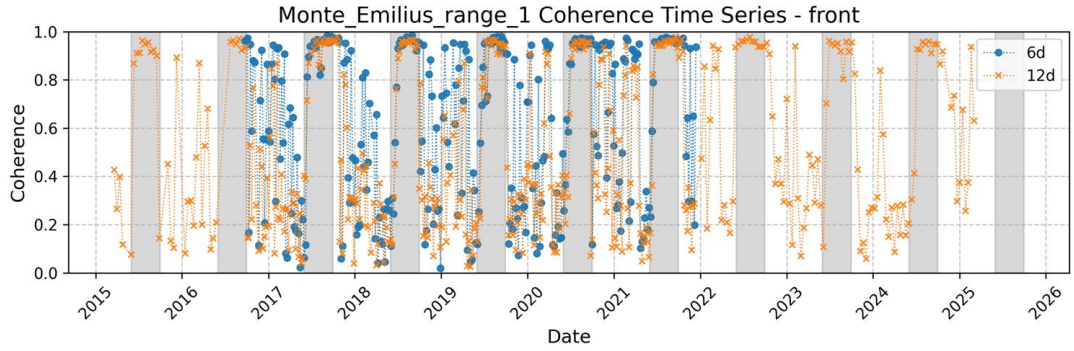

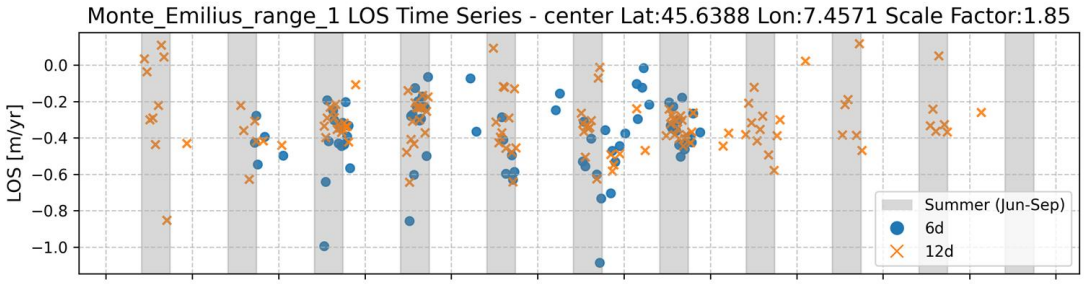

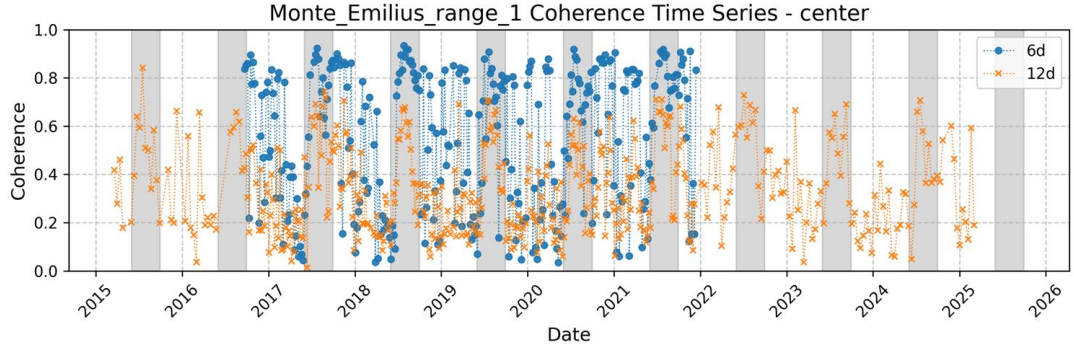

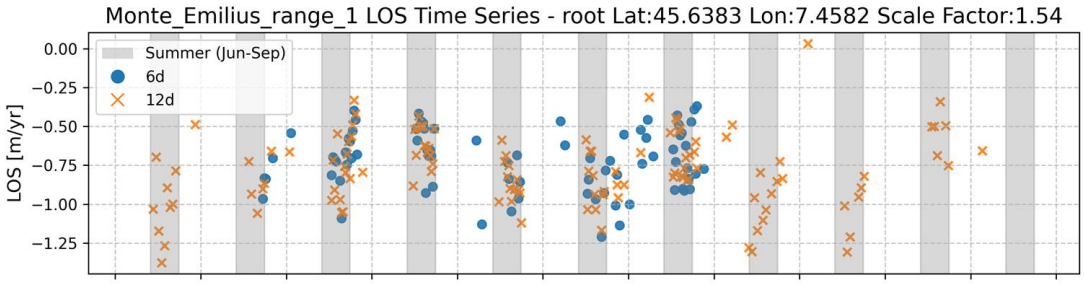

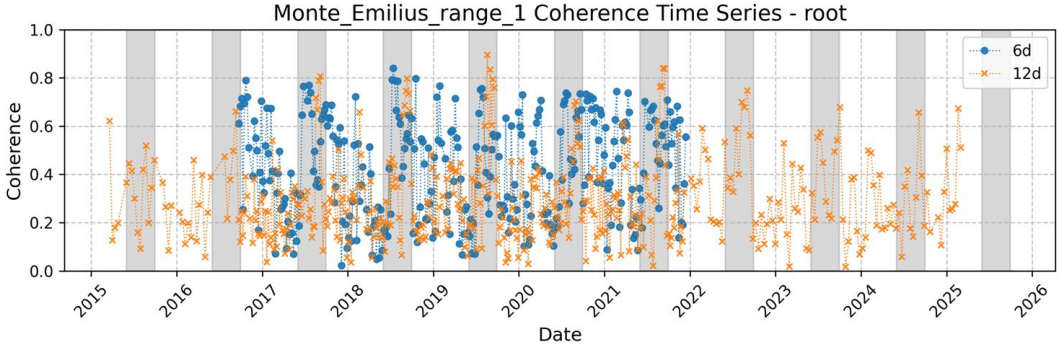

RG Monte Emilius Range 1
RGV Analysis – Descending orbit 139

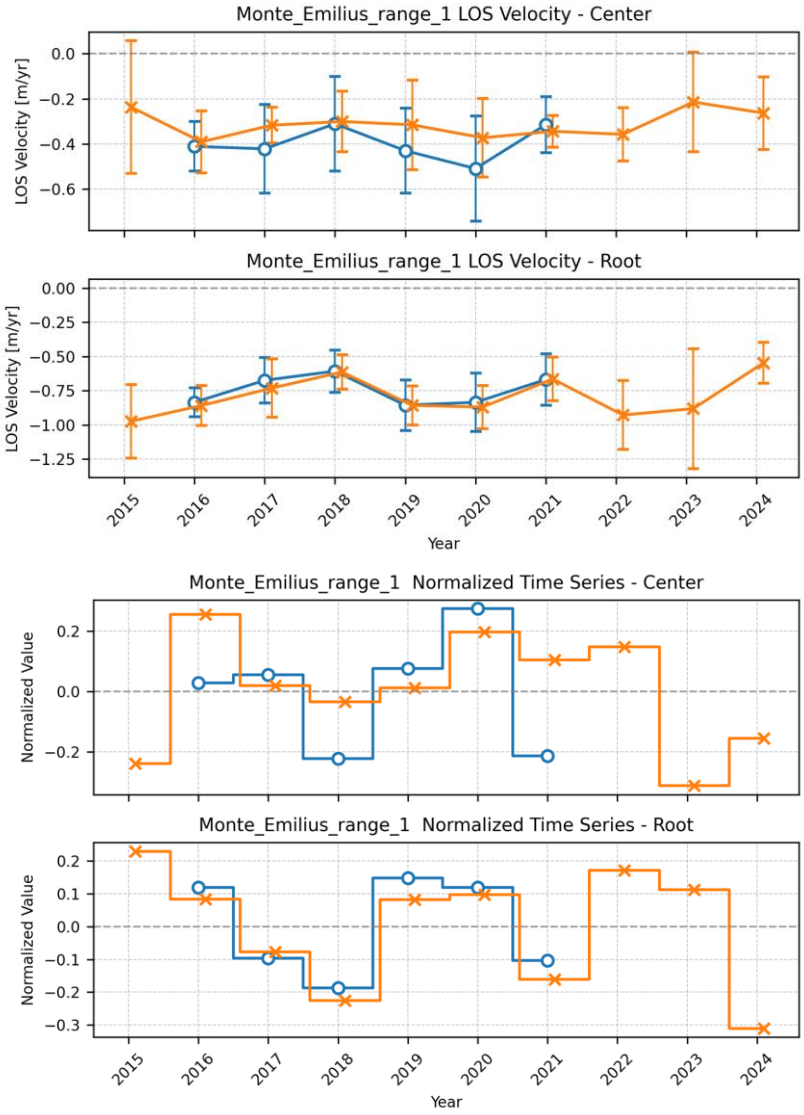

Velocity variation over the years: We averaged the obtained LOS velocity rates from the monitoring points center and root to generate yearly velocity estimates. For the location front the LOS velocities are below the sensitivity thresholds. In the top two figures, the averaged LOS velocities per summer are shown. The error bars represent the standard deviation per year. The two bottom figures show the normalized values ((Avg_year/mean_overall)-1) to highlight relative changes independent of the absolute velocities. Note that higher variations are expected as the measured velocities approach the sensitivity/noise level.

The center and root locations show error bars of roughly +/- 0.2 m/yr. The center and root display stronger seasonal variations, with slower movement in 2018 and 2021. Note that variation of the 12d data for point Center is not matching the other time-series. The variation is also relatively small with large error bars. The result should thus be interpreted with caution.

Monte Emilius Range 2 RGV Analysis

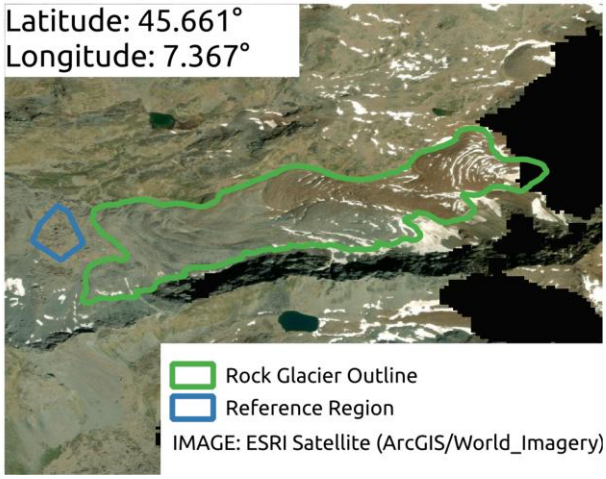

T088A

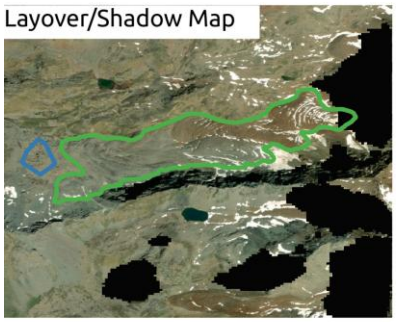

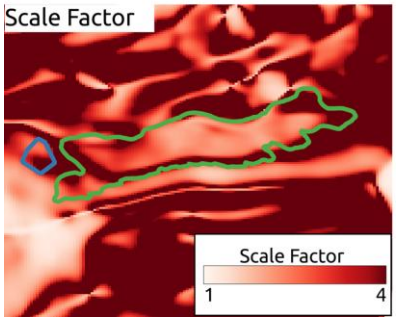

T139D

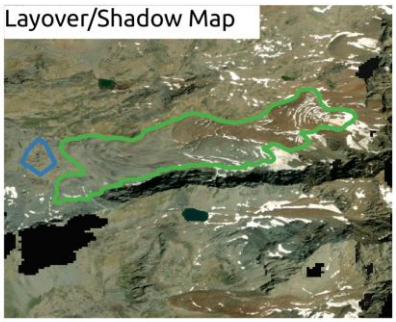

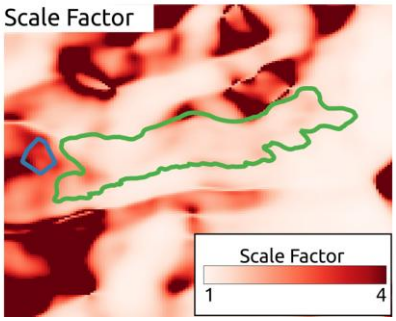

Layover/Shadow
Sentinel-1 data are acquired from two orbits (T088A and T139D). In both orbits the rock glacier region is not affected by layover or shadow effects.

Scale Factor:
T088A exhibits a more unfavorable viewing geometry than T139D with a Scale Factor from 2.2 to 4 and above. The Line-of-Sight for orbit T139D aligns better with the flow direction of the RG. Scale Factors for orbit T139D are in the range 1.3 to 2.5 over the RG.

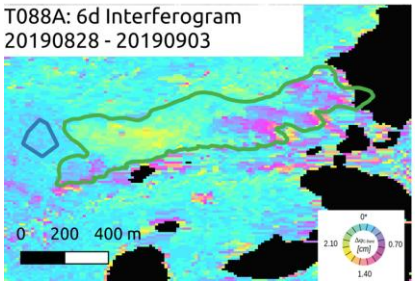

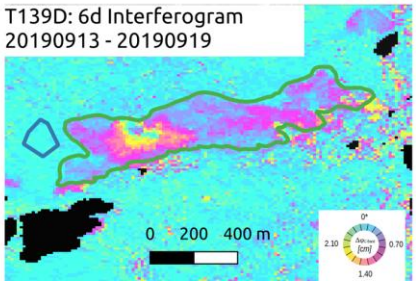

Initial assessment
The T139D interferogram reveals substantial movement across most of the RG, with deformation rates up to 1cm/6d (equivalent to approximately 0.6m/yr), sensitivity ~0.2m/yr. One sector exhibits significantly faster displacement rates approaching 3.3cm/6d (2m/yr). The extreme velocity contrast necessitates thorough verification of phase unwrapping during processing, with manual corrections likely required to ensure accurate deformation measurements. The T088A interferograms show smaller displacements due to the different viewing geometry.

Line-of-Sight

For the RGV Analysis use orbit T139D

RG Monte Emilius Range 2
RGV Analysis – Descending orbit 139

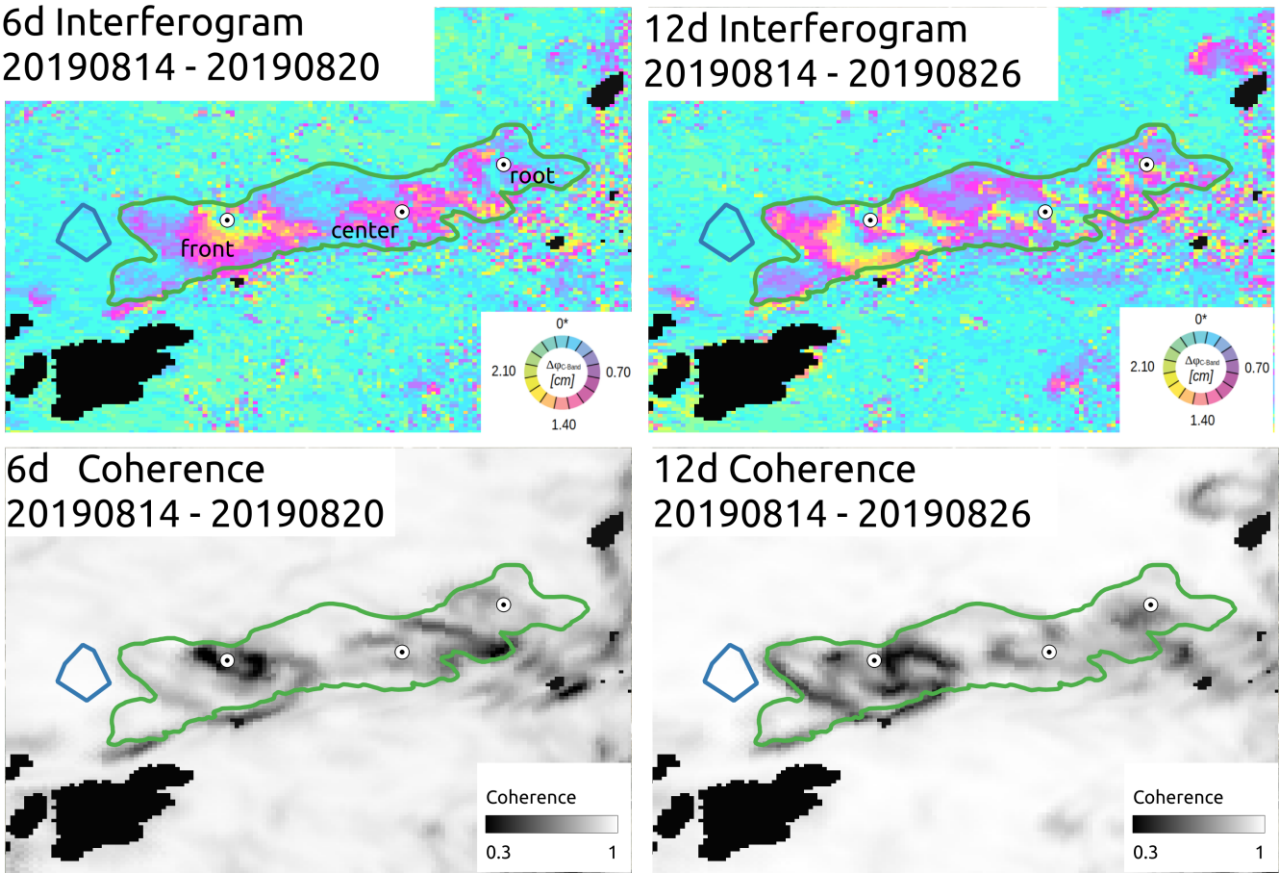

Overview

The figure above shows a 6d and 12d interferogram as well as the associated coherence from mid to late summer 2019. A selection of coherent interferograms was made manually for the further analysis. Many unwrapping issues are present due to high LOS velocities (up to 2 m/yr in the lower parts of the RG) as well as abrupt changes. We selected three points (front, center, root) across the RG to extract LOS velocities time series.

Point Time Series

For the three monitoring points (front [45.6608, 7.3609], center [45.6612, 7.3677], and root [45.6630, 7.3716]) highlighted in the upper figures, we extracted LOS velocity time series, carefully checking and correcting any unwrapping issues. Each figure showing the time series on the next page displays the LOS displacement rates in m/yr in the top panel and the coherence in the bottom panel. For the LOS displacements, the coherent values are shown. For the coherence time series, all available pairs are shown. The coherence was obtained at the point location in the individual interferograms. Blue circles represent 6-day interferometric measurements, while orange crosses show 12-day measurements, with summer months (June-September) highlighted by gray vertical bands. In general, the 12-day interferogram coherence values are lower than the 6-day. For the locations center and root the coherence values in the summer season are generally high (>0.8), while for the front location the coherence values in summer are overall slightly lower. Higher velocities as well as unfavorable conditions such as snow cover can decrease the coherence.

The highest velocities are measured at the front location (~1.5-2.2 m/yr ~> 1.8-2.7 m/yr when assuming slope-parallel movement) with fluctuations due to the low data quality (see figure on next page). At the center, the velocities fluctuate from 0.5 up to 1 m/yr with strong seasonal variations. The LOS velocity at the root is overall lowest with values generally within the sensitivity threshold of 0.2 m/yr but reaching 0.6 m/yr in the summers of 2017 and 2019. Scale Factors for the three points are 1.23 for front, 1.49 for center and 1.53 for root.

RG Monte Emilius Range 2
RGV Analysis – Descending orbit 139

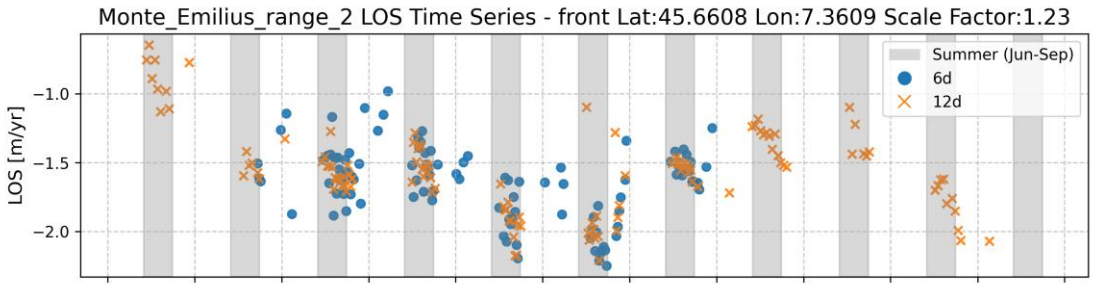

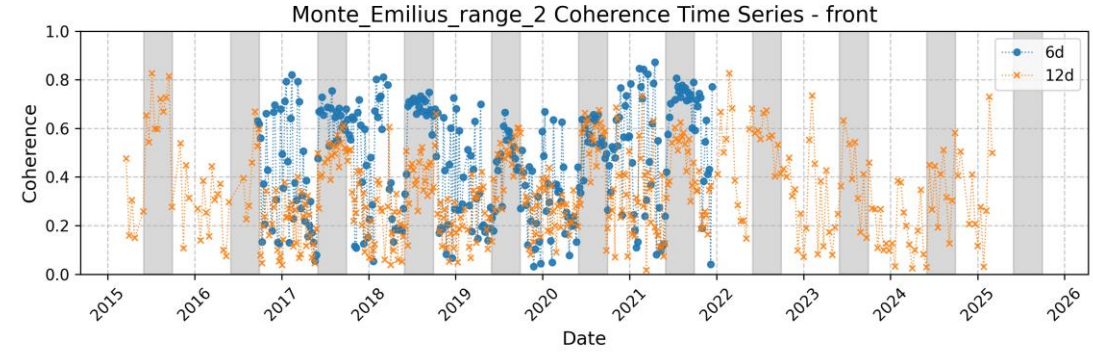

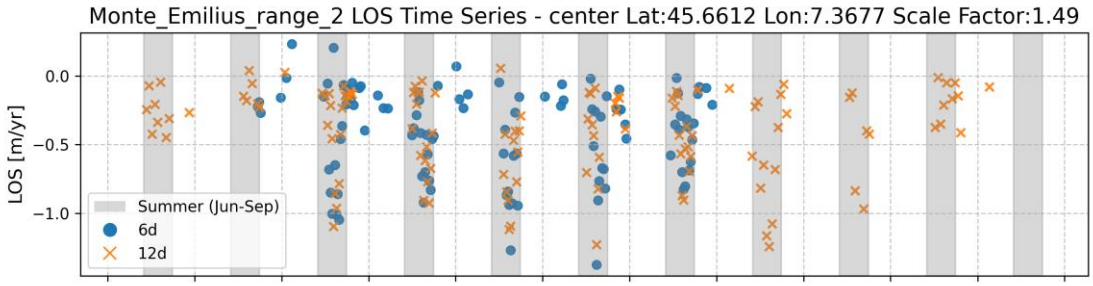

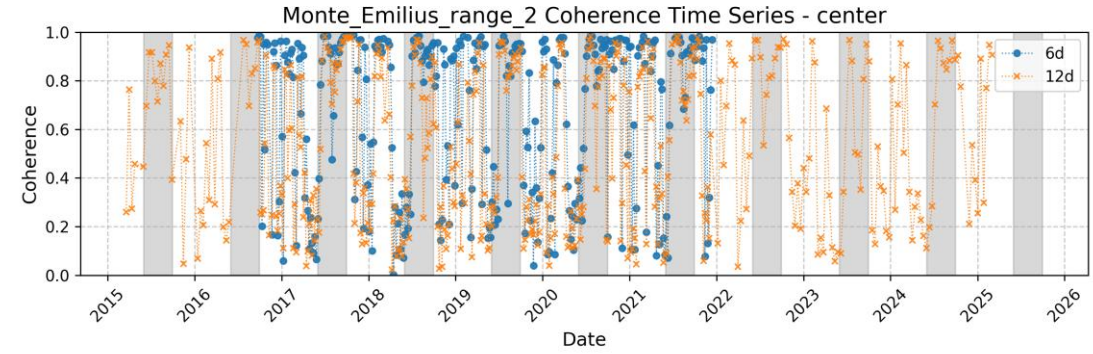

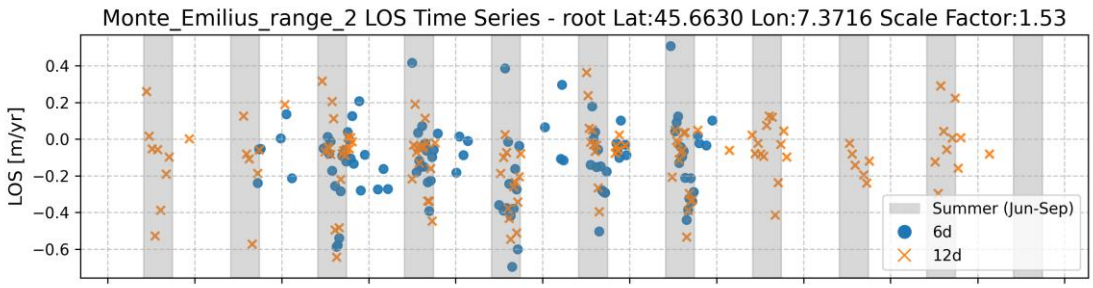

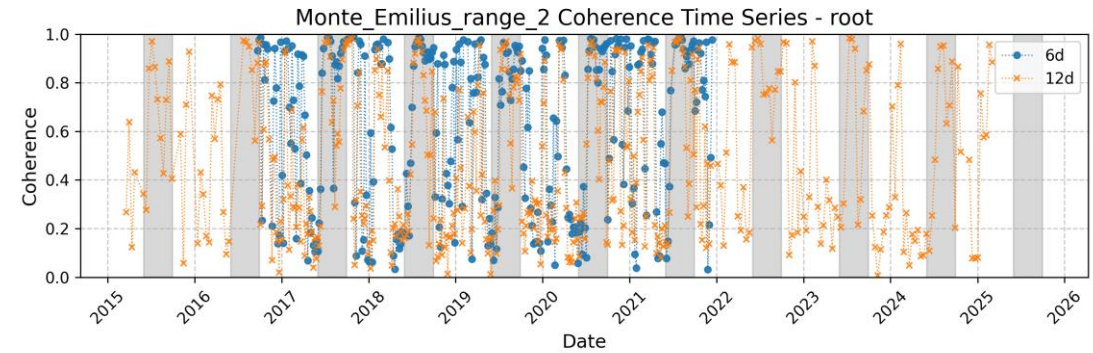

RG Monte Emilius Range 2
RGV Analysis – Descending orbit 139

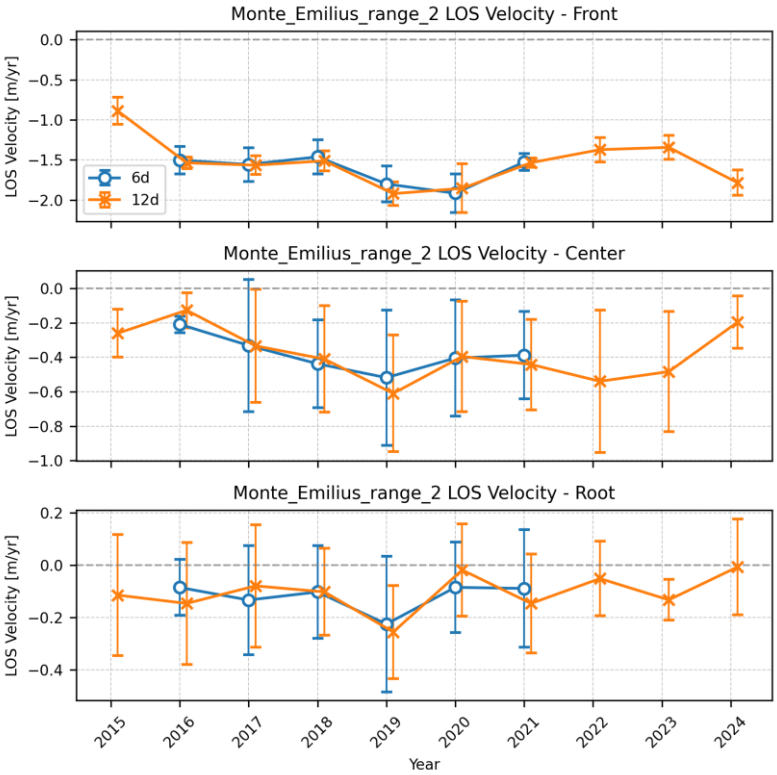

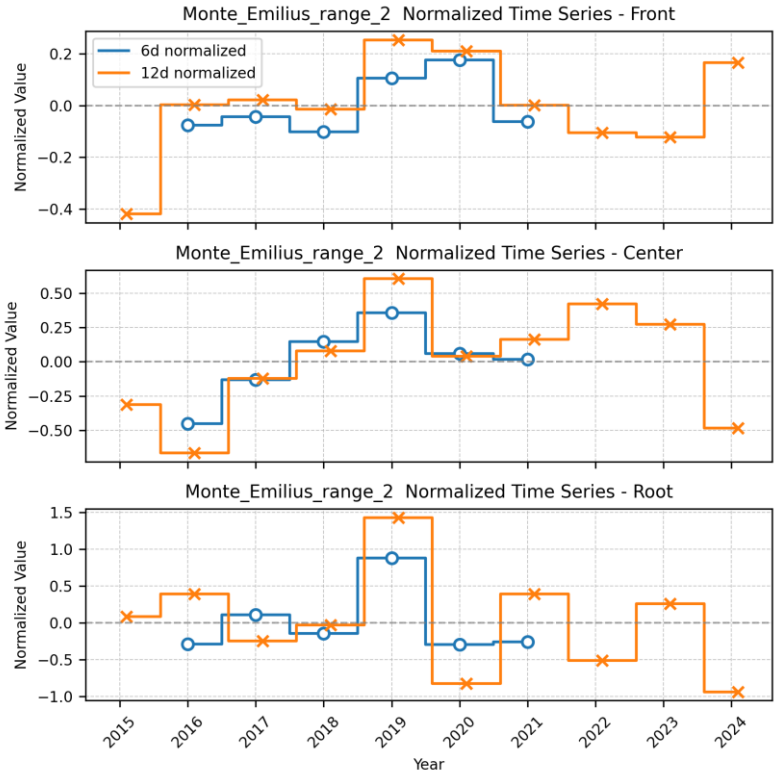

Velocity variation over the years: We averaged the obtained LOS velocity rates from all three monitoring points to generate yearly velocity estimates. In the top three figures, the averaged LOS velocities per summer are shown. The error bars represent the standard deviation per year. The three bottom figures show the normalized values ((Avg_year/mean_overall)-1) to highlight relative changes independent of the absolute velocities. Note that higher variations are expected as the measured velocities approach the sensitivity/noise level.

All locations show error bars of roughly +/- 0.2-0.4 m/yr. The front shows the overall highest LOS velocities with a very good agreement between 6-day and 12-day measurements. The center and root display stronger seasonal variations, with lowest overall velocities at the root location that largely remain within the sensitivity threshold of 0.2 m/yr and the time series displayed should thus be interpreted with caution.

North Arpignan RGV Analysis

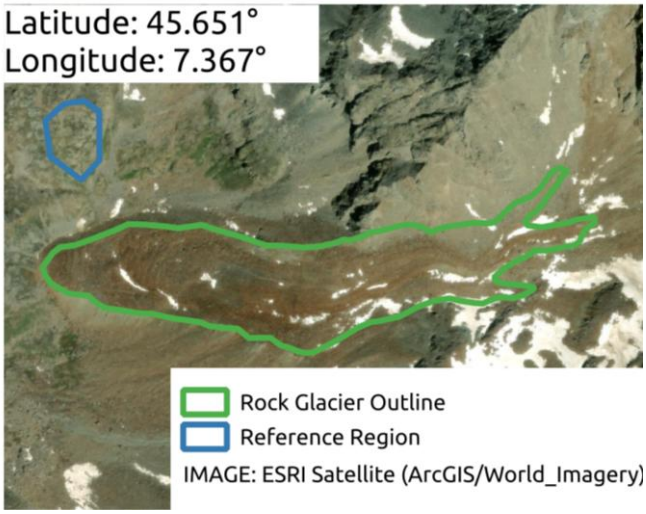

T088A

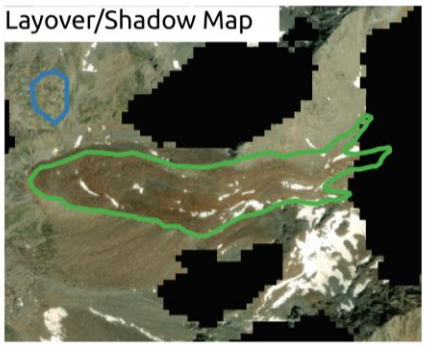

T139D

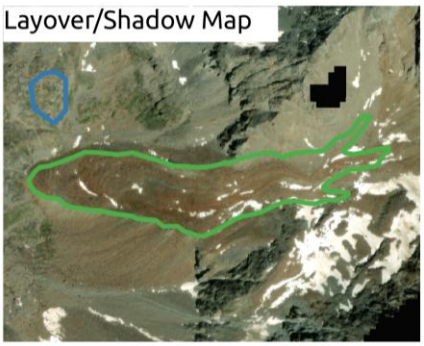

Layover/Shadow
Sentinel-1 data are acquired from two orbits (T088A and T139D). In both orbits the rock glacier region is not affected by layover or shadow effects.

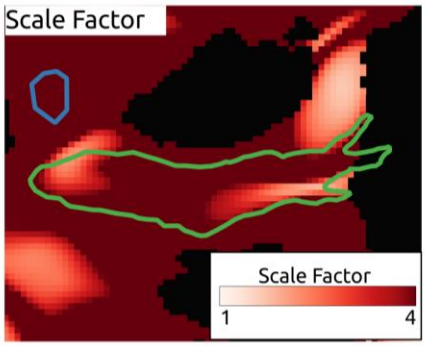

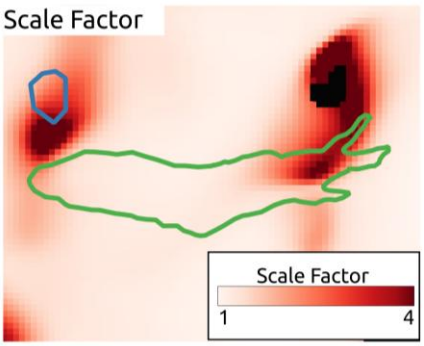

Scale Factor:
T088A exhibits an unfavorable viewing geometry with a Scale Factor above 4. The Line-of-Sight for orbit T139D aligns well with the flow direction of the RG. Scale Factors for orbit T139D are in the range 1.1 to 2 over the majority of the RG. At the root of the RG there is a small region that is not well aligned and shows scale factors above 4.

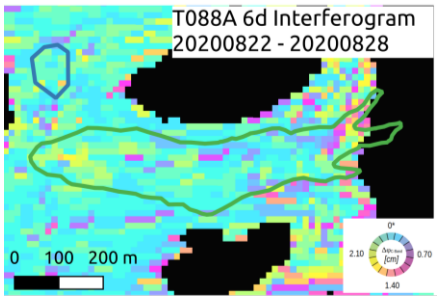

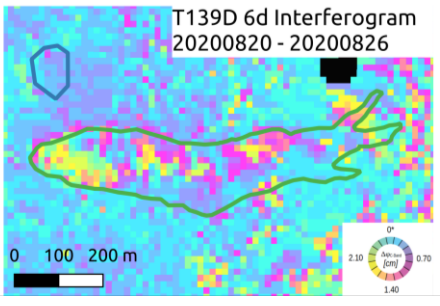

Line-of-Sight

Initial assessment
The T139D interferogram shows contrasting deformation patterns within the RG. The upper part at the root exhibits slow movement at or below the detection limit (sensitivity ~0.2m/yr), while the lower and center part displays faster movement of up to 2.2cm/6d (equivalent to approximately 1.2m/yr). Sharp velocity transitions towards the edges of the RG may introduce phase unwrapping challenges during processing.

For the RGV Analysis we use orbit T139D descending data.

North Arpignan RGV Analysis – Descending orbit 139

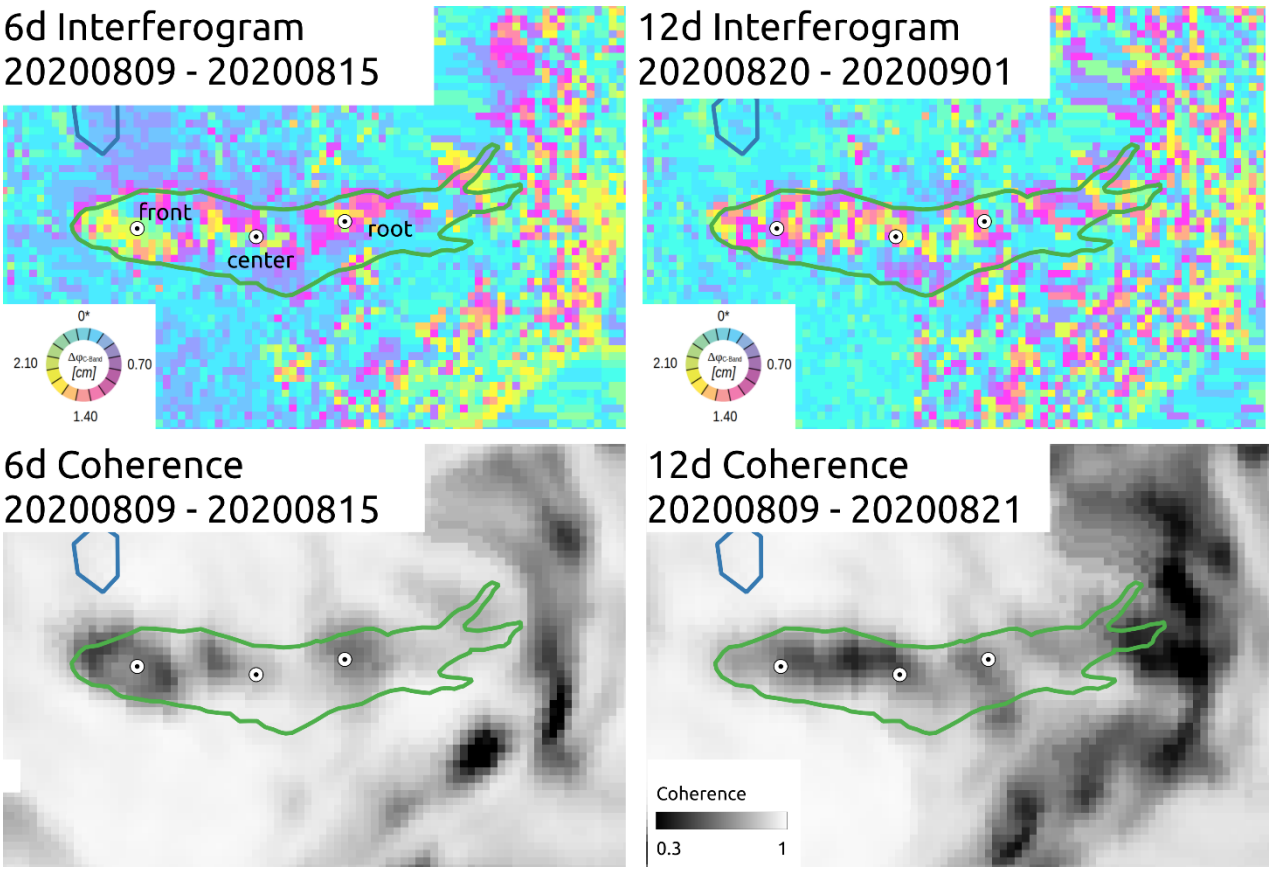

Overview

The figure above shows a 6d and 12d interferogram as well as the associated coherence from mid summer 2020. A selection of coherent interferograms was made manually for the further analysis. Many unwrapping issues are present due to high LOS velocities (> 1.2 m/yr) as well as abrupt changes. We selected three points (front, center, root) across the RG to extract LOS velocities time series.

Point Time Series

For the three monitoring points (front [45.6514, 7.3649], center [45.6513, 7.3678], and root [45.6516, 7.3699]) highlighted in the upper figures, we extracted LOS velocity time series, carefully checking and correcting any unwrapping issues. Each figure showing the time series on the next page displays the LOS displacement rates in m/yr in the top panel and the coherence in the bottom panel. For the LOS displacements, the coherent values are shown. For the coherence time series, all available pairs are shown. The coherence was obtained at the point location in the individual interferograms. Blue circles represent 6-day interferometric measurements, while orange crosses show 12-day measurements, with summer months (June-September) highlighted by gray vertical bands. In general, the 12-day interferogram coherence values are lower than the 6-day. For all locations, the coherence values in the summer season are generally high (>0.6). Higher velocities as well as unfavorable conditions such as snow cover can decrease the coherence.

The highest velocities are measured at the center location with velocities up to 2.5 m/yr (2.8 m/yr when assuming slope-parallel movement). The high velocities did not all to correct the unwrapping error for the 12d interferograms. At the front and root location LOS velocities were lower approaching 1.2 m/yr. The root location showed the large fluctuations during the summer months (acceleration and deceleration). Scale Factors for the three points are 1.30 for front, 1.13 for center and 1.59 for root.

North Arpignan RGV Analysis – Descending orbit 139

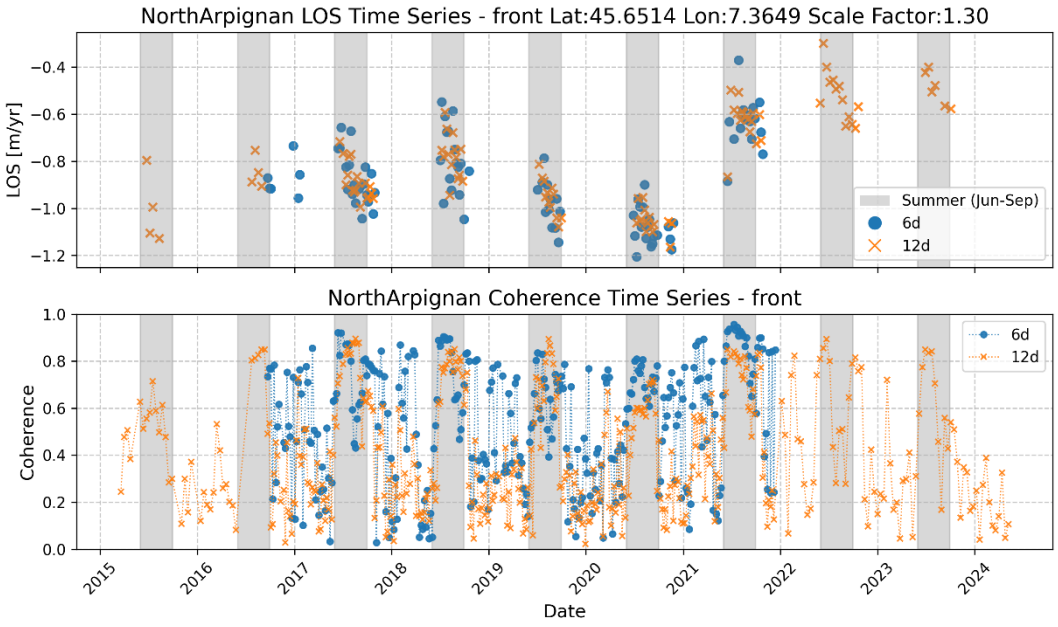

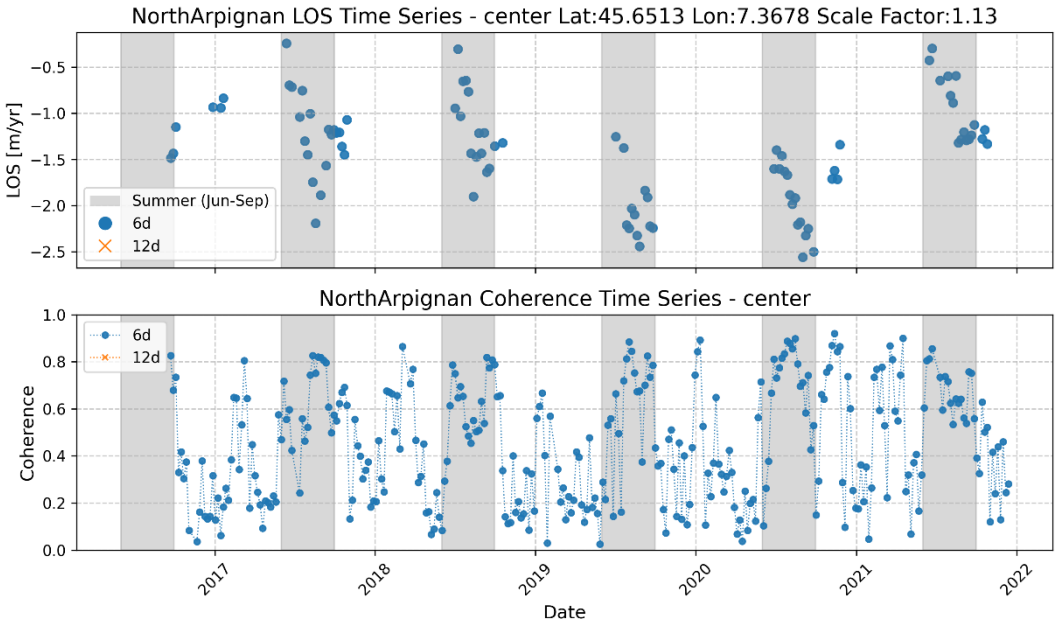

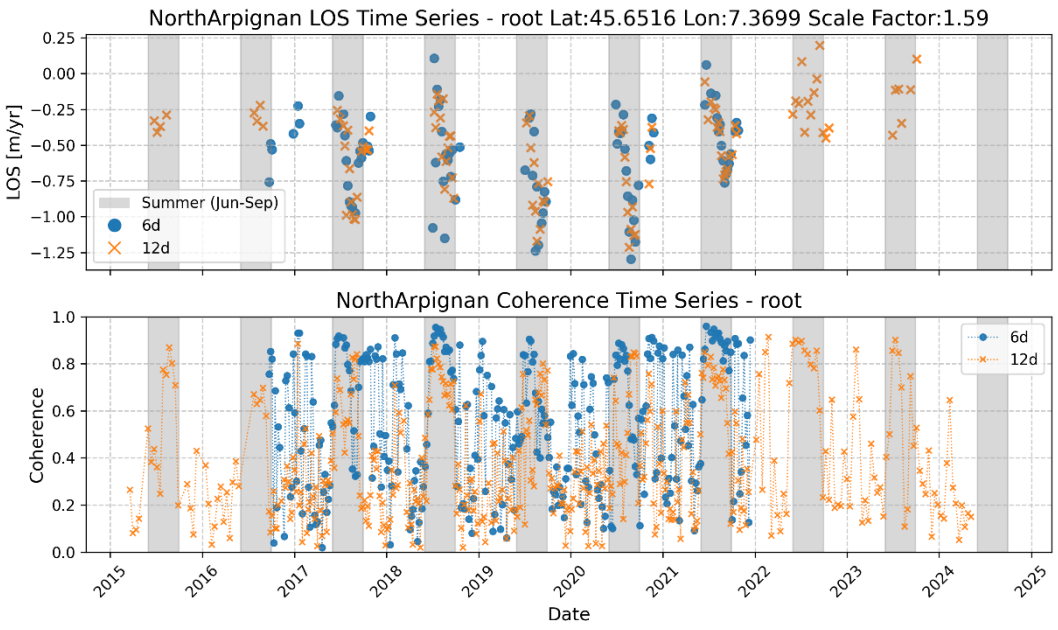

North Arpignan RGV Analysis – Descending orbit 139

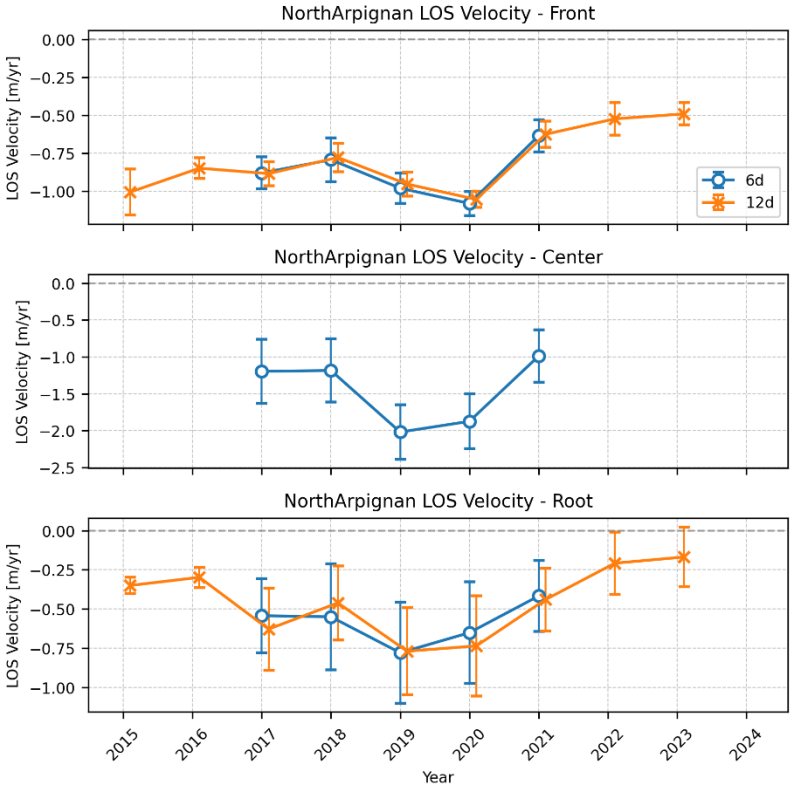

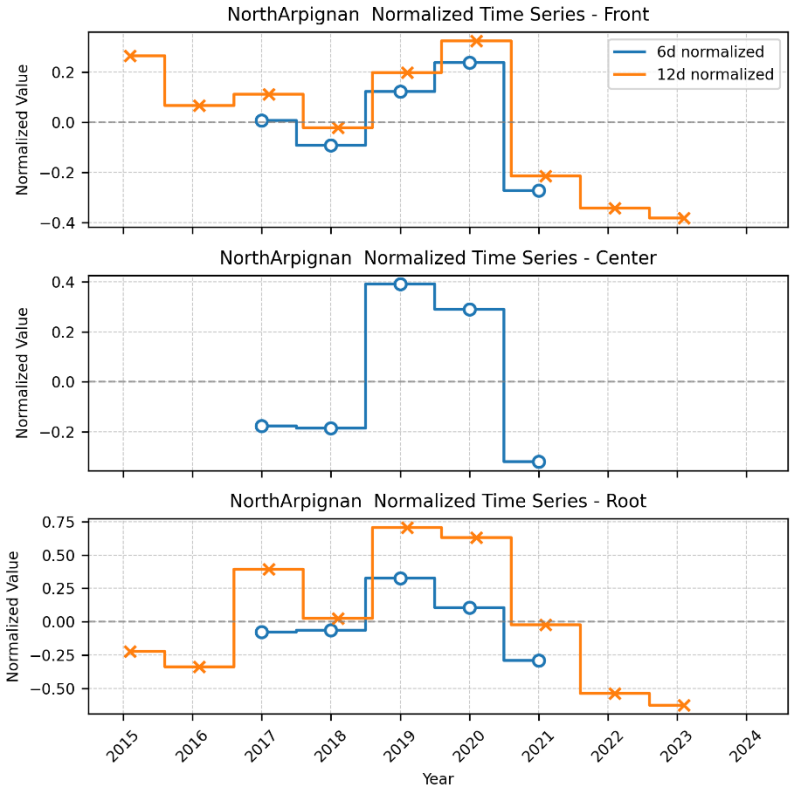

Velocity variation over the years: We averaged the obtained LOS velocity rates from all three monitoring points to generate yearly velocity estimates. In the top three figures, the averaged LOS velocities per summer are shown. The error bars represent the standard deviation per year. The three bottom figures show the normalized values ((Avg_year/mean_overall)-1) to highlight relative changes independent of the absolute velocities. Note that higher variations are expected as the measured velocities approach the sensitivity/noise level.

All three points show significant changes during the observation period. In general, the behavior of all three points as well as the 6-day and 12-day period match well. The fasters years are in 2020 and 2021. The error bar are larges for the root point due to the large seasonal acceleration and deceleration.

Rhemes RGV Analysis

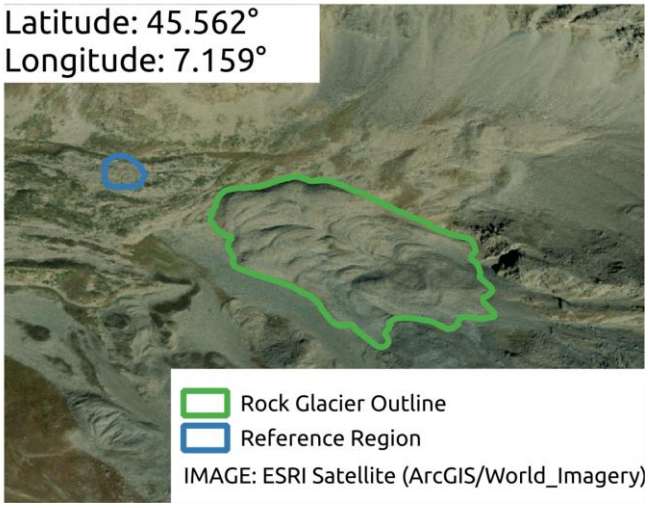

T088A

T139D

Layover/Shadow
Sentinel-1 data are acquired from two orbits (T088A and T139D). In both orbits the rock glacier region is not affected by layover or shadow effects.

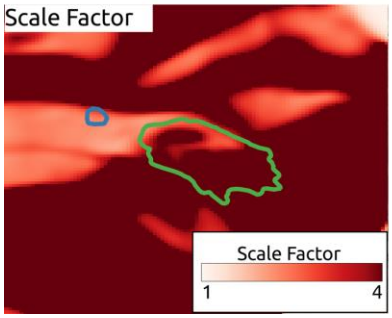

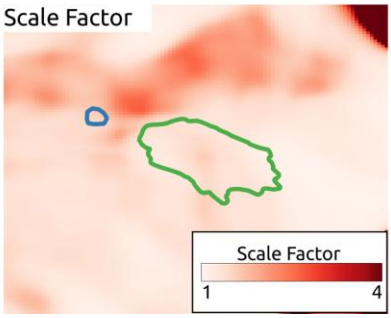

Scale Factor
T088A exhibits an unfavorable viewing geometry with a Scale Factor above 4. The Line-of-Sight for orbit T139D aligns better with the flow direction of the RG. Scale Factors for orbit T139D are in the range of 1.2 to 1.6 over the RG.

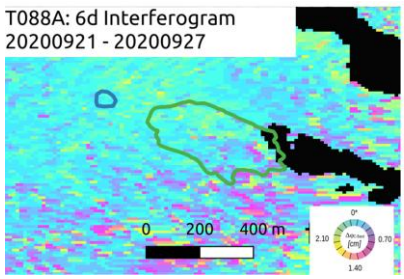

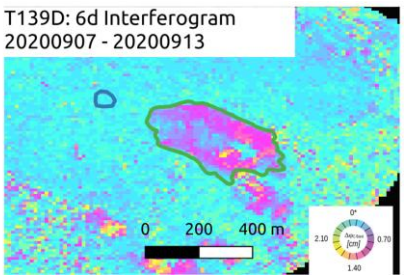

Initial assessment
The T139D interferogram shows movement of about 0.5 to 1 cm/6d (0.3 to 0.6m/yr) over most of the RG. A section in the center exhibits potentially faster displacement rates, which may present phase unwrapping challenges during subsequent processing stages.

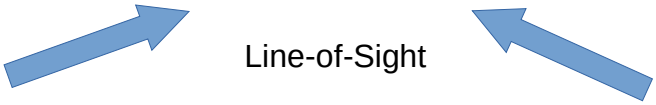

For the RGV Analysis we use orbit T139D descending data.

Rhemes RGV Analysis – Descending orbit 139

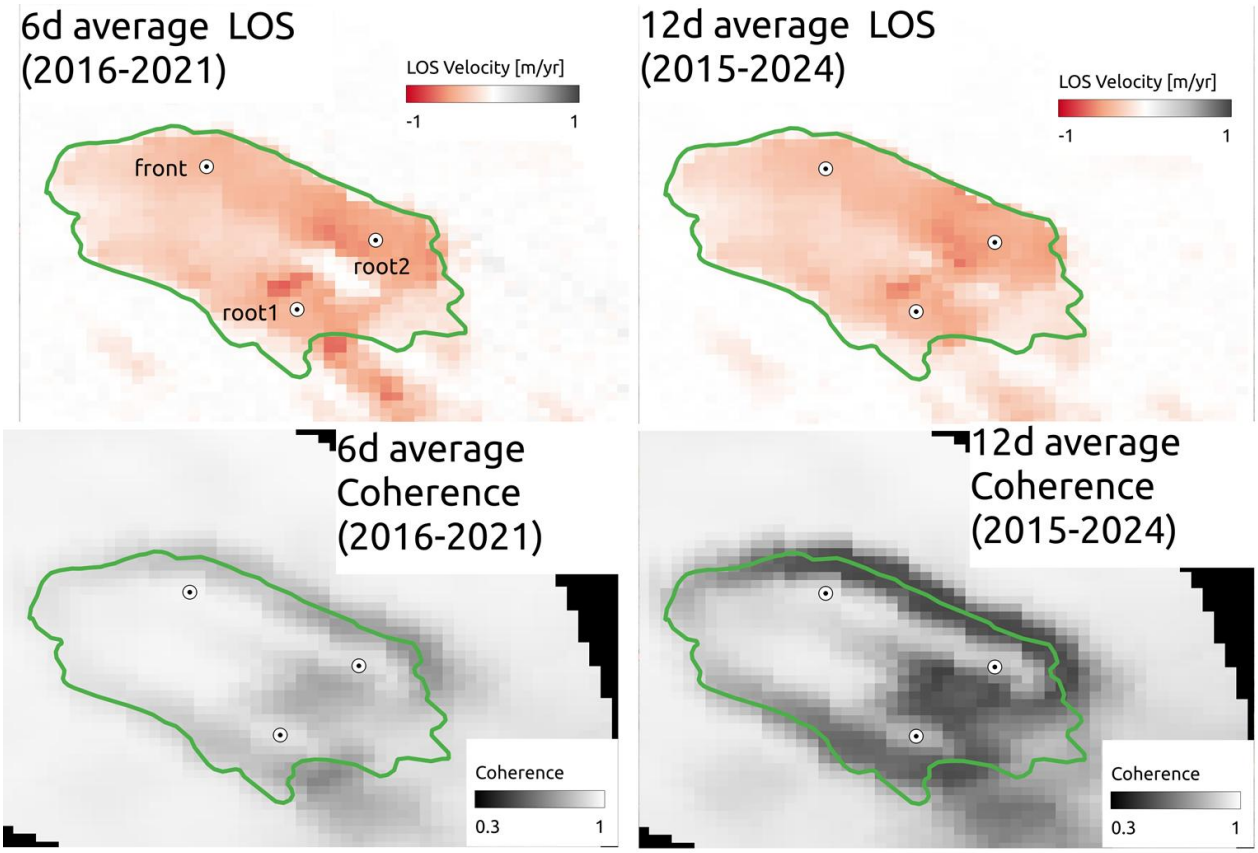

Overview
The figures above show averaged Line-of-Sight (LOS) velocities over all available summer seasons (July to October) (top) as well as the average coherence over the same period (bottom). 6-day interferograms are available from October 2016 to December 2021, 12-day interferograms are available from October 2015 to the start of 2025. Negative LOS values indicate a displacement away from the sensor. A selection of coherent interferograms was made manually for the further analysis. We selected three points (front, root1 and root2) to extract LOS velocities time series.

Point Time Series
For the three monitoring points (front [45.5628, 7.1575], root1 [45.5606, 7.1589], and root2 [45.5617, 7.1602]) highlighted in the upper plots, we extracted LOS velocity time series, carefully checking and correcting any unwrapping issues. Each figure showing the time series on the next page displays the LOS displacement rates in m/yr in the top panel and the coherence in the bottom panel. For the LOS displacement, only the coherent measurements are shown. For the coherence time series, all available pairs are shown. The coherence was obtained at the point location in the individual interferograms. Blue circles represent 6-day interferometric measurements, while orange crosses show 12-day measurements, with summer months (June-September) highlighted by gray vertical bands.
For the selected interferograms the coherence values are generally high (>0.6-0.8) and are obtained mainly in the summer season. In general, the 12-day interferogram coherence values are lower than the 6-day. Higher velocities as well as unfavorable conditions such as snow cover can decrease the coherence.
The highest velocities are measured at the root2 location (~0.8-0.9 m/yr ~> 0.9-1.0 m/yr when assuming slope-parallel movement) with acceleration and deceleration during the summer of about 0.3-0.4 m/yr. Root1 shows similar behavior with slightly higher fluctuations within the summer of 0.4 m/yr. At the front, the velocities are overall lower and range between 0.2 m/yr and 0.6 m/yr, with few accelerations up to 0.7 m/yr in the summers of 2019 and 2020.
Scale Factors for the three points are 1.36 for front, 1.34 for root1 and 1.17 for root2.

Rhemes RGV Analysis – Descending orbit 139

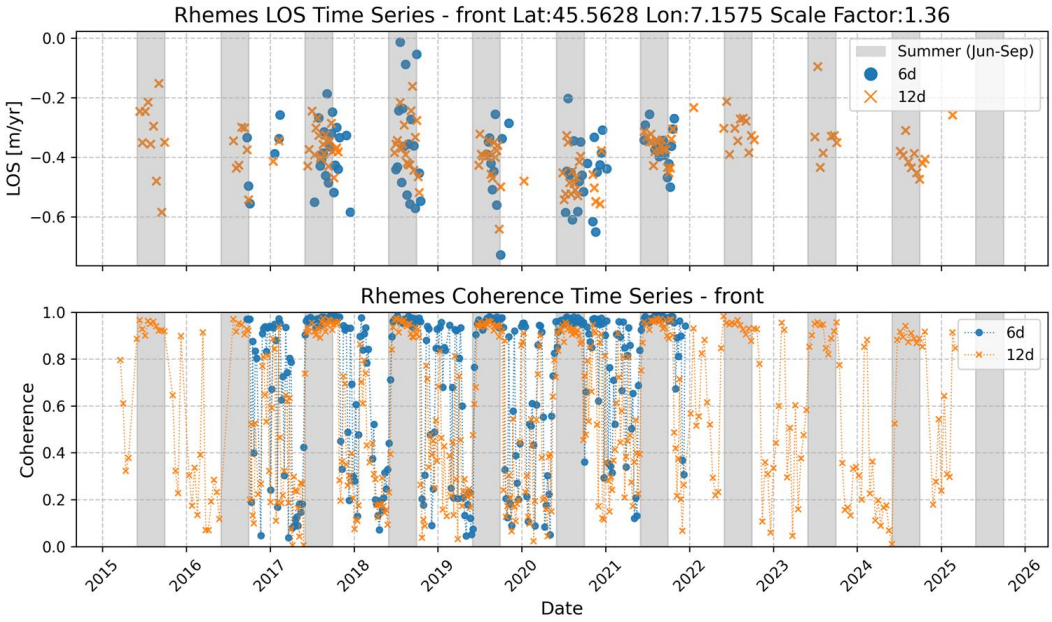

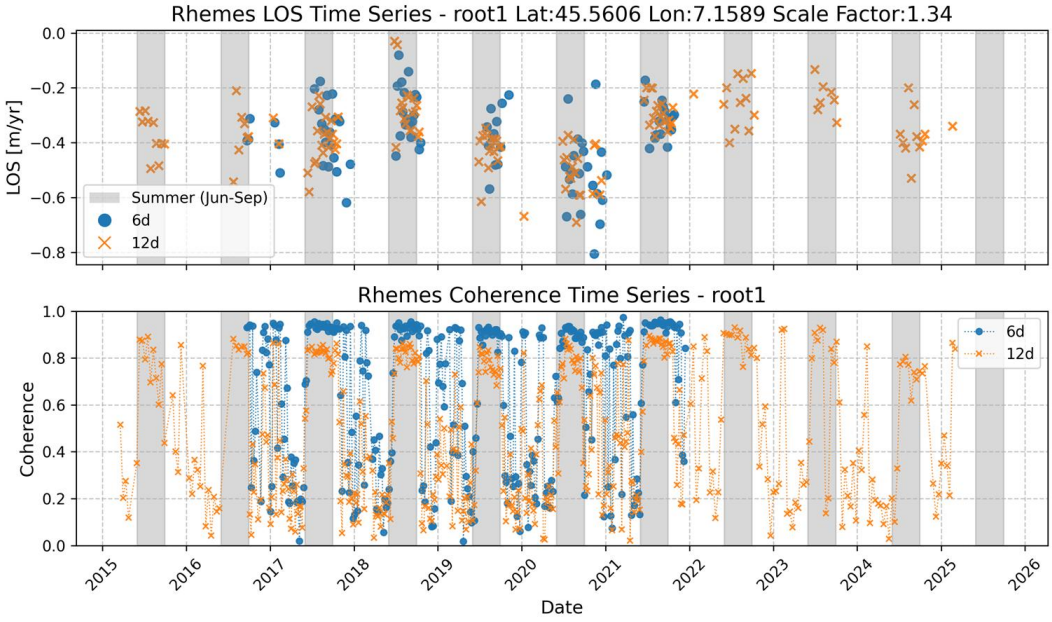

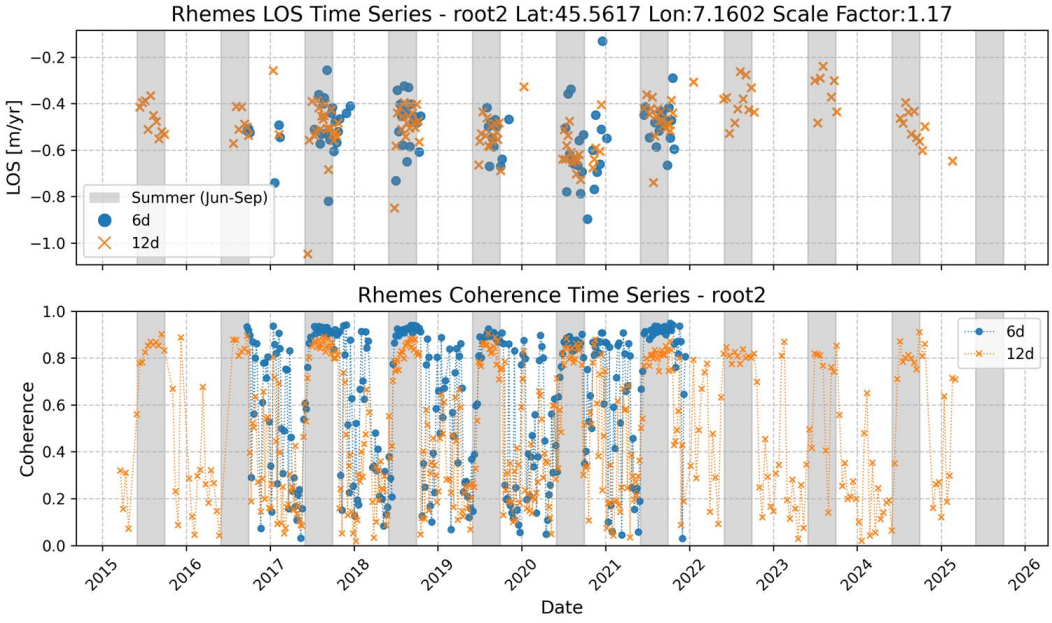

Rhemes RGV Analysis – Descending orbit 139

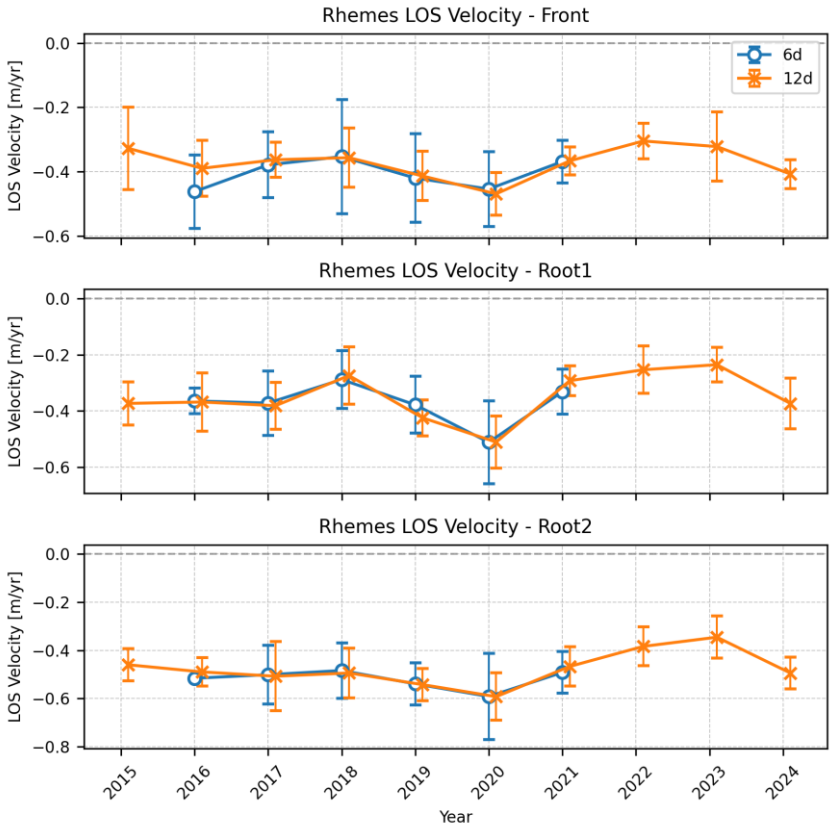

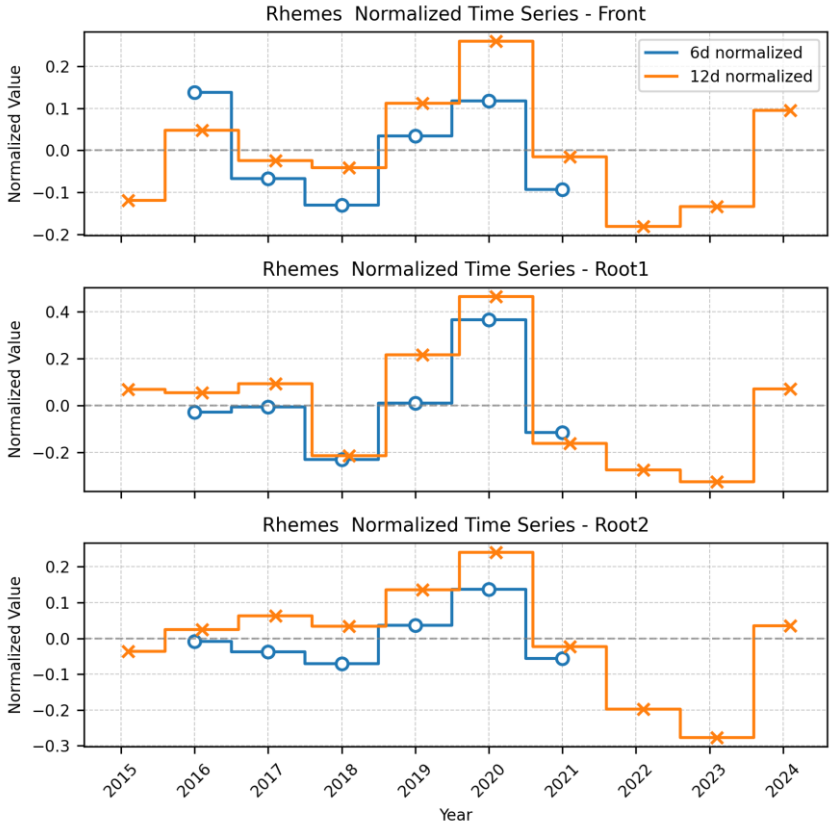

Velocity variation over the years: We averaged the obtained LOS velocity rates from all three monitoring points to generate yearly velocity estimates. In the top three figures, the averaged LOS velocities per summer are shown. The error bars represent the standard deviation per year. The three bottom figures show the normalized values ((Avg_year/mean_overall)-1) to highlight relative changes independent of the absolute velocities. Note that higher variations are expected as the measured velocities approach the sensitivity/noise level.

All three locations exhibit fluctuations and seasonal variations, showing a relatively consistent temporal pattern: stable displacement in 2015 to 2018, followed by a strong acceleration in 2019 and 2020 and a subsequent deceleration until 2023, with a renewed acceleration in 2024. The similar pattern between all three points in the normalized plot indicates that while absolute movement intensity differs between locations, the proportional changes over time are consistent. The good agreement between 6-day (blue circles, 2016-2021) and 12-day (orange crosses, 2015-2024) interferometric measurements indicates reliability in the observations.

Rhemes RGV Analysis – Descending orbit 139

The number of unwrapping errors over the whole RG was small which allowed the spatial aggregation of LOS velocities for all points on the RG. We kept points with average LOS displacement rates above the approximate sensitivity (0.2m/yr for 6d and 0.1m/yr for the 12d). The points above the sensitivity limit can be seen in the bottom figures and the relative changes averaged over all points in the bottom plot.

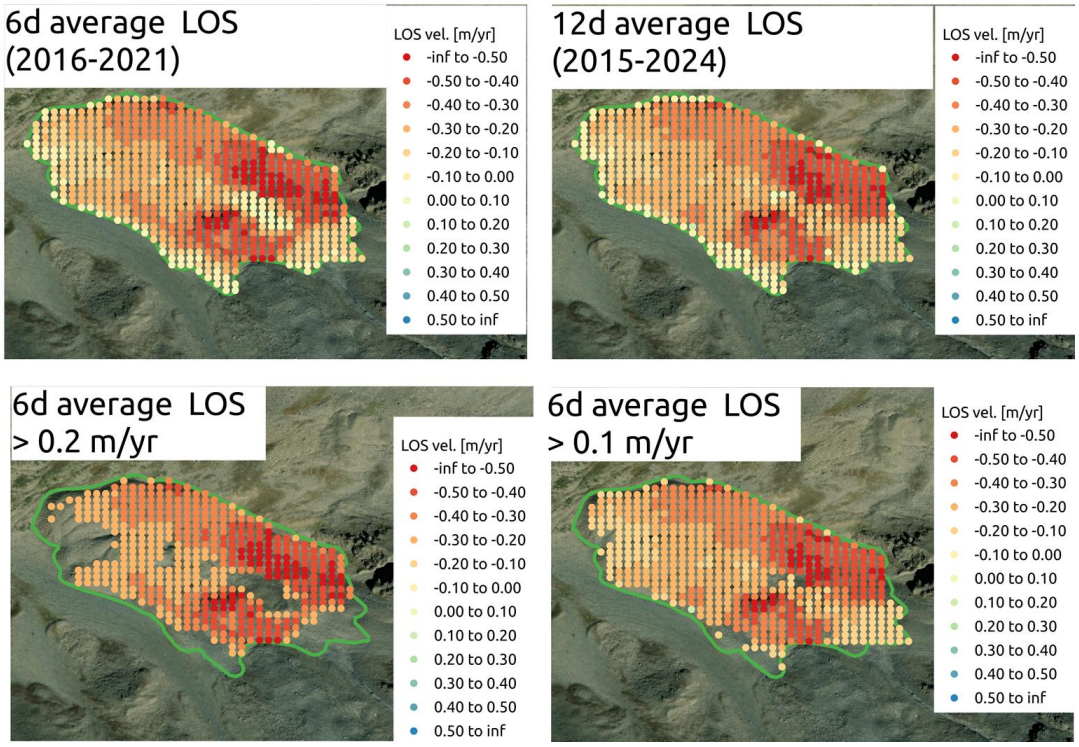

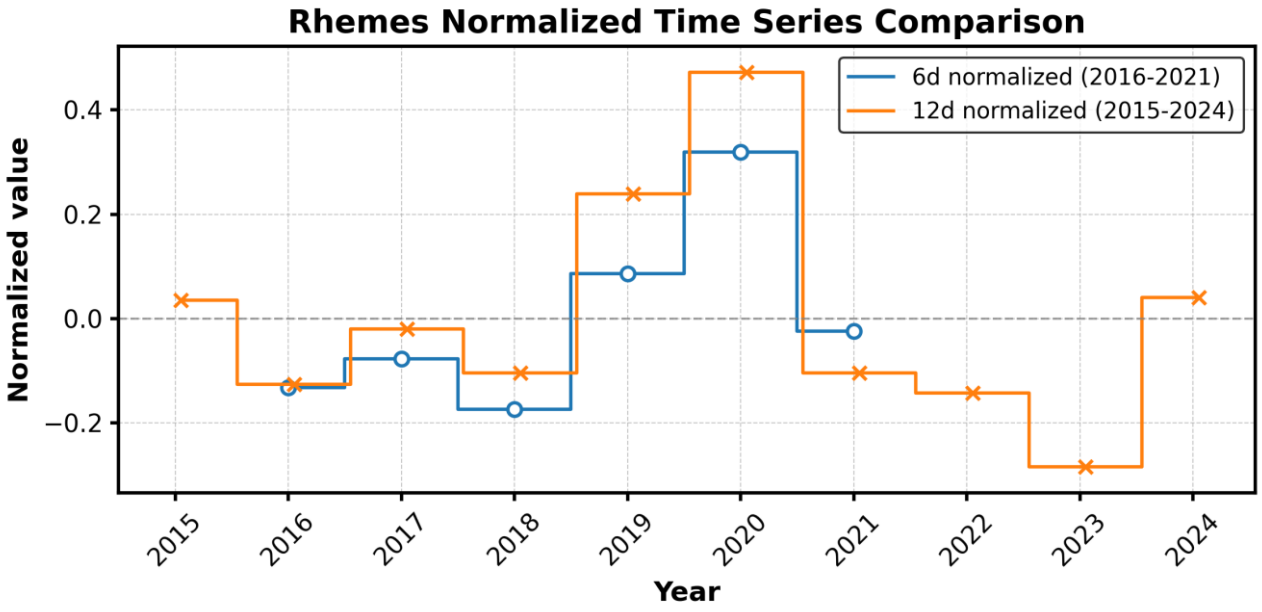

Val Grisenche 2 RGV Analysis

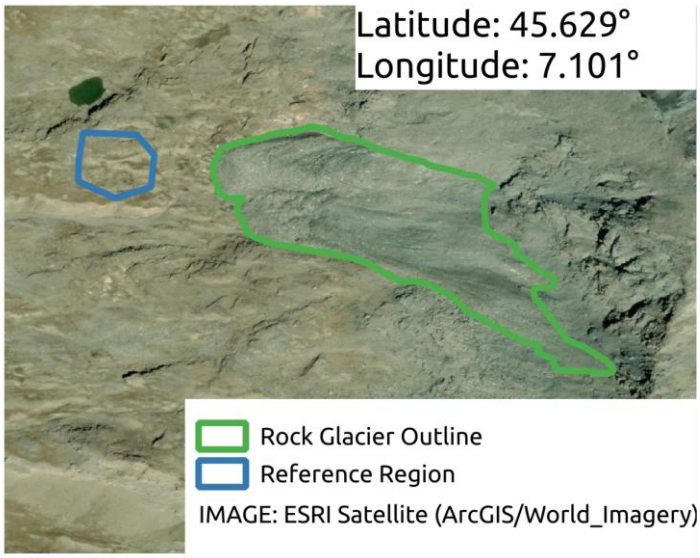

T088A

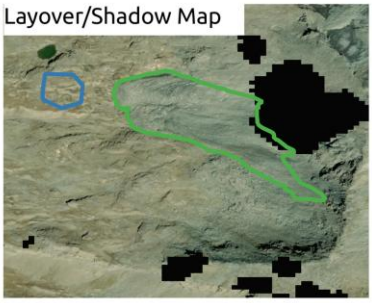

T139D

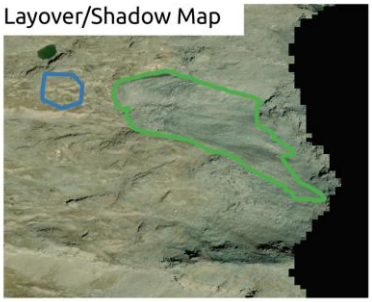

Layover/Shadow
Sentinel-1 data are acquired from two orbits (T088A and T139D). In both orbits the rock glacier region is not affected by layover or shadow effects.

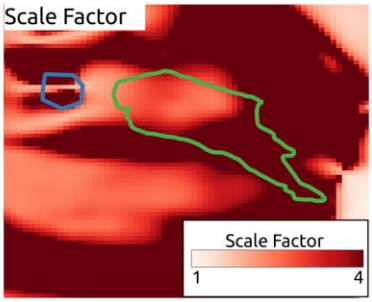

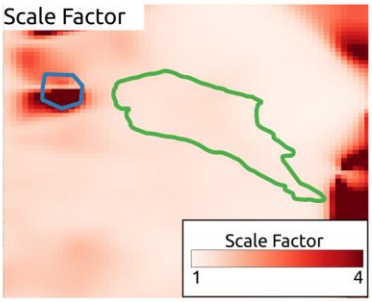

Scale Factor
T088A exhibits an unfavorable viewing geometry with a Scale Factor mostly above 4.
The Line-of-Sight for orbit T139D aligns well with the flow direction of the RG.
Scale Factors for orbit T139D are in the range 1.1 to 1.5 over the RG.

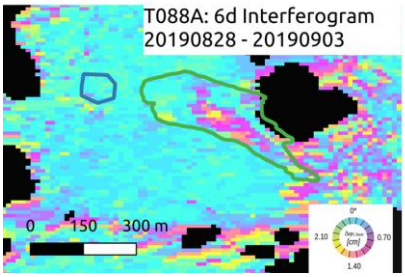

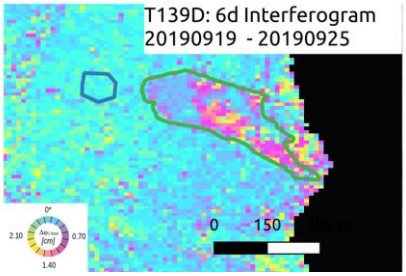

Initial assessment
The T139D interferogram shows velocities up to 1.5 to 2 cm/6d (approximately 0.9 to 1.2 m/yr). Challenging conditions are evident with notable phase noise quality issues. These factors may make processing potentially challenging, requiring careful attention during subsequent analysis steps.

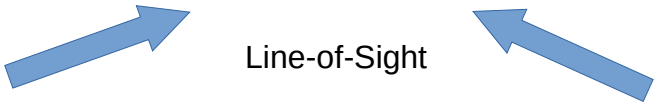

For the RGV Analysis we use orbit T139D descending data.

Val Grisenche 2 RGV Analysis – Descending orbit 139

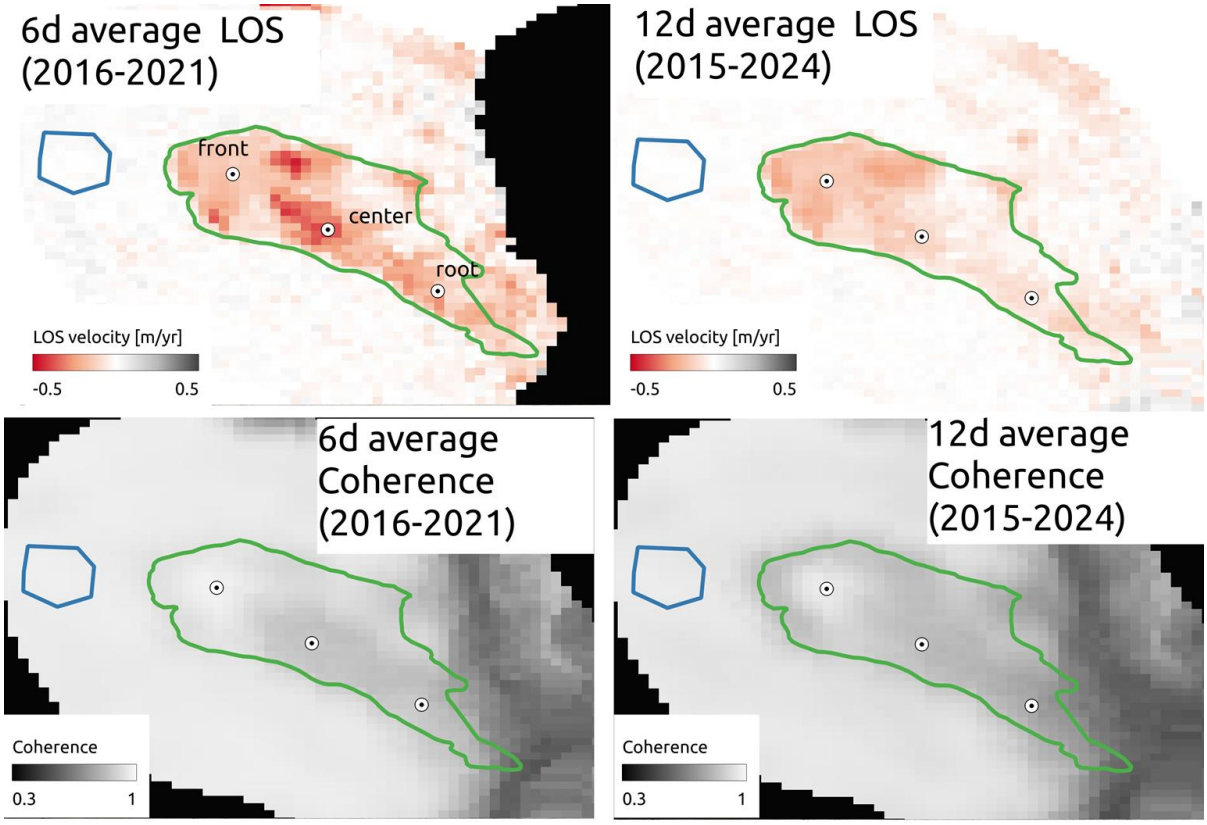

Overview

The figures above show averaged Line-of-Sight (LOS) velocities over all available summer seasons (July to October) (top) as well as the average coherence over the same period (bottom). 6-day interferograms are available from October 2016 to December 2021, 12-day interferograms are available from October 2015 to the start of 2025. Negative LOS values indicate a displacement away from the sensor. A selection of coherent interferograms was made manually for the further analysis. We selected three points (front, center and root) to extract LOS velocities time series.

Point Time Series

For the three monitoring points (front [45.6303, 7.1000], center [45.6293, 7.1016], and root [45.6283, 7.1035]) highlighted in the upper figures, we extracted LOS velocity time series, carefully checking and correcting any unwrapping issues. Each figure showing the time series on the next page displays the LOS displacement rates in m/yr in the top panel and the coherence in the bottom panel. For the LOS displacement, only the coherent measurements are shown. For the coherence time series, all available pairs are shown. The coherence was obtained at the point location in the individual interferograms. Blue circles represent 6-day interferometric measurements, while orange crosses show 12-day measurements, with summer months (June-September) highlighted by gray vertical bands.

For the selected interferograms the coherence values are generally high (>0.6-0.8) and are obtained mainly in the summer season. In general, the 12-day interferogram coherence values are lower than the 6-day. Higher velocities as well as unfavorable conditions such as snow cover can decrease the coherence.

The highest velocities are measured at the center (~1.2-1.5 m/yr ~> 1.6-2.0 m/yr when assuming slope-parallel movement) with acceleration and deceleration during the summer of up to 1 m/yr. The root location shows similar behavioral patterns in summer, reaching LOS velocities of 0.6-0.8 m/yr (~> 0.8-1.1 m/yr when assuming slope-parallel movement) with slightly lower fluctuations of about 0.5 m/yr. The velocities are lowest at the front and range between 0.2 m/yr, thus inside the sensitivity limit, and 0.4 m/yr. Scale Factors for the three points are 1.31 for front, 1.37 for center and 1.25 for root.

Val Grisenche 2 RGV Analysis – Descending orbit 139

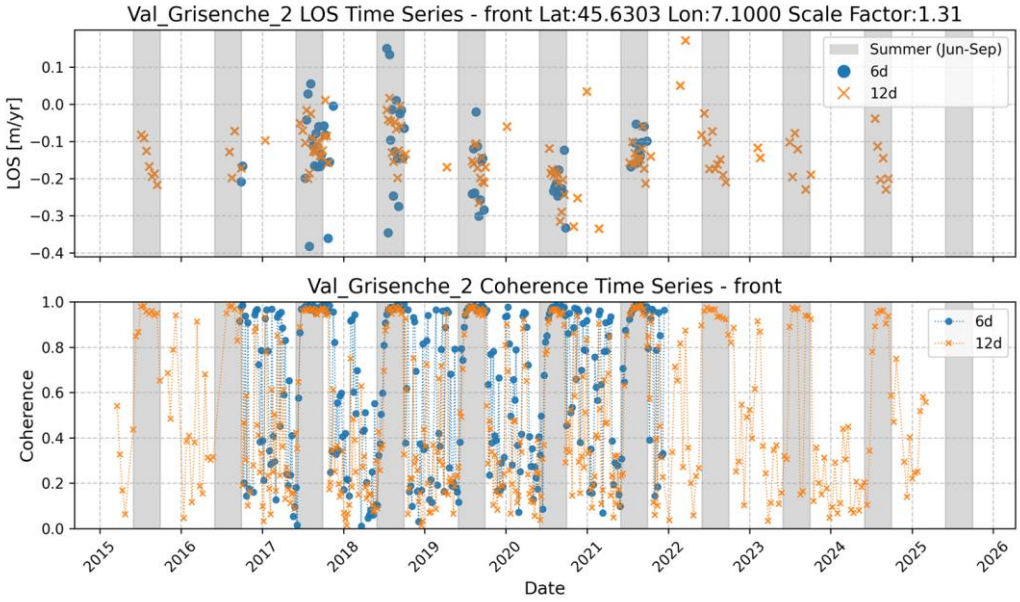

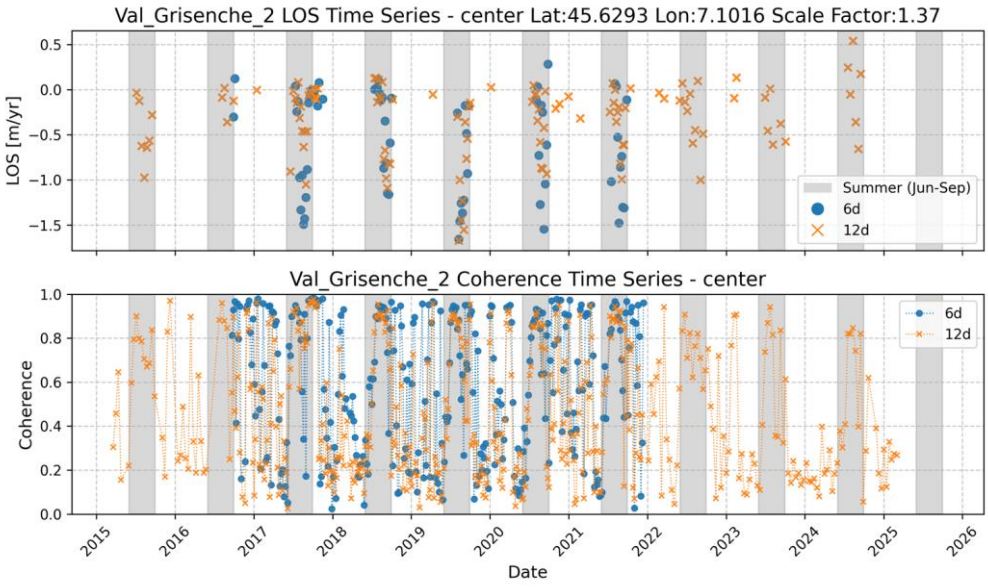

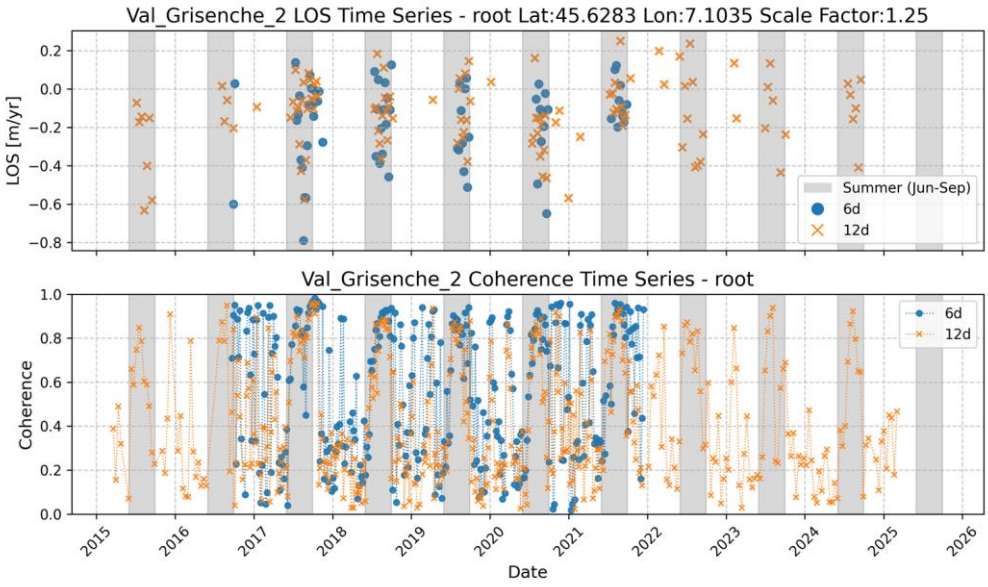

Val Grisenche 2 RGV Analysis – Descending orbit 139

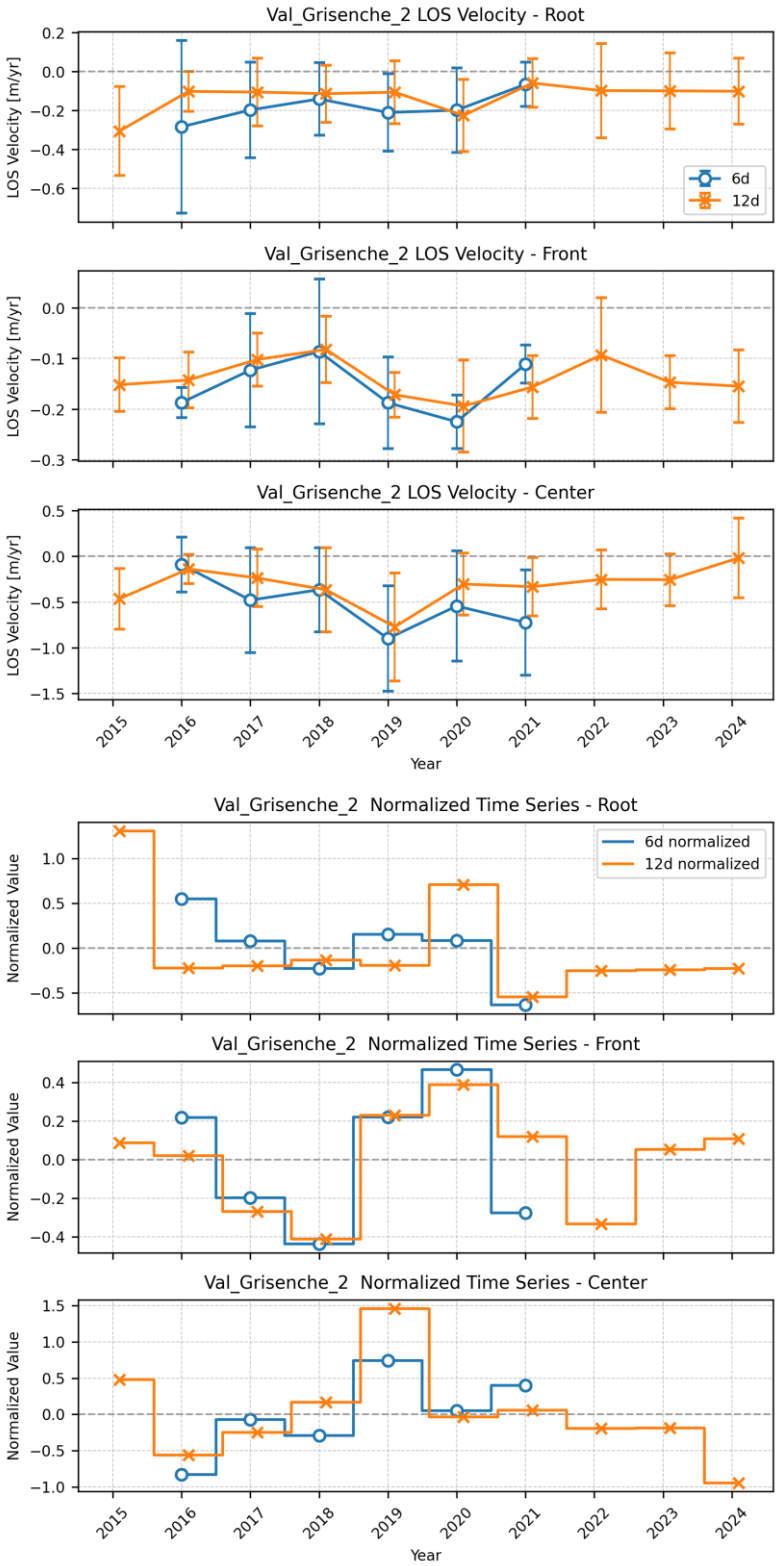

Velocity variation over the years: We averaged the obtained LOS velocity rates from all three monitoring points to generate yearly velocity estimates. In the top three figures, the averaged LOS velocities per summer are shown. The error bars represent the standard deviation per year. The three bottom figures show the normalized values ((Avg_year/mean_overall)-1) to highlight relative changes independent of the absolute velocities. Note that higher variations are expected as the measured velocities approach the sensitivity/noise level.

All three locations exhibit some fluctuations and seasonal variations and show different temporal patterns. 6-day displacement at the root appears relatively stable throughout the time series following a slight deceleration from 2015 to 2017 and lies largely within the sensitivity limit of 0.2 m/yr. The relative changes should thus be interpreted with caution. The center and front locations show a better overlap between 6-day and 12-day measurements and overall larger fluctuations. The front indicates a slight deceleration in LOS velocity from 2015 to 2018, followed by an acceleration until 2020 and a renewed subsequent deceleration. LOS velocity at the center increases from 2016 until 2019, after which a sharp deceleration occurs in 2020 with subsequent largely stable displacement. The overall good agreement between 6-day (blue circles, 2016-2021) and 12-day (orange crosses, 2015-2024) interferometric measurements particularly at the front location indicates reliability in the observations.

Val Grisenche 2 RGV Analysis – Descending orbit 139

The number of unwrapping errors over the whole RG was small which allowed the spatial aggregation of LOS velocities for all points on the RG. We found some small unwrapping issues in the 12d interferograms in the region around the front location which leads to an underestimation in the 12d average LOS displacement rates.
We kept points with average LOS displacement rates above the approximate sensitivity (0.2m/yr for 6d and 0.1m/yr for the 12d). The points above the sensitivity limit can be seen in the top figures and the relative changes averaged over all points in the bottom plot.

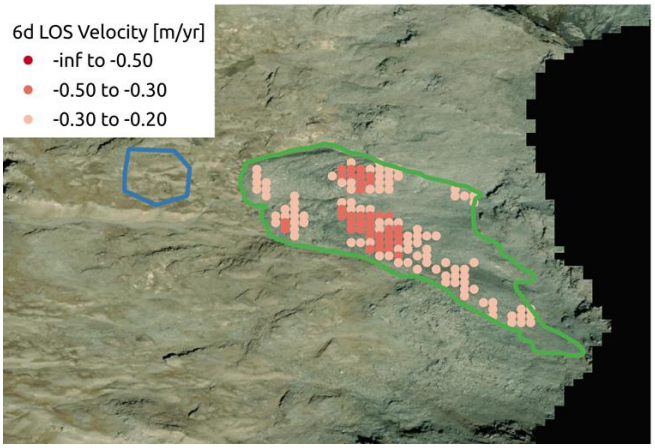

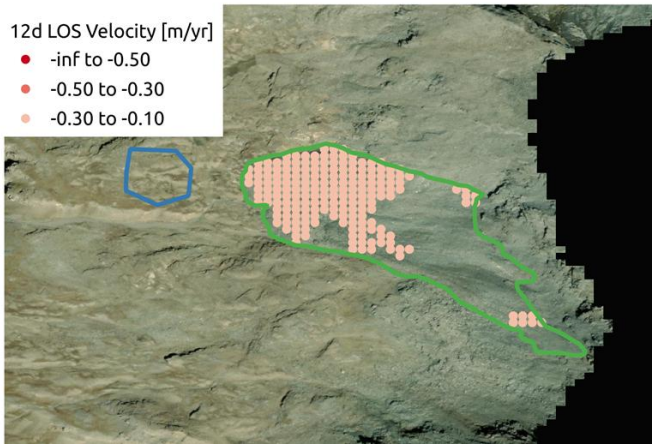

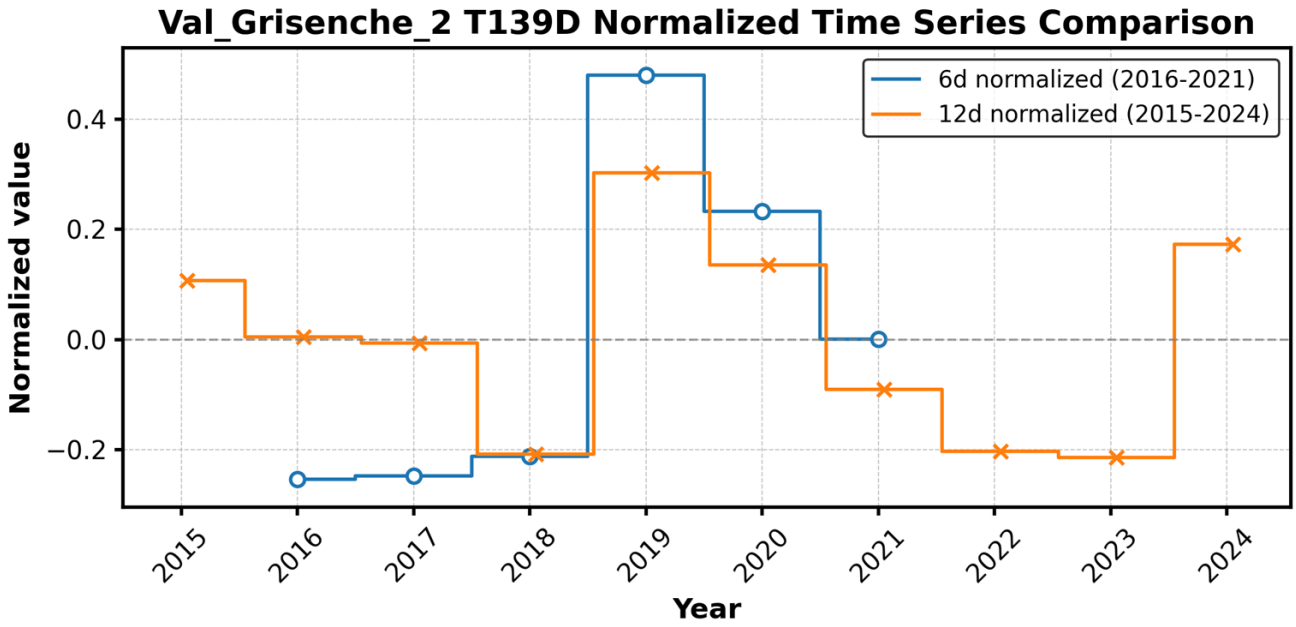

Val Grisenche 3 RGV Analysis

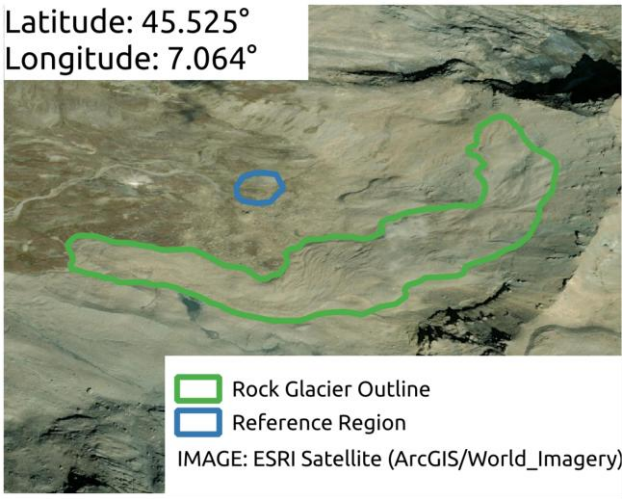

T088A

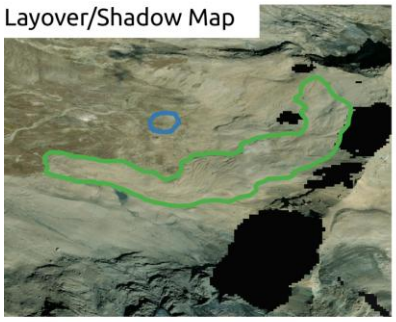

T139D

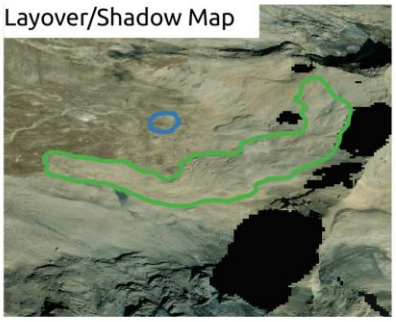

Layover/Shadow
Sentinel-1 data are acquired from two orbits (T088A and T139D). In both orbits the rock glacier region is not affected by layover or shadow effects.

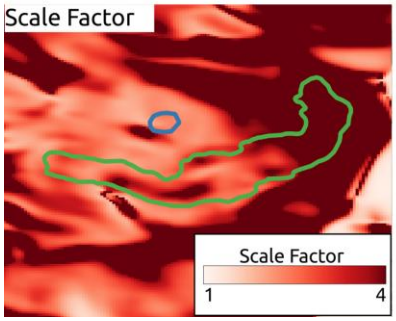

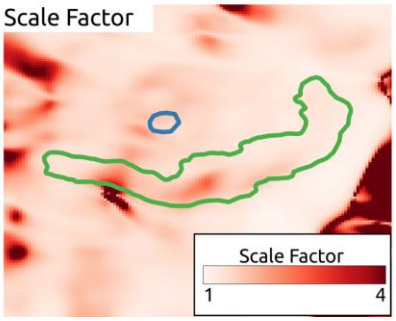

Scale Factor
T088A exhibits a more unfavorable viewing geometry with a Scale Factor mostly above 4.
The Line-of-Sight for orbit T139D aligns well with the flow direction of the RG.
Scale Factors for orbit T139D are in the range 1.2 to 2.6 over the RG.

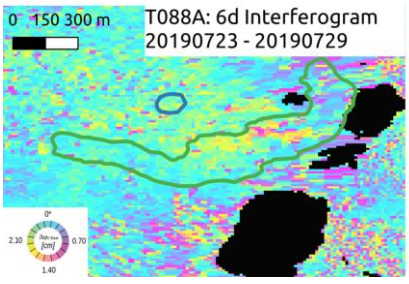

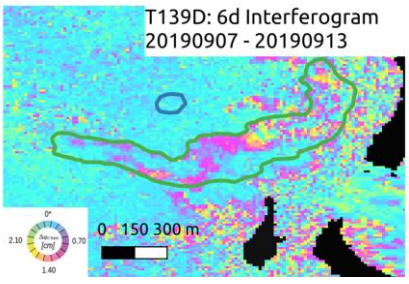

Initial assessment
The T139D interferogram reveals movement up to 2cm/6d (approximately 1.2m/yr) across the RG, with one region in the center potentially exceeding 2.5cm/6d (approximately 1.5m/yr). The northeast section shows deteriorating quality, possibly due to variations in velocity. These complex deformation patterns present processing challenges in several parts of the interferogram.

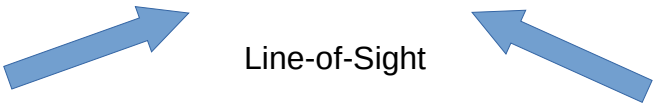

For the RGV Analysis we use orbit T139D descending data.

Val Grisenche 3 RGV Analysis – Descending orbit 139

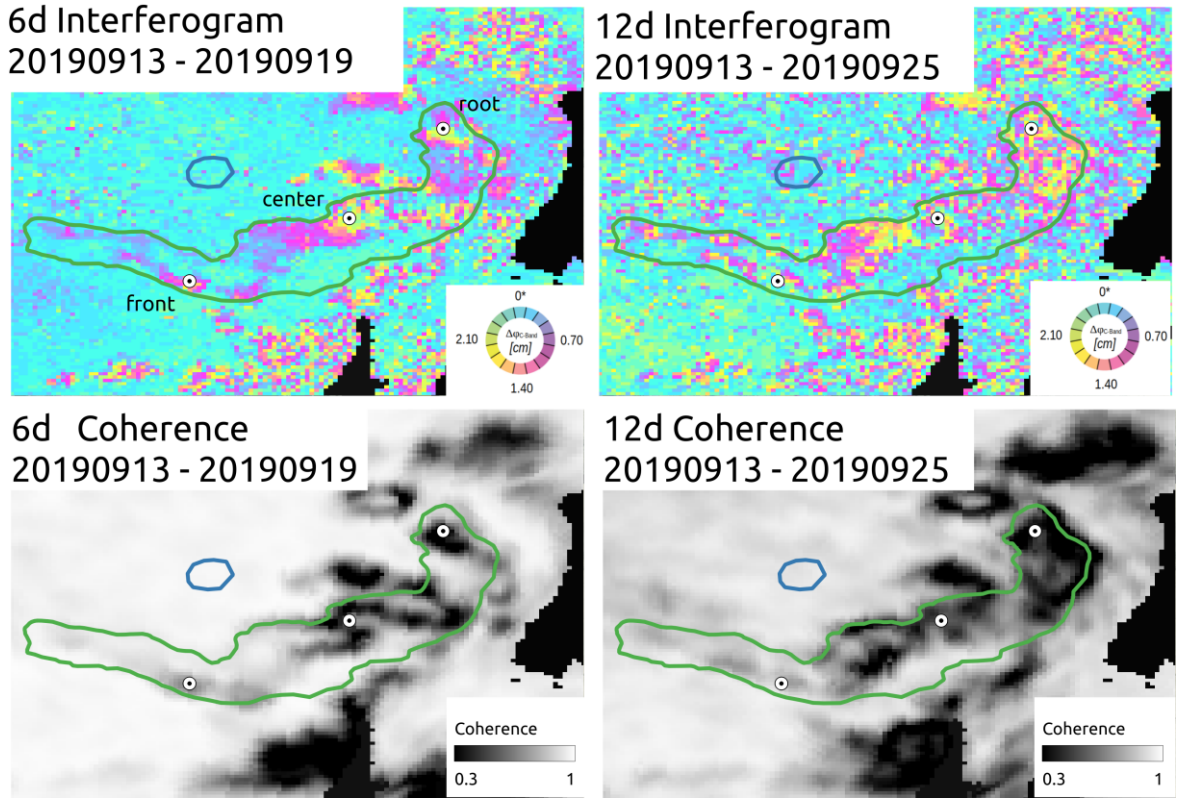

Overview

The figure above shows a 6d and 12d interferogram as well as the associated coherence from late summer 2019. A selection of coherent interferograms was made manually for the further analysis. Many unwrapping issues are present due to high LOS velocities (> 1.2 m/yr) as well as abrupt changes. We selected three points (front, center, root) across the RG to extract LOS velocities time series.

Point Time Series

For the three monitoring points (front [45.5302, 7.0464], center [45.5326, 7.0524], and root [45.5360, 7.0560]) highlighted in the upper figures, we extracted LOS velocity time series, carefully checking and correcting any unwrapping issues. Each figure showing the time series on the next page displays the LOS displacement rates in m/yr in the top panel and the coherence in the bottom panel. For the LOS displacements, the coherent values are shown. For the coherence time series, all available pairs are shown. The coherence was obtained at the point location in the individual interferograms. Blue circles represent 6-day interferometric measurements, while orange crosses show 12-day measurements, with summer months (June-September) highlighted by gray vertical bands. In general, the 12-day interferogram coherence values are lower than the 6-day. For the front location the coherence values in the summer season are generally high (>0.6), while for the root and center locations the coherence values in summer are overall slightly lower. Higher velocities as well as unfavorable conditions such as snow cover can decrease the coherence.

The highest velocities are measured at the center location (~1.8-2.2 m/yr ~> 2.2-2.7 m/yr when assuming slope-parallel movement). At the front, the velocities are lowest but show larger fluctuations within summer from about 0.5 up to 1.3 m/yr, and exceeding 1.5 m/yr in the summers of 2017 and 2019. The LOS velocity at the root shows similar fluctuations of +/- 0.8 m/yr with overall higher velocities reaching 1.8 m/yr. Scale Factors for the three points are 1.65 for front, 1.22 for center and 1.31 for root.

Val Grisenche 3 RGV Analysis – Descending orbit 139

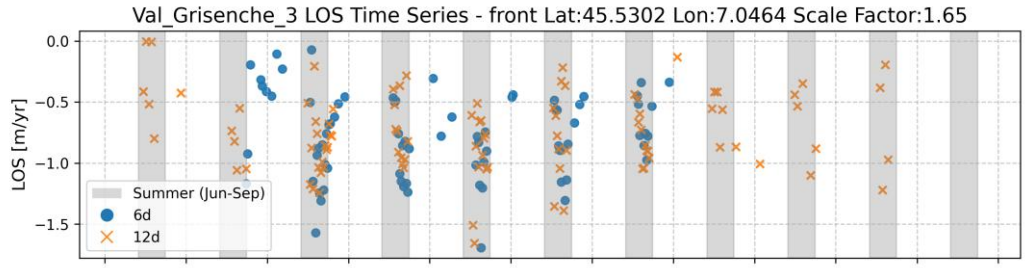

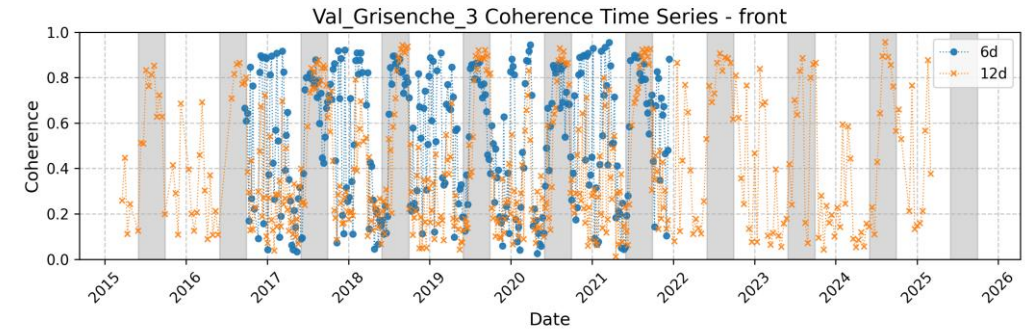

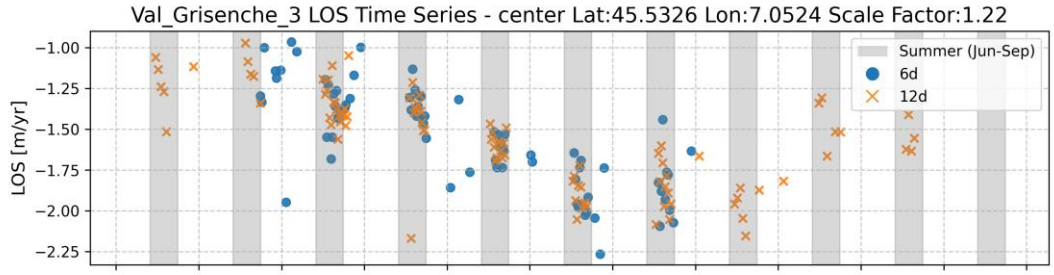

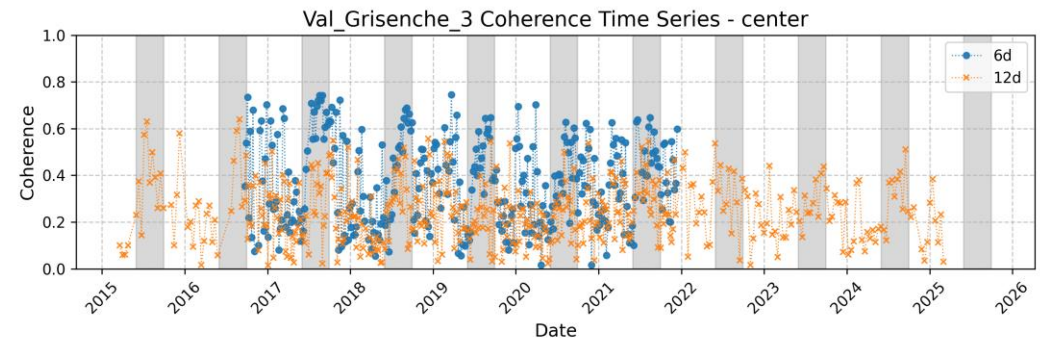

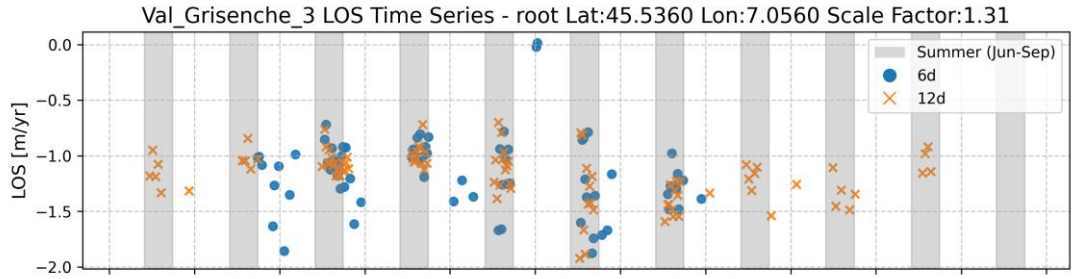

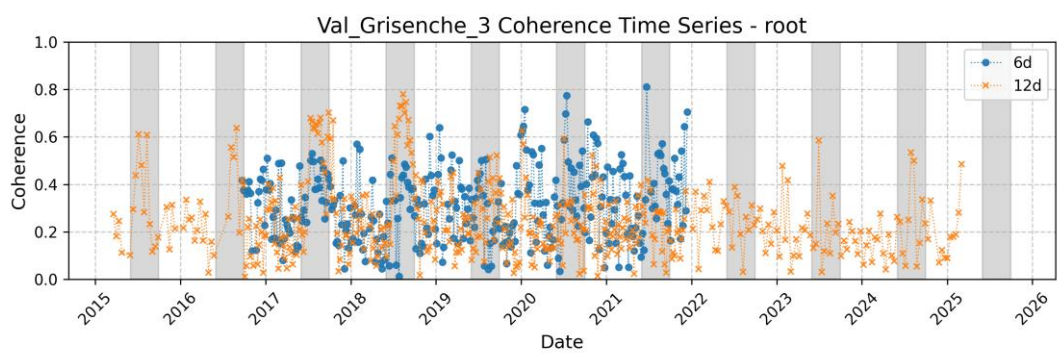

Val Grisenche 3 RGV Analysis – Descending orbit 139

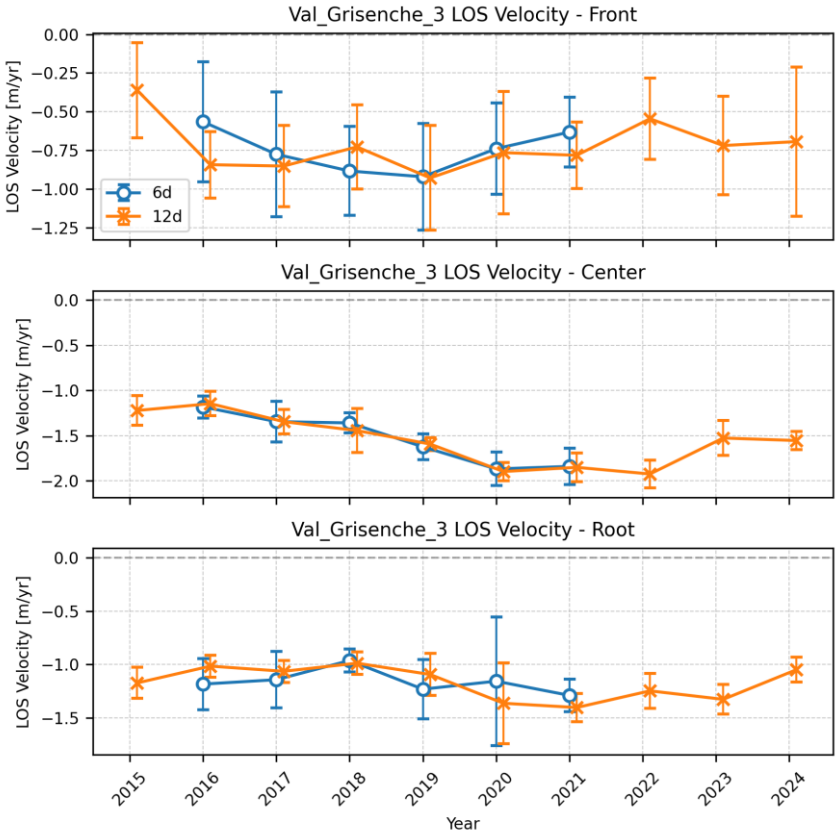

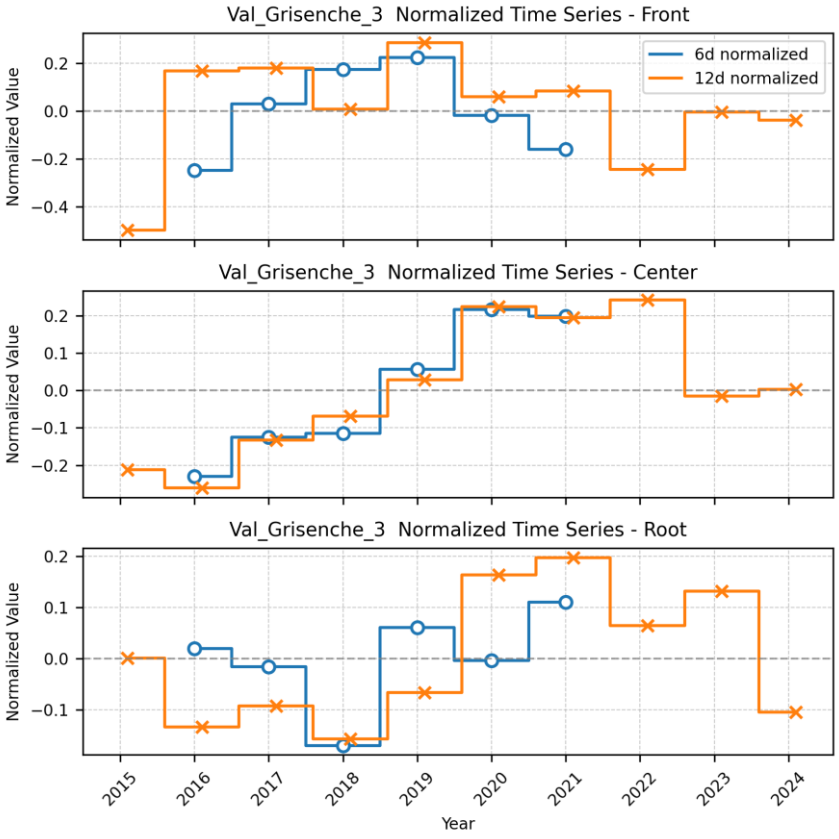

Velocity variation over the years: We averaged the obtained LOS velocity rates from all three monitoring points to generate yearly velocity estimates. In the top three figures, the averaged LOS velocities per summer are shown. The error bars represent the standard deviation per year. The three bottom figures show the normalized values ((Avg_year/mean_overall)-1) to highlight relative changes independent of the absolute velocities. Note that higher variations are expected as the measured velocities approach the sensitivity/noise level.

The center and root locations show small error bars of roughly +/- 0.2 m/yr, while the front shows larger error bars of up to +/- 0.5. The center location shows a very good correlation between 6-day and 12-day interferograms, while less overlap is apparent at the front of the RG. Here the data quality is the lowest. In the root location, measurements in 2020 shows large variations. The normalized time-series should be interpreted with caution.

Valnontey RGV Analysis

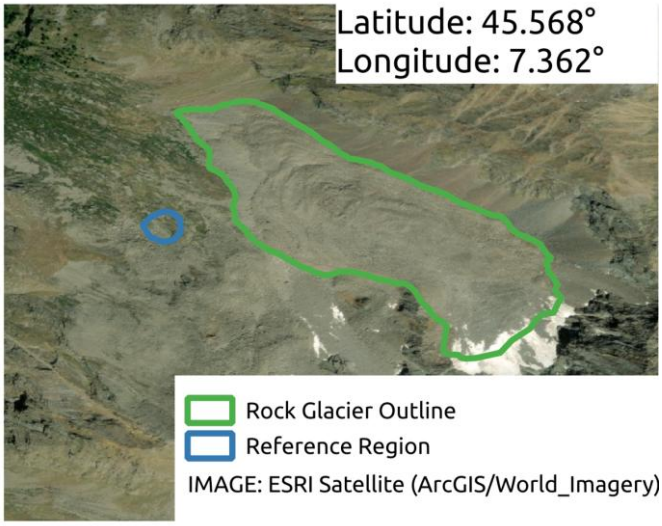

T088A

T139D

Layover/Shadow
Sentinel-1 data are acquired from two orbits (T088A and T139D). In both orbits the rock glacier region is not affected by layover or shadow effects.

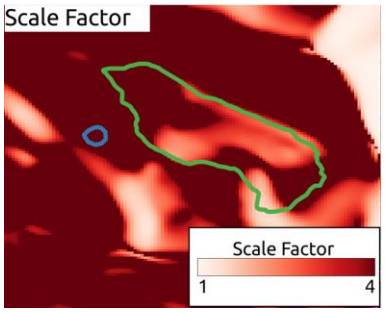

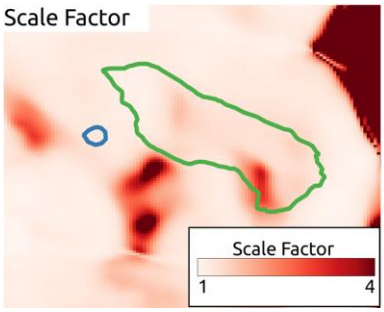

Scale Factor:
T088A exhibits a more unfavorable viewing geometry with a Scale Factor mostly above 4.
The Line-of-Sight for orbit T139D aligns well with the flow direction of the RG.
Scale Factors for orbit T139D are in the range 1.1 to 3 over the RG.

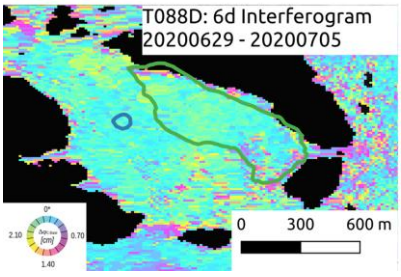

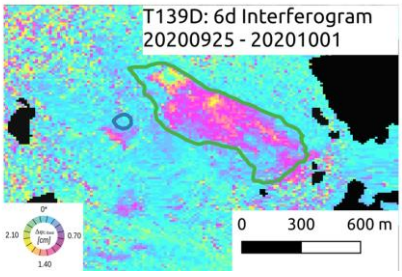

Initial assessment
The T139D interferogram shows movement with displacement reaching approximately 1.4-2.1cm/6d (equivalent to 0.8-1.2m/yr). The pronounced deformation pattern shows a clear gradient, with the highest velocities concentrated in the upper right section of the outlined area. These higher deformation rates may present phase unwrapping challenges during processing, particularly at the boundaries where velocity gradients are steepest.

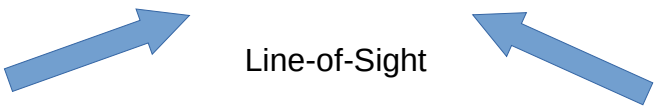

For the RGV Analysis we use orbit T139D descending data.

Valnontey RGV Analysis – Descending orbit 139

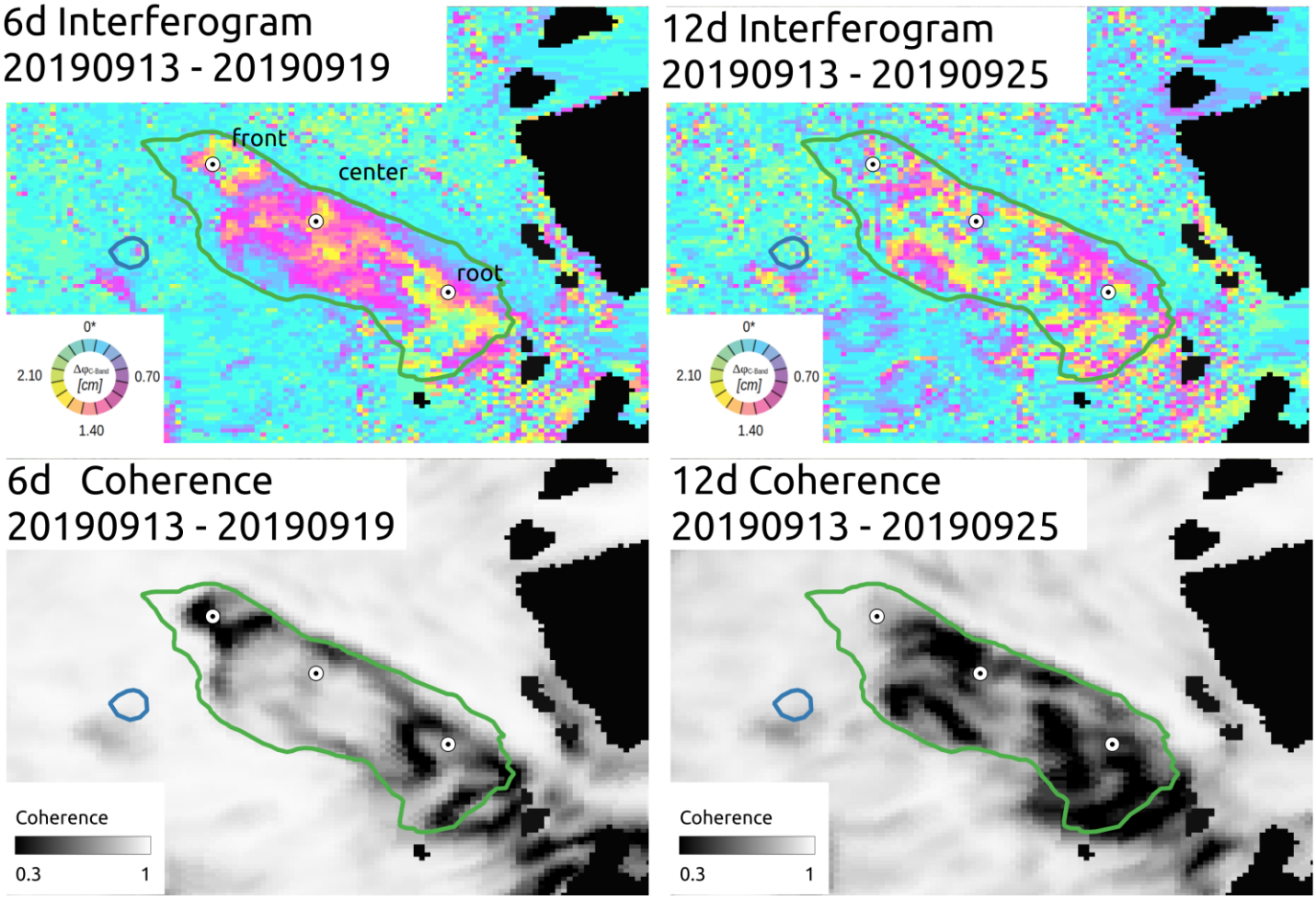

Overview

The figure above shows a 6d and 12d interferogram as well as the associated coherence from late summer 2019. A selection of coherent interferograms was made manually for the further analysis. Many unwrapping issues are present due to high LOS velocities (> 0.8 m/yr) as well as abrupt changes. We selected three points (front, center, root) across the RG to extract LOS velocities time series.

Point Time Series

For the three monitoring points (front [45.5725, 7.3504], center [45.5707, 7.3536], and root [45.5685, 7.3578]) highlighted in the upper figures, we extracted LOS velocity time series, carefully checking and correcting any unwrapping issues. Each figure showing the time series on the next page displays the LOS displacement rates in m/yr in the top panel and the coherence in the bottom panel. For the LOS displacements, the coherent values are shown. For the coherence time series, all available pairs are shown. The coherence was obtained at the point location in the individual interferograms. Blue circles represent 6-day interferometric measurements, while orange crosses show 12-day measurements, with summer months (June-September) highlighted by gray vertical bands. In general, the 12-day interferogram coherence values are lower than the 6-day. For the locations center and root the coherence values in the summer season are generally high (>0.6-0.8), while for the front location the coherence values in summer are overall slightly lower. Higher velocities as well as unfavorable conditions such as snow cover can decrease the coherence.

The highest velocities are measured at the center location (~1.2-1.5 m/yr ~> 1.7-2.1 m/yr when assuming slope-parallel movement) with large fluctuations in summer. At the front, the velocities also fluctuate from by +/- 0.6 m/yr within summer and exceed values of 1.2 m/yr in 2019 and 2020. The LOS velocity at the root is overall lowest with values of 0.8-0.9 m/yr in 2018-2020 and similar fluctuations in summer. Scale Factors for the three points are 1.12 for front, 1.41 for center and 1.39 for root.

Valnontey RGV Analysis – Descending orbit 139

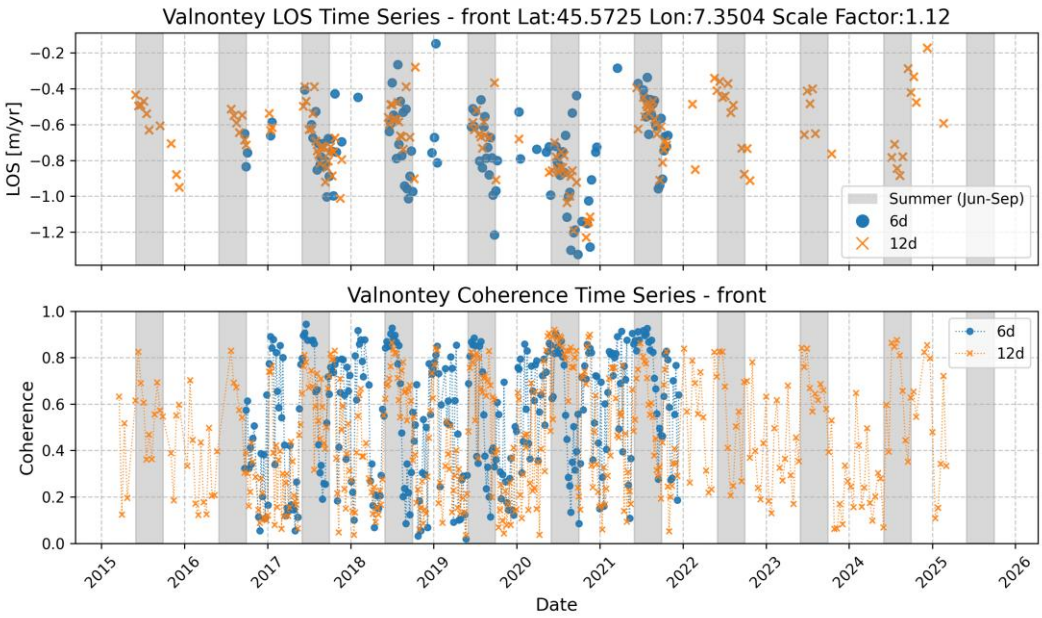

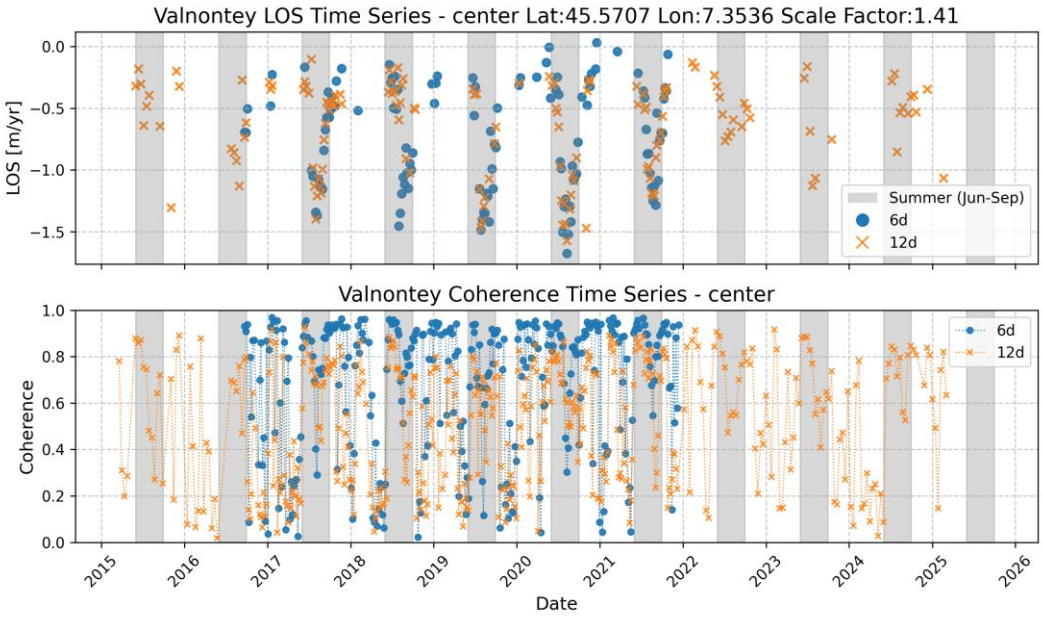

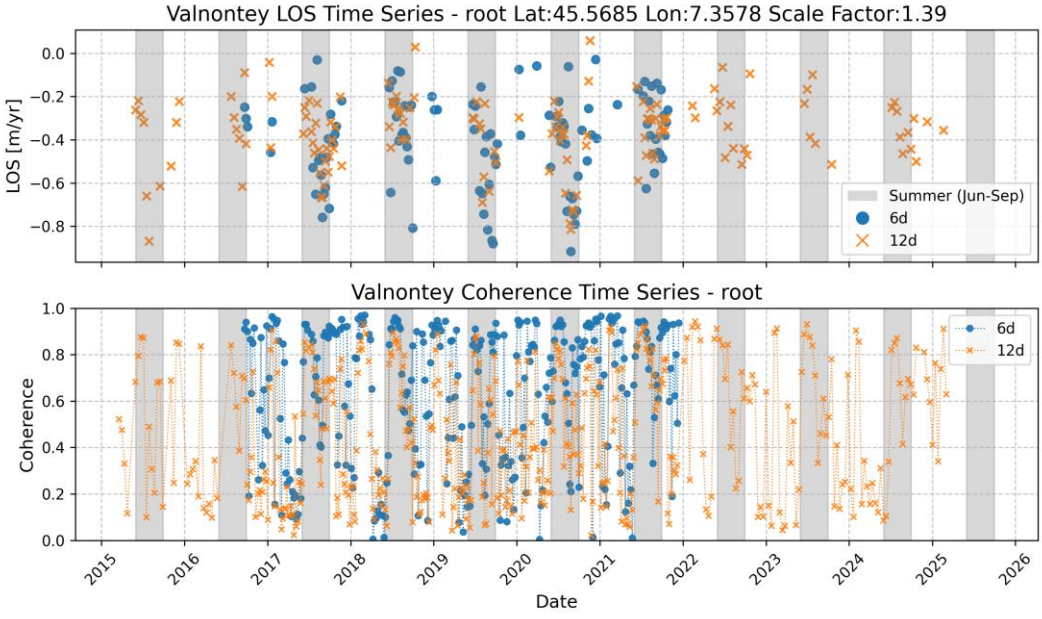

Valnontey RGV Analysis – Descending orbit 139

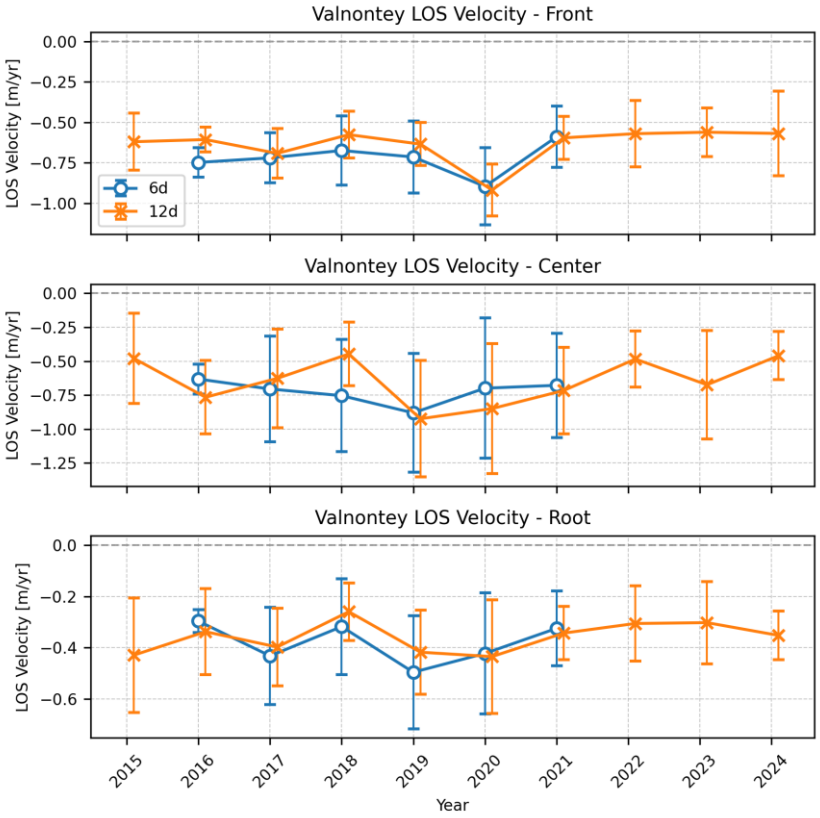

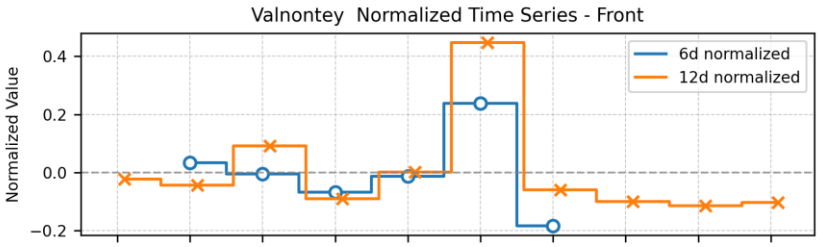

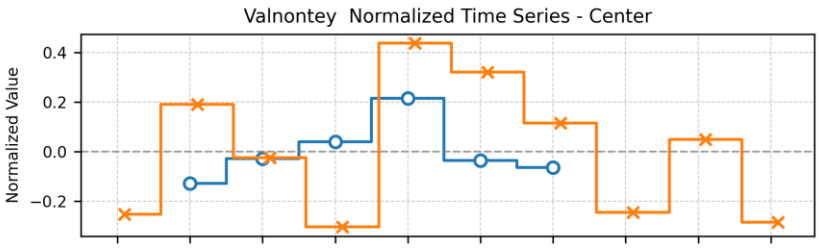

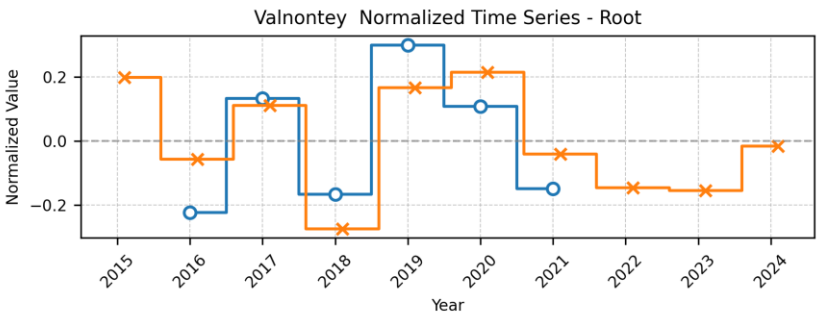

Velocity variation over the years: We averaged the obtained LOS velocity rates from all three monitoring points to generate yearly velocity estimates. In the top three figures, the averaged LOS velocities per summer are shown. The error bars represent the standard deviation per year. The three bottom figures show the normalized values ((Avg_year/mean_overall)-1) to highlight relative changes independent of the absolute velocities. Note that higher variations are expected as the measured velocities approach the sensitivity/noise level.

The front location shows overall smaller error bars compared to the RG center and root, possibly due to less fluctuations in LOS velocity during the summer season. The front and root locations show overall good overlap between 6-day and 12-day interferograms, with relatively stable displacement at the front apart from a strong acceleration in summer 2019 followed by a deceleration in 2020. The center and root locations show more variable displacement patterns with larger seasonal fluctuations. The selection of which points to use in the analysis thus plays a significant role. The time series displayed should thus be interpreted with caution.

Valsavarenche 1 RGV Analysis

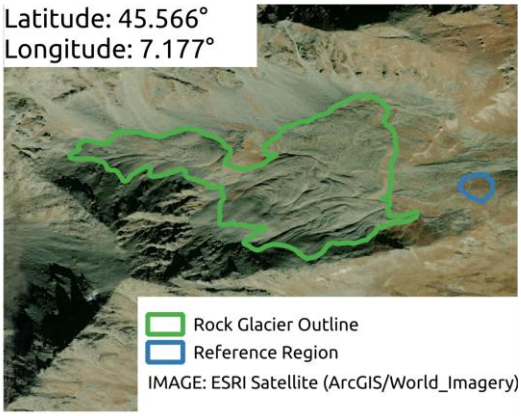

T088A

T139D

Layover/Shadow
Sentinel-1 data are acquired from two orbits (T088A and T139D). In both orbits the rock glacier region is not affected by layover or shadow effects.

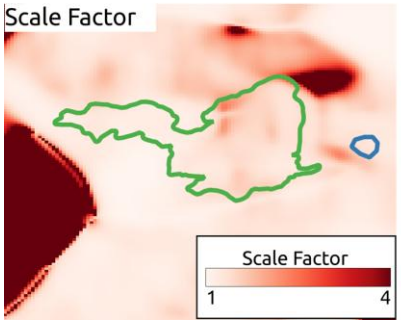

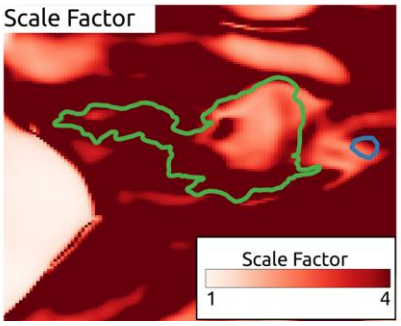

Scale Factor
T139D exhibits a more unfavorable viewing geometry with a Scale Factor mostly above 4.
The Line-of-Sight for orbit T088A aligns well with the flow direction of the RG.
Scale Factors for orbit T088A are in the range 1.1 to 2.4 over the RG.

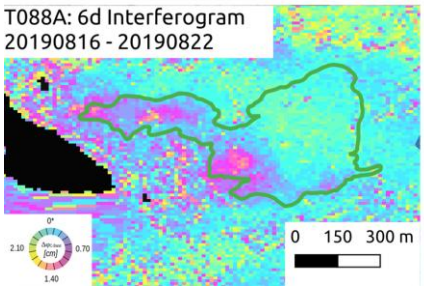

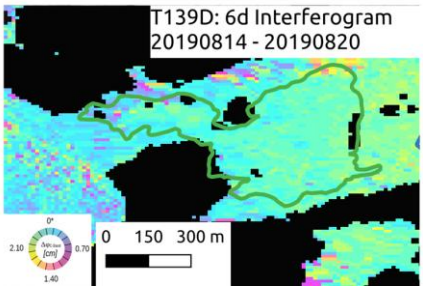

Initial assessment
The T088A interferogram shows movement across the western portion of the RG, with displacement patterns reaching approximately 0.7-1.4cm/6d (equivalent to 0.4-0.8m/yr). The eastern part of the RG exhibits minimal displacement. This spatial variation in movement rates may require careful attention during phase unwrapping procedures, though the moderate velocity magnitudes should allow for successful processing without extensive manual intervention.

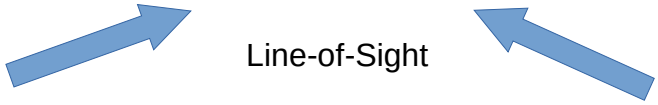

For the RGV Analysis we use orbit T088A ascending data.

Valsavarenche 1 RGV Analysis – Ascending orbit 88

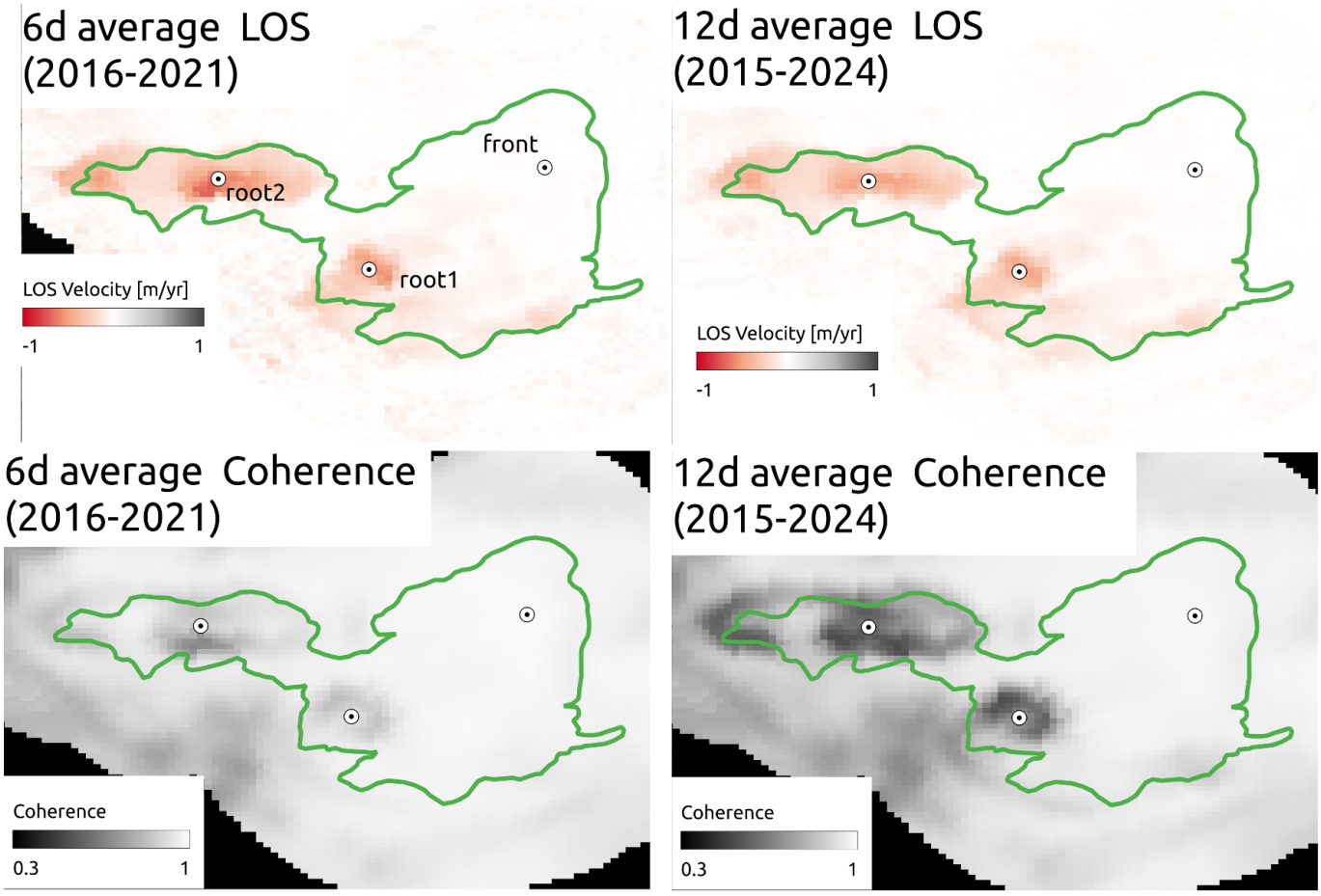

Overview

The figures above show averaged Line-of-Sight (LOS) velocities over all available summer seasons (July to October) (top) as well as the average coherence over the same period (bottom). 6-day interferograms are available from October 2016 to December 2021, 12-day interferograms are available from October 2015 to the start of 2025. Negative LOS values indicate a displacement away from the sensor. A selection of coherent interferograms was made manually for the further analysis. We selected three points (front, root1 and root2) to extract LOS velocities time series.

Point Time Series

For the three monitoring points (front [45.5677, 7.1794], root1 [45.5652, 7.1752], and root2 [45.5674, 7.1716]) highlighted in the upper plots, we extracted LOS velocity time series, carefully checking and correcting any unwrapping issues. Each figure showing the time series on the next page displays the LOS displacement rates in m/yr in the top panel and the coherence in the bottom panel. For the LOS displacement, only the coherent measurements are shown. For the coherence time series, all available pairs are shown. The coherence was obtained at the point location in the individual interferograms. Blue circles represent 6-day interferometric measurements, while orange crosses show 12-day measurements, with summer months (June-September) highlighted by gray vertical bands.

For the selected interferograms the coherence values are generally high (>0.8) and are obtained mainly in the summer season. In general, the 12-day interferogram coherence values are lower than the 6-day. Higher velocities as well as unfavorable conditions such as snow cover can decrease the coherence.

The highest velocities are measured at the root2 location (~1.0-1.2 m/yr ~> 1.2-1.4 m/yr when assuming slope-parallel movement) with acceleration and deceleration during the summer of about 0.4-0.6 m/yr. Root1 shows similar behavior with overall lower LOS velocities reaching about 0.7-0.8 m/yr. At the front, the velocities are lowest and remain largely within the sensitivity threshold of 0.2 m/yr. Scale Factors for the three points are 1.46 for front, 1.29 for root1 and 1.17 for root2.

Valsavarenche 1 RGV Analysis – Ascending orbit 88

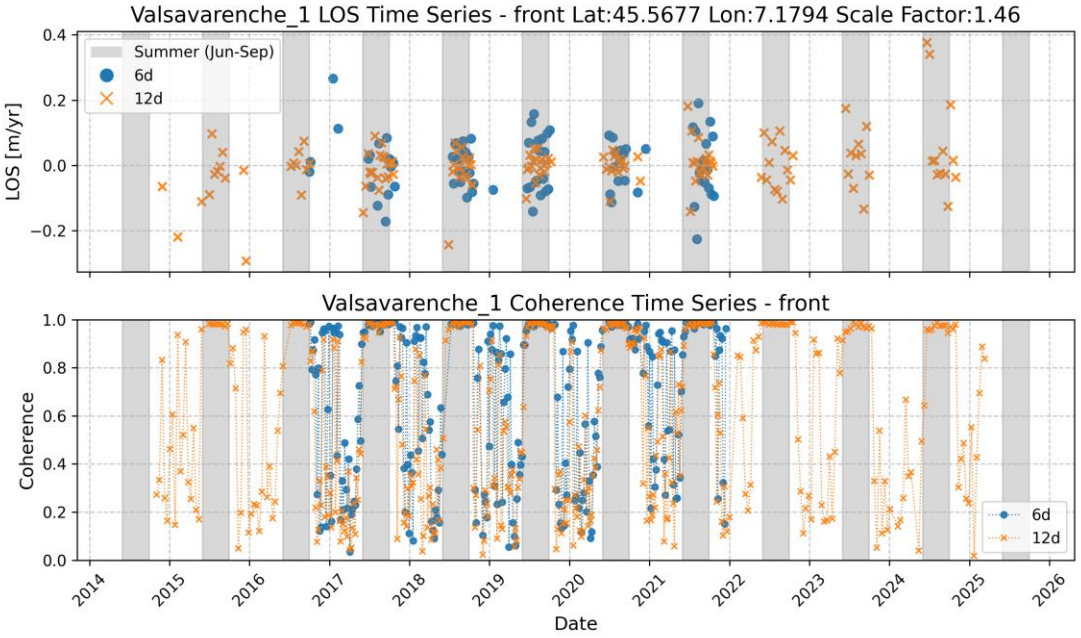

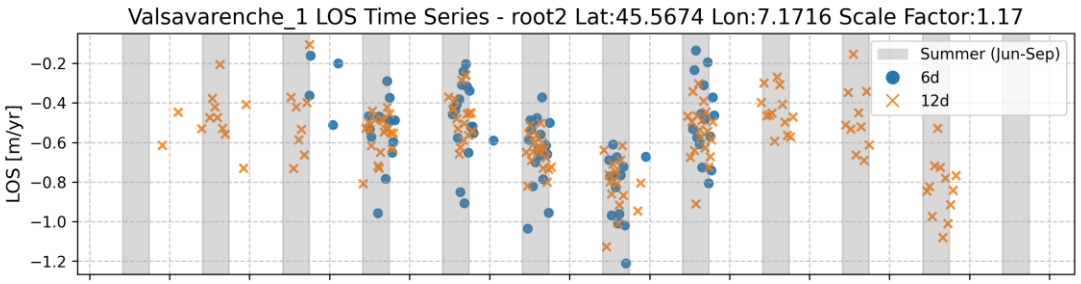

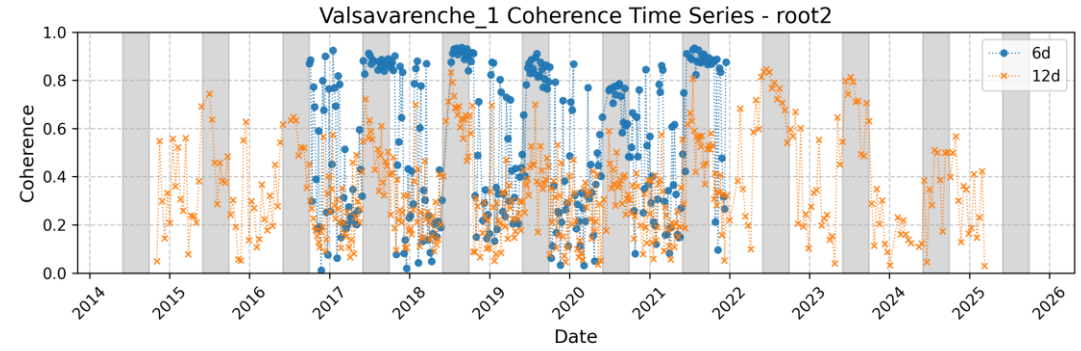

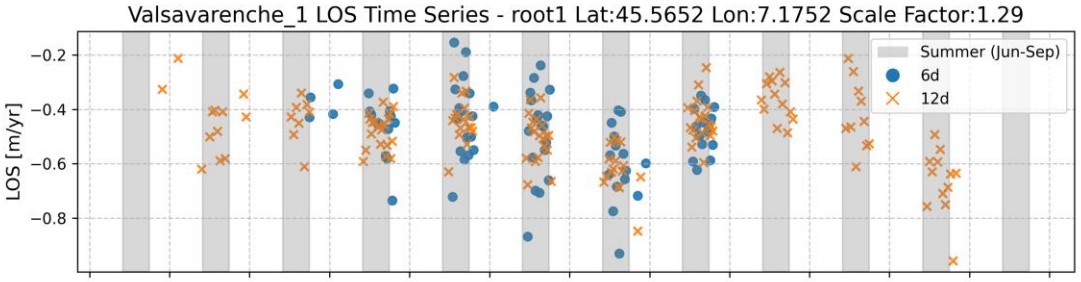

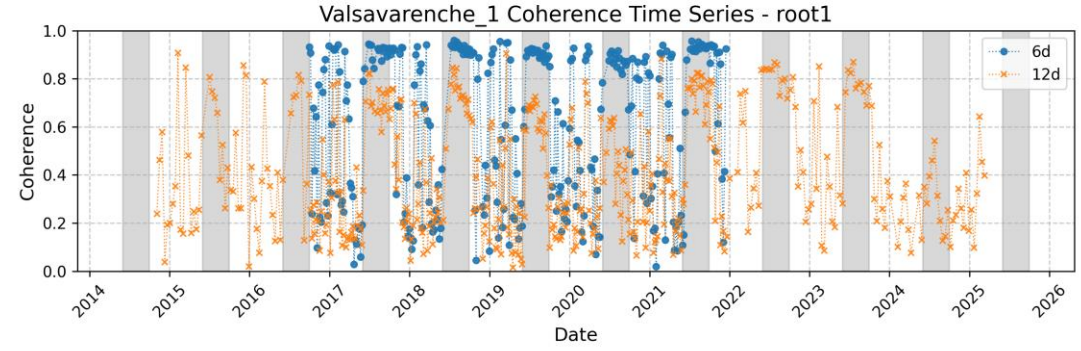

Valsavarenche 1 RGV Analysis – Ascending orbit 88

Velocity variation over the years: We averaged the obtained LOS velocity rates from the two root location monitoring points to generate yearly velocity estimates. In the top two figures, the averaged LOS velocities per summer are shown. The error bars represent the standard deviation per year. The two bottom figures show the normalized values ((Avg_year/mean_overall)-1) to highlight relative changes independent of the absolute velocities. Note that higher variations are expected as the measured velocities approach the sensitivity/noise level.

Both root locations exhibit fluctuations and seasonal variations, showing a relatively consistent temporal pattern: stable displacement in 2015 to 2018, followed by a strong acceleration in 2019 and 2020, with a renewed deceleration through 2021 and 2022 and subsequent acceleration. The similar pattern between both points in the normalized plot indicates that while absolute movement intensity differs between locations, the proportional changes over time are consistent. The good agreement between 6-day (blue circles, 2016-2021) and 12-day (orange crosses, 2015-2024) interferometric measurements indicates reliability in the observations.

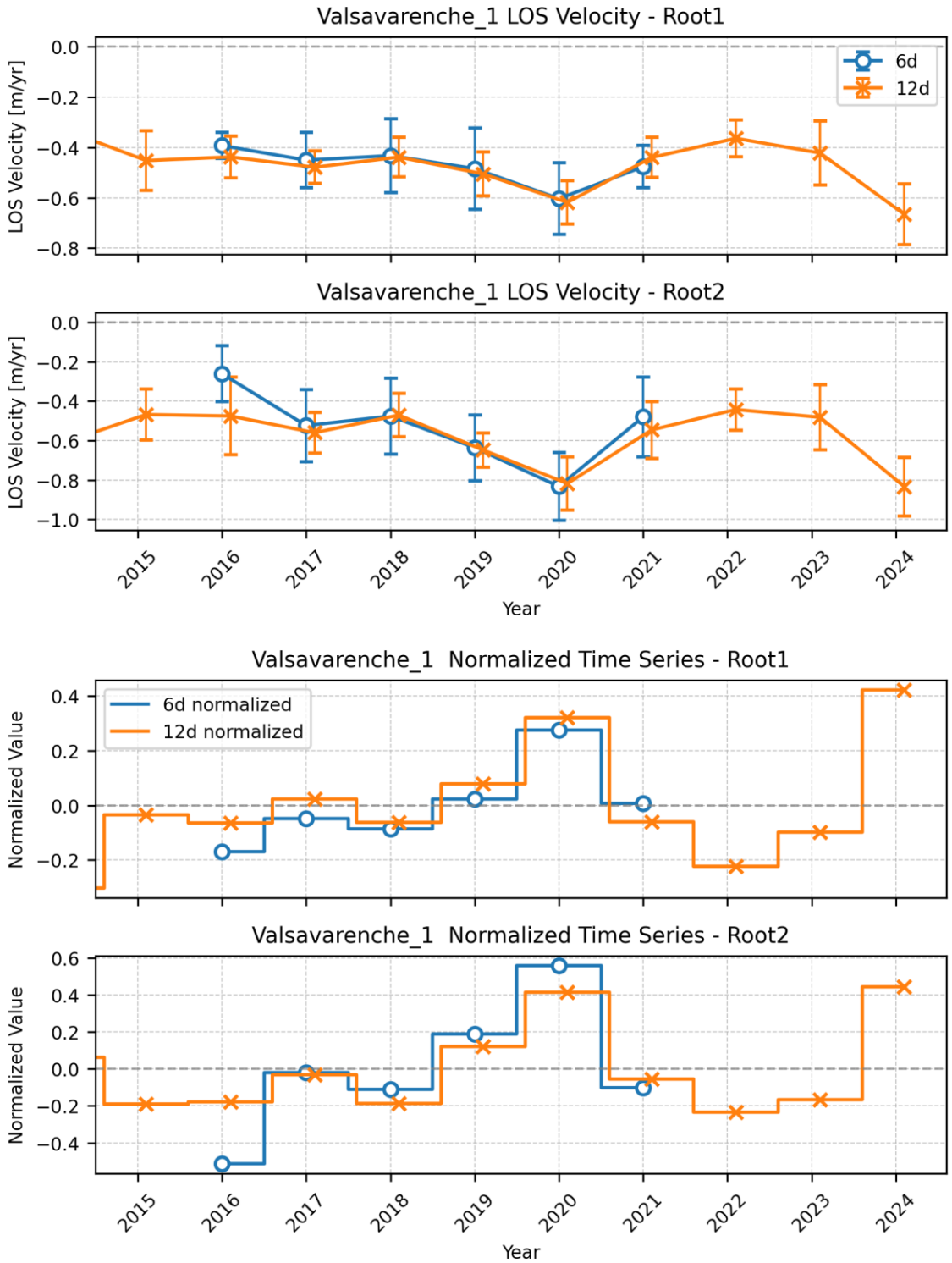

Valsavarenche 1 RGV Analysis – Ascending orbit 88

The number of unwrapping errors over the whole RG was small which allowed the spatial aggregation of LOS velocities for all points on the RG. We found some small unwrapping issues in the 12d interferograms in the region between root and front which lead to an underestimation in the 12d average LOS displacement rates.
We kept points with average LOS displacement rates above the approximate sensitivity (0.2m/yr for 6d and 0.1m/yr for the 12d). The points above the sensitivity limit can be seen in the top figures and the relative changes averaged over all points in the bottom plot.

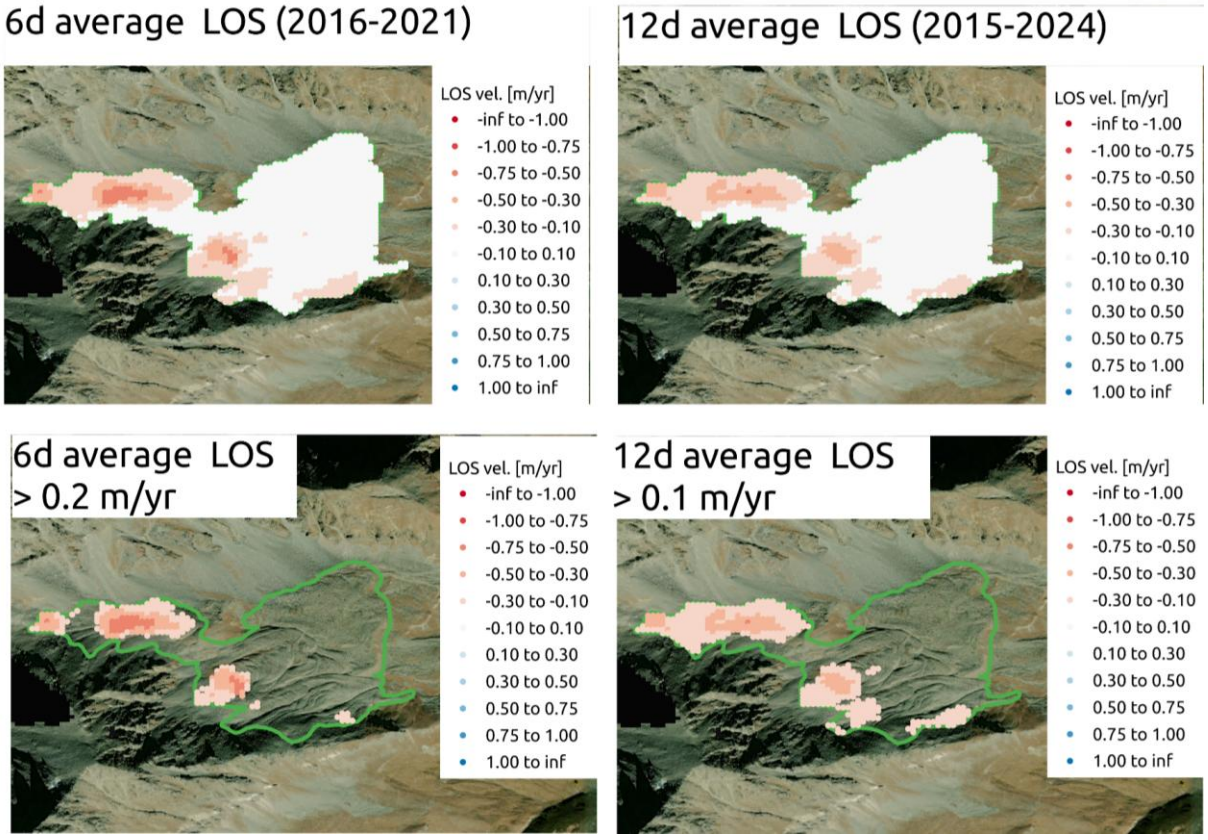

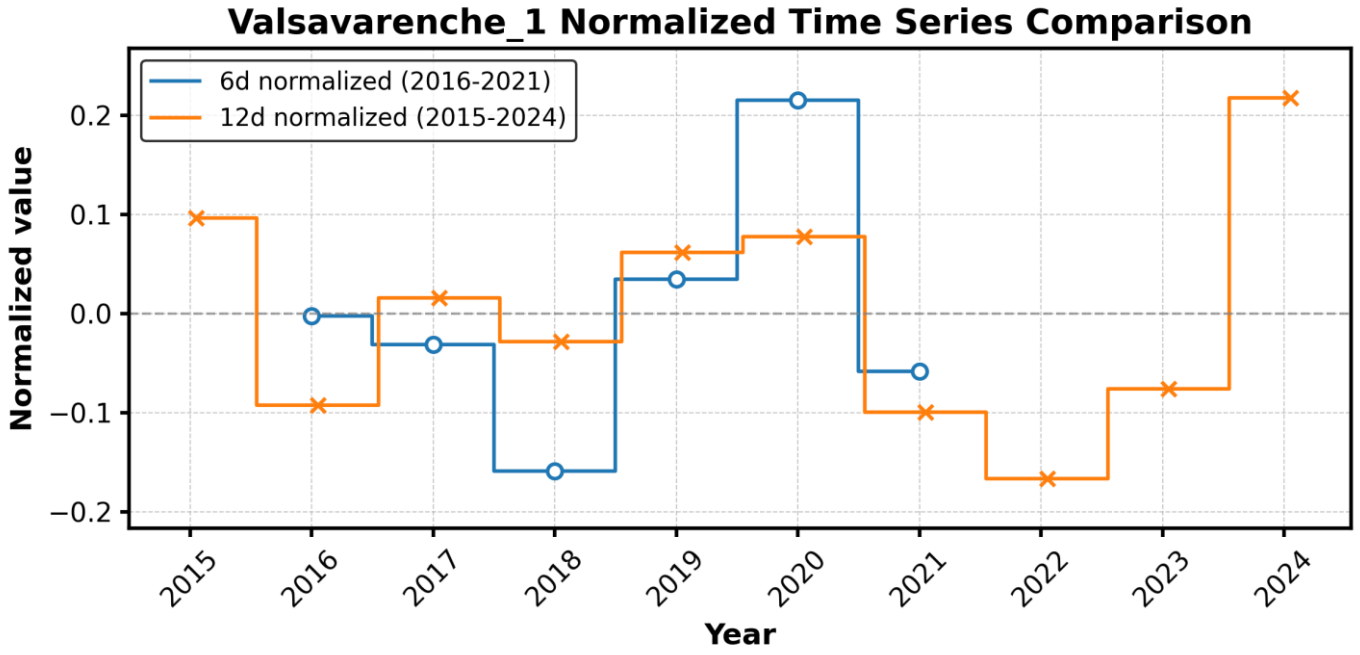

Valsavarenche 3 RGV Analysis

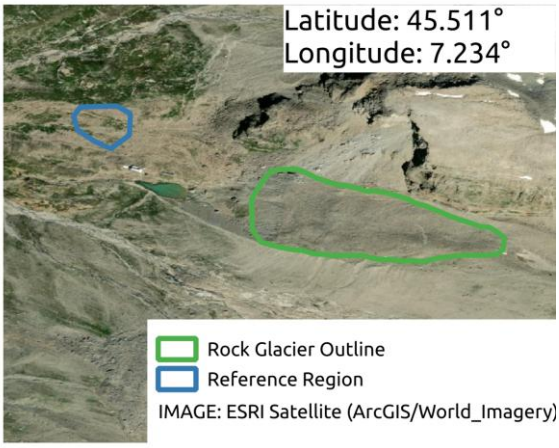

T088A

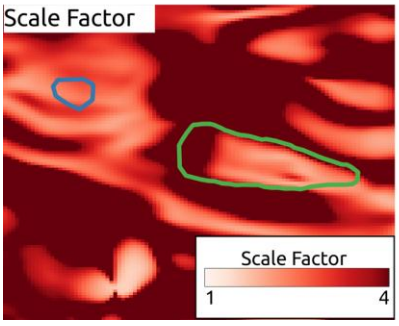

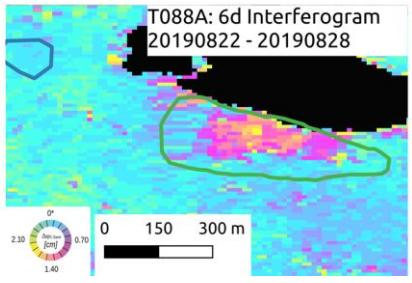

T139D

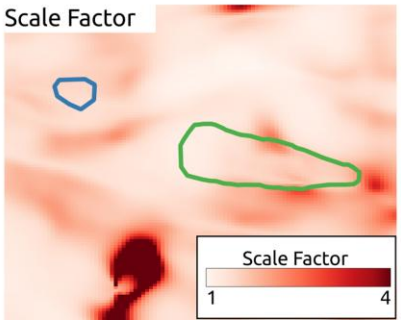

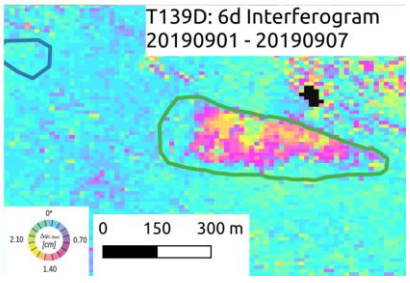

Line-of-Sight

For the RGV Analysis we use both orbits.

Layover/Shadow
Sentinel-1 data are acquired from two orbits (T088A and T139D). In both orbits the rock glacier region is not affected by layover or shadow effects.

Scale Factor
T088A exhibits a more unfavorable viewing geometry with a Scale Factor mostly above 4.
The Line-of-Sight for orbit T139D aligns well with the flow direction of the RG.
Scale Factors for orbit T130D are in the range 1.1 to 2.4 over the RG.

Initial assessment
The T139D interferogram shows significant movement across the RG, with deformation rates ranging from 0.7-1.4cm/6d (approximately 0.4-0.8m/yr). The displacement pattern exhibits notable spatial variation, with higher velocities concentrated in the central to eastern portions of the outlined area. These variations create moderate velocity gradients that may require attention during phase unwrapping, though the overall coherent pattern suggests processing should proceed without major complications.

Valsavarenche 3 RGV Analysis – Descending orbit 139

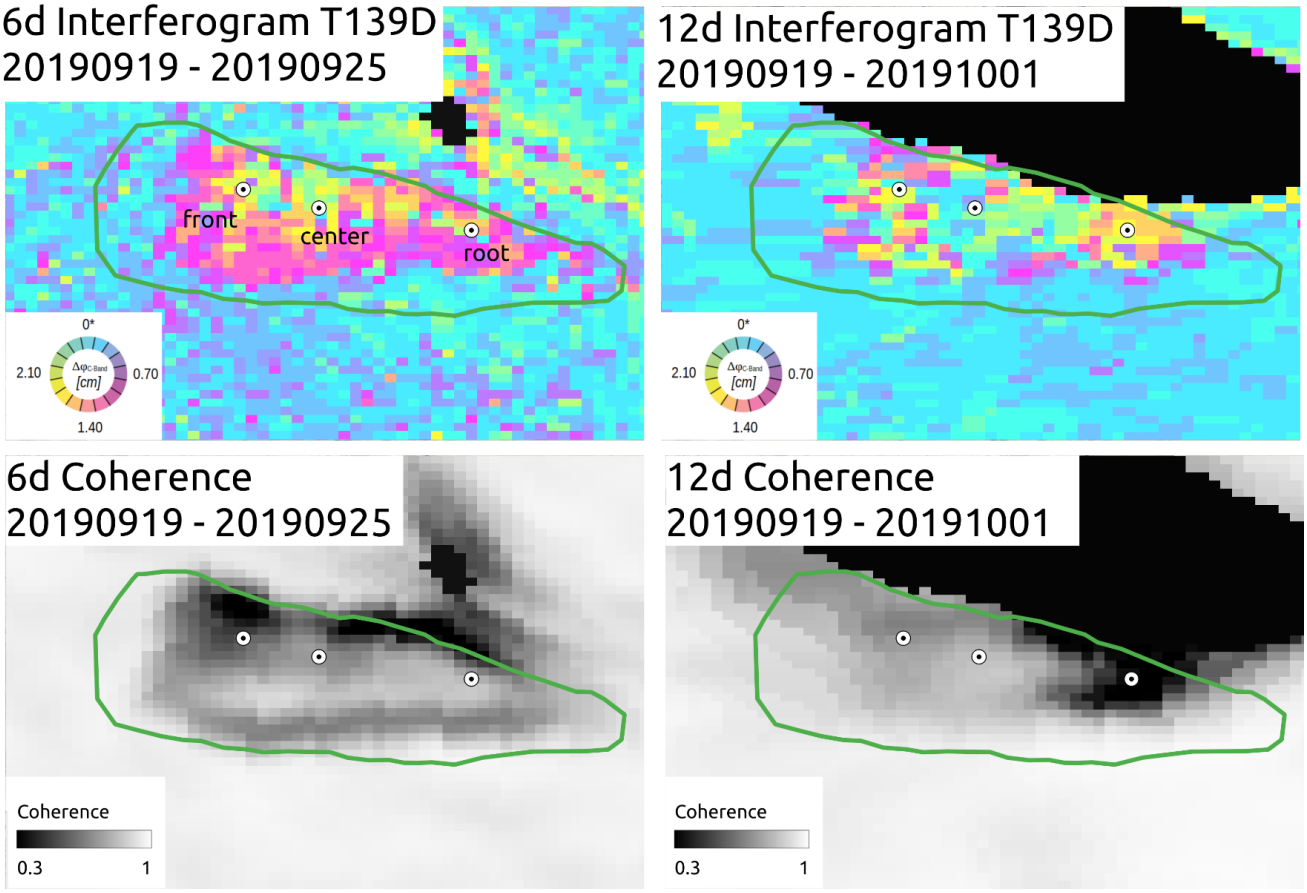

Overview

The figure above shows a 6d and 12d interferogram as well as the associated coherence from end of summer 2019. A selection of coherent interferograms was made manually for the further analysis. Many unwrapping issues are present due to high LOS velocities (> 1.5 m/yr) as well as abrupt changes, leading to an exclusion of 12-day interferograms for the analysis. We selected three points (front, center, root) across the RG to extract LOS velocities time series.

Point Time Series

For the three monitoring points (front [45.5117, 7.2356], center [45.5114, 7.2367], and root [45.5111, 7.2391]) highlighted in the upper figures, we extracted LOS velocity time series, carefully checking and correcting any unwrapping issues. Each figure showing the time series on the next page displays the LOS displacement rates in m/yr in the top panel and the coherence in the bottom panel. For the LOS displacements, the coherent values are shown. For the coherence time series, all available 6-day pairs are shown. The coherence was obtained at the point location in the individual interferograms. Blue circles represent 6-day interferometric measurements, while orange crosses show 12-day measurements, with summer months (June-September) highlighted by gray vertical bands. 12-day measurements were excluded due to poor unwrapping results. For all three locations the coherence values in the summer season are generally high (>0.6). Higher velocities as well as unfavorable conditions such as snow cover can decrease the coherence.

The highest velocities are measured at the center location (~1.5-2.0 m/yr ~> 2.4-3.2 m/yr when assuming slope-parallel movement) with large fluctuations. The front location shows high velocities of up to 1.5-1.6 m/yr (~> 2.0-2.1 m/yr when assuming slope-parallel movement), with equally large fluctuations in summer. LOS velocities at the root are slightly lower but reach 1-5 m/yr in the summers of 2019 and 2020. Scale Factors for the three points are 1.35 for front, 1.61 for center and 1.65 for root.

Valsavarenche 3 RGV Analysis – Descending orbit 139

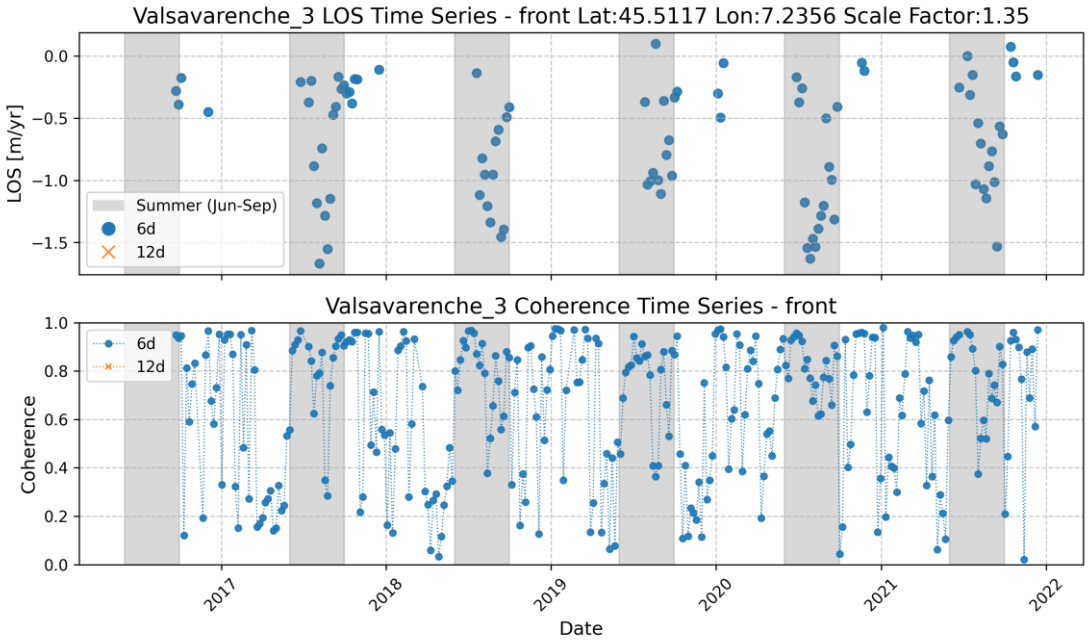

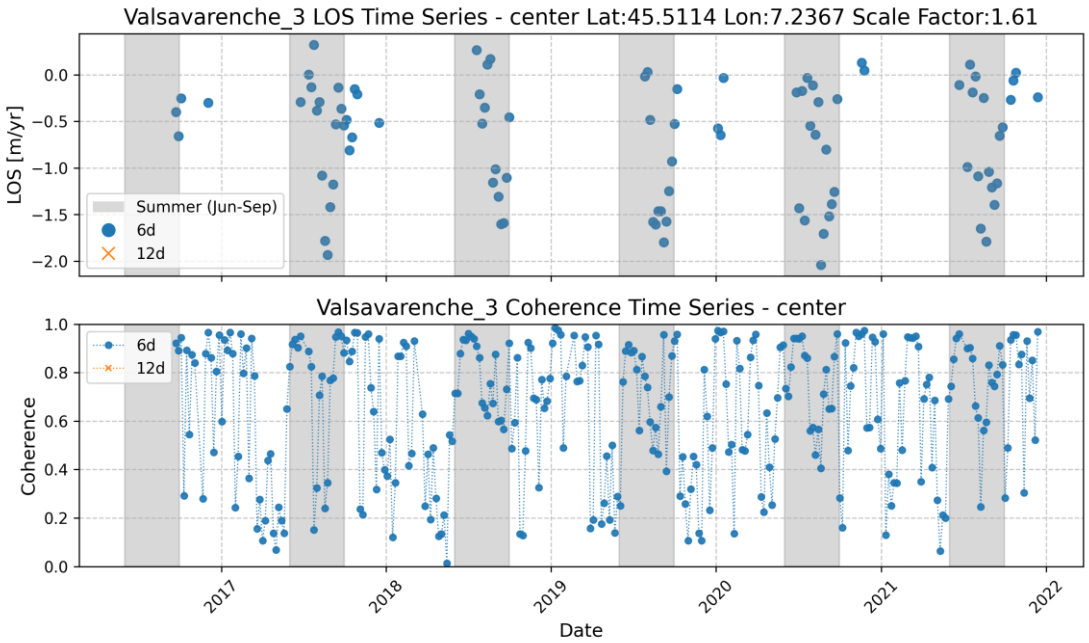

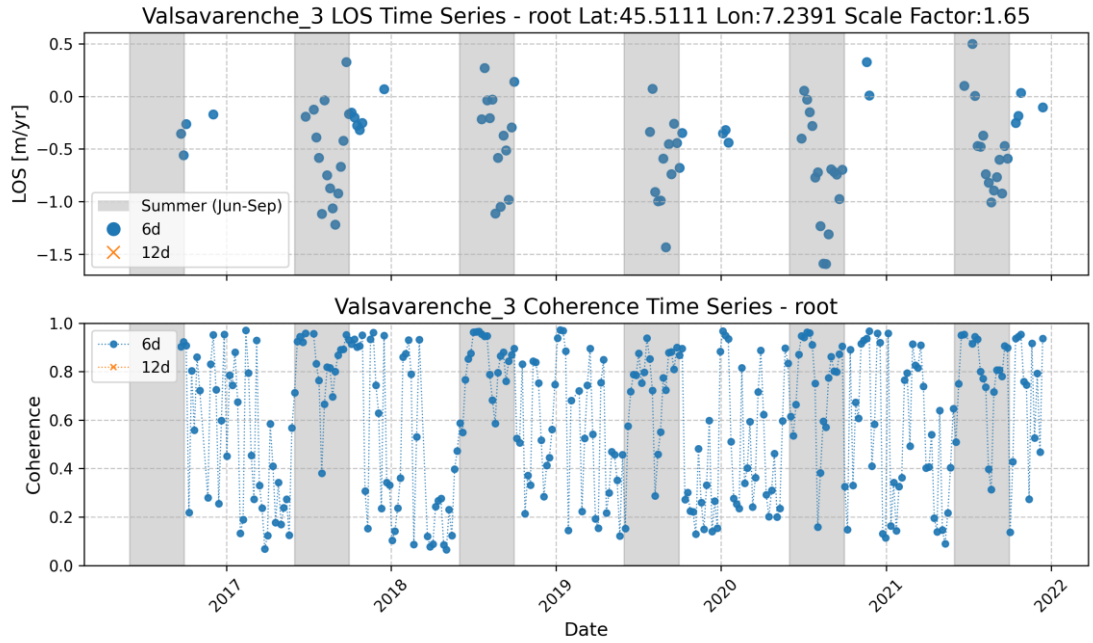

Valsavarenche 3 RGV Analysis – Descending orbit 139

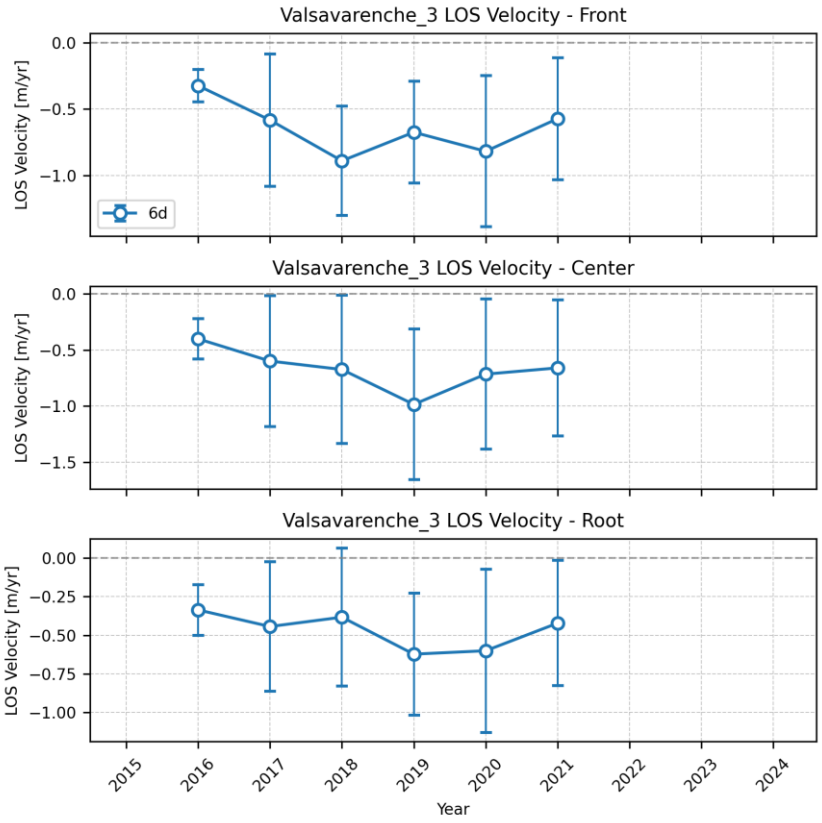

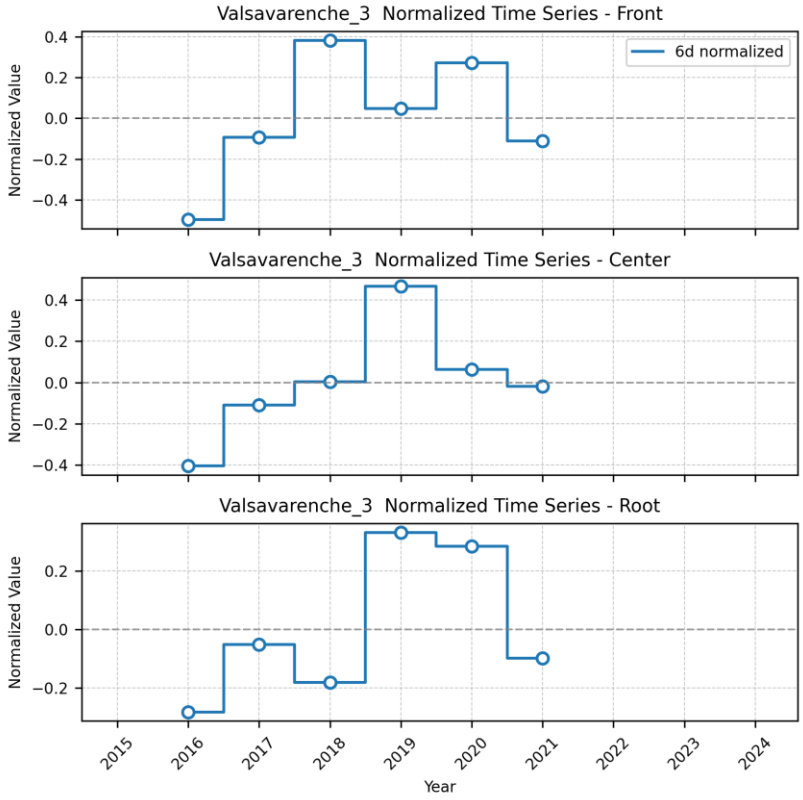

Velocity variation over the years: We averaged the obtained LOS velocity rates from all three monitoring points to generate yearly velocity estimates. In the top three figures, the averaged LOS velocities per summer are shown. The error bars represent the standard deviation per year. The three bottom figures show the normalized values ((Avg_year/mean_overall)-1) to highlight relative changes independent of the absolute velocities. Note that higher variations are expected as the measured velocities approach the sensitivity/noise level.

All three locations show a very similar temporal pattern, with slightly higher error bars at the center location compared to the root and front. The LOS displacement shows an overall acceleration from 2016 to 2018/2019, followed by a subsequent deceleration in 2020 and 2021. The lack of good quality 12-day interferograms underlines the overall lower reliability of the data. The time series displayed should thus be interpreted with caution.

Valsavarenche 3 RGV Analysis – Ascending orbit 88

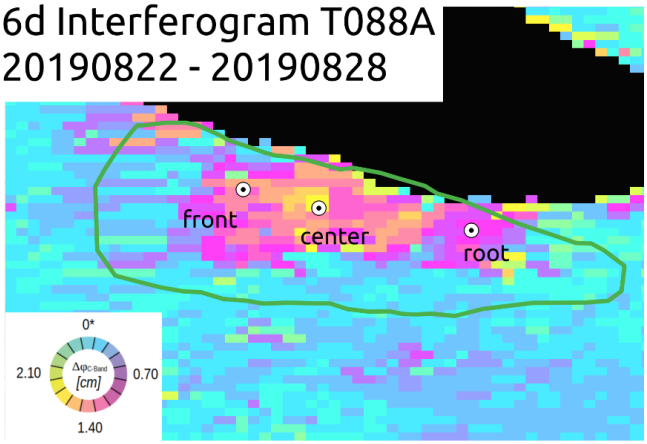

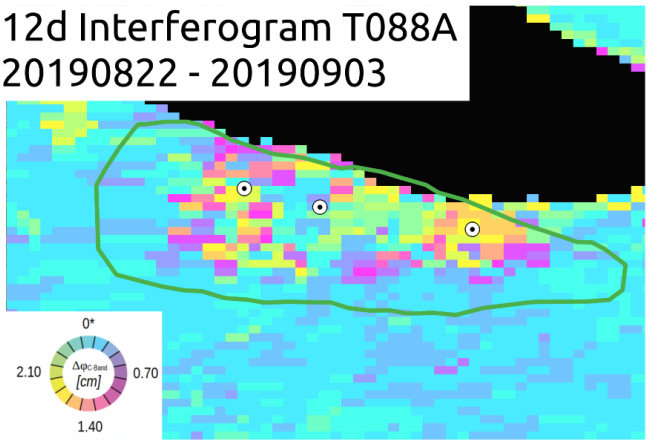

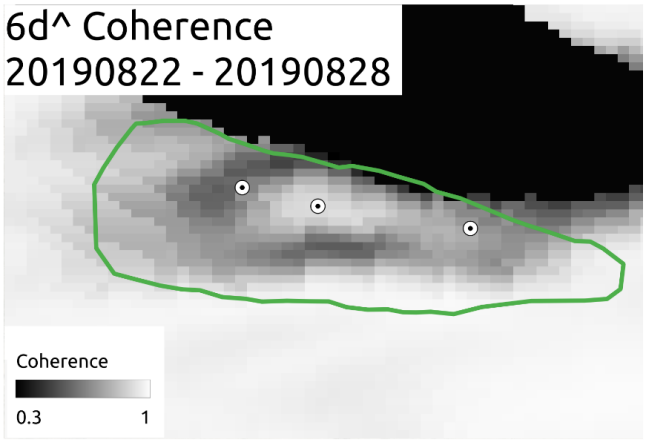

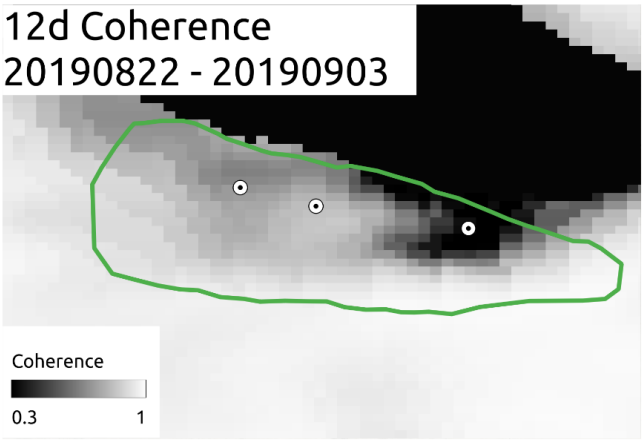

Overview

The figure above shows a 6d and 12d interferogram as well as the associated coherence from mid summer 2019. A selection of coherent interferograms was made manually for the further analysis. Many unwrapping issues are present due to high LOS velocities (> 1.5 m/yr) as well as abrupt changes, leading to an exclusion of 12-day interferograms for the analysis. We selected three points (front, center, root) across the RG to extract LOS velocities time series.

Point Time Series

For the three monitoring points (front [45.5117, 7.2356], center [45.5114, 7.2367], and root [45.5111, 7.2391]) highlighted in the upper figures, we extracted LOS velocity time series, carefully checking and correcting any unwrapping issues. Each figure showing the time series on the next page displays the LOS displacement rates in m/yr in the top panel and the coherence in the bottom panel. For the LOS displacements, the coherent values are shown. For the coherence time series, all available 6-day pairs are shown. The coherence was obtained at the point location in the individual interferograms. Blue circles represent 6-day interferometric measurements, while orange crosses show 12-day measurements, with summer months (June-September) highlighted by gray vertical bands. 12-day measurements were excluded due to poor unwrapping results. For all three locations the coherence values in the summer season are generally high (>0.6). Higher velocities as well as unfavorable conditions such as snow cover can decrease the coherence.

The ascending orbit is unfavorable with respect to the RG flow direction, yielding high scale factors. The highest velocities are measured at the center location (~1.0-1.2 m/yr ~> 2.1-2.5 m/yr when assuming slope-parallel movement) with fluctuations during the summer season. The front and root locations show similar fluctuations with LOS velocities of up to 0.7-1.0 m/yr. Scale Factors for the three points are 2.85 for front, 2.10 for center and 2.44 for root.

Valsavarenche 3 RGV Analysis – Ascending orbit 88

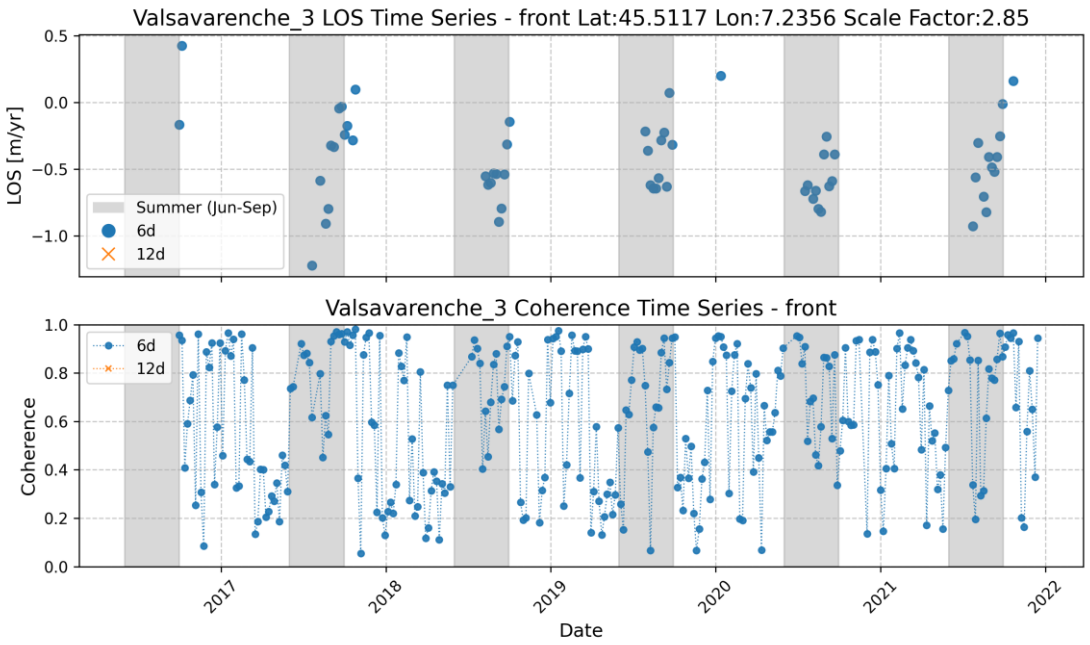

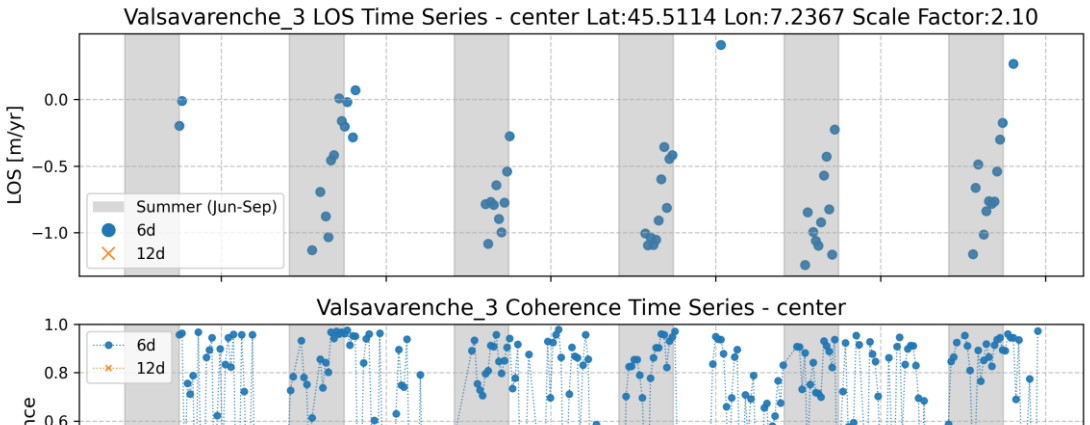

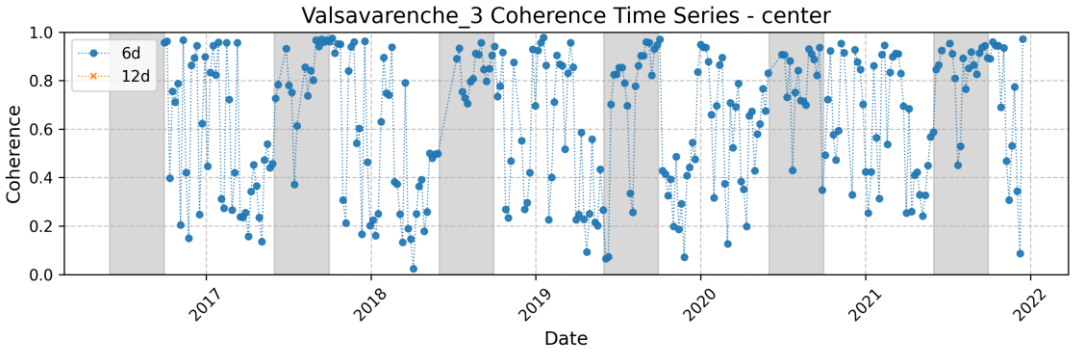

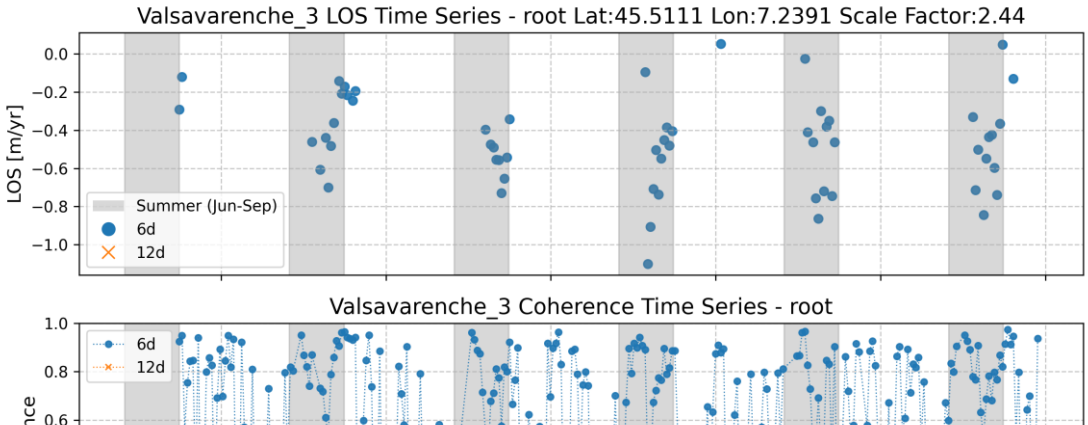

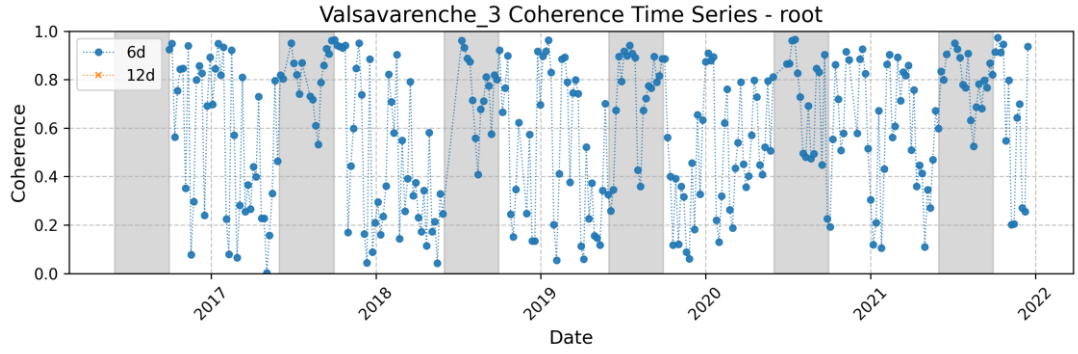

Valsavarenche 3 RGV Analysis – Ascending orbit 88

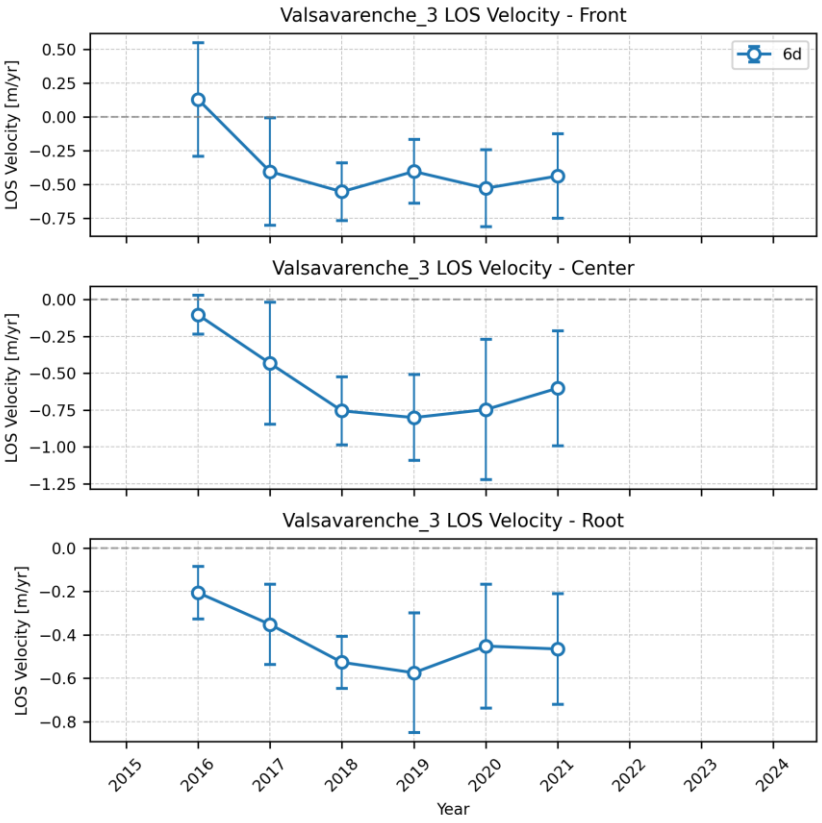

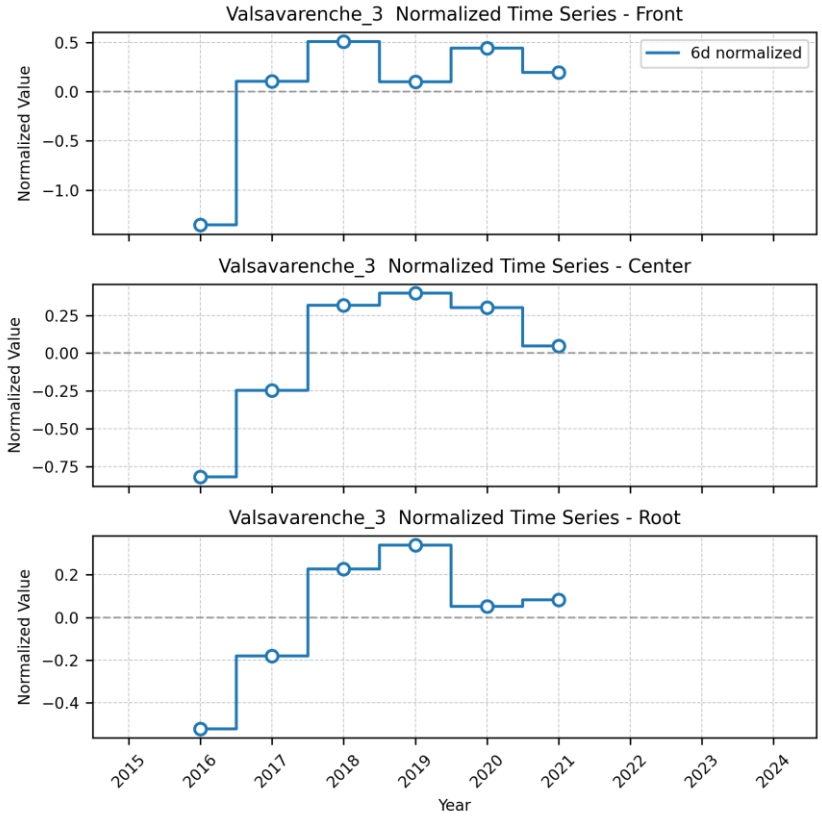

Velocity variation over the years: We averaged the obtained LOS velocity rates from all three monitoring points to generate yearly velocity estimates. In the top three figures, the averaged LOS velocities per summer are shown. The error bars represent the standard deviation per year. The three bottom figures show the normalized values ((Avg_year/mean_overall)-1) to highlight relative changes independent of the absolute velocities. Note that higher variations are expected as the measured velocities approach the sensitivity/noise level.

All three locations show a similar temporal pattern, with error bars of +/- 0.2-0.5 m/yr. The LOS displacement shows an overall acceleration from 2016 to 2018/2019, followed by a subsequent deceleration in 2020 and 2021. The lack of good quality 12-day interferograms underlines the overall lower reliability of the data. The time series displayed should thus be interpreted with caution.

Lazaun RGV Analysis

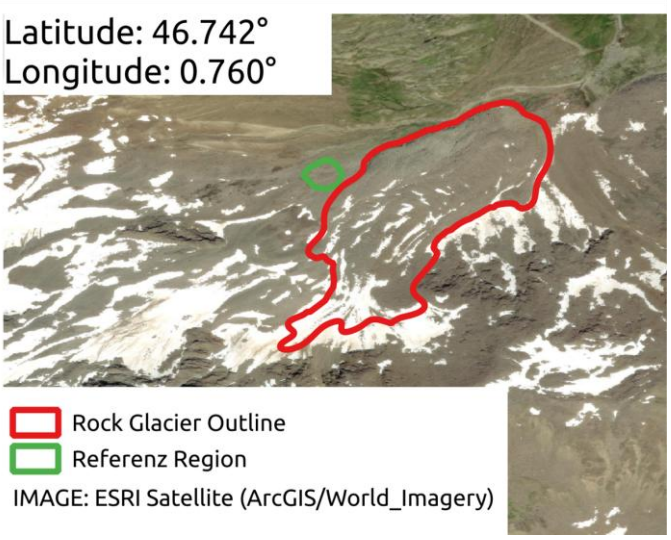

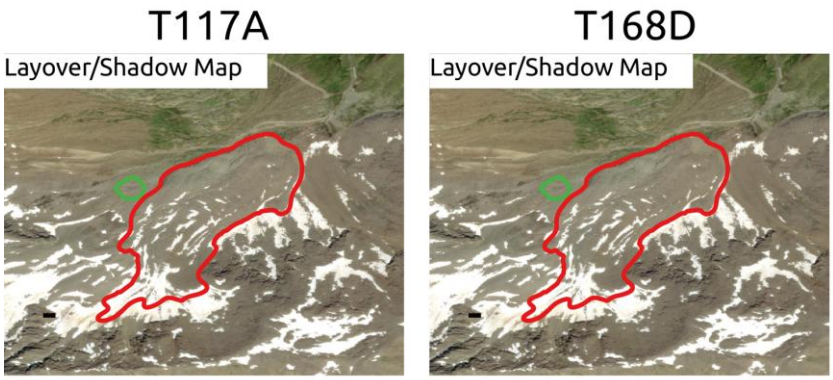

Layover/Shadow
Sentinel-1 data are acquired from two orbits (T117A and T168D). In both orbits the rock glacier region is not affected by layover or shadow effects.

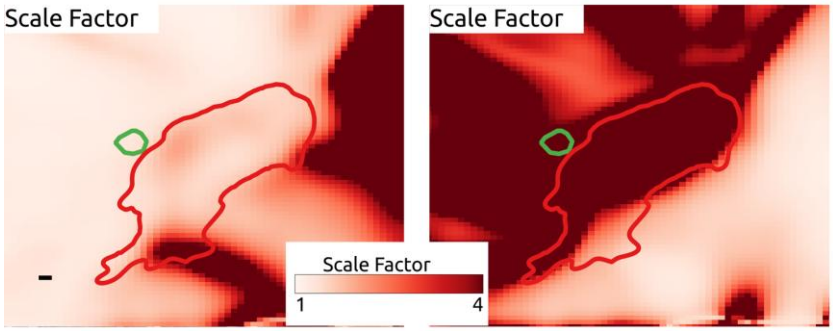

Scale Factor:
T168D exhibits an unfavorable viewing geometry with a Scale Factor above 4. The Line-of-Sight for orbit T117A aligns well with the general flow direction of the RG. Scale Factors for orbit T117A are in the range 1.2 to 1.8. Nevertheless, the most southern part at the top of the RG shows scale factors above 4.

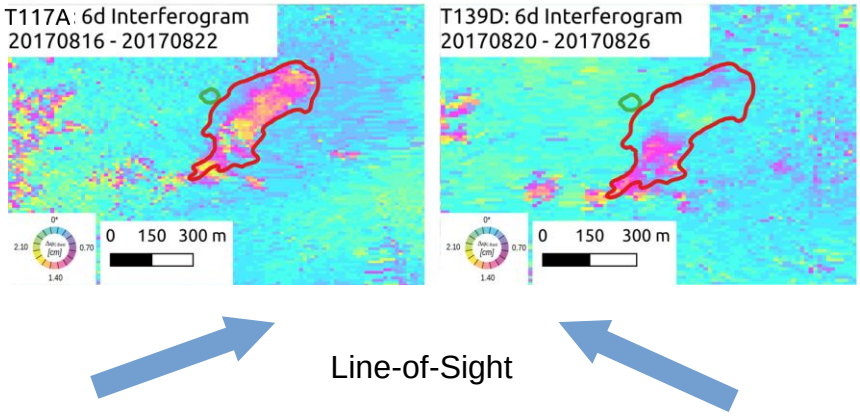

Initial assessment
The T117A interferogram shows movement in all parts of the RG, reaching up to half a phase cycle (2cm/6d or approximately 1m/yr). In the upper part some decorrelated regions are visible. Due to the high velocities, phase unwrapping problems are likely to occur during processing.
The T139D interferogram shows no/minimal movement as expected due to the high Scale Factor.

For the RGV Analysis we use orbit T117A ascending data.

Lazaun RGV Analysis – Ascending orbit 117

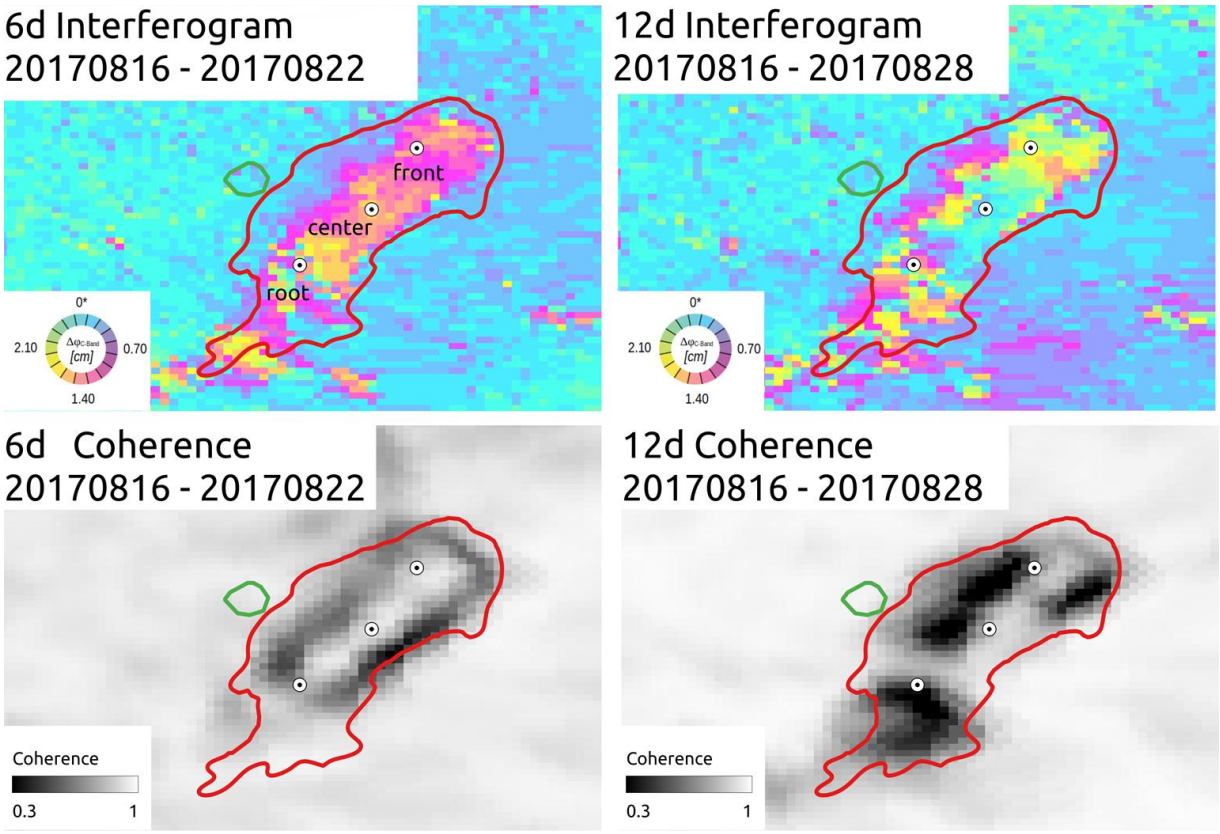

Overview

The figure above shows a 6d and 12d interferogram as well as the associated coherence from end of summer 2017. A selection of coherent interferograms was made manually for the further analysis. Many unwrapping issues are present due to high LOS velocities (up to 2 m/yr) as well as abrupt changes. We selected three points (front, center, root) across the RG to extract LOS velocities time series.

Point Time Series

For the three monitoring points (front [46.7474, 10.7560], center [46.7461, 10.7551], and root [46.7450 10.7537]) highlighted in the upper figures, we extracted LOS velocity time series, carefully checking and correcting any unwrapping issues. Each figure showing the time series on the next page displays the LOS displacement rates in m/yr in the top panel and the coherence in the bottom panel. For the LOS displacements, the coherent values are shown. For the coherence time series, all available pairs are shown. The coherence was obtained at the point location in the individual interferograms. Blue circles represent 6-day interferometric measurements, while orange crosses show 12-day measurements, with summer months (June-September) highlighted by gray vertical bands. In general, the 12-day interferogram coherence values are lower than the 6-day. For the locations center and root the coherence values in the summer season are generally high (>0.6). For the root location the coherence was lowest and only a processing of the 6d-interferograms was possible. Higher velocities as well as unfavorable conditions such as snow cover decrease the coherence.

The highest velocities are measured at the center and root location (~1.5-2 m/yr ~> 2-3 m/yr when assuming slope-parallel movement) with large fluctuations due to the low data quality (see figure on next page). At the front, the velocities slightly lower (<1.5m/yr). Scale Factors for the three points are 1.64 for front, 1.41 for center and 1.59 for root.

Lazaun RGV Analysis – Ascending orbit 117

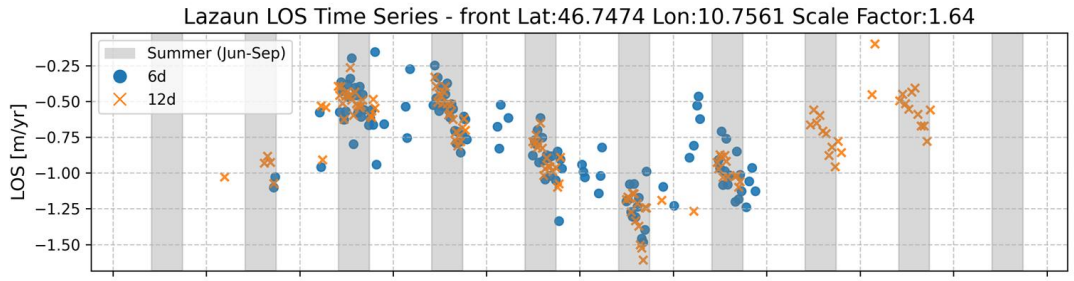

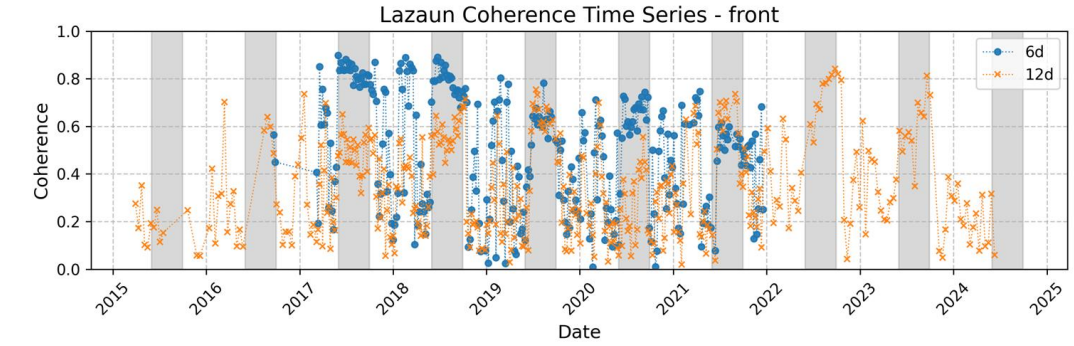

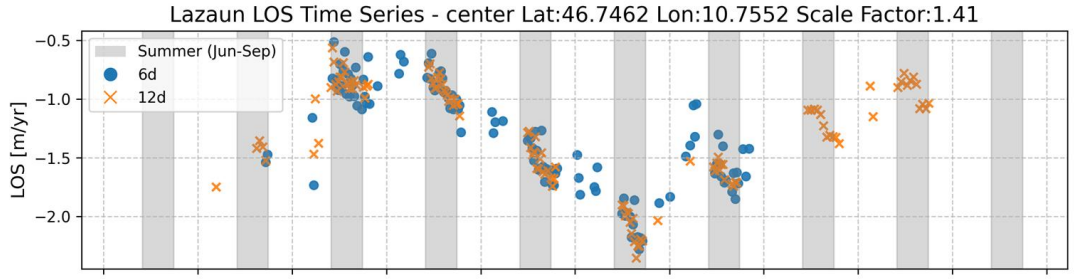

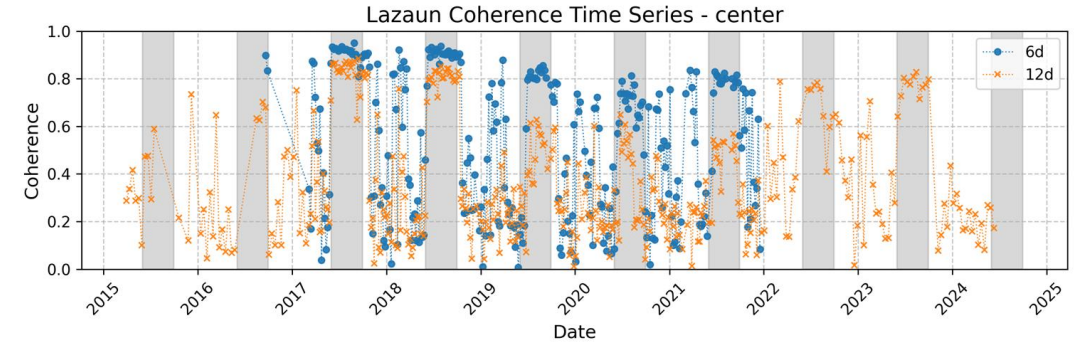

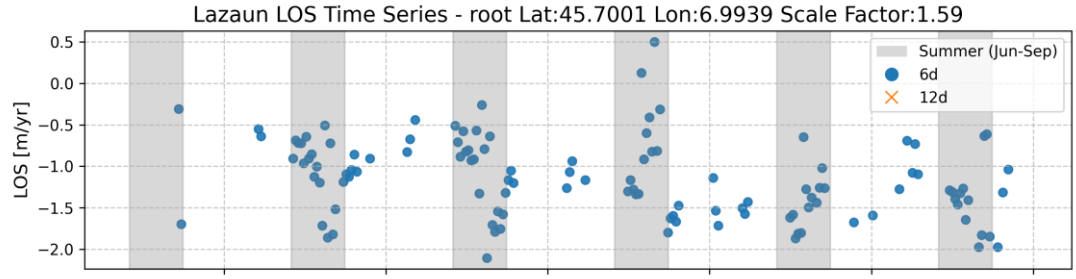

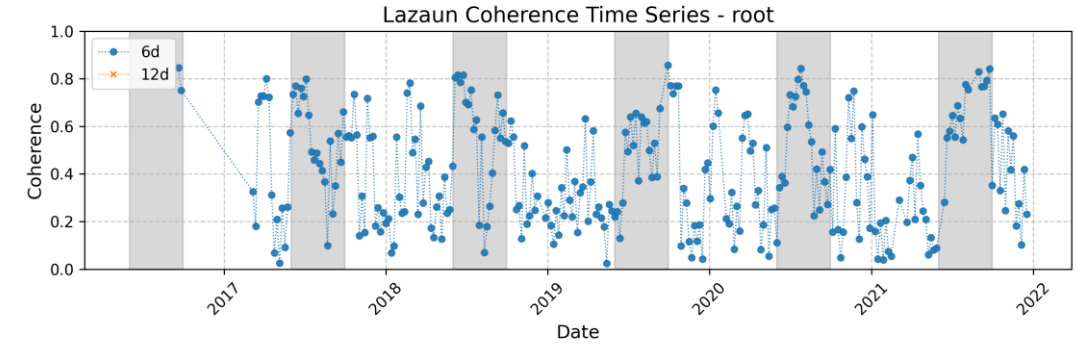

Lazaun RGV Analysis – Ascending orbit 117

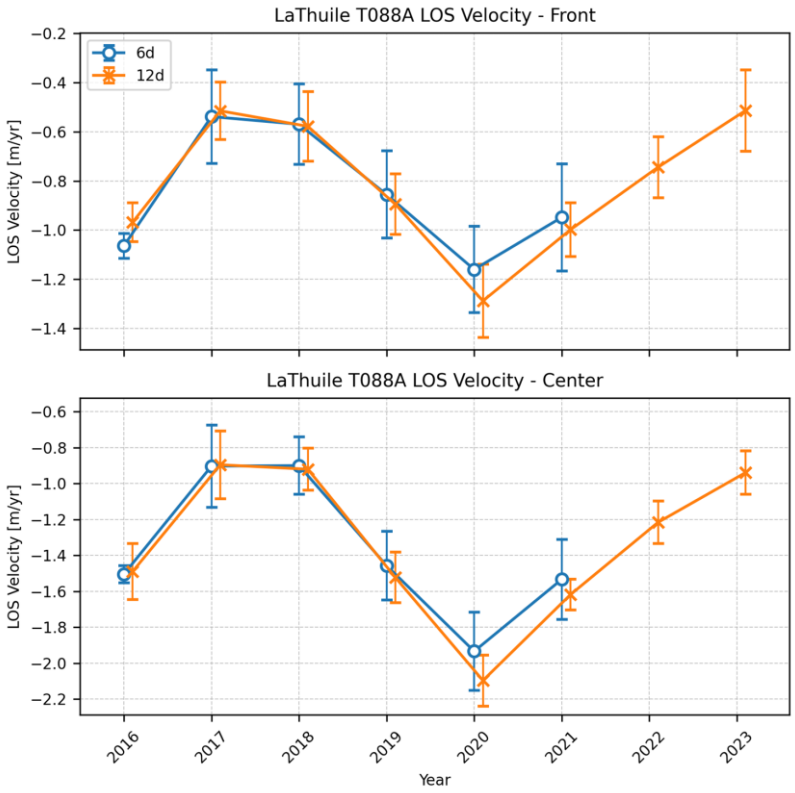

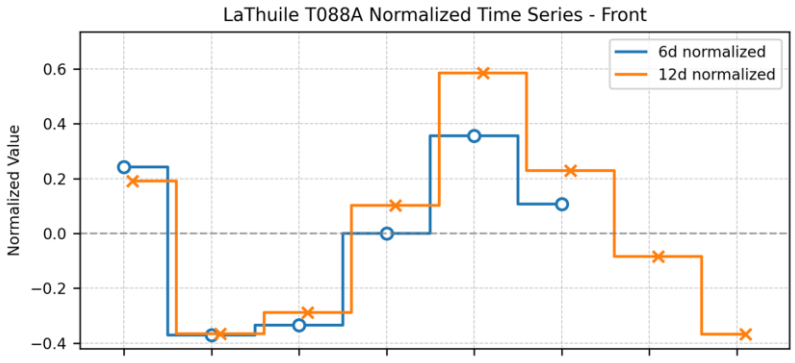

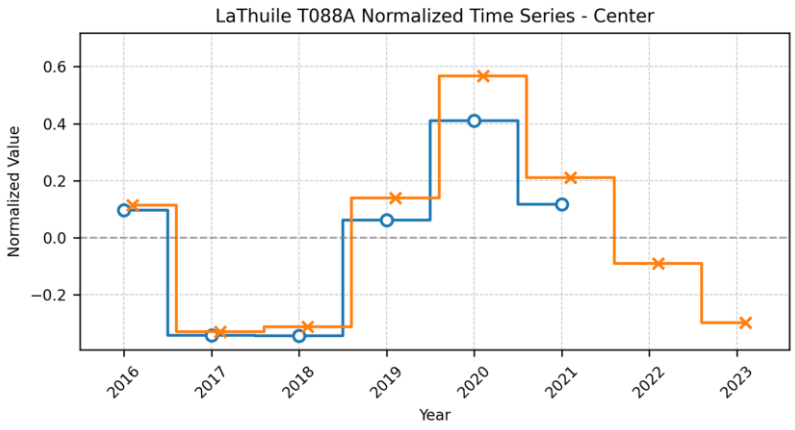

Velocity variation over the years: We averaged the obtained LOS velocity rates from the root and front monitoring points to generate yearly velocity estimates. In the top two figures, the averaged LOS velocities per summer are shown. The error bars represent the standard deviation per year. The two bottom figures show the normalized values ((Avg_year/mean_overall)-1) to highlight relative changes independent of the absolute velocities. Note that higher variations are expected as the measured velocities approach the sensitivity/noise level.

For location root the obtained measurements are very noise and we do not show the results here. Both other points (front and center) show a strong yearly change which is consistent for both points and Interferogram interval. The velocities decrease from 2016 to 2017/18, followed by a strong increase from 2018 to 2020, and again a decrease from 2020 to 2023 afterwards.

Similaun RGV Analysis

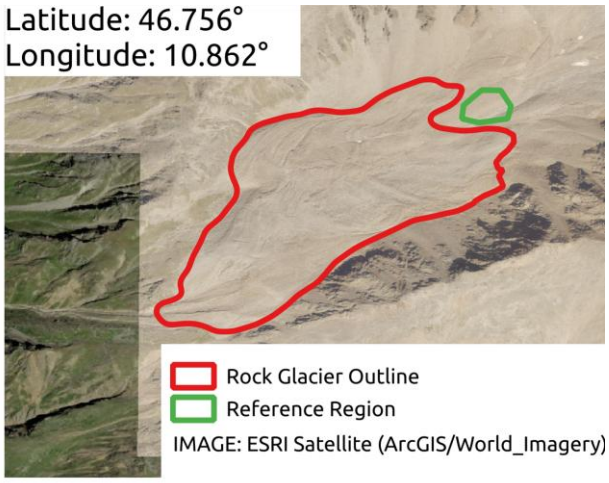

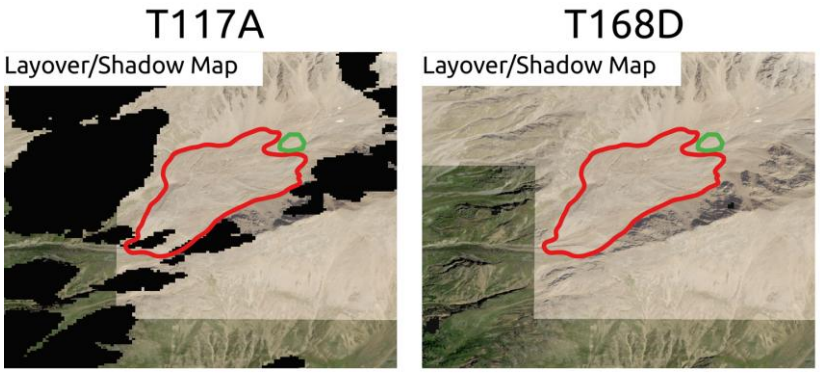

Layover/Shadow
Sentinel-1 data are acquired from two orbits (T117A and T168D). In orbit T117A the western front of the rock glacier region is affected by layover/shadow effects. Orbit T168D is not affected by layover/shadow effects.

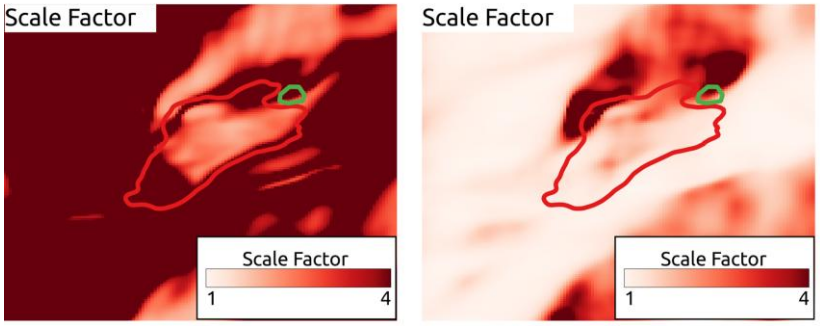

Scale Factor:
T117A exhibits an unfavorable viewing geometry with a Scale Factor approaching or above 4.
The Line-of-Sight for orbit T168D aligns better with the general flow direction of the RG except for a small region in the center. Scale Factors for orbit T117A are in the range 1.1 to 2.5.

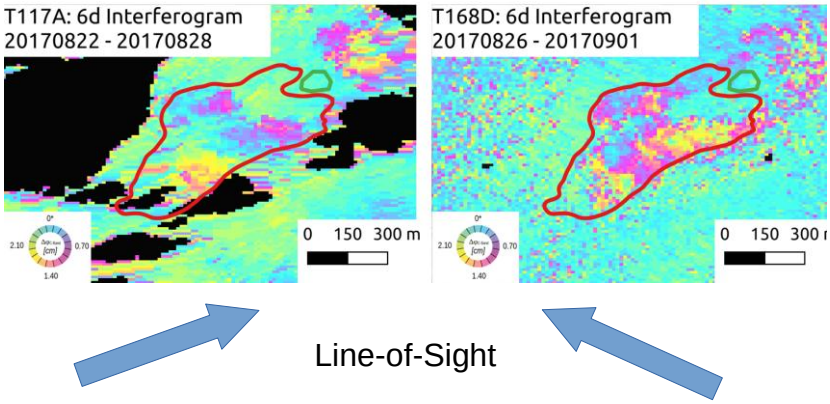

Initial assessment
The T168D interferogram shows contrasting deformation patterns within the RG. The upper and lower part at the root exhibits slow movement at or below the detection limit (sensitivity ~0.2m/yr), while the center part displays faster movement of up to 2.2cm/6d (equivalent to approximately 1.2m/yr). Sharp velocity transitions from this center region towards the edges of the RG may introduce phase unwrapping challenges during processing.

For the RGV Analysis we use orbit T168D descending data.

Similaun RGV Analysis
Descending orbit 168

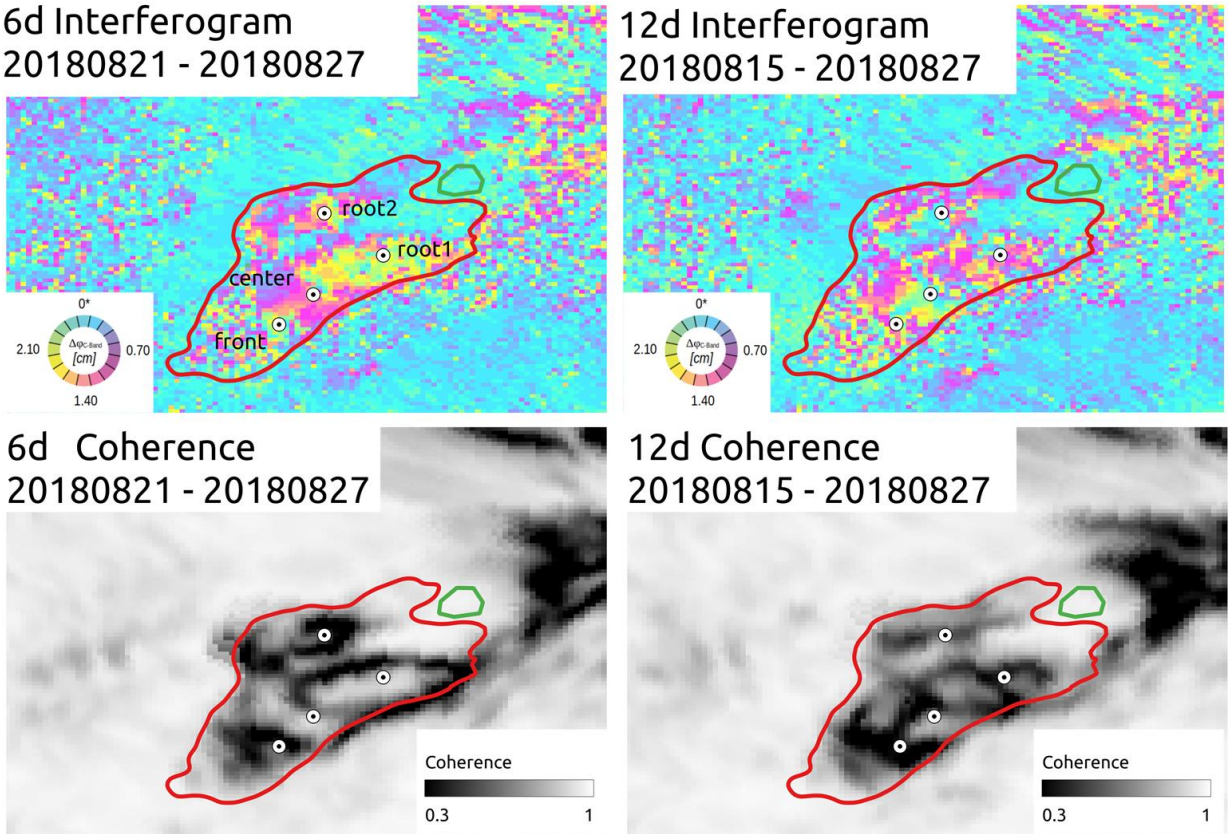

Overview

The figure above shows a 6d and 12d interferogram as well as the associated coherence from mid summer 2018. A selection of coherent interferograms was made manually for the further analysis. Many unwrapping issues are present due to high LOS velocities (> 1.2 m/yr) as well as abrupt changes. We selected four points (front, center, root1, root2) across the RG to extract LOS velocities time series.

Point Time Series

For the three monitoring points (front [46.7545, 10.8608], center [46.7555, 10.8620], root1 [46.7569, 10.8644] and root2 [46.7582, 10.8624]) highlighted in the upper figures, we extracted LOS velocity time series, carefully checking and correcting any unwrapping issues. Each figure showing the time series on the next page displays the LOS displacement rates in m/yr in the top panel and the coherence in the bottom panel. For the LOS displacements, the coherent values are shown. For the coherence time series, all available pairs are shown. The coherence was obtained at the point location in the individual interferograms. Blue circles represent 6-day interferometric measurements, while orange crosses show 12-day measurements, with summer months (June-September) highlighted by gray vertical bands. In general, the 12-day interferogram coherence values are lower than the 6-day. For all locations, the coherence values in the summer season are generally high (>0.6). Higher velocities as well as unfavorable conditions such as snow cover can decrease the coherence.

The highest velocities are measured at the front location with velocities up to 2 m/yr (~3 m/yr when assuming slope-parallel movement). For root1 location show a very strong increase from 0.5m/yr to 1.5m/yr each summer season. Due to the high velocity increase it was not possible to correct the unwrapping error for the 12d interferograms. At root2 a similar behavior is visible at slightly lower velocities. At the center location LOS velocities were lower approaching 1.2 m/yr. Scale Factors for the three points are 1.56 for front, 1.71 for center, 1.40 for root1 and 1.98 for root2.

Similaun RGV Analysis
Descending orbit 168

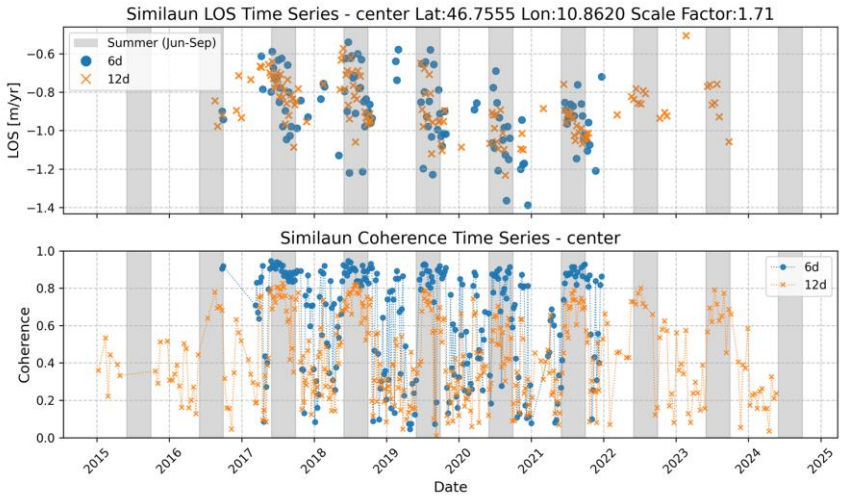

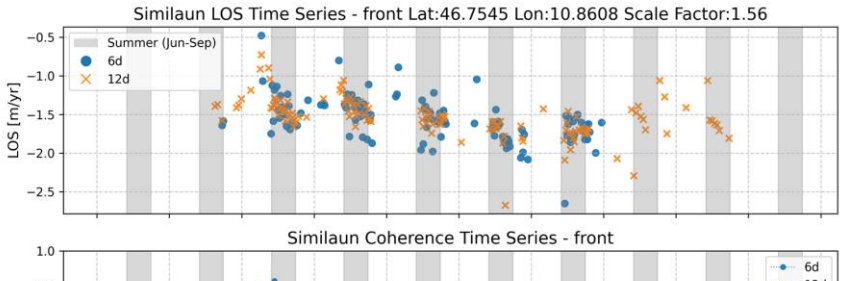

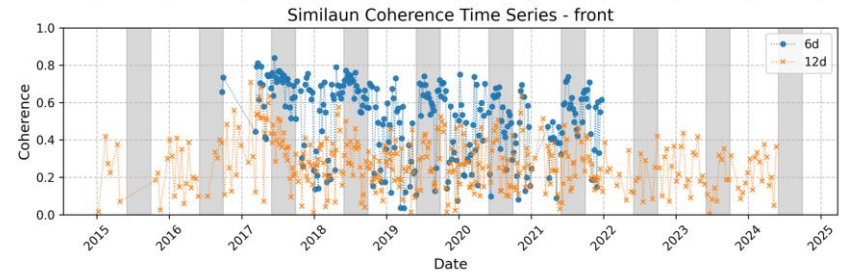

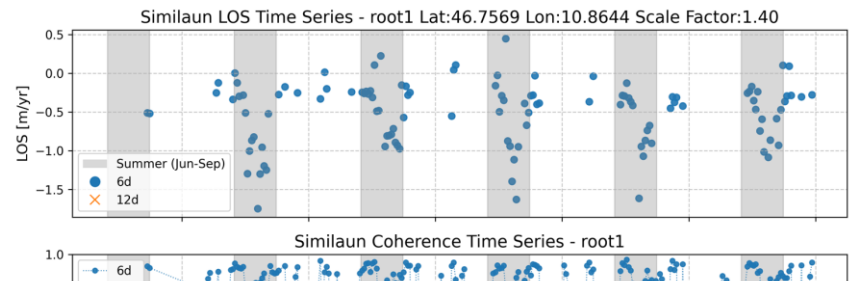

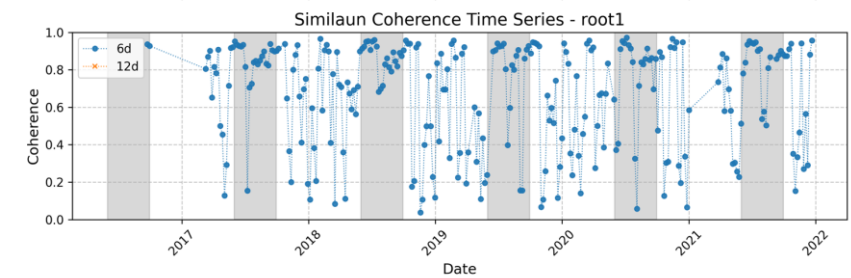

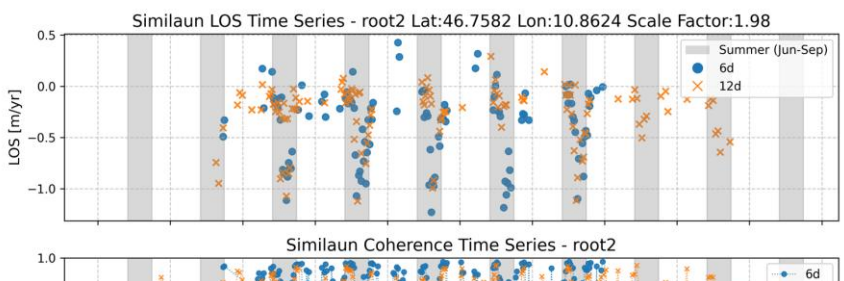

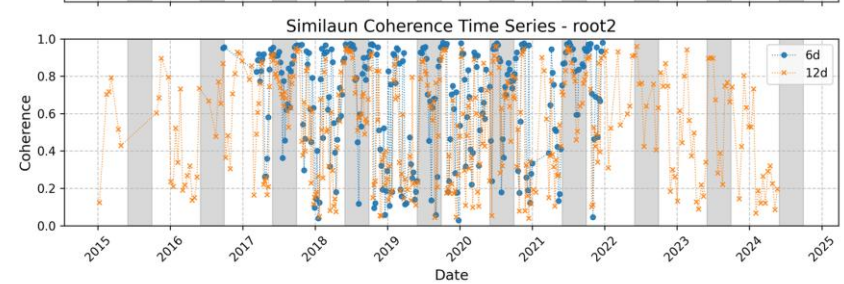

Similaun RGV Analysis
Descending orbit 168

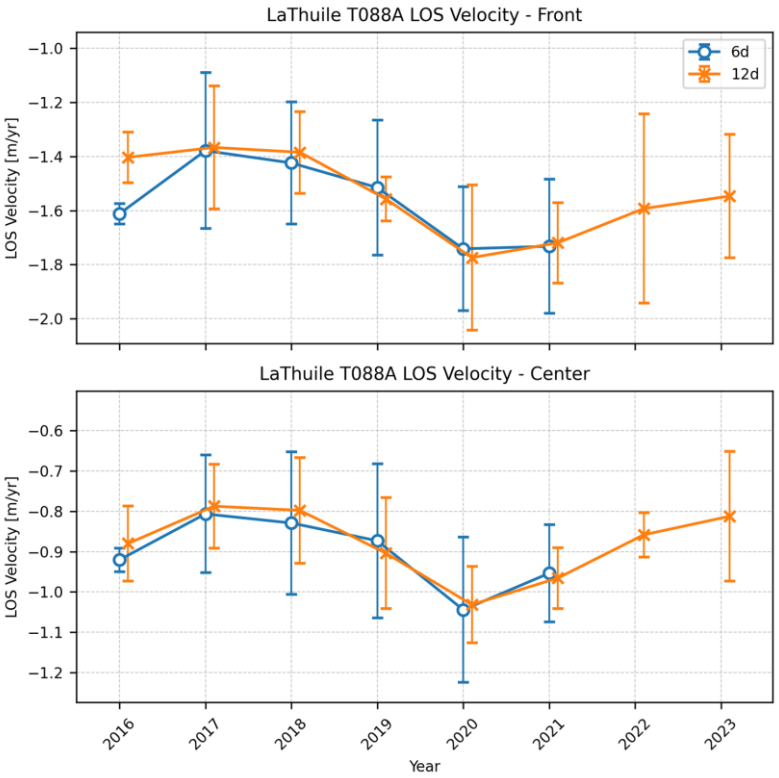

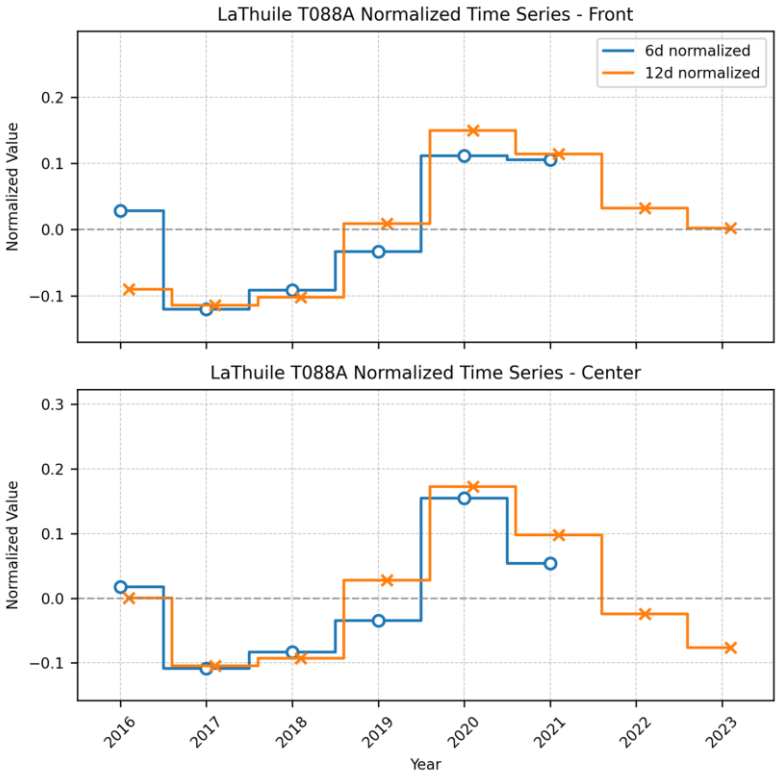

Velocity variation over the years: We averaged the obtained LOS velocity rates from all three monitoring points to generate yearly velocity estimates. In the top three figures, the averaged LOS velocities per summer are shown. The error bars represent the standard deviation per year. The three bottom figures show the normalized values ((Avg_year/mean_overall)-1) to highlight relative changes independent of the absolute velocities. Note that higher variations are expected as the measured velocities approach the sensitivity/noise level.

Due to the large velocity variations during the summer months at the two root location we do not show them here. The front and center location show significant changes during the observation period. In general, the behavior of the two points as well as the 6-day and 12-day period match well. The fasters year is in 2020.

Laurichard RGV Analysis

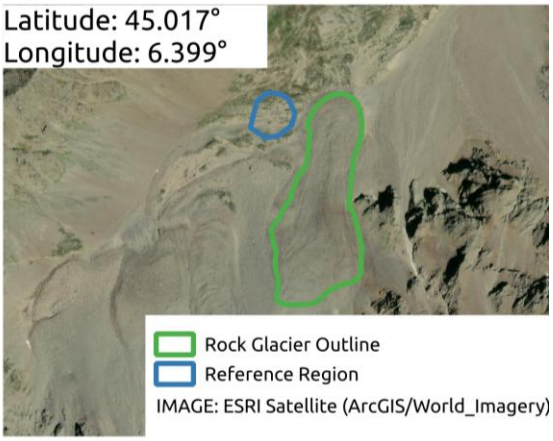

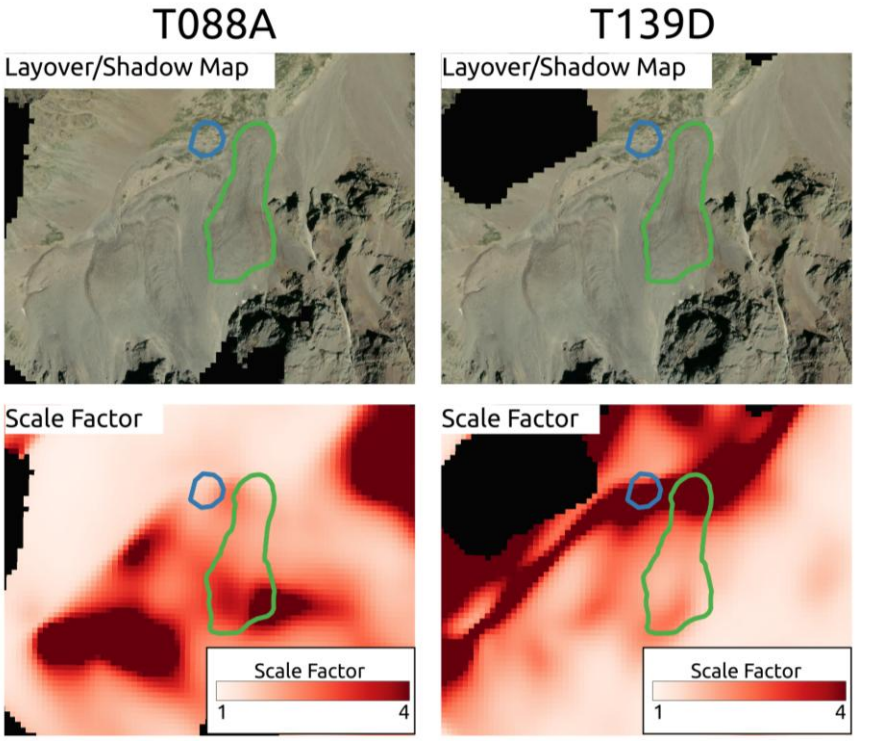

Layover/Shadow
Sentinel-1 data are acquired from two orbits (T088A and T139D). In both orbits the rock glacier region is not affected by layover or shadow effects.

Scale Factor:
Both orbits show low and high scale factors across the RG. T088A exhibits a more unfavorable viewing geometry at the root of the RG, T139D on the other side shows unfavorable scale factors at the front.
Respective Scale Factor at the front for T088A are 1.3 to 2 and for T139D at the root of 1.8 to 2.4.

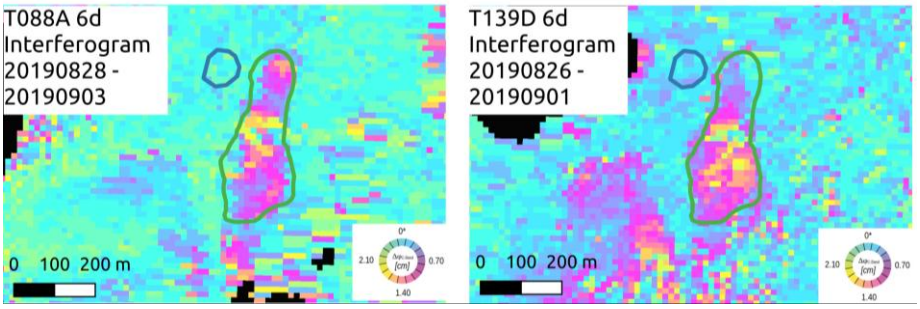

Line-of-Sight

Initial assessment
Both interferograms reveals substantial movement across most of the RG, with deformation rates up to 2cm/6d (equivalent to approximately 1.2m/yr). In the transition zone between the front and root of the RG faster displacement rates are visible approaching 3.3cm/6d (2m/yr). The extreme velocity contrast necessitates thorough verification of phase unwrapping during processing, with manual corrections likely required to ensure accurate deformation measurements.

For the RGV Analysis use both orbits

Laurichard RGV Analysis – Descending orbit 139

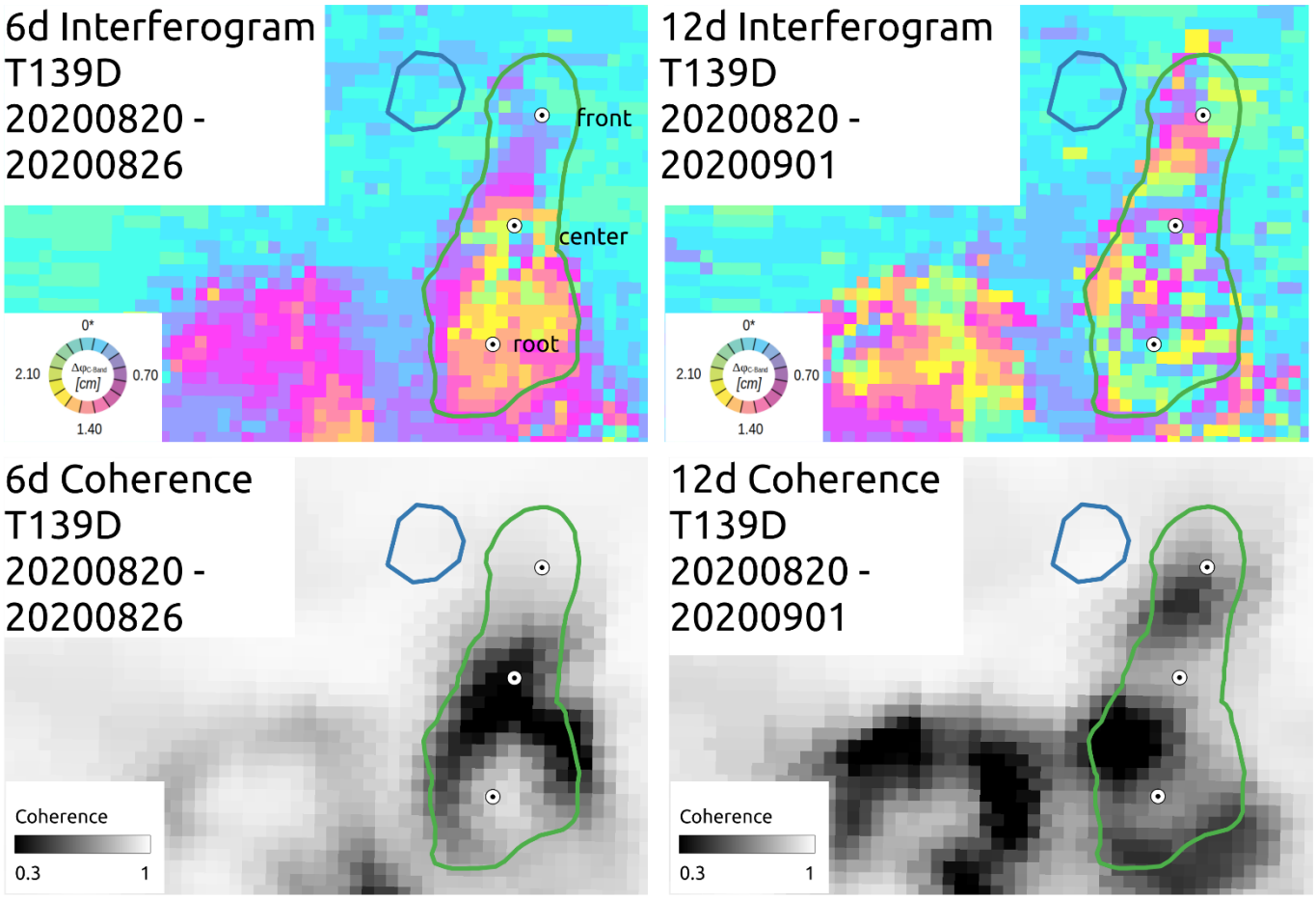

Overview

The figure above shows a 6d and 12d interferogram as well as the associated coherence from mid to late summer 2020. A selection of coherent interferograms was made manually for the further analysis. Many unwrapping issues are present due to high LOS velocities (up to 2 m/yr in the center of the RG) as well as abrupt changes. We selected three points (center, root) across the RG to extract LOS velocities time series. We did not analysis location front here due to high scale factors (see previous page)

Point Time Series

For the two monitoring points (center [45.0172, 6.3996], and root [45.0160, 6.3994]) highlighted in the upper figures, we extracted LOS velocity time series, carefully checking and correcting any unwrapping issues. Each figure showing the time series on the next page displays the LOS displacement rates in m/yr in the top panel and the coherence in the bottom panel. For the LOS displacements, the coherent values are shown. For the coherence time series, all available pairs are shown. The coherence was obtained at the point location in the individual interferograms. Blue circles represent 6-day interferometric measurements, while orange crosses show 12-day measurements, with summer months (June-September) highlighted by gray vertical bands. In general, the 12-day interferogram coherence values are lower than the 6-day. For the root locations the coherence values in the summer season are generally high (>0.8), while for the center location the coherence values can drop to 0.4 to 0.5. Higher velocities as well as unfavorable conditions such as snow cover can decrease the coherence.

The highest velocities are measured at the center location (~1.2-1.6 m/yr ~> 2.5-3.2 m/yr when assuming slope-parallel movement) with large fluctuations of up to 0.8 m/yr during the summer months. At the root, the velocities are slower (up to 0.8m/yr) but also show strong acceleration and deceleration during the summer. Scale Factors for the two points are 2.09 for center and 2.13 for root.

Laurichard RGV Analysis – Descending orbit 139

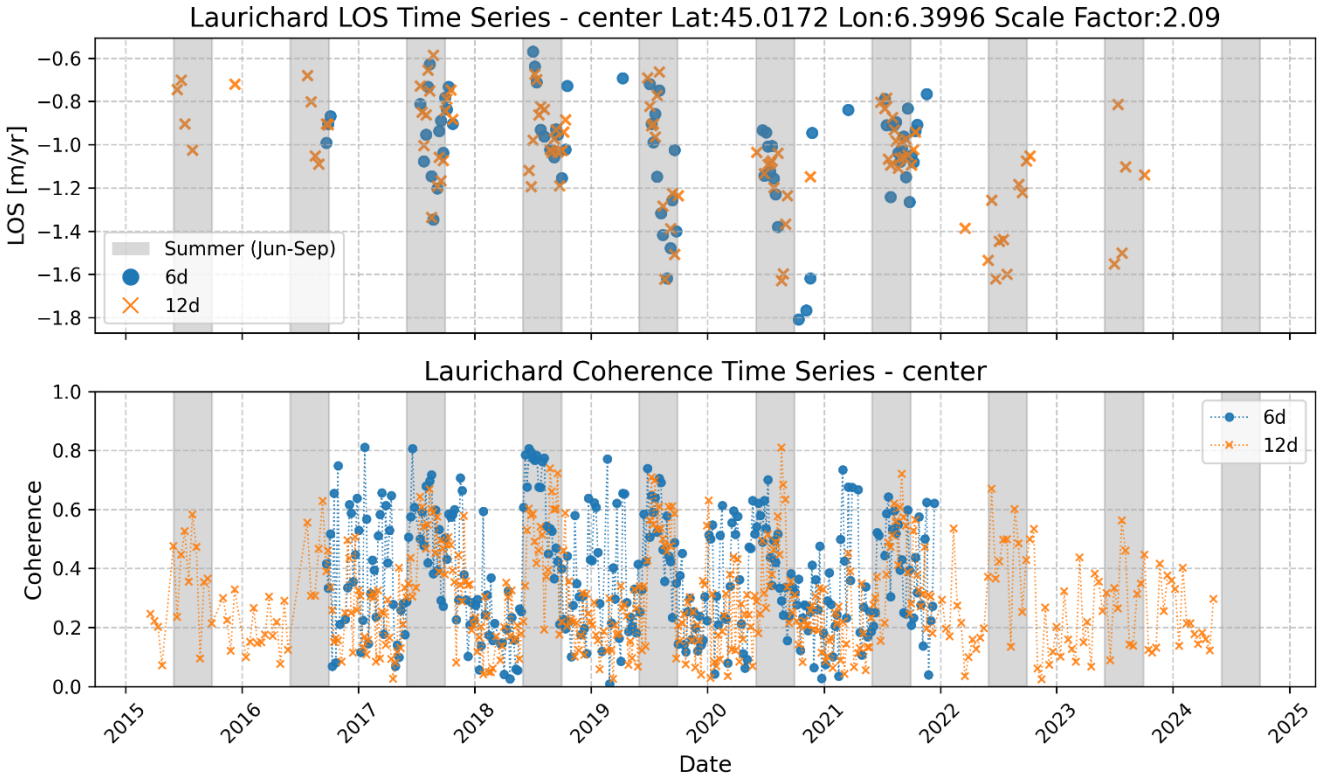

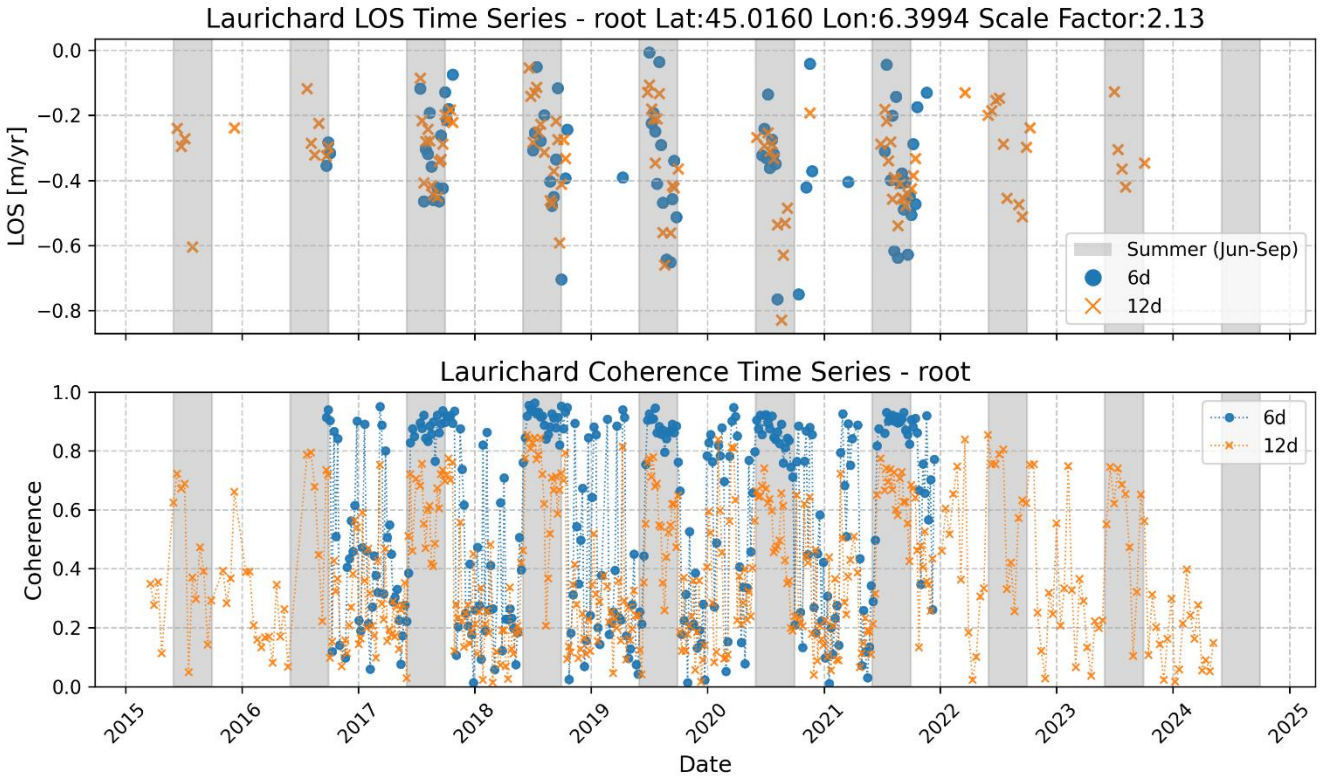

Laurichard RGV Analysis – Ascending orbit 88

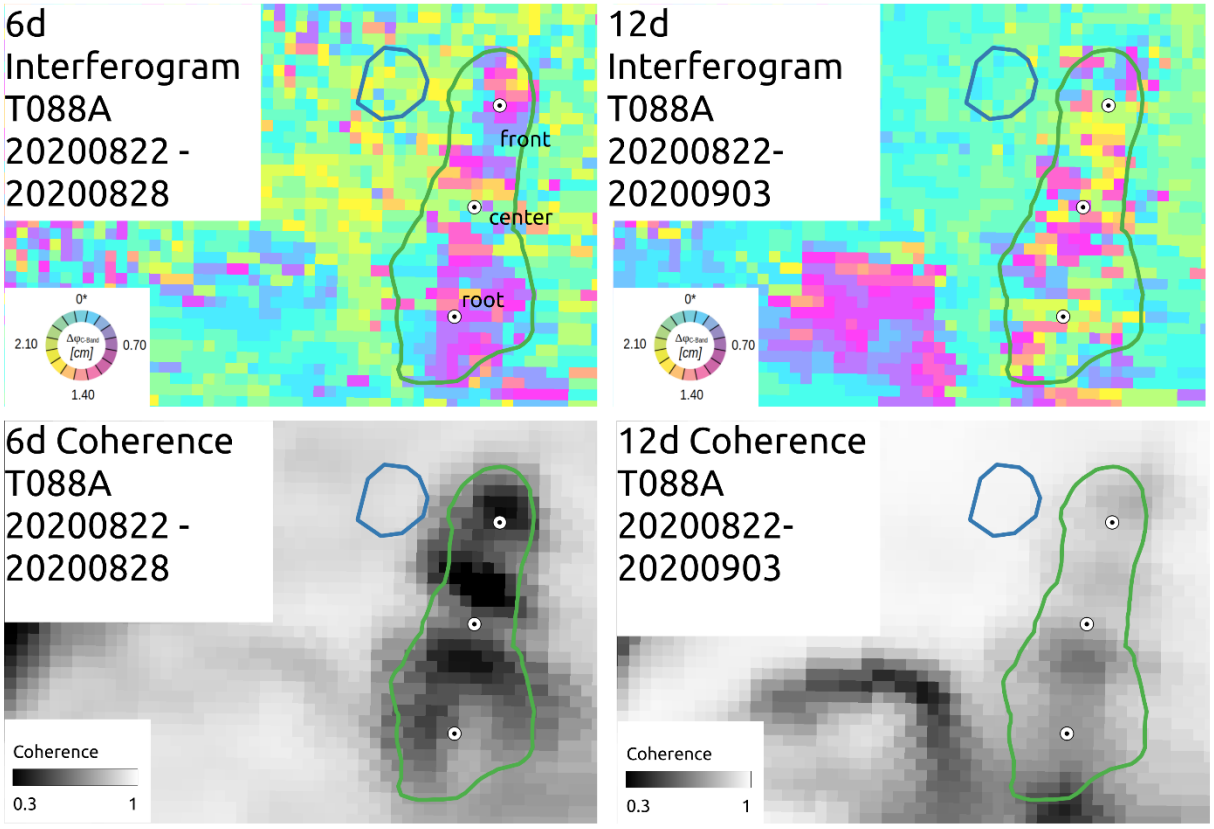

Overview

The figure above shows a 6d and 12d interferogram as well as the associated coherence from end of summer 2019. A selection of coherent interferograms was made manually for the further analysis. Many unwrapping issues are present due to high LOS velocities (up to 2 m/yr) as well as abrupt changes. We selected three points (front, center, root) across the RG to extract LOS velocities time series.

Point Time Series

For the three monitoring points (front [45.0184, 6.4000], center [45.0172, 6.3996], and root [45.0160 6.3994]) highlighted in the upper figures, we extracted LOS velocity time series, carefully checking and correcting any unwrapping issues. Each figure showing the time series on the next page displays the LOS displacement rates in m/yr in the top panel and the coherence in the bottom panel. For the LOS displacements, the coherent values are shown. For the coherence time series, all available pairs are shown. The coherence was obtained at the point location in the individual interferograms. Blue circles represent 6-day interferometric measurements, while orange crosses show 12-day measurements, with summer months (June-September) highlighted by gray vertical bands. In general, the 12-day interferogram coherence values are lower than the 6-day. For the locations center and root the coherence values in the summer season are generally high (>0.6). For the center location the coherence was significantly lower (0.4 to 0.6) and only a processing of the 6d-interferograms was possible. Higher velocities as well as unfavorable conditions such as snow cover decrease the coherence.

The highest velocities are measured at the center location (~1.5-2.0 m/yr ~> 3-4 m/yr when assuming slope-parallel movement) with large fluctuations due to the low data quality. At the front and root locations, the velocities are up to 0.8 m/yr. Here also large fluctuation in the summer months of up to 0.6m/yr are visible. Scale Factors for the three points are 1.86 for front, 2.03 for center and 3.47 for root.

Laurichard RGV Analysis – Ascending orbit 88

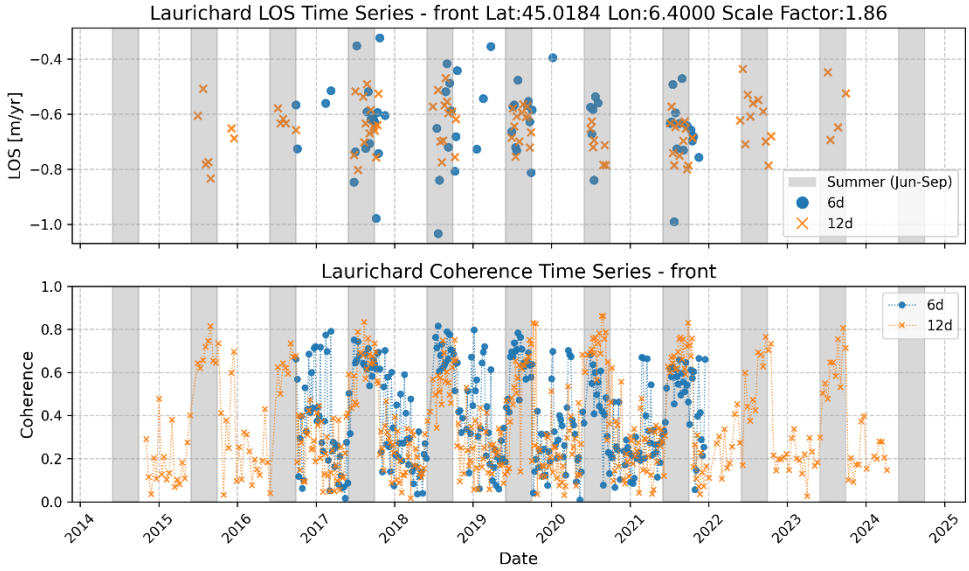

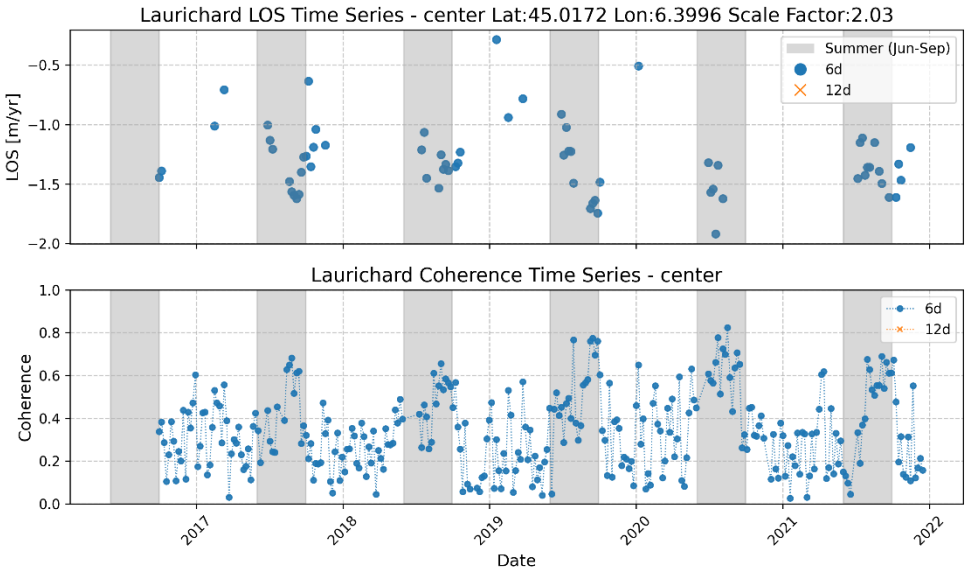

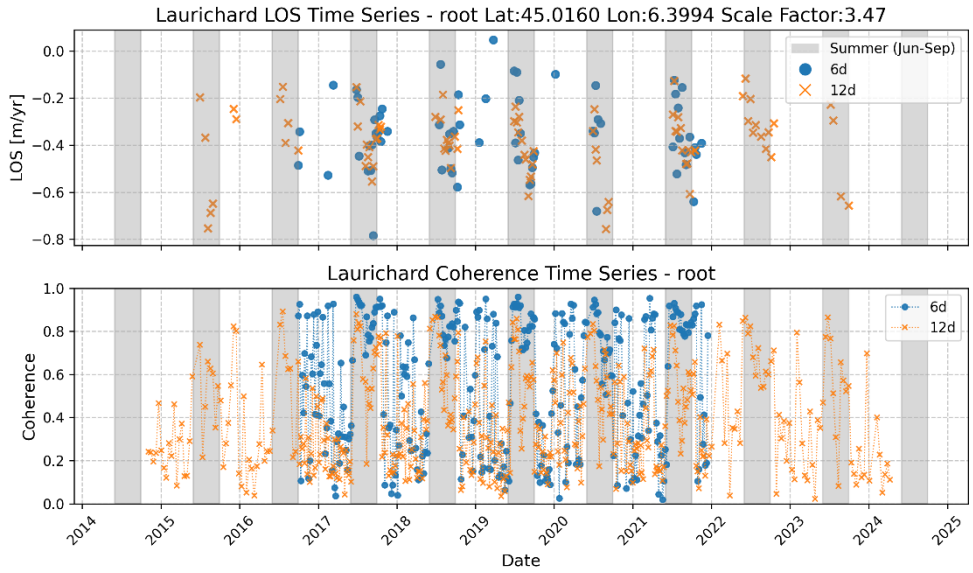

Laurichard RGV Analysis – Ascending orbit 88

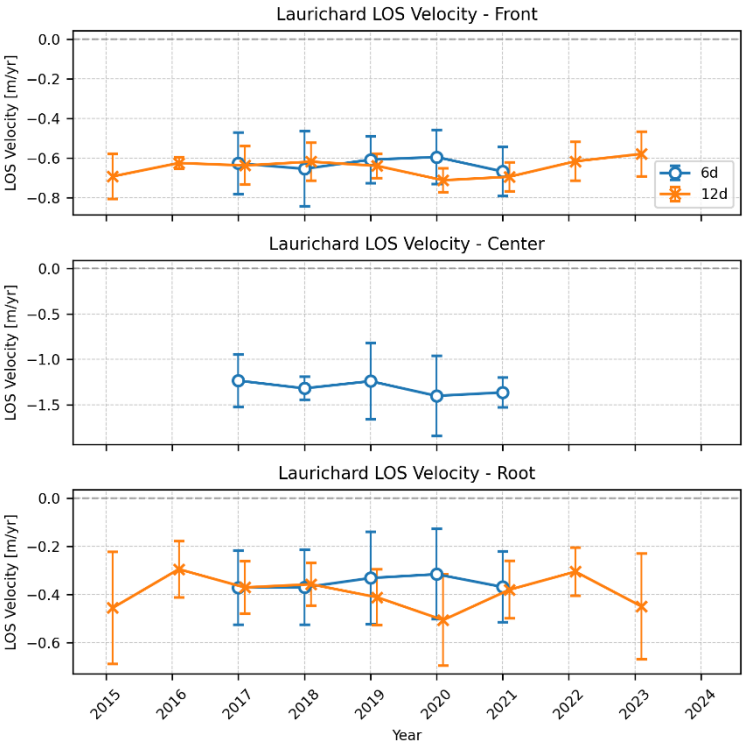

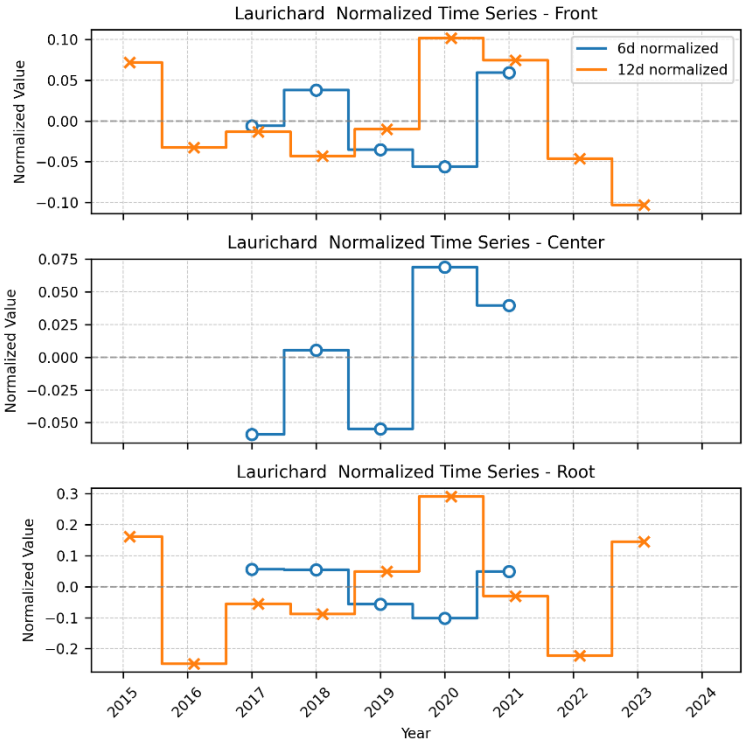

Velocity variation over the years: We averaged the obtained LOS velocity rates from all three monitoring points to generate yearly velocity estimates. In the top three figures, the averaged LOS velocities per summer are shown. The error bars represent the standard deviation per year. The three bottom figures show the normalized values ((Avg_year/mean_overall)-1) to highlight relative changes independent of the absolute velocities. Note that higher variations are expected as the measured velocities approach the sensitivity/noise level.

All three points show show realitivy small variations over the year, especially considering the error bars. All years show stronger seasonal variations. The selection of which points to use in the analysis thus plays a significant role. The time series displayed should thus be interpreted with caution.